Longitudinal characterisation of neuropathology in transgenic and knock-in Huntington's disease mouse lines

This thesis is submitted for the degree of Doctor of Philosophy at Cardiff University

Zübeyde Bayram-Weston

Supervisors:

Dr. Simon P. Brooks

Professor Stephen B. Dunnett

Cardiff University

September 2011

I dedicate this thesis to the memory of my grandmother, Fikriye Ekinci.

Declatation

This work has not previously been accepted in substance for any degree and is not concurrently submitted in candidature for any degree.

Signed …… (candidate) Date ……

STATEMENT 1

This thesis is being submitted in partial fulfillment of the requirements for the degree of PhD.

Signed …… (candidate) Date ……

STATEMENT 2

This thesis is the result of my own independent work/investigation, except where otherwise stated.

Other sources are acknowledged by explicit references.

Signed …… (candidate) Date ……

STATEMENT 3

I hereby give consent for my thesis, if accepted, to be available for photocopying and for inter-library loan, and for the title and summary to be made available to outside organisations.

Signed …… (candidate) Date ……

STATEMENT 4: PREVIOUSLY APPROVED BAR ON ACCESS

I hereby give consent for my thesis, if accepted, to be available for photocopying and for inter-library loans **after expiry of a bar on access previously approved by the Graduate Development Committee.**

Signed …… (candidate) Date ……

Thesis Summary

The work presented in this thesis consists of 4 manuscripts, focussed on characterising the distribution of mutant huntingtin protein in transgenic and knock-in mouse models of Huntington's disease.

The mouse lines showed a different expression level of mutant huntingtin across the different time points. In the R6/1 mice, the inclusions were present and widespread from 3.5 weeks of age. In the YAC128 mice, inclusions were not present until 15 months of age, but then developed rapidly throughout the brain. In the *Hdh*Q92 and *Hdh*Q150 mice, intra nuclear inclusions (NIIs) were apparent at 10 and 5 months of age, respectively, and spread anterior to posterior and ventral-dorsal directions. In this thesis, the study has shown no increase in GFAP immunoactivity in the striatum of each mice line. However we detected a small increase in GFAP immunoactivity in the cortex of transgenic mouse models. With electron microscopy, we observed ultrastructural pathology with vacuolization, uneven cell membrane and degenerated mitochondria in these mouse lines along side with the presence of inclusions. Each mouse line showed different levels of degeneration such as YAC128 and *Hdh*Q92 mice exhibited apoptitic neurons, whereas *Hdh*Q150 mice has shown signs of necrosis.

The results demonstrate that each of the mouse lines studied has a unique pattern of development of neuropathology. Inclusion formations may not be pathogenic per se, but may be representative of the dysfunctional neuronal populations that underpin the functional disturbances found in each of these mouse lines. Electron microscopy shows different cell death morphology in these mouse lines

.

Acknowledgements

First of all I would like to thank my supervisors Stephen Dunnett and Simon Brooks for giving me this opportunity to work with them. Your support and enthusiasm has inspired me and made me believe I can do this, thank you ever so much! I would also like to thank Lesley Jones for her helpful advice. The High Q meetings have always motivated me and kept me on my toes and have ensured I met the targets I set myself.

A massive thank to my old room mates Ulrike Weyrauch, Sophie Precious, Dr. Steve Fielding and present office mates, Gaynor Smith, Andreas Heuer, Amy Evans and Narawadeee Choompoo, you are all amazing scientists. Dr Steve, thank you! Your tips, guidance, and endless humour were great medicine. Sophie thank you so much for your help over the last three years. Andi thank you so much for your support! Your cake made my day, which I will never forget. Gaynor, I have been encouraged by your positive outlook and am sure Harvard will be a great success for you. Thank you all again, for believing in me and supporting me all the way.

A special thank you to Becky Trueman, I cannot thank you enough for all your support, advice and inspiration throughout my work.

A big thank you to the rest of the members of the Brain Repair Group, past and present, Anne Rosser, Claire Kelly, Eduardo Torres, Rike Zietlow, Alex Klein, Mariah Lelos, Emma Lane, Hanna Lindgreen, Andrew Hollins, Sarah Minster, Jenny Townhill, Mate Dobrosy, Ludivine Breger, Marijia Fjodorova, Victoria Roberton, Ellen Murphy, Susannah Williams, Ali Blaird, Anne-Marie McGorrian, Nari Jangra, Ngoc Nga Vinh, Jane Heath, Harri Harrison and Gemma Higgs for the help and supports. It is a pleasure to work with such a wonderful team of scientists and I am gereatful for a creating a wonderful enviorement to work.

An enormous thank to Antony Hann and other members of electron microscopy unit. Hann, thank you so much for your guidance and expertise on the electron microscopy. I have enjoyed working with you.

Sevgili ailem, annem Şükriye, babam Mustafa, kardeşlerim, Timuçin ve Sitki, buraya kadar sizin sayenizde geldim, sizin sevgi ve desteğiniz olmadan bunların hiçbirini yapamazdim. Sizlerle gurur duyuyorum. Bana olan sonsuz sevginiz, inancınız ve desteğiniz icin çok teşşekkur ederim.

I want to special thanks to my husband Mark for his endless support and being there whenever I was in need. I would not have been able to get through this without you.

Last but definitely not least an extra special thanks to my beautiful son Sami who wasn't around when I started this work. You have brought me great joy and have made me the proudest mum in the world.

Summary of the papers presented in the thesis

Paper 1

Light and electron microscopic characterization of the evolution of cellular pathology in R/1 Huntington's disease transgenic mice.
Bayram-Weston Z, Jones L., Dunnett S.B. and Brooks S.P.

Brain Res Bull. 2011 Jul 23

Paper 2

Light and electron microscopic characterization of the evolution of cellular pathology in YAC128 Huntington's disease transgenic mice.
Bayram-Weston Z, Jones L., Dunnett S.B., Brooks S.P.

Brain Res Bull. 2011 May 18.

Paper 3

Light and electron microscopic characterization of the evolution of cellular pathology in Hdh(Q92) Huntington's disease knock-in mice. Bayram-Weston Z., Jones L., Dunnett S.B. and Brooks S.P.

Brain Res Bull. 2011, Apr 13.

Paper 4

Light and electron microscopic characterization of the evolution of cellular pathology in the Hdh((CAG)150) Huntington's disease knock-in mouse.
Bayram-Weston Z**.**, Torres E.M., Jones L., Dunnett S.B., and Brooks S.P. Brain Res Bull. 2011 Apr 13.

Summary of additional publications

In Brain Repair Group, I have been involved in publications, outside of this thesis and these are listed below:

Longitudinal analysis of the behavioural phenotype in R6/1 (C57BL/6J) Huntington's disease transgenic mice. Brooks S.P., Janghra N., Workman V.L., Bayram-Weston Z., Jones L. and Dunnett SB. Brain Res Bull. 2011 Jan 25.

Selective cognitive impairment in the YAC128 Huntington's disease mouse. Brooks S.P., Janghra N., Higgs G., Bayram-Weston Z., Heuer A., Jones L. and Dunnett S.B. Brain Res Bull. 2011 May 20.

Profiles of motor and cognitive impairment in the transgenic rat model of Huntington's disease. Fielding S.A., Brooks S.P., Klein A., Bayram-Weston Z., Jones L. and Dunnett S.B. Brain Res Bull. 2011(in press)

Abbreviations

3-NP	3-Nitropropionic acid
AChE	Acetylcholinesterase
ALS	Amyotrophic lateral sclerosis
Amygdala BL	Basolateral amygdala
Amygdala CL	Central amygdala
BDNF	Brain-derived neurotrophic factor
BSA	Bovine serum albumin
CAG	Glutamate
CNS	Central nervous system
CREB	cAMP-responsive element- binding protein
CV	Cresyl fast violet
D1	Dopamine receptor 1
D2	Dopamine receptors 2
DAB	3,3'-diaminobenzidine
DNA	Deoxyribonucleic acid
DRPLA	Dentatorubral pallidoluysian atrophy
E	Embryonic day
ENK	Enkephalin
ENNIs	Extra-nuclear inclusions
ER	Endoplasmic reticulum
GABA	γ- Aminobutyric acid
GFAP	Glial fibrillary acidic protein
GP	Globus pallidus
GPi	Globus pallidus internal
GPe	Globus pallidus external

HD	Huntington's disease
HTT	Huntingtin gene (human)
HTT	Huntingtin protein (human)
Htt	Huntingtin gene (mouse and rat)
Htt	Huntingtin protein (mouse and rat)
IHC	Immunohistochemisty
IT15	Interesting transcript 15
KI	Knock-in
mTOR	mammalian target of rapamycin
MSNs	medium spiny neurons
NADPH	Nicotinamide adenine dinucleotide phosphate
NIIs	Intra nuclear inclusions
NOS	nitric oxide synthase
PD	Parkinson's disease
PBS	Phosphate buffered saline
PFA	Paraformaldehyde
PolyQ	Polyglutamine
SBMA	Spinal and bulbar muscular atrophy
SCA	Spinocerebellar ataxia
SNc	Substantia nigra pars compacta
SNr	Substantia nigra pars reticulate
STN	Subthalamic nucleus
Sub P	substance P
$TAF_{II}130$	TBP-associated factor
TEM	Transmission electron microscopy
TBP	TATA- binding protein

TBS	Tris buffered saline
UPR	Unfolded-protein response
UPS	Ubiquitin-proteasome system
YAC	Yeast artificial chromosome
WT	Wild-type

Table of Contents

Chapter 1

General Introduction

1.1 Huntington's disease

1.1.1. The Historical Perspective of Huntington's disease

Huntington's disease (HD) is an autosomal dominant, progressive neurodegenerative disorder which was first described in 1872 by George Huntington in and an article entitled "On Chorea" in *The Medical and Surgical Reporter (Philadelphia),* a weekly journal of the time*.* The Huntington family were physicians in East Hampton, New York and practiced medicine throughout almost all of the nineteenth century. George Huntington was the youngest of his generation of Huntingtons. "On Chorea" describes his own observations of affected families under his care in combination with the valuable knowledge he gained from the further observations of his father and grandfather at the same practice before him (Harper, 2002). In this classic paper, Huntington identifies three marked traits of the disease: its hereditary nature, a tendency towards insanity and suicide, and its manifestation as a grave disease that appears only in adult life (Huntington, 2003).

While, the recognition of HD was spreading rapidly throughout the world in the late nineteenth century, an attempt was made to identify families in the New England region which were believed to be the source of the spreading of the HD gene. Comprehensive pedigrees were collected by Jelliffe in 1908 and Davenport and Muncey in 1916 and they were linked back to the possible founding members. Most of these people seemed to originate in the early seventeenth century from the East Anglian regions of England and subsequently migrated to the USA. Furthermore, it had been claimed by Vessie in 1932 that HD originated from three individuals from the village of Bures in Suffolk. This was also supported in other studies by Critchley in 1934 and later by Maltsbereger in 1961 and van Zwanenberg in 1974. However, in 1975, Caro and Haines produced genealogical evidence in both England and the USA, and discredited the previous findings which were shown to be flawed and inadequate. Nonetheless, New England played a central role on spreading HD genes from Europe throughout the USA. It was suggested by Scrimgeour in 1983 that HD might have spread to some Pacific Island

communities by visiting New England whaling ships in the early nineteenth century (Harper, 2002).

1.1.2. Clinical features of Huntington's disease

The frequency of HD in the Caucasian population is approximately 5-10 cases per 100000 individuals (Harper, 1992). The first symptoms usually occur between the ages of 40 to 50 years old. The symptoms and signs gradually change with disease progression and leading to death 15-20 years after the motor symptom onset (Roos et al., 1993). Prior to the identification of the HD gene and availability of a definitive genetic test, HD was diagnosed by three criteria: a family history of HD; a progressive motor disability with chorea and psychiatric disturbance with progressive dementia (Vonsattel and DiFiglia, 1998). However, today, following identification of the HD gene, HD can be confirmed by deoxyribonucleic acid (DNA) analysis of blood samples taken from gene carriers.

The disease is characterized by progressive development of cognitive, psychiatric and motor symptoms (Roos et al., 1993). Symptoms can vary between individuals, even members of the same family (Georgiou et al., 1999; Howeler et al., 1989). Affected individuals may exhibit mild personality changes in initial stage of the disease. Other psychiatric symptoms can include the irritability, depression, anxiety, apathy and changes in sleeping patterns (for a rewiew, see (Kremer and ., 2002; Roos, 2010)).

Prior to the appearance of motor deficits, some affected individuals have been shown to perform poorly on cognitive tests (Campodonico et al., 1996) and the presence of cognitive deficits is reported in HD gene carriers at the 'pre-symptomatic' stage, well before the onset of the motor symptoms that define the disease. Therefore, it has been suggested that affected individuals may pass through an early asymptomatic stage, and that HD can start with nonspecific cognitive impairments rather than motor impairments (Ho et al., 2003; Kirkwood et al., 2000; Lawrence et al., 1996; Lawrence et al., 1998;

Lemiere et al., 2004; Robins Wahlin et al., 2007). However, questionnaires filled by family members of affected individuals reveal that involuntary movements may still be one of the earliest symptoms followed by mental and emotional symptoms including sadness, depression and “difficult to get along with” (Kirkwood et al., 2001). Some patients may exhibit minor motor impairments such as disturbed saccadic eye movement and slowness of rapid alternating movements before showing any sign of dominant motor abnormalities. However, as the disease progresses, there is a clear appearance of increased motor impairment including chorea (an involuntary writhing movement of the trunk, head and limbs), hypokinesia and rigidity (Penney, Jr. et al., 1990). In the early–middle stage of the disease, affected individuals have been reported to display motor signs of clumsiness, lack of motivation, sexual problems and paranoia. In the middle stage, patients experience motor difficulties that interfere with functional activities such as unsteadiness, trouble holding onto things, and trouble walking. In addition to motor difficulties, few patients suffer from delusions and hallucinations. In the middle- late stage, patients begin to experience speech difficulties and weight loss. In the late stage, motor symptoms worsen with increased chorea, hypertonic rigidity, dystonia (slow abnormal movements and abnormal posturing), bradykinesia (slow movements), rigidity, gait disturbances, speech abnormalities and dysphagia (swallowing impairment) (Kremer and ., 2002) and individuals have difficulties with bowel and bladder control (Kirkwood et al., 2001). In addition to these symptoms, cognitive decline is more obvious with difficulties in concentration, obtaining new information, impairment of language skills and dementia in late stage of the diseases (Kremer and ., 2002). Therefore, this broad range of clinical phenotypes results in a varying degree of HD, in terms of the age of onset, manifestation and speed of progression.

The symptoms usually get worse and patients lose their independence requiring assistance and need care for activities in daily living. Pneumonia (33%) is the leading cause of death in affected individuals, followed by heart

problems, choking, nutritional deficiencies, chronic skin ulcers (Lanska et al., 1988) and suicide (Harris and Barraclough, 1994).

1.2. The basal ganglia and Huntington's Disease

HD is widely considered to be first and foremost a disease of the basal ganglia. Basal ganglia diseases are associated with a range of movement disorders such as Parkinson's disease (hypokinesia), chorea and dystonia (hyperkinesia) (Mink, 2003). The basal ganglia consists of the striatum (caudate and putamen), the subthalamic nucleus (STN), globus pallidus (internal and external segments), and the substantia nigra pars compacta (SNc) and pars reticulata (SNr) (Alexander et al., 1986). Together, these nuclei form multiple circuits linking the basal ganglia both to the cortex and to the thalamus and brainstem. Alexander and Crutcher have proposed that there are at least five structurally and functionally distinct circuits in parallel (Figure 1; (Alexander et al., 1986). These circuits are thought to originate in discrete functional areas of the neocortex and then to funnel through distinct regions of the basal ganglia and thalamus and then project back to discrete regions of the frontal cortex which has a unique function. For instance, the putamen is mainly involved in motor control as the result of its connections with the supplementary motor and premotor cortex. Conversely, the ventromedial part of the head of the caudate nucleus is involved in the normal functions of limbic system such as reward, emotion and motivation. The dorsalateral part of the head of caudate forms is part of the dorsalateral prefrontal circuit which is involved in cognitive functions. The body of the caudate nucleus is part of the oculomotor circuit and involved in saccadic eye movement. The ventral striatum is part of the cingulate cortex and is also involved in limbic functions (Alexander et al., 1986; Alexander et al., 1990). Hence, the striatum can be separated into three distinct striatal regions including sensorimotor, associative and limbic territories. However, some researchers have suggested that this separation is incomplete and there is cross talk between the loops which is reviewed in Parent and Hazrati (1995).

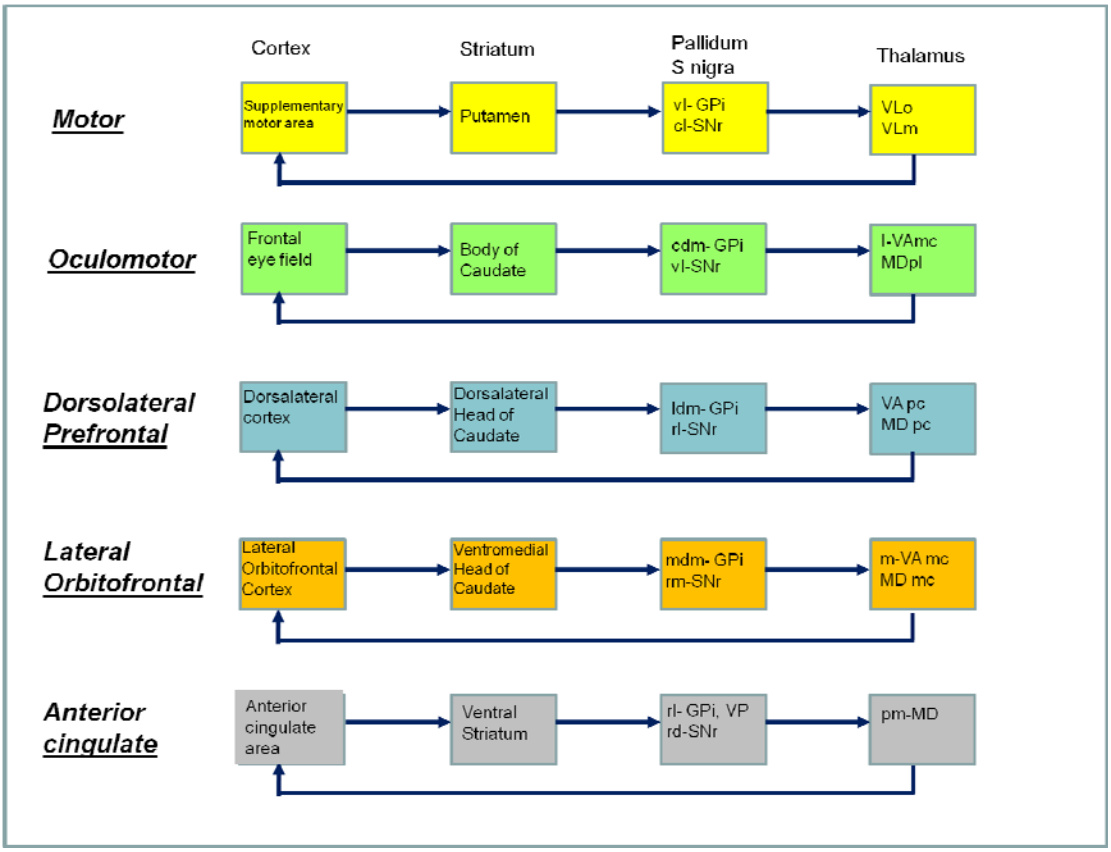

Figure 1; The five proposed basal ganglia- thalamocortical circuits. Each circuits Abbreviations: GPi, internal segment of globus pallidus; MD, medialis dorsalis; MDpl, medialis dorsalis pars paralamellaris; MDmc, medialis dorsalis pars magnocellularis; MDpc, medialis dorsalis parsparvocellularis; SNr, sunstantia nigra pars reticulata; VAmc, ventralis anterior pars magnocellularis; Vapc, ventralis anterior pars parsparvocellularis; VLm, ventralis lateralis pars medialis; VLo, ventralis lateralis pars oralis; VP, ventral pallidum; cl, caudolateral; cdm, caudal dorsamedial;dl, dorsolateral; l, lateral; ldm, lateral dorsomedial; pm, posteromedial; rd, rostrodorsal; rl, rostrolateral; rm, rostromedial; vm, ventromedial; vl, ventrolateral;

In addition to the globus pallidus and substantia nigra, the largest part of the basal ganglia comprises a group of structurally similar nuclei known collectively as the ‘striatum’. Anatomically, there are minor differences in the organisation of the basal striatum in rodents and primates (Parent, 1986). In the primate striatum, the caudate nucleus and putamen comprise similar populations of neurons at a cellular level but are divided into two discrete nuclei by the sheet of fibres comprising the internal capsule. However, in the rodent brain, the internal capsule is present, not as a sheet but as multiple small bundles of fibres so that the caudate nucleus and putamen can not be resolved but are jointly referred to as ‘dorsal’ striatum (or ‘neostriatum’). The

more ventral parts of the striatum of both primates and rodents contain the nucleus accumbens and olfactory tubercle (Nauta, 1979).

The neuronal population of striatum consist of 90% medium spiny neurons (MSNs) and 10% interneurons in rodents (Kawaguchi et al., 1995; Kawaguchi, 1997). Figure 2 below shows the striatal neuron populations and neurotransmitters used.

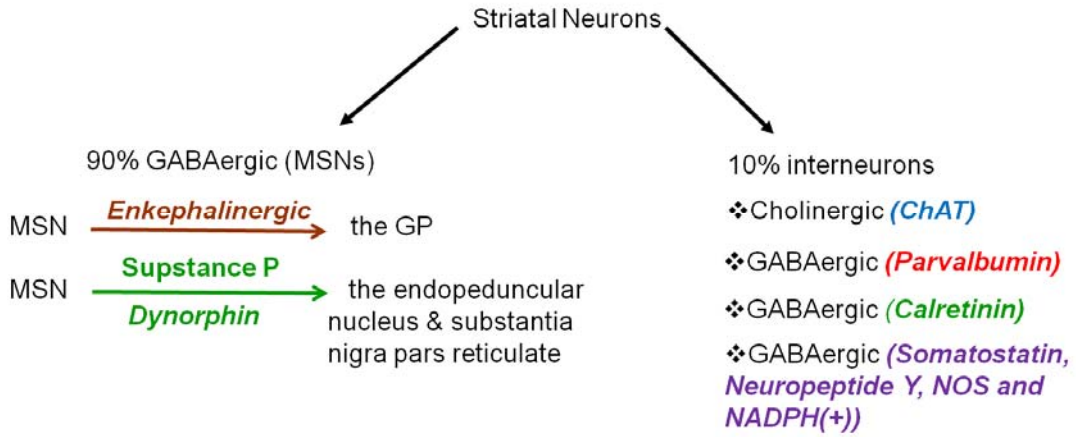

Figure 2. Neurons of the striatum with their neurotransmitters. 90% GABAergic MSNs and 10% interneurons with corresponding neurotransmitters. Abbreviations: GP, globus pallidus; ChAT, choline acetyltransferase; NOS, nitric oxide synthase; NADPH, nicotinamide adenine dinucleotide phosphate diaphorase.

The MSNs are γ- aminobutyric acid (GABA)-ergic, in addition to GABA, they also contain neuropeptides co-transmitters, such as enkephalin and substance P and/or dynorphin (Gerfen and Young, III, 1988). Striatal efferents contain different neurotransmitters and project to different nuclei. The MSNs are distinguished from the interneurons as being the major projection neurons of the striatum, with different neurotransmitters corresponding to the different projection targets. The MSN can be divided into two relatively equal sized populations based on these axonal projections. These main output pathways called ‘direct’ and ‘indirect’ pathways due to their connections (Alexander and Crutcher, 1990) (Figure 3: inputs and outputs of basal ganglia). In the “direct pathway”, striatal neurons containing GABA and substance P project to the SNr/globus pallidus internal (GPi). The pathway then goes through the

thalamus via the GABA projection and then to the cortex via the excitatory glutamate projections. In the “indirect pathway”, striatal neurons containing GABA and enkephalin (ENK) project to the globus pallidus external (GPe), which then project to the subthalamic nucleus through a GABAergic pathway, and finally to the SNr /GPi via glutamatergic neurons. These two populations of MSNs are morphologically identical and are not topographically separated within the striatum. However the distinct destination and transmitter types of two populations may offer a kind of functional separation within the striatum (Alexander and Crutcher, 1990; Bates et al., 2002; Chenery et al., 2008).

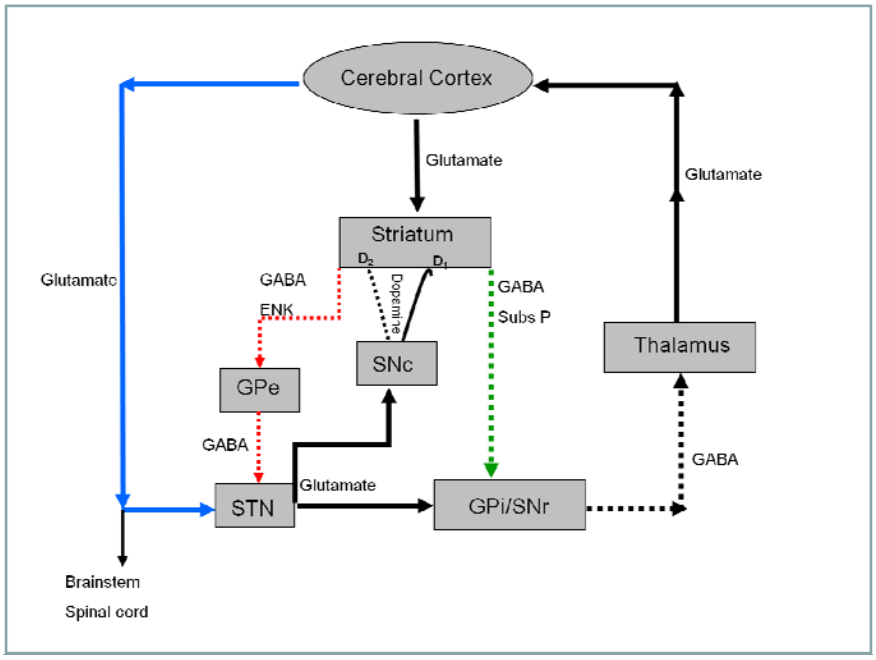

Figure 3: The inputs and outputs of the basal ganglia (Adapted from Alexander & Cruther, 1990 and Chenery et al 2008). Inhibitory projections are shown as dashed lines and excitatory projections are shown block lines. Green line, direct pathway; red line, indirect pathway; blue line, hyperdirect pathway. GPi, globus pallidus internal; GPe, globus pallidus external; STN, subthalamic nucleus; SNr, substantia nigra pars reticulate; SNc, substantia nigra pars compacta; GABA, gamma-aminobutyric acid; ENK, enkephalin; Sub P, substance P; D_1, dopamine receptor 1; D_2, dopamine receptors 2.

Additionally, there is a second characteristic feature of these two pathways which is they have different expression of dopamine (DA) receptors. The striatum receives dopaminergic input from the sunstantia nigra pars compacta and all five DA receptors (D_1-D_5) are expressed within the striatum. However, D_1 DA receptor (Drd1a) and D_2 DA (Drd2) are the most abundant receptors. D_1 receptors are selectively expressed by MSNs of the direct

pathway, whereas, D_2 receptors are expressed by MSNs of the indirect pathway. These two different receptors have different intracellular signalling cascades and targets, causing different cellular responses to extracellular DA (Gerfen et al., 1990). As mentioned earlier, MSNs of the direct pathway express high levels of substance P and dynorphin, whereas MSNs of the indirect pathway express enkephalin. After DA–depleting lesions, striatal enkephalin levels are elevated and substance P levels are depressed, suggesting that DA differently regulates these two MSNs populations (Young, III et al., 1986). Furthermore, it has been shown that the antagonists of D_1 and D_2 receptor restored substance P and enkephalin levels, respectively (Gerfen et al., 1990). However, there is debate as whether cells with D_1 and D_2 receptors are completely separate or these two receptors are colocalized on some cells. For example, an electrophysiological study has showed that both D_1 and D_2 receptor antagonists have effects on the same striatal neurons (White and Wang, 1986) indicating the complexity of the circuits and making it difficult to separate these two receptors. Nonetheless, recent studies support the idea that there is a reasonably clear-cut dichotomy of D_1 and D_2 receptor expression on MSN of the direct- and indirect pathways, respectively (Gertler et al., 2008; Valjent et al., 2009) and the impact of DA within the striatal circuitry has been reviewed in Gerfen and Surmeier (2010).

In HD, a decrease of dopaminergic neurons (Huot et al., 2007; Oyanagi et al., 1989; Yohrling et al., 2003) and a degeneration of nigrostriatal projections (Ferrante and Kowall, 1987; Ginovart et al., 1997) have been reported. Furthermore, a down regulation of D_1 and D_2 receptors has been observed in HD brains (Ginovart et al., 1997). In addition to these findings, one study has suggested that loss of D_2 receptors is a sensitive early marker of neuronal impairment in presymptomatic HD patients (van Oostrom et al., 2005). Taken together, these results suggest the presence of dysfunctional nigrostriatal pathways which may be involved in motor and cognitive deficits in HD.

In addition to MSNs in the striatum, there are four subtypes of striatal interneurons which can be characterized by their chemical constituents, size and dendritic morphology. These interneurons are; cholinergic interneurons,

which contain a large soma, widespread dendritic trees and receive direct dopaminergic inputs and contains choline acetyltransferase (ChAT); a second subtype GABAergic interneurons which express parvalbumin; a third subtype GABAergic interneurons that express calretinin and a fourth subtype, which are GABAergic express somatostatin, neuropeptide Y, nitric oxide synthase (NOS) and nicotinamide adenine dinucleotide phosphate (NADPH)-diaphorase (+) (Kawaguchi et al., 1995).

In HD, the GABAergic projection neurons are the most severely affected neurons in the striatum in HD (Ferrante, 2009). In early and mid stage of HD, it has been observed that enkephalin-containing neurons of the striatum are more vulnerable than substance P-containing neurons, causing an imbalance between the direct and indirect pathways. However, it has been suggested that substance P-containing neurons may also be affected during early stages of the disease. Although, in late stage of HD, it has been reported that the loss of all projections are prominent (Albin et al., 1992; Reiner et al., 1988). The large cholinergic neurons (Ferrante et al., 1987a) and striatal interneurons (containing somatostatin, neuropeptides Y or NADPH-diaphorase) remain selectively preserved in the caudate nucleus of HD patients (Ferrante et al., 1985). Additionally, it has been reported that parvalbumin containing interneurons are also spared in HD (Mitchell et al., 1999). But, a recent study has suggested that the cholinergic system might be affected in HD patients (Smith et al., 2006).

The striatum is also characterised with two neurochemically distinct compartments, the patch and matrix. The patch compartment (striosomes) is identified by patches of dense opiate receptor binding, and is enriched in substance P and enkephalin immunoreactivity. The matrix compartment has high acetylcholinesterase (AChE) reactivity and stains more densely for somatostatin, neuropeptide Y, NADPH- diaphorase and calbindin. These two compartments receive different afferents from the cortex and the midbrain (Gerfen, 1984; Gerfen et al., 1985). The matrix mainly projects to the pallidum and the SNr, which together make up the main GABAergic systems. In contrast, the outputs of patch project to the dopamine-containing SNc and/or it's near surrounds suggesting that the patch linked to some branches of the

limbic system, change part of the dopaminergic input to the striatum. There are noticeable, but selective cross connections between these two compartments and reviewed in Graybiel (1990).

In early-stage HD, a study has suggested that cell loss is restricted to the patch compartment (Hedreen and Folstein, 1995), however, other studies have found that the matrix compartment is the more vulnerable (Ferrante et al., 1987b; Seto-Ohshima et al., 1988). Interestingly, a previous study has shown that the pathology of the patch compartment is greater in patients with mood symptoms (Tippett et al., 2007). The role of patch/matrix distinction in both normal function and neuropathology remains unresolved and is diffucult to marry the more widely adopted direct/indirect pathways characterisation.

1.2.1. Neuropathology of Huntington's disease

Mutant huntingtin is responsible for the neurodegeneration of the basal ganglia and cerebral cortex which is preceded by neuronal dysfunction in HD (Vonsattel, 2008).The most noticeable neurodegenerative changes in the post-mortem brains of HD patients are found in the caudate and putamen with neuronal loss and astrogliosis being a feature (Vonsattel et al., 1985; Vonsattel and DiFiglia, 1998). The severe loss of striatal medium spiny neurons (MSNs) is a neuropathlogical hallmark of HD. Striatal MSNs receive a major source of afferents from the cortex, and there is considerable speculation over whether loss of the striatal cells may be an anterograde consequence of cortical atrophy (Graveland et al., 1985; Rosas et al., 2002; Rosas et al., 2003; Rosas et al., 2008) or conversely that loss of cortical cells may be a retrograde response to loss of their targets (Cudkowicz and Kowall, 1990). Loss of MSNs leads to a noticeable decrease in striatal volume leading to an equivalent enlargement of the lateral ventricles (Vonsattel et al., 1985), the pattern of neuronal loss has been shown to appear earliest and to be most extensive in dorso-medial sectors of the striatum and to progress ventrally, laterally and caudally as the disease develops (Hedreen and Folstein, 1995; Mitchell et al., 1999). Unfortunately, by the time of clinical diagnosis, more

than 50% of the striatum has atrophied and the total brain weight could have reduced by as much as 30% by the time of death (Rosas et al., 2003).

Brains from HD patients are classified from grade 0 to 4 based on the severity of striatal neuropathology. In grade 0, no striatal pathology is found despite a positive family history; in the grade 1 brain, there is limited neuronal loss and astrogliosis; in grade 2 HD, there is caudate nucleus atrophy; in grade 3, atrophy of the caudate-putamen is evident; and in the highest grade, grade 4, severe caudate-putamen and nucleus accumbens atrophy are found (Vonsattel et al., 1985). The same study has reported that motor and cognitive impairments can appear before any obvious neuronal cell loss, suggesting that initially these impairments are caused by a neuronal dysfunction, rather than cell death *per se*. However, the some evidence show that there can be a significant striatal atrophy even in presymtomatic patients (Aylward et al., 2004; Kassubek et al., 2004; Ruocco et al., 2006; van den Bogaard et al., 2011) and it has been suggested that the striatal atrophy begins well before the presence of motor symptoms or clinical diagnosis (Aylward et al., 2004).

In addition to the striatum, cortical atrophy has been observed in grade 3 and 4 patients. Earlier post mortem studies indicated that the most affected layers are especially III, V and IV with a reduction of a subset of pyramidal neurons (Sotrel et al., 1991; Vonsattel and DiFiglia, 1998). More recently, neuroimaging techniques have exposed important correlations between cortico-striatal atrophy and cognitive impairment such as attention, working memory and executive functions in HD patients (Montoya et al., 2006). Some studies have reported that the presence of cortical atrophy in early to mid-stages of HD by MRI scan (Kassubek et al., 2004; Rosas et al., 2003). However, some recent studies have failed to show cortical atrophy in presymtomatic patients (Aylward et al., 2011; Hobbs et al., 2010; Kipps et al., 2005).

Although, the neuropathology is most prominent in the neostriatum and the cerebral cortex, other brain areas such as amygdala, hippocampus (Rosas et al., 2003), globus pallidus (GP) and the nucleus accumbens (van

den Bogaard et al., 2011) are also affected in the early stages of the disease. With the disease progression, the other regions of brain for example substantia nigra (SN) (Vonsattel et al., 1985; Vonsattel and DiFiglia, 1998), hippocampus (Spargo et al., 1993), thalamus (de la Monte et al., 1988) hypothalamus (Kremer et al., 1991) and the cerebellum (Herishanu et al., 2009; Jeste et al., 1984; Rodda, 1981) have also found to be atrophied. Although, it is important to mention that some studies reported that the cerebellum is generally spared in the adult onset form of HD (Rosas et al., 2003; Ruocco et al., 2006). The recent MRI scans also showed the atrophy of the white and gray matter in early HD (Aylward et al., 2011; Hobbs et al., 2010; Kipps et al., 2005). Therefore, although the principal focus of HD is on the cortico-striatal tracts and degeneration of the cortex and striatum, the disease, is a disease of the whole brain, and many of the areas outside of the cortex and striatum degenerate in early and later stage of the disease process.

1.2.2. GFAP expression in the HD brain

Astrocytes are one of the most abundant cell types in the central nervous system (CNS) and are involved in a number of different physiological and pathological processes in the brain (Ransom et al., 2003). Their full role in the brain is still unclear. They fill the spaces between neurons and provide structural support for neuronal migration and positioning, and mediate the chemical content of the extracellular space. For instance, astrocytes surround synaptic junctions in the brain thus restricting the spread of released neurotransmitters and recycling certain neurotransmitter substances such as glutamate. The membrane of astrocytes contains special proteins which actively remove many neurotransmitters from the synaptic cleft. Additionally, astrocytes regulate the concentration of potassium ions in extracellular fluid for example cleaning up potassium ions, during intense neuronal activity. Unlike neurons, astrocytes can multiply at any time. In particular, after CNS injury, the proliferation of astrocytes and their processes results in dense glial scar tissue, gliosis (Bear M.F. et al., 2006). The transition of astrocytes from

the resting to active state is associated with the expression of new molecules which are not detectible in resting astrogilia. This list of new molecules was reviewed by Eddleston and Mucke (1993). Molecular tools also suggest that astrocytes contribute to the elimination of neutotoxins by both enhanced uptake and metabolic turnover (Eddleston and Mucke, 1993).

An intermediate filament protein, glial fibrillary acidic protein (GFAP) is expressed primarily by reactive astrocytes and provides a marker for astroglial activation (Bignami et al., 1972; Dahl et al., 1981). The brain reacts to neuronal injuries with an increase in number and size of cells expressing GFAP, this is called reactive astrogliosis. Hence GFAP immunostaining has been used to identify reactive astrogliosis and an early marker of CNS damage in HD (Yu et al., 2003). Astrogliosis is observed in human HD (Galatioto, 1996; Hedreen and Folstein, 1995; Maat-Schieman et al., 2007). The suppression of GFAP expression in human glial cells line suggests that GFAP is required for stabilizing glial processes in response to neuronal signals (Weinstein et al., 1991). It is also important to emphasize that the response of CNS to neurologic injury involves many cell types other than astrocytes including microglia, macrophages, and other invading inflammatory and immune cells.

1.2.3. Ultrastructural neuropathology in HD

Ultrastructural neuropathology has been reported in the brain samples (Butterworth et al., 1998; DiFiglia et al., 1997; Goebel et al., 1978; Gutekunst et al., 1999; Portera-Cailliau et al., 1995; Roizin et al., 1974; Roizin et al., 1979; Roos and Bots, 1983; Roos et al., 1985; Tellez-Nagel et al., 1974) and peripheral tissues (Squitieri et al., 2009) by transmission electron microscopy (TEM) in HD patients. In addition to that seen in patients, ultrastructural neuropathology has also been observed in mouse models of HD with TEM (Davies et al., 1997; Gray et al., 2008; Iannicola et al., 2000; Ikeda et al., 1996; Montoya et al., 2006; Morton et al., 2000; Panov et al., 2002; Portera-Cailliau et al., 1995; Stack et al., 2005; Yu et al., 2003).

Ultrastructural pathology in HD brain includes: the alterations of nuclear membranes (Goebel et al., 1978; Roizin et al., 1974; Roos and Bots, 1983; Roos et al., 1985), the accumulations of large lipofucsin granules (Goebel et al., 1978; Roizin et al., 1974; Tellez-Nagel et al., 1974), irregular distributions of the rough endoplasmic reticulum, enlargements of Golgi apparatus (Roizin et al., 1974), disorganizations of nuclei, reduction of the number of ribosomes (Roos and Bots, 1983; Roos et al., 1985) and DNA fragmentation (Butterworth et al., 1998; Portera-Cailliau et al., 1995). Several studies have reported severe ultrastructural changes in mitochondria, including enlarged mitochondria, mitochondria accumulation, and an increased degenerated mitochondrial population in HD patients (DiFiglia et al., 1997; Goebel et al., 1978; Squitieri et al., 2006; Tellez-Nagel et al., 1974), supporting other evidence that mitochondrial dysfunction and oxidative stress play a role in the neurodegenerative process of the disease (Damiano et al., 2010; Deschepper et al., 2011; Kim et al., 2010; Lin and Beal, 2006; Shirendeb et al., 2011).

Neuronal intra-nuclear inclusions (NIIs) were originally observed in 1979 in biopsy samples of HD patients using electron microscopy (Roizin et al., 1979), and then were discovered in the post-mortem tissues of affected individuals with the light and electron microscopes. At the ultrastructural level, NIIs are highly heterogeneous in composition and consist of a mixture of granules, straight and twisted filaments with no membrane separating it from its surroundings (Davies et al., 1997; DiFiglia et al., 1997). Extranuclear inclusions (ENNIs) were not detected with conventional TEM analysis, however they been identified in the dendrites and axons by immunogold TEM (Gutekunst et al., 1999).

Electron microscopic examination of transgenic mouse striatum revealed the presence of striatal neurons with inclusions (Davies et al., 1997), and large accumulations of lipofucsin granules and enlarged mitochondria (Iannicola et al., 2000). The localization of mutant huntingtin on the mitochondrial membrane of transgenic mice were observed by immunogold TEM analysis (Panov et al., 2002). Ikeda and co-workers showed ultrastructurally that expanded polyQ induces cell death *in vitro* and *in vivo*.

These dying cells have a punctate staining and show features of apoptotic cell death with cytoplasmic fragmentation, condensed nuclei and DNA fragmentation in the nuclei (Ikeda et al., 1996). Other studies have also reported that the presence of increased shrunken, angular, dark neurons with reduced cytoplasm and nucleoplasm in the brains of transgenic mice (Gray et al., 2008; Stack et al., 2005; Turmaine et al., 2000). The presence of ENNIs in the synaptic densities of the neurons in mice were observed with immunogold TEM (Morton et al., 2000). However, one research group have highlighted novel ENNIs which are easily identified without immunogold labelling by TEM examination in the R6/2 mouse (Morton et al., 2009).

1.3. Genetic background of Huntington's disease

The gene responsible for HD was first mapped in 1983 and it was reported that the HD locus resides on the short arm of human chromosome 4 (Gusella et al., 1983). A decade later, a mutation of HD gene, 'interesting transcript *15' (IT15)* was found on exon 1 of the short arm of chromosome 4. The *IT15* gene, now known as *huntingtin,* codes for the protein huntingtin (HTT), a large ubiquitous 350kDa protein, The Huntington's Disease Collaborative Research Group (1993), which is essential for normal embryonic development (Duyao et al., 1995; Nasir et al., 1995; Zeitlin et al., 1995). The HD gene consists of 67 exons and extends over 170kb of DNA (Ambrose et al., 1994), and contains a polymorphic stretch of repeated CAG trinucleotides which encodes polyglutamine (polyQ). Normal individuals may have between 6 and 35 CAG repeats, and it is when the numbers of repeats increases above 35 (36 to 39), that HD might occur and show partial affects, however 40 and more repeats will always cause the disease within a normal lifespan (Rubinsztein et al., 1996). Similarly, a previous study is also reported that the range between 29-35 CAG repeats are unstable which is likely to cause changes in the onset of the disease in the next generation (Trottier et al., 1994). Age of onset of HD can vary from early childhood to very old age, largely depending on the extent of the repeat length (Wexler et al., 2004).

CAG repeat length is inversely correlated with the age of onset (Andrew et al., 1993; Djousse et al., 2003) and accounts for about 50% of the variance in age of onset. Although HD patients carry the same mutation, two patients who have the same number of CAG repeat lengths do not necessarily exhibit the same cognitive, psychiatric and motor impairments at the same age (Gusella and MacDonald, 2009), and are thought to depend upon a range of genetic and environmental modifiers. Thus studies of a pair of monozygotic HD twins, who share identical CAG repeat length showed differences both in clinical symptoms and behavioural abilities (Georgiou et al., 1999; Gomez-Esteban et al., 2007). This supports the idea that other genetic and environmental factors are also involved in determining onset of the disease (Djousse et al., 2004; Wexler et al., 2004). No significant differences in age of onset, symptoms and progression of illnesses have been observed between affected HD homozygote and HD heterozygote patients (Wexler et al., 1987). However, a recent study has shown that homozygotes had a more severe cilincal course and affects the phenotype and the rate of the disease progression (Squitieri et al., 2003).

An inverse correlation between repeat lengths and the age of onset of the disease has been found (Andrew et al., 1993; Djousse et al., 2003). However, no correlation has been reported between duration of the disease and CAG repeat length on the adult form of HD (Ruocco et al., 2006). Despite these findings, a correlation between the atrophy of the striatum and CAG repeat length has been reported (Becher et al., 1998; Myers et al., 1988). In addition, a few previous studies have emphasised the presence of somatic instability in trinucleotide diseases in human HD (Kennedy et al., 2003; Telenius et al., 1994) and mouse models (Fortune et al., 2000; Gonitel et al., 2008; Kennedy and Shelbourne, 2000; Mangiarini et al., 1997; Wheeler et al., 1999), and showed that whereas all tissues displayed some repeat mosaicism, the greatest level is found in the brain and sperm. The basal ganglia and the cortex show the greatest neuropathology and display the greatest mosaicism (Telenius et al., 1994). Further, a correlation mechanism has been proposed between somatic repeat expansion and disease onset

and it has been suggested that the somatic CAG repeat expansion reaches a pathological threshold within the life time of patients. The disease becomes more apparent when this CAG repeat extends beyond a certain threshold in cells of the brain (Kaplan et al., 2007).

Longer CAG repeats, of ~ 65 or more are associated with juvenile HD defined as having onset occurring before 21 years of age (van Dijk et al., 1986). Under normal circumstances, the duration of the disease is usually 15-20 years after onset (Roos et al., 1993), but, juvenile HD progresses more rapidly, and death occurs within 7-10 years of onset (Ho et al., 2001b; Petersen et al., 1999; Roos et al., 1993). The juvenile form of HD differs from the adult form with a distinctive combination of parkinsonian symptoms such as rigidity, tremor and often epileptic seizures, but never chorea (Telenius et al., 1993). The cognitive and behavioural disturbances are similar in nature for children and adults, however, juveniles display a more severe disease progression (Wexler et al., 1991). In addition, the pattern of the neurodegeneration is less selective in juvenile onset. There are histopathological differences between juvenile and adult onset HD. Juvenile patients have extensive cell loss and gliosis in the cortex with neuronal reduction of the dentate nuclei and inferior olivary nuclei (Goebel et al., 1978) which is not seen in adult HD. Similarly, it has been revealed that there is neurodegeneration in the Purkinje cells of the cerebellum (Robitaille et al., 1997).

1.3.1. Role of Normal Huntingtin

Huntingtin is expressed within the CNS and peripheral organs (Zuccato et al., 2010), and is a necessary protein for the normal function of the basal ganglia. A murine homolog of the human HD gene has been created (Duyao et al., 1995; Nasir et al., 1995; Zeitlin et al., 1995). Homozygote animals have embryonic lethality before gastrulation and formation of the nervous system, however, heterozygote animals do not differ from wild type litter mates at birth (Nasir et al., 1995). Huntingtin has been shown to be involved in wide range

of functions other than embryonic development including neurogenesis (Dragatsis et al., 2000; Reiner et al., 2007; White et al., 1997), vesicle trafficking (Metzler et al., 2001; Velier et al., 1998), microtubule-dependent retrograde transport of membranous organelles (Li et al., 1998), axonal transport (Gunawardena et al., 2003), apoptosis (Gunawardena et al., 2003; Rigamonti et al., 2000), neuroprotection (Ho et al., 2001a; Que, Jr. et al., 1975; Rigamonti et al., 2001), energy homeostasis (Clabough and Zeitlin, 2006) and spermatogenesis (Dragatsis et al., 2000). Within the cell, wild-type huntingtin is mostly present in the cytoplasm, associated with organelles such as mitochondria, the Golgi apparatus, the endoplasmic reticulum and synaptic vesicles (DiFiglia et al., 1995; Kegel et al., 2002; Sharp et al., 1995), with a small amount being intra-nuclear (Hoogeveen et al., 1993).

It has been indicated that wild-type huntingtin has a role in membrane trafficking in the cytoplasm and interacts with many other proteins which may be involved in transcriptional regulation, intracellular trafficking and cytoskeletal organization (Li et al., 2003; Singaraja et al., 2002). Recently, 234 high-confidence huntingtin associated proteins have identified (Kaltenbach et al., 2007). Some of these huntingtin-binding proteins such as HAP1, HIP1 and HIP14 have been isolated (associated with endocytosis). However, their role in selective neuropathology has not been demonstrated (Li et al., 1995; Singaraja et al., 2002; Wanker et al., 1997). Huntingtin also regulates transcription of brain-derived neurotrophic factor (BDNF), a pro-survival factor produced by cortical neurons, that is necessary for survival of striatal neurons in the brain (Zuccato et al., 2001). Caspases have been associated in the cleavage of both wildtype and mutant huntingtin (Goldberg et al., 1996; Wellington et al., 1998; Kawaguchi et al., 1995). Depletion of huntingtin causes cells to become more vulnerable to apoptotic cell death and increases caspase-3 activity (Zhang et al., 2006). It has been assumed that the mutant protein has a toxic gain of function from an abnormal conformation of the mutant huntingtin protein which harms neurons. However, loss of wild-type huntingtin may also contribute to the death of striatal neurons (Cattaneo and Calabresi, 2002). Over-expression of normal huntingtin in the YAC128 mice

has been reported to show a mild improvement in the striatal neuropathology but not motor function, suggesting that mutant huntingtin is responsible for the striatal neuropathology seen in these mice (Van Raamsdonk et al., 2006).

1.3.2. Mutant Huntingtin

Normal and mutant huntingtin is expressed in both post-mortem human HD brains and mice (Bhide et al., 1996). In addition to the CNS, peripheral organs such as the colon, liver, pancreas and testes express mutant huntingtin (Strong et al., 1993). Within the brain, mutant huntingtin is present in the cytoplasm and nucleus of neurons (DiFiglia et al., 1997). A small amount of mutant huntingtin has been found in some subcellular organelles including the plasma membrane, mitochondria, lysosomes and endoplasmic reticulum (Kegel et al., 2002; Kegel et al., 2005; Orr et al., 2008; Panov et al., 2002). In addition to cell bodies, it has been also observed that an N-terminus of mutant huntingtin with 115-156 glutamine repeats accumulates in dystrophic neurite in the cortex and striatum (DiFiglia et al., 1997) and occasionally in astrocytes of HD patients post-mortem brains (Shin et al., 2005; Singhrao et al., 1998; Turmaine et al., 2000). Despite the widespread expression of mutant huntingtin in all body tissues throughout life, the most affected cells are MSNs of the striatum (Gusella and MacDonald, 2006). It has been suggested that selective degeneration of MSNs in HD may be due to the enhanced expression of the mutant huntingtin protein (Kosinski et al., 1997). A previous study has also showed that the existence of toxicity of the N-terminal fragment of huntingtin protein were present in the absence of CAG repeat expansion, although the study has confirmed that the presence of CAG repeats aggravates the toxicity of mutant huntingtin (O'Kusky et al., 1999).

1.3.2.1. Aggregate formation

HD is not the only disease caused by a CAG/polyglutamine repeat expansion. Glutamine expansion within other genes can cause at least nine

other neurodegenerative disorders such as spinal and bulbar muscular atrophy (SBMA), dentatorubral pallidoluysian atrophy (DRPLA) and spinocerebellar ataxia (SCA) types 1, 2, 3, and 7 (Bates et al., 1997; Schilling et al., 1999; Yamamoto et al., 2000; Timchenko and Caskey, 1999). These diseases share many common features such as subcortical and cortical atrophy, a progressive phenotype (Yamamoto et al., 2000; Davies et al., 1998) and the formation of neuronal intra-nuclear inclusions (NIIs) (Davies et al., 1998).

All these PolyQ diseases are associated with protein misfolding which is initiated by the expanded polyQ repeats. Protein folding is the process by which a polypeptide of amino acids folds into three-dimensional structure. It has been described that CAG repeats form a “polar zipper” structure causing the formation of the aggregates which may lead to neuronal damage (Perutz et al., 1994). Molecular chaperones remove misfolded protein from the cytoplasm, thus preventing the possibility of protein aggregation (Johnston et al., 1998). The genetic mutation such as HD can cause a failure in protein folding processes due to amino acid mis-incorporation (Johnston et al., 1998; Vidair et al., 1996). Previously, aggregation was considered to involve non-specific coagulated polypeptide chains (Zettlmeissl et al., 1979). However, it has subsequently been shown that aggregation is the result of a specific interaction of certain conformations rather than non-specific coagulation (Speed et al., 1996). Many misfolded proteins are targeted for degradation by the proteasome. It has been suggested that protein aggregation happens when the capacity of the proteasome degradation is exceeded. Therefore, Johnston and co-workwers have suggested two possible ways, either an increased substrate expression or decreased proteasome activity (Johnston et al., 1998). Huntingtin can be cleaved by apopain which is involved in ubiquitin-dependant proteolosis system and the rate of cleavage increases with the length of PolyQ (Goldberg et al., 1996). Following this it was shown that inclusions were also stained with an anti-ubiquitin antibody in post mortem tissues of HD, indicating that inclusions are ubiquitinated (Davies et al., 1997). The presence of ubiquitin in the NIIs has also been reported in all other PolyQ diseases (Saunders and Bottomley, 2009). These aggregates

can sequester proteins including those that have normal functions in the cells. This may suggest that aggregation of proteins disrupts cellular function by removing one or several vital cellular proteins. Additionally, the presence of huntingtin aggregates might inhibit the ubiquitin proteasome system (UPS) which is the primary cellular proteolytic pathway that normally manages protein misfolding. Ubiquitin is involved in both the normal non-lysosomal degregading pathway (Ciechanover, 1994) and the UPS is responsible for the turnover of most proteins within cells. This provides an important role in degrading key short-lived regulatory proteins (Hershko and Ciechanover, 1998). One theory regarding the pathogenic properties of the mutant protein is that the expanded CAG sequence causes the mutated protein to misfold and recruits some protein components of the UPS (Davies et al., 1997; DiFiglia et al., 1997; Kopito, 2000). The inhibition of ubiquitin could cause an aberrant accumulation of other proteins that would normally digested by the proteolytic pathway as part of normal protein turnover (Bence et al., 2001). Molecular chaperones mediate protein folding and assure that proteins retain their native conformations (Hartl and Hayer-Hartl, 2002). They are also responsible for the translocation of many proteins across cellular membrane and promote the transfer of misfolded proteins to the proteasome for degradation (Muchowski, 2002). It has been reported that the presence of molecular chaperones and components of the UPS are also a common feature in other neurodegenerative diseases (Clark and Muchowski, 2000) including HD, which supports the idea that impairment of the UPS may play a key role in neurodegenerative diseases. In addition to UPS, it has been suggested that the autophagy-lysosomal degradation pathway is impaired in HD (Martinez-Vicente et al., 2010; Pandey et al., 2007; Ravikumar et al., 2004). Another theory has suggested that misfolded proteins initiate a protective stress response which is also called the unfolded-protein response (UPR) in the endoplasmic reticulum. This may postpone a cellular disaster for a while, but will not last long and eventually cause activation of a suicide pathway (Bredesen et al., 2006).

Recently, nuclear pore complexes have been shown to deteriorate with age. This process leads to an increased nuclear permeability and causes a leakage of cytoplasmic proteins into the nucleus in old neurons. The same study has also revealed that cytoplasmic proteins such as intranuclear tubulin aggregates into large filamentous structures which cause severe morphological chromatin abnormalities (D'Angelo et al., 2009). Moreover, the Tpr protein, which is responsible for exporting molecules from the nucleus and localized at intra-nuclear side of nuclear pore complex, has been shown to be involved in the nuclear localization of small N-terminal huntingtin, and the polyQ domain does not interact with this protein. A faulty nuclear export of N-terminal huntingtin might be important for nuclear pathology (Cornett et al., 2005).

However several general mechanisms of pathology have been suggested for HD, including excitotoxiticity, DA toxicity, metabolic impairment, mitochondrial dysfunction, oxidative stress, apoptosis and autophagy alongside NIIs. These mechanisms develop slowly over time and appear prominent at late stage of the disease (Gil and Rego, 2008). Mutant huntingtin may also cause neurons to be dysfunctional by a variety of pathogenic mechanisms such as abnormal energy metabolism (Seong et al., 2005), decreased mitochondrial calcium buffering capacity (Panov et al., 2002), and impaired gene transcription (Cha et al., 1998). These factors may initiate the cell death of neurons in HD single-handedly or in cooperation (Guidetti et al., 2006). For example, mutant huntingtin can lead to abnormal protein-protein interactions with other nuclear proteins such as pro-apoptotic transcription factor p53 and directly interact with several transcription factors such as TATA-binding protein (TBP) (Schaffar et al., 2004), cAMP-responsive element- binding protein (CREB) (Steffan et al., 2000), specific protein -1 and the TBP-associated factor ($TAF_{II}130$) (Dunah et al., 2002). This process results in recruiting these proteins into the aggregates and inhibiting their transcriptional activity (Gil and Rego, 2008). Furthermore, several studies suggest that mutant huntingtin can influence synaptic dysfunction by

interfering in a variety of synaptic proteins and their receptors (Gil and Rego, 2008; Li et al., 2003).

1.3.2.2. Role of NIIs

Intra-nuclear inclusions are formed by the misfolding of mutant huntingtin and are a pathological marker of the disease both in mice and humans (Davies et al., 1997; DiFiglia et al., 1997). Two types of inclusion body formation have been proposed. Firstly, protein aggregation directly deposits a single or limited number of inclusions and, secondly, proteins are merged from individual aggregates into a single or number of inclusions (Kopito, 2000). Roizen and co-workers originally observed them as fibrillar and filamentous dense structures in biopsy samples of human patients, by electron microscopy (Roizin et al., 1979). Later on, they were discovered in a transgenic mouse model of HD (Davies et al., 1997) and then in humans (DiFiglia et al., 1997). After the discovery of NIIs in both HD patients and mouse models, they became a focus for many research groups who are investigating the NII formation in HD pathology. The data from *in vivo* and *in vitro* studies suggest that there are three possible scenarios for the role of NIIs in CAG/polyglutamine repeated diseases. Firstly, NIIs are toxic to cells and initiate the pathology (Ross, 1997; Ross et al., 1997; Rubinsztein et al., 1999; Rubinsztein, 2006). Secondly, they protect the cell from toxic proteins (Arrasate et al., 2004; Ravikumar et al., 2004; Saudou et al., 1998). Thirdly, they are side products and have no function in cell death (Sisodia, 1998).

There are several possible mechanisms that have been proposed for the mechanism of action of mutant huntingtin in neuronal cell death. It has been suggested that mutant huntingtin abnormally binds to interacting proteins which may lead to new protein interactions and subsequently disrupt the normal function of the huntingtin protein causing cell death (Li et al., 2003). Recent evidence suggests that diffuse huntingtin aggregates dysregulate cell machinery before they become insoluble NIIs (Bennett et al., 2007; Landles et al., 2010). Some studies have also suggested that the

soluble forms of huntingtin, such as monomers and oligomers, might be toxic (Menalled et al., 2003; Van Raamsdonk et al., 2005a) and the toxicity is induced by aggregates (Waelter et al., 2001). It has been reported that mutant huntingtin aggregates impair mitochondrial motility and trafficking in striatal neurons more than in cortical neurons, therefore producing selective neurodegeneration (Chang et al., 2006). When the effects of aggregate localization in both polyglutamine peptides of Q20 and Q42 were compared, it was found that the fibrillar forms of neither polyglutamine peptides is toxic to the cytoplasm, but, they both lead to cell death when they are directed in the nucleus (Chen et al., 2001; Chen and Wetzel, 2001; Yang et al., 2002). Similarly, inhibition of aggregate formation with Congo red treatment in a transgenic mouse model of HD exerted beneficial effects on survival, weight loss and motor function (Sanchez et al., 2003). However, an indepented study replicating this research has shown that Congo red treatment failed to ameliorate motor and cognitive functions (Wood et al., 2007). Therefore, it has been suggested that early nuclear localization of mutant huntingtin may be a key pathogenic event in HD (Van Raamsdonk et al., 2005a; Wheeler et al., 2000).

Although these studies have suggested that NIIs might be toxic, some studies have proposed that NIIs may not be the cause of cell death *per se,* but rather they recruit other cell proteins to initiate a neuroprotective mechanism (Arrasate et al., 2004; Saudou et al., 1998). For example, in cell models, transgenic mice and human brain, mammalian target of rapamycin (mTOR) was sequestered in aggregates. Inhibition of mTOR protects cells by induced autophagy, a principal clearance pathway for mutant huntingtin and reduces huntingtin accumulation (Ravikumar et al., 2004), suggesting that NIIs might be neuroprotective. Saudou and colleagues indicated that mutant huntingtin acts in the nucleus to induce neurodegeneration by an apoptotic mechanism that is cell specific. However, they have also shown that nuclear aggregates are not sufficient to initiate neurodegeneration and are not correlated with huntingtin–induced apoptosis. Unknown mechanisms and/or pathways trigger apoptosis in these cells (Saudou et al., 1998). Likewise, it

has been shown that the neurons that contained NIIs had an improved survival compared to those that did not (Arrasate et al., 2004).

CAG repeat length has also been associated with inclusion formation (Becher et al., 1998; Martindale et al., 1998) and the rate of cortical atrophy (Halliday et al., 1998). It has been observed that a 36 CAG repeat may result in NIIs to a variable degree, as shown in HD brain tissues (Gomez-Tortosa et al., 2001), however 39 or above always causes NIIs (DiFiglia et al., 1997; Gomez-Tortosa et al., 2001; Gourfinkel-An et al., 1998; Gutekunst et al., 1999; Maat-Schieman et al., 2007). Based on these correlations between CAG repeat length, inclusion formation and toxicity, it has been suggested that inclusion formation can mediate neurodegeneration in HD (Legleiter et al., 2009). There is variability in the distribution and areas of NIIs in post mortem brains of HD between different laboratories. However all agree that the cortex contains pronounced NIIs. Table 1 summarises the distribution and areas of NIIs in various human studies undertaken on post-mortem tissues.

Table 1. The deposition of inclusions in post mortem human studies

NIIs in human HD	Difigia et al., 1997	Sapp et al., 1997	Gourfinkel-An et al., 1998	Maat- Schierman et al., 1999	Gutekunst et al., 1999
Antibody	Ab 1 (both wt-htt and mhtt) and ubiquitin	Ab585 (both wt-htt and mhtt)	Ubiquitin and 1C2	Ubiquitin	EM48
Patients	6 adult onset HD (Grade 2-3) 3 Juvenile (Grade 3-4)	12 adult onset HD (Grade 1-4) 3 Juvenile	5 adult onset HD (Grade 2-3)	5 adult onset HD (Grade 3-4) 2 Juvenile	12 adult onset HD (Grade 1-4)
Most abundant	Present all layers of cortex (3-6 % of total neuron) More frequent in juveniles (38-52%)	Robust staining the cortex	Most abundant in cerebral cortex (all layers) and the striatum	Most abundant in the neocortex	Most abundant in the cortex (More frequent layer V and VI, differences between cortical areas within individual HD brains)
Less abundant	Less abundant in the striatum	Reduced labelling in medial and dorsal regions of the striatum and in the globus pallidus (G:1-3)	Less abundant in pallidum, thalamus and subthamus	Hippocampus	Less abundant in caudate, putamen, substantia nigra, hypotalamic nuclei, thalamus and brain stem
Rare	Not reported	Not reported	Extremely rare in the ventral striatum	Rare in the neotriatum	Rare in the globus pallidus, hippocampus and cerebellum
Absent	Absent in the globus pallidus and cerebellum	Not reported	Absent in the cerebellum	Absent in the cerebellum Substantia nigra and pallidum	

It has been revealed that there is a close relationship between neuronal degeneration and the existence of neuronal inclusions. Even short CAG repeat expansions are associated with NIIs in HD patients (Gourfinkel-An et al., 1998).

In post-mortem brains of HD patients, the cortex is more intensely stained for NIIs than the striatum. In the study by DiFiglia and co-workers (1997), it was found that the position of NIIs is variable throughout the nucleus of cells. Intra-nuclear inclusions are larger than the nucleolus and of different shapes: 55% globular, 30% ovoid and 15% elliptical. Most neurons usually contain one NII, however, 5-7% of labelled neurons contain two or three NIIs per neuron. Intra-nuclear inclusions are present in all layers of the cortex and are more frequent in juvenile patients than adult onset patients. Intra-nuclear inclusions are also present in MSNs in the striatum. However, NIIs are absent in the globus pallidus and cerebellum. ENNIs were mainly present in 5^{th} and 6^{th} layers of the cortex, where they satained densely, and had morphology consistent with localisation in dystrophic neurites. However, their distribution was uneven. ENNIs were more common in adult onset patients than juvenile onset patients. While, NIIs are not detected in the presymptomatic patient, ENNIs are observed in layer 6 of the cortex of the same presymptomatic patient (DiFiglia et al., 1997; Gourfinkel-An et al., 1998; Gutekunst et al., 1999).

It has been reported that Grade 0 patients do not contain cortical inclusions. However it is important to note that Grade 0 patients, effectively by definition, do not show HD pathology (Maat-Schieman et al., 2007). Inclusions are found in the cortex of HD brains while many medium spiny neurons lack inclusions despite the presence of neuronal loss (Gutekunst et al., 1999). There is some variability between human studies, for example, in another study (Sapp et al., 1997), the medial and dorsal regions of the striatum showed reduced mutant huntingtin staining, whereas the cortex exhibited robust staining. A reduced mutant huntingtin staining was also observed in the globus pallidus of adult onset HD. Interestingly, Grade 1 patients contain pronounced nuclear staining of neuronal nuclei and an increased axonal staining in the cortex of both adult and juvenile onset HD patients (Sapp et al.,

1997). Due to the presence of NIIs in symptomatic patients and the absence of presymptomatic patients, it has been suggested that inclusions develop before neurological symptoms (Davies et al., 1998).

1.4. Animal Models of Huntington's disease

Experimental animal models of HD have been sought to replicate the degeneration seen in the human disease. None of these models exactly mimics the human disease, but, they do permit the study of the disease processes in relative detail and have helped to develop and improve new strategies for therapies. The first animal models were generated using excitotoxic lesions, by either central or systemic administration of excitotoxins and metabolic toxins. Subsequently transgenic and knock-in (KI) mouse lines expressing HD have been successfully developed, following the identification of the HD gene. These models differ in the promoter used, the length of the huntingtin protein, and the length of CAG repeats (Gray et al., 2008; Hodgson et al., 1999; Lin et al., 2001; Lloret et al., 2006; Mangiarini et al., 1996; Reddy et al., 1998; Schilling et al., 1999; Slow et al., 2003; White et al., 1997).

1.4.1. Excitotoxic lesions

Until the discovery of the Huntingtin gene in 1993, excitotoxic lesion models were the most widely studied models of the disease. These models involve the injection of excitotoxins (kainic acid, ibotenic acid or quinolinic acid) into the striatum of experimental animals to induce a pattern of cell loss that resembles the pathology of HD. The first excitotoxic model was the injection of kainic acid into the striatum of the rat which caused clear neuronal loss (Coyle and Schwarcz, 1976). It was subsequently identified that kainic acid caused remote damage and epileptic side-effects and was replaced, initially, by ibotenic acid, and then quinolinic acid, both of which offer a more selective striatal cell loss that more closely resembles the neuropathologic and neurochemical characteristics of HD (Dunnett and Rosser, 2004; Mason et al., 1978; Schwarcz et al., 1983). More recently, 3-nitropropionic acid (3-NP) lesions have been proposed as an alternative HD model due to their

histological and pathological similarities with human HD (Wang and Qin, 2006). The mechanism of action of 3-NP differs from excitotoxic lesions in that 3-NP irreversibly disrupts mitochondrial energy metabolism, leading to very selective striatal degeneration and functional deficits such as hyperactivity (seen in early HD) or hypoactvity (seen in late HD) (Borlongan et al., 1997). 3-NP has the added facility that it causes selective striatal degeneration even after peripheral administration, but suffers from a considerable variability in toxicity from animal to animal that makes designed experiments difficult to execute. Although requiring central administration, the excitotoxic lesion models have proved more reliable, and reproduce similar patterns of striatal cell loss as well as many motor and cognitive symptoms of HD. Consequently they are useful for studying mechanisms to repair the damage caused by HD and replace the lost cells. However, excitoxically-lesioned rats fail to display specific chorea- like movements (Wang and Qin, 2006) and cannot clarify the underlying molecular mechanisms of pathogenesis in human HD, which is of its very essence a genetically defined disease.

1.4.2. Genetic models

Genetically modified models of HD have been developed in different species: *Drosophila melanogaster* (Warrick et al., 1998), *Caenorhabditis elegans* (Faber et al., 2002), zebrafish (Schiffer et al., 2007), non-human primates (Yang et al., 2008), pig (Matsuyama et al., 2000) and rodents (Lin et al., 2001; Mangiarini et al., 1996; Menalled et al., 2002; Menalled et al., 2003; Schilling et al., 1999; Slow et al., 2003; Slow et al., 2005; Von Horsten et al., 2003; Wheeler et al., 2000). Of these, rodent models have proved to be the most widespread and flexible, incorporating the complexity of the mammalian brain necessary to make them suitable for behavioural studies, cell replacement and drug development strategies. These models have different CAG repeat lengths and different expression levels of mutant huntingtin protein. The inserted mutant allele is either truncated or full length.

Ideally, an animal model should mimic key features of HD, including adult onset; progressive motor and cognitive impairments; cell loss in the

striatum and cortex; and expression, distribution and progression of aggregates/inclusions. Today, no animal models of HD can replicate precisely all the features of HD; however rodent models maintain their importance, because they are key tools to provide valuable sources of data for discovering the pathology of HD and allowing new potential therapeutic targets for clinical treatments. The selection of animal model depends on the type of experiment planned. For instance, R6 mouse lines progress rapidly and better represents juvenile-onset form of HD as such they are more useful for the therapeutic approach (Mangiarini et al., 1996). On the other hand, cognitive and behaviour experiments need a longer life span to allow for extended training, and relativelyselective fronto-striatal pathology to match the cognitive symptoms observed in patients, and for these studies knock-in models have been found to be more suitable. A multiplicity of genetic models of HD is now proving to offer useful tools for the study both of disease pathology and the elaboration of novel therapeutic strategies.

1.4.2.1. Knock-out models

Studies into the geraneration of knock-out HD mouse models showed that null mutants did not survive and suffered early embryonic lethality at around embryonic days (E)7.5 (Duyao et al., 1995; Nasir et al., 1995; Zeitlin et al., 1995). This finding showed that huntingtin is essential for embryonic development and made this model unsuitable for further studies. However, heterozygous litters for this mutation completed the major events of gastrulation and they have demonstrated motor and cognitive impairments with reductions of neurons in the subthalamic nucleus (Nasir et al., 1995).

1.4.2.2. Transgenic models

Transgenic models contain either a fragment of, or the full-length human gene with an expanded CAG repeat region which is randomly inserted into the rodent genome under the control of a promoter. The R6 mouse line was the first transgenic model of HD (Mangiarini et al., 1996). The R6/1 and the R6/2 mice express the N- terminal fraction of the human HD gene

containing a highly expanded ~116 and ~150 CAG repeats, respectively. The R6/2 transgenic model has been one of the most widely used models of HD, because R6 mice show a progressive phenotype which includes motor impairments (such as tremor, shuddering, stereotypic movements) and cognitive abnormalities (Carter et al., 1999; Lione et al., 1999; Mangiarini et al., 1996). Their characteristic features have been well documented. R6/2 mice first display symptoms at 5-6 weeks of age, with death occurring at about 12-15 week (Mangiarini et al., 1996). Neuronal loss and reduced brain volume have been observed at very late stage of the disease in these mice (Stack et al., 2005). Aggregates were initially reported in the cortex and striatum of R6/2 mice at 3.5 and 4.5 months of age, respectively (Davies et al., 1997). However, another study has reported that the appearance of intra-nuclear inclusions in R6/2 transgenic mice is present as early as postnatal day (P) 1 (Stack et al., 2005) and demonstrated that both numbers and size of intra-nuclear inclusions increases with the disease progression (Li et al., 1999; Stack et al., 2005). It has recently been shown that the different CAG repeat size alters the onset of appearance of NIIs in the R6/2 transgenic mice, with mice containing shorter repeat lengths exhibiting NIIs earlier than mice with longer repeat lengths (Morton et al., 2009).

In R6/1 mice, the earliest motor deficit with hyperactivity occurs at 4 weeks of age (Bolivar et al., 2004) and as the diseases progresses, motor deficits become apparent with foot clasping at 14 weeks of age (Naver et al., 2003). Cognitive (Hodges et al., 2008) and behavioural (Naver et al., 2003) deficits are present at 15 weeks of age and by 22 weeks of age, a decrease in body weight has been observed (Naver et al., 2003). A decrease in striatal volume is evident by approximately 20 weeks of age (Mangiarini et al., 1996; van Dellen et al., 2000). Impairment of hippocampal neurons has also been observed (Grote et al., 2005; Lazic et al., 2006). It has been suggested that R6/1 mice have deficits in short-term hippocampal-dependent memory prior to the onset of motor symptoms (Nithianantharajah et al., 2008). The degree of motor impairment is associated with the number of striatal neurons containing NIIs (Hansson et al., 2001). There is variability between studies showing the presence of NIIs. For example, NIIs have been reported in the hippocampus at 4 weeks of age (Milnerwood et al., 2006), whereas, another study failed to

show the appearance of NIIs in the hippocampus at early age (van der and Brundin, 2007). It has been reported that the reduced BDNF expression levels enhance the number of aggregates in the R6/1 mouse (Pineda et al., 2005). There is also conflicting literature on the effects of the environmental enrichment on this model. Van Dellen and co-workers have reported that the environmental enrichment delays onset of motor deficits but does not alter protein aggregate density in R6/1 mice (van Dellen et al., 2008). However, a more recent study has shown that the environmental enrichment has an effect on decreasing aggregate formation in this mouse line (Benn et al., 2010).

Another mouse model is the N-171-82Q mouse which has a longer N-terminal fragment of huntingtin (exon 1 and exon 2) with 82 CAG repeats. This model displays less severe behavioural phenotype than that of R6/2 mice. It has been observed NIIs are more prominent in the cortex than in the striatum with widespread in other regions of the brain including hippocampus and cerebellum (Schilling et al., 1999).

Another transgenic mouse model is the yeast artificial chromosome (YAC) mouse model which contains the full length human HD gene, including the entire regulatory element (Hodgson et al., 1999; Slow et al., 2003). The YAC128 mouse contains the full length human HD gene and has been characterized by Slow and colleagues in 2003 (Slow et al., 2003; Van Raamsdonk et al., 2005a). Motor and behavioural abnormalities arise at 3 months of age with increased activity in the open field test, followed decreased performance on the rotorod at 6 months. Yet, by 12 months of age the open field activity declined in transgenic animals in comparison to their wildtype litter mates. Cognitive deficit has been reported on the simple swimming test at 8 months of age. Minor striatal atrophy was present at 9 months of age, and by 12 months of age cortical atrophy was detected with striatal atrophy. NIIs were not observed until 18 months of age, but, high nuclear immunoreactivity was seen from 2 months onwards in the striatum. No changes have been observed in hippocampal volume (Van Raamsdonk et al., 2005b). Interestingly, a recent study showed a decline in hippocampal cell proliferation (Simpson et al., 2010). Similar results were observed in the R6/2 transgenic mice (Gil et al., 2005) suggesting hippocampal dysfunction in R6/2

mouse model (Murphy et al., 2000). It has been suggested that in transgenic mouse models, onset of the symptoms is associated with synaptic and neuronal dysfunction and then neuronal death occurs (Turmaine et al., 2000; van Dellen et al., 2005).

In addition, a conditional HD mouse model in which the mutant huntingtin gene can be switched off has been also generated. The mice expressing mutant huntingtin protein, “gene on” demonstrated NIIs with motor impairments. However, blockade of expression in these mice caused a disappearance of NIIs with improved behavioural phenotype (Yamamoto et al., 2000).Figure 4 summarises the other transgenic models of HD.

1.4.2.3 Knock-in models

Knock-in HD mouse models are created by inserting a linearized targeting vector into their own murine huntingtin gene (*Htt*) which is the homologue of human *HTT*. Therefore, they are the most faithful genetic replication of human HD. These mice can be homozygous or heterozygous for the mutation and have been less studied than transgenics. They contain different CAG repeats. For example, $Hdh^{(CAG)Q150}$ mice contains approximately 150 CAG repeats and show motor deficit with hyperactivity and clasping at 3 months of age (Lin et al., 2001). Cognitive impairment became prominent on a set shifting task at 6 months of age (Brooks et al., 2006) and with age increases, mice show behavioural impairment at 15 months of age. Aggregates are first observed in the striatum at 6 months of age (Tallaksen-Greene et al., 2005; Woodman et al., 2007). Other knock-in mouse models are Hdh^{Q92} and Hdh^{Q111} mouse models. They contain ~ 90 and 109 CAG repeats, respectively (Wheeler et al., 2000). Hdh^{Q92} mice exhibit cognitive deficit at 4 months of age (Trueman et al., 2007), behavioural and motor deficit become apparent with age (Trueman et al., 2009). Aggregates were observed at 1.5 months of age (Wheeler et al., 2000). Some of the most common knock-in models are summarised in figure 5.

Initially, knock-in models were not reported to exhibit obvious neurological symptoms and early motor abnormalities (Petersen et al., 1999;

Shelbourne et al., 1999; Wang and Qin, 2006; Wheeler et al., 2000). However, more recent studies show that with more sensitive behavioural analysis, most knock-in models do display neurological symptoms and early behavioural abnormalities (Brooks et al., 2010b; Brooks et al., 2010c; Brooks et al., 2006; Hickey et al., 2008; Lin et al., 2001; Menalled et al., 2002; Menalled et al., 2003; Trueman et al., 2007; Trueman et al., 2008). Similarly, in early studies, it has been observed that aggregates/nuclear inclusions occur in the brains of knock-in mice later than in those of transgenic mice (Levine et al., 1999; Lin et al., 2001; Vonsattel, 2008). However, it has been confirmed that the appearance of the aggregates in most knock-in models occurs at a relatively early stage (Menalled et al., 2003; Tallaksen-Greene et al., 2005; Wheeler et al., 2000; Woodman et al., 2007).

Figure 4. Transgenic models of HD. Frist appereance of Aggregates/inclutions, behavioral, cognitive and motor symotoms of age. Left column illustrates the genetic construct used to generate the transgenic model, indicates survival and emergence of phenotypes in weeks and months. Right column represents % of a life span.

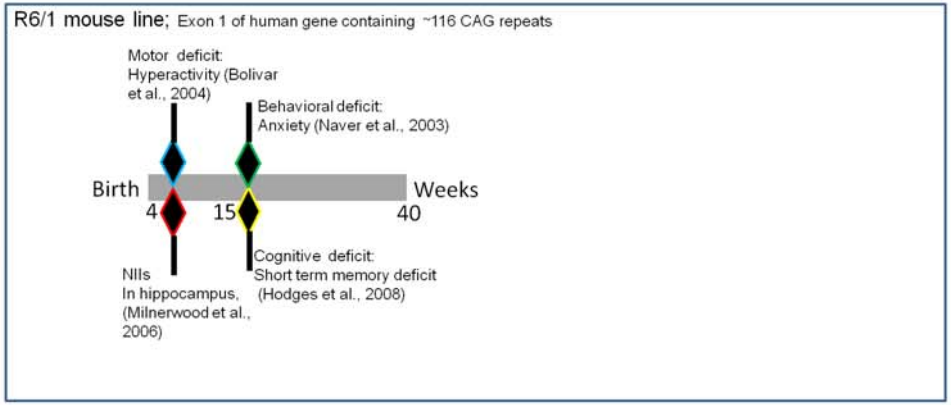

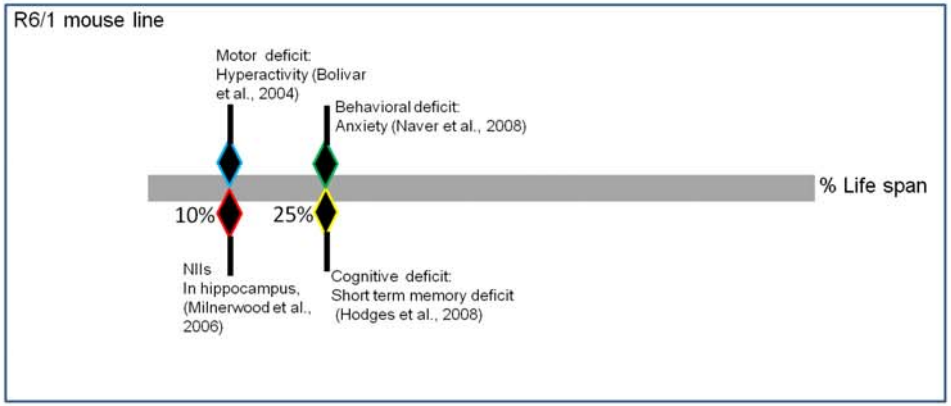

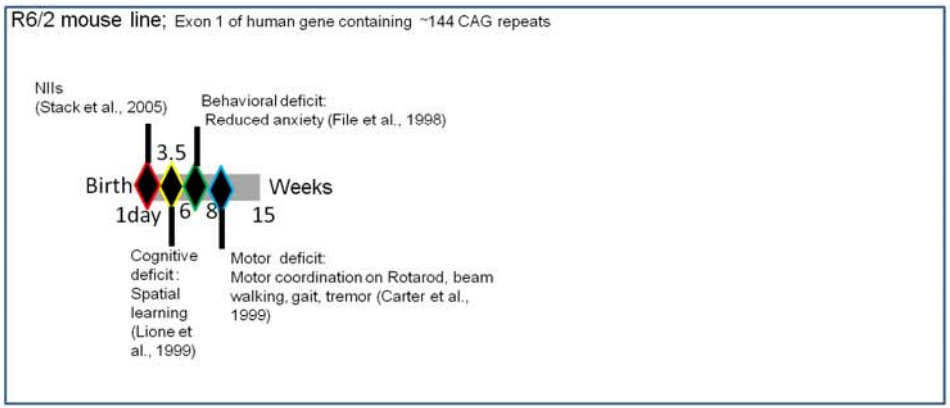

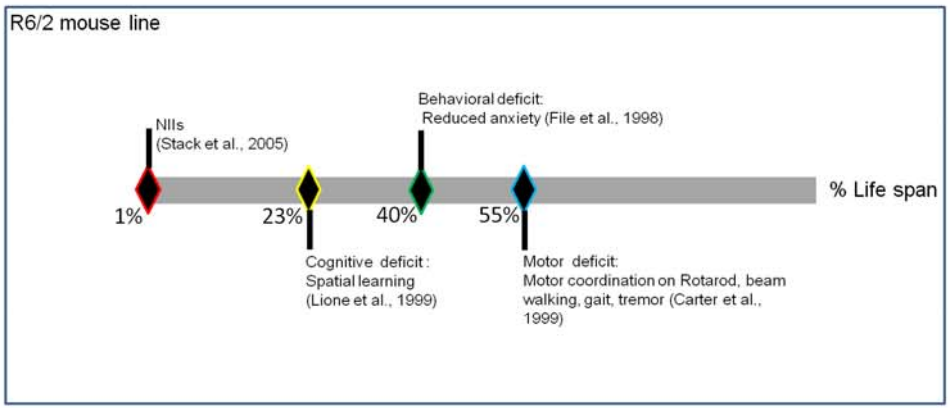

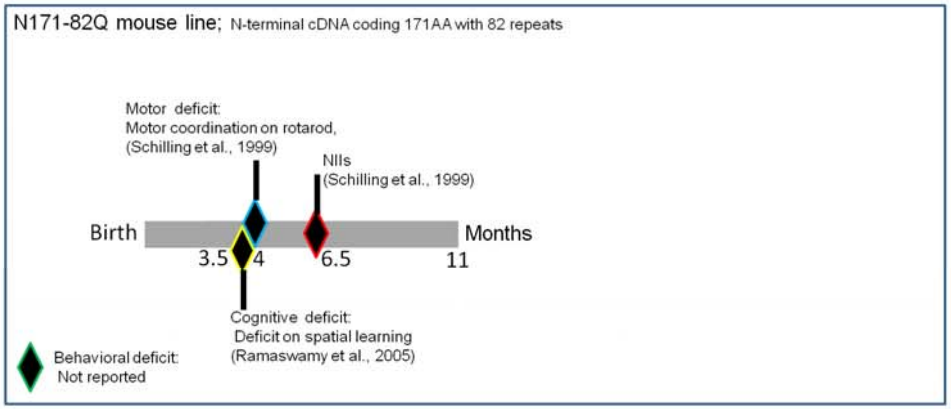

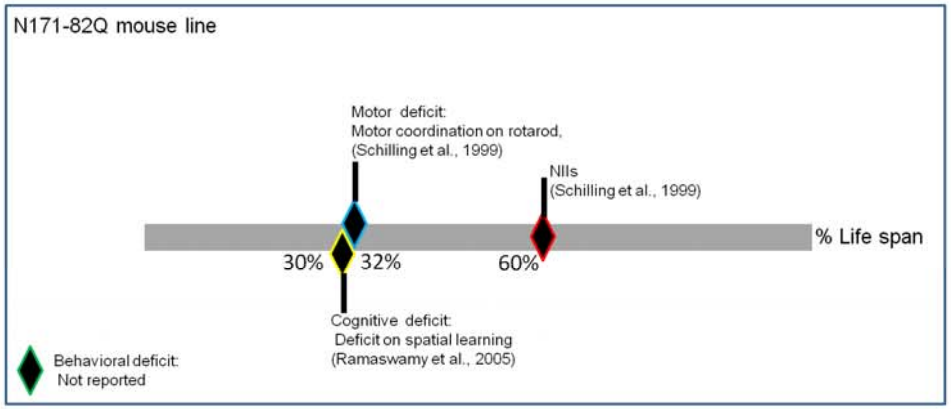

YAC128 mouse line; Yeast artificial chromosome expressing entire human protein with 128 repeats

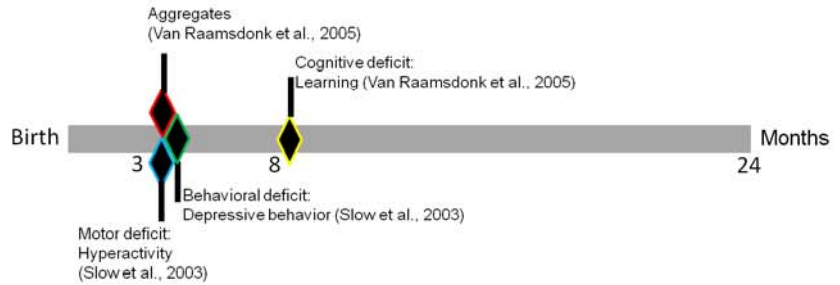

YAC128 mouse line

YAC72 mouse line; Yeast artificial chromosome expressing entire human protein with 72 repeats

YAC72 mouse line

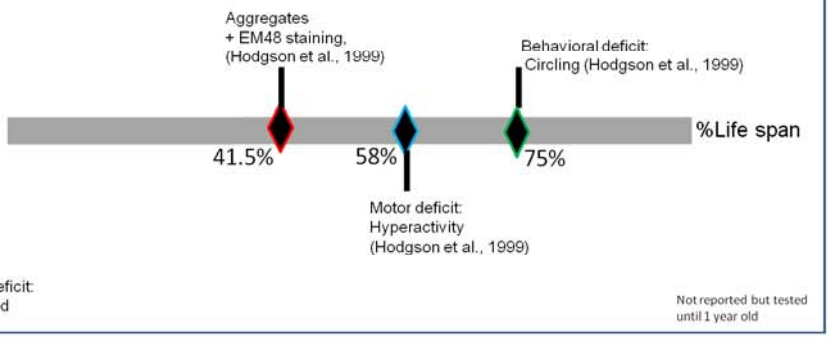

Shortstop mouse line; Yeast artificial chromosome expressing exon 1 and 2 with 120 repeats

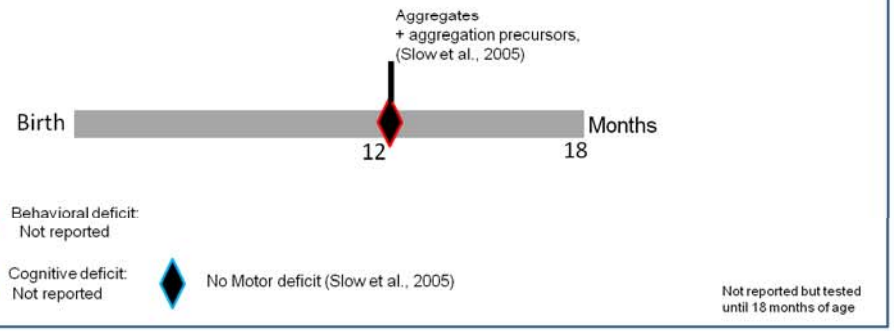

Shortstop mouse line

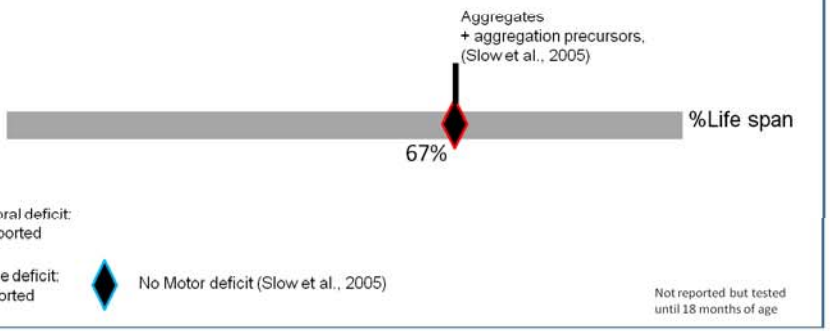

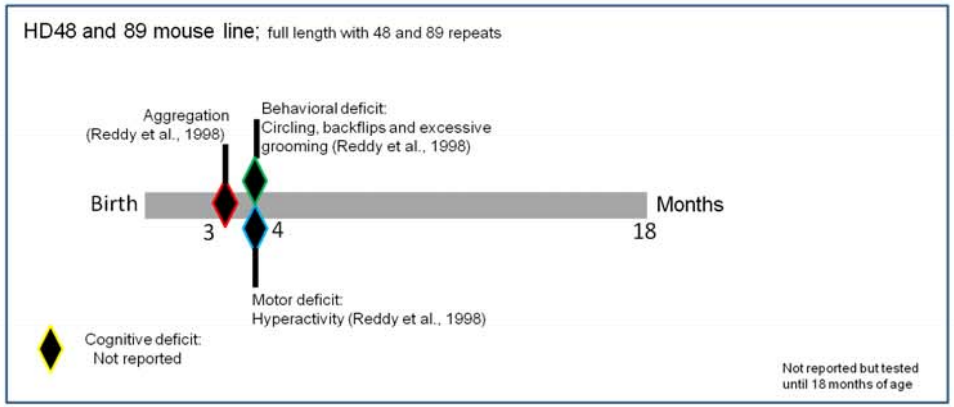
HD48 and 89 mouse line; full length with 48 and 89 repeats
Aggregation
(Reddy et al., 1998)
Behavioral deficit:
Circling, backflips and excessive
grooming (Reddy et al., 1998)
Birth
Months
3
4
18
Motor deficit:
Hyperactivity (Reddy et al., 1998)
Cognitive deficit:
Not reported
Not reported but tested
until 18 months of age

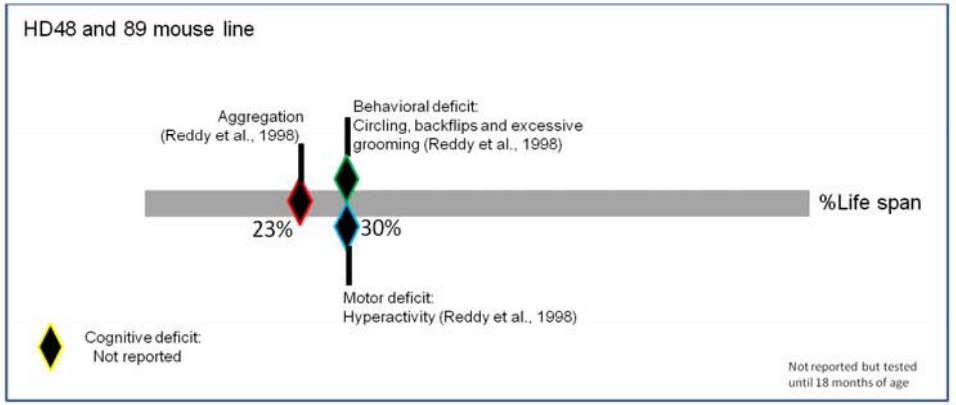
HD48 and 89 mouse line
Aggregation
(Reddy et al., 1998)
Behavioral deficit:
Circling, backflips and excessive
grooming (Reddy et al., 1998)
%Life span
23%
30%
Motor deficit:
Hyperactivity (Reddy et al., 1998)
Cognitive deficit:
Not reported
Not reported but tested
until 18 months of age

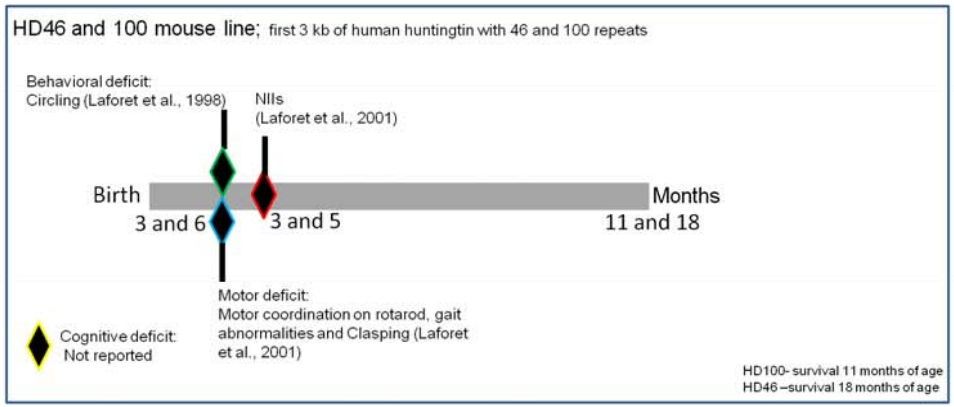
HD46 and 100 mouse line; first 3 kb of human huntingtin with 46 and 100 repeats
Behavioral deficit:
Circling (Laforet et al., 1998)
NIIs
(Laforet et al., 2001)
Birth
Months
3 and 6
3 and 5
11 and 18
Motor deficit:
Motor coordination on rotarod, gait
abnormalities and Clasping (Laforet
et al., 2001)
Cognitive deficit:
Not reported
HD100- survival 11 months of age
HD46 –survival 18 months of age

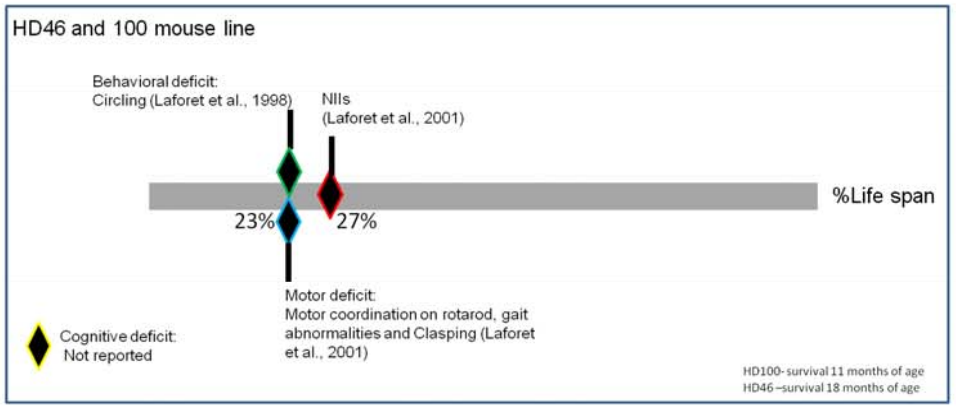
HD46 and 100 mouse line
Behavioral deficit:
Circling (Laforet et al., 1998)
NIIs
(Laforet et al., 2001)
%Life span
23%
27%
Motor deficit:
Motor coordination on rotarod, gait
abnormalities and Clasping (Laforet
et al., 2001)
Cognitive deficit:
Not reported
HD100- survival 11 months of age
HD46 –survival 18 months of age

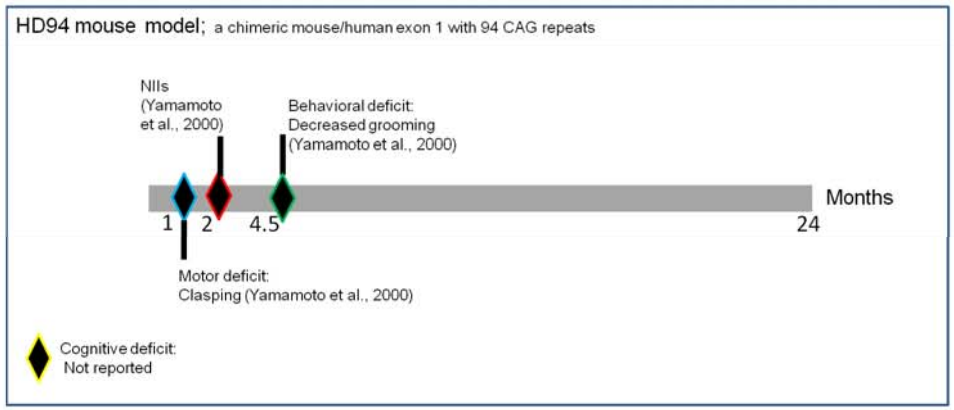
HD94 mouse model; a chimeric mouse/human exon 1 with 94 CAG repeats
NIIs
(Yamamoto
et al., 2000)
Behavioral deficit:
Decreased grooming
(Yamamoto et al., 2000)
Months
1
2
4.5
24
Motor deficit:
Clasping (Yamamoto et al., 2000)
Cognitive deficit:
Not reported

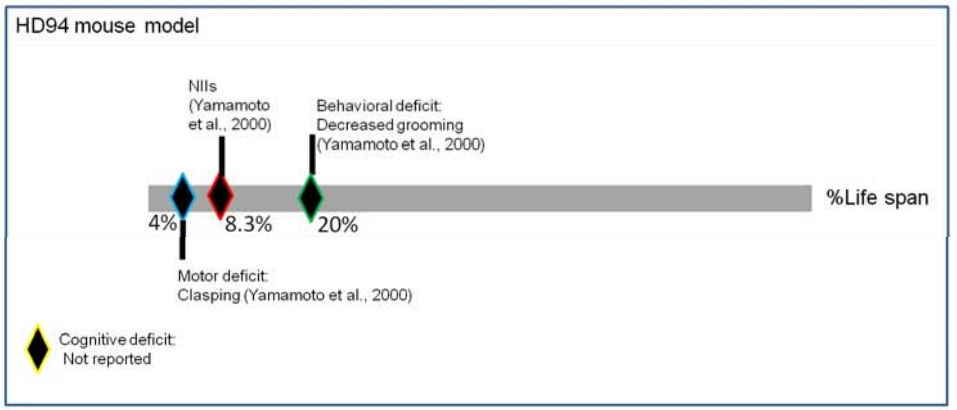
HD94 mouse model
NIIs
(Yamamoto
et al., 2000)
Behavioral deficit:
Decreased grooming
(Yamamoto et al., 2000)
%Life span
4%
8.3%
20%
Motor deficit:
Clasping (Yamamoto et al., 2000)
Cognitive deficit:
Not reported

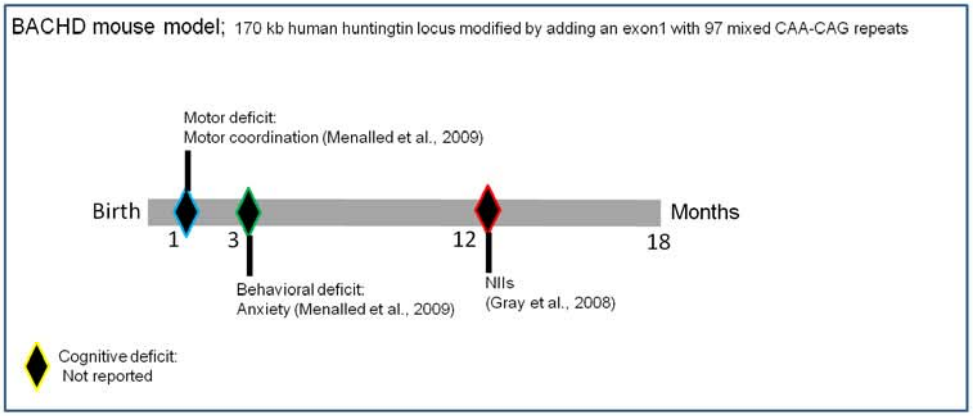
BACHD mouse model; 170 kb human huntingtin locus modified by adding an exon1 with 97 mixed CAA-CAG repeats
Motor deficit:
Motor coordination (Menalled et al., 2009)
Birth
Months
1
3
12
18
Behavioral deficit:
Anxiety (Menalled et al., 2009)
NIIs
(Gray et al., 2008)
Cognitive deficit:
Not reported

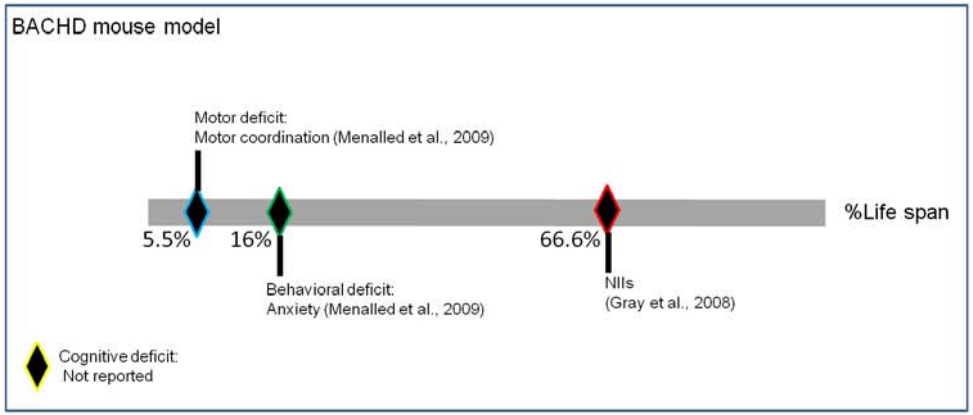
BACHD mouse model
Motor deficit:
Motor coordination (Menalled et al., 2009)
%Life span
5.5%
16%
66.6%
Behavioral deficit:
Anxiety (Menalled et al., 2009)
NIIs
(Gray et al., 2008)
Cognitive deficit:
Not reported

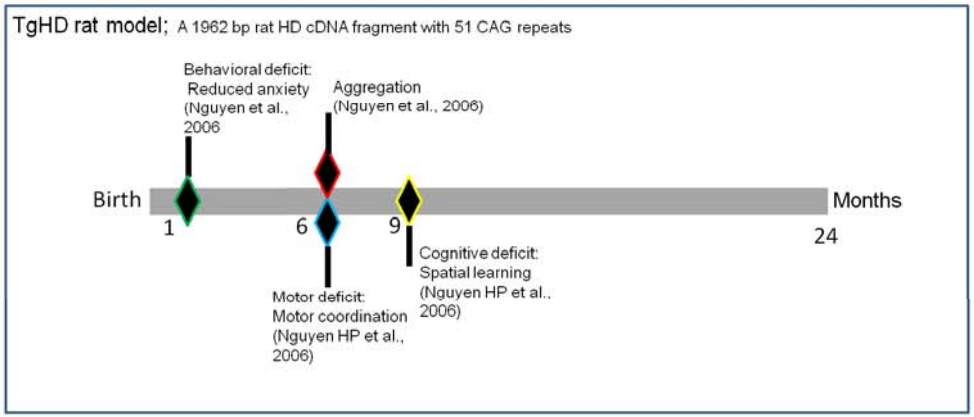
TgHD rat model; A 1962 bp rat HD cDNA fragment with 51 CAG repeats
Behavioral deficit:
Reduced anxiety
(Nguyen et al., 2006
Aggregation
(Nguyen et al., 2006)
Birth
Months
1
6
9
24
Cognitive deficit:
Spatial learning
(Nguyen HP et al., 2006)
Motor deficit:
Motor coordination
(Nguyen HP et al., 2006)

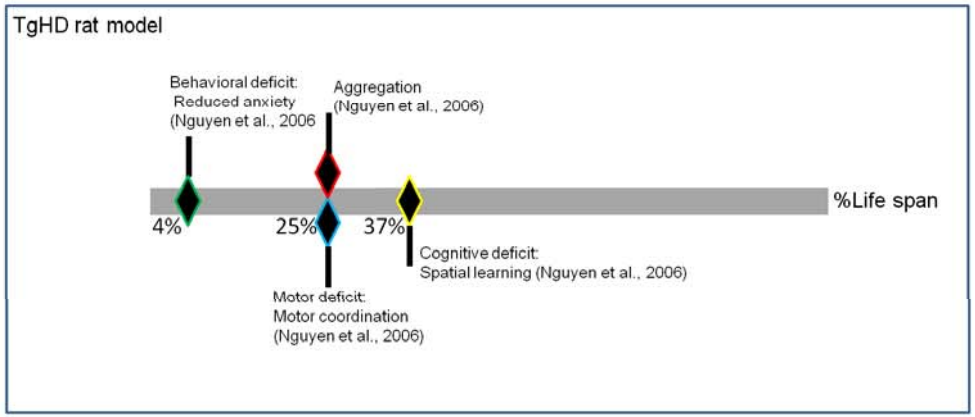
TgHD rat model
Behavioral deficit:
Reduced anxiety
(Nguyen et al., 2006
Aggregation
(Nguyen et al., 2006)
%Life span
4%
25%
37%
Cognitive deficit:
Spatial learning (Nguyen et al., 2006)
Motor deficit:
Motor coordination
(Nguyen et al., 2006)

Figure 5. Knock-in models of HD. Frist appereance of aggregates/inclutions, behavioral, cognitive and motor symotoms of age. Left column illustrates the genetic construct used to generate the knock-in model, indicates survival and emergence of phenotypes in weeks and months. Right column represents % of a life span.

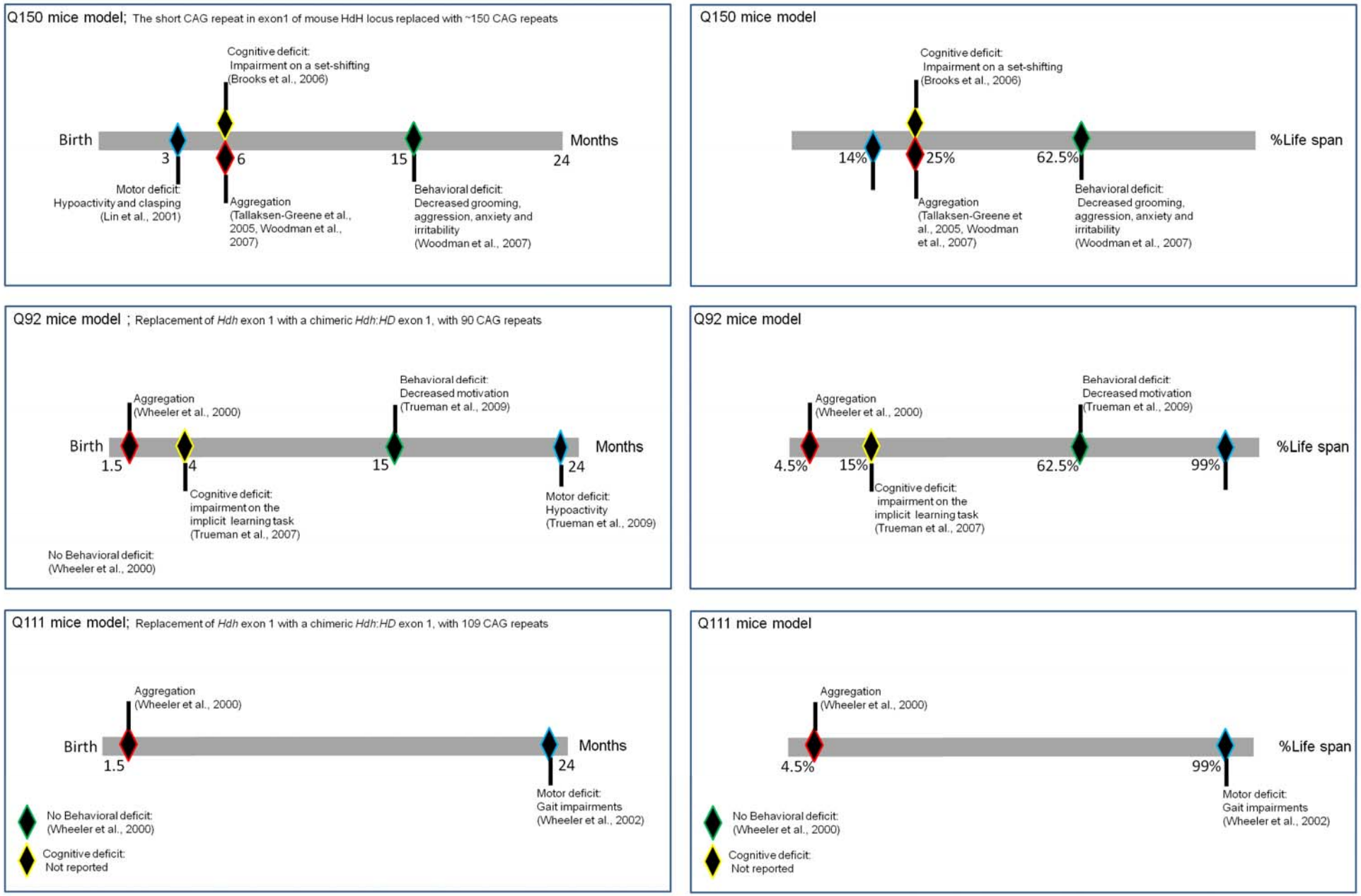

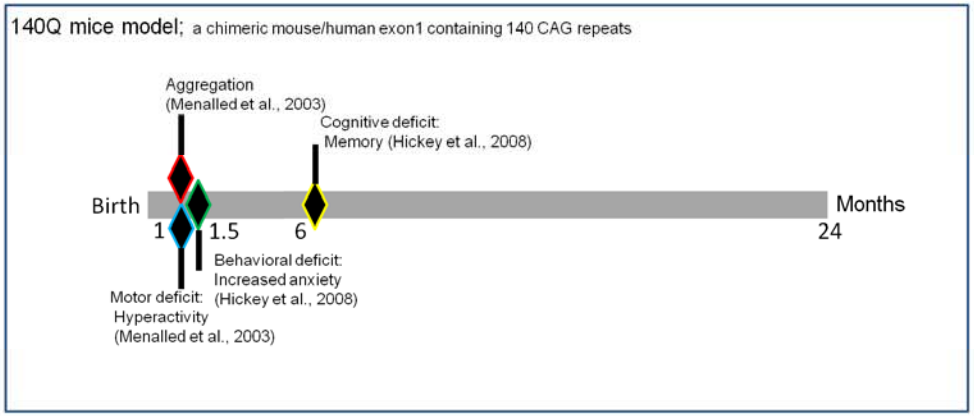
140Q mice model; a chimeric mouse/human exon1 containing 140 CAG repeats
Aggregation
(Menalled et al., 2003)
Cognitive deficit:
Memory (Hickey et al., 2008)
Birth
Months
1
1.5
6
24
Behavioral deficit:
Increased anxiety
(Hickey et al., 2008)
Motor deficit:
Hyperactivity
(Menalled et al., 2003)

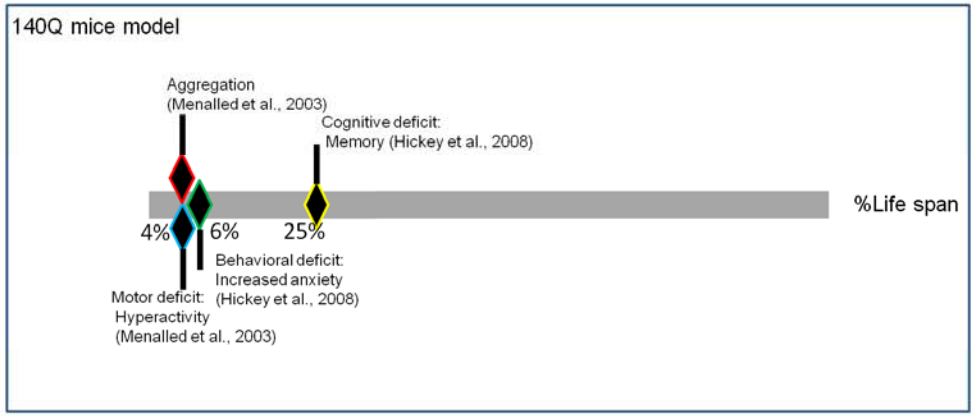
140Q mice model
Aggregation
(Menalled et al., 2003)
Cognitive deficit:
Memory (Hickey et al., 2008)
%Life span
4%
6%
25%
Behavioral deficit:
Increased anxiety
(Hickey et al., 2008)
Motor deficit:
Hyperactivity
(Menalled et al., 2003)

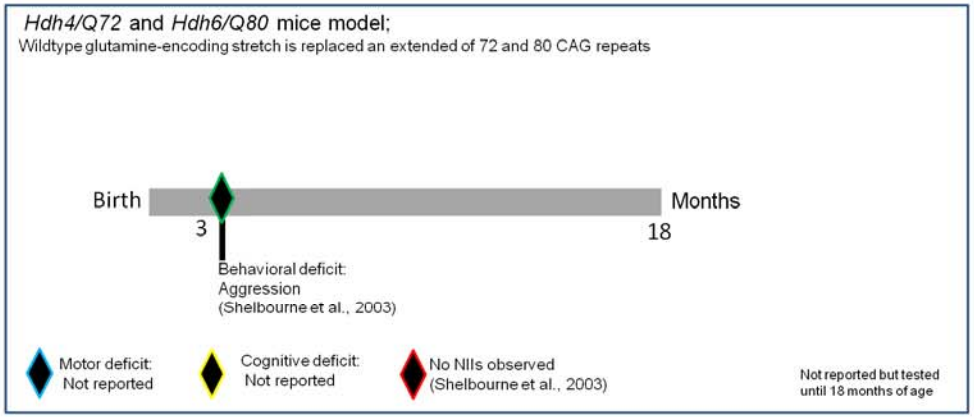
Hdh4/Q72 and Hdh6/Q80 mice model;
Wildtype glutamine-encoding stretch is replaced an extended of 72 and 80 CAG repeats
Birth
Months
3
18
Behavioral deficit:
Aggression
(Shelbourne et al., 2003)
Motor deficit:
Not reported
Cognitive deficit:
Not reported
No NIIs observed
(Shelbourne et al., 2003)
Not reported but tested
until 18 months of age

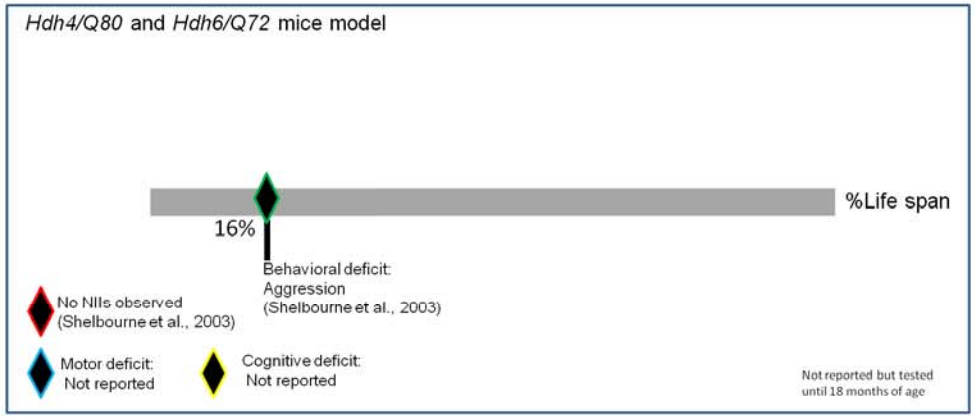
Hdh4/Q80 and Hdh6/Q72 mice model
%Life span
16%
Behavioral deficit:
Aggression
(Shelbourne et al., 2003)
No NIIs observed
(Shelbourne et al., 2003)
Motor deficit:
Not reported
Cognitive deficit:
Not reported
Not reported but tested
until 18 months of age

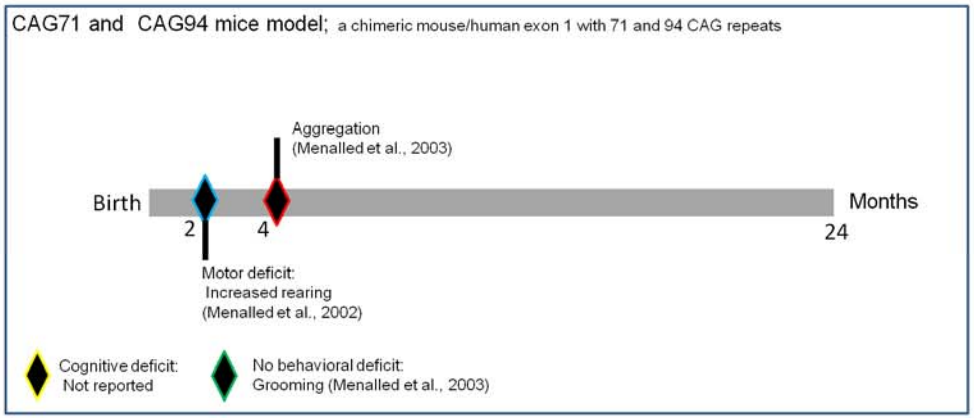
CAG71 and CAG94 mice model; a chimeric mouse/human exon 1 with 71 and 94 CAG repeats
Aggregation
(Menalled et al., 2003)
Birth
Months
2
4
24
Motor deficit:
Increased rearing
(Menalled et al., 2002)
Cognitive deficit:
Not reported
No behavioral deficit:
Grooming (Menalled et al., 2003)

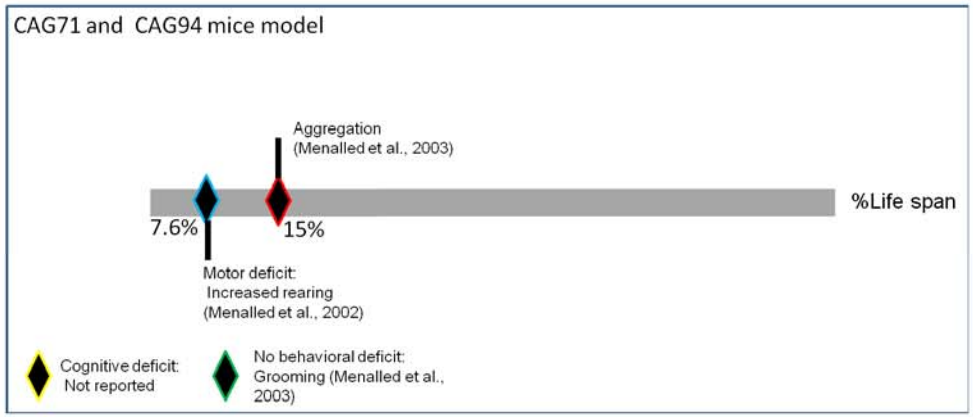
CAG71 and CAG94 mice model
Aggregation
(Menalled et al., 2003)
%Life span
7.6%
15%
Motor deficit:
Increased rearing
(Menalled et al., 2002)
Cognitive deficit:
Not reported
No behavioral deficit:
Grooming (Menalled et al.,
2003)

Recently, it has been proposed that nuclear and cytosolic aggregates have different functions and behave differently (Weiss et al., 2008). An independent study has reported that in R6/2 transgenic mice, there is a progressive appearance of NIIs and ENNIs in striatum, cortex and hippocampus (Morton et al., 2000). Additionally, recently it has been shown that the difference in CAG repeat size alters the onset of appearance of NIIs. it has been shown that mice with shorter repeat length show earlier onset of appearance of NIIs, whereas with longer repeat lengths there is delayed onset of appearance of NIIs (Morton et al., 2009). The cytoplasmic/ENNIs are suggested as possible precursors of intra-nuclear inclusions (Lunkes and Mandel, 1998).

Importantly, astrogliosis is also observed in some knock-in mouse models such as $Hdh^{(CAG)Q150}$, $Hdh^{(CAG)Q200}$ (Heng et al., 2010; Lin et al., 2001) and some transgenic mouse models such as HD89 transgenic mouse line (Reddy et al., 1998) However, it has not been reported in the R6/2 transgenic mice, which have the reduced brain size (Mangiarini et al., 1996). However one recent study has shown that chimeric R6/2 mice which crossed with ROSA26 mice (bear a *lacZ* transgene, used as wildtype) exhibited increased reactive gliosis (Reiner et al., 2007). In addition to astrocytes, microglia abnormalities are also observed in this mouse model (Simmons et al., 2007).

Of the available mouse lines, four lines are of particular interest to us as they are representative of the disease in terms of their functional deficits but have been created with very different genetic constructs. The *Hdh*Q92 mouse line is a targeted insertion of a chimeric human-mouse exon 1with 90 CAG repeats (Wheeler et al., 2000), the *Hdh*Q150 is constructed by insertion of approximately 150 CAG repeats into in exon 1 of the mouse *Htt* locus using a two step gene targeting strategy (Lin et al., 2001; Ordway and Detloff, 1996). The R6/1 mice line is generated by insertion of exon 1 of human gene into the genome (Mangiarini et al., 1996), whereas, YAC128 mice contains the entire HD gene including the promoter region (Slow et al., 2003).

1.5. Aims of this thesis

There is still much more to learn about all these animal models. For example, the exact relationship between the genetic mutation and molecular changes in the cell remains unknown, and the impact of these behavioural phenotypes has not been fully elucidated. We hypothesise that the behavioural symptoms are driven by the pathology in particular cells and regions of the brain. Consequenty if we can identify the different patterns and time courses of pathological changes in the brain expressed in different genetically modified mouse lines, alongside the profile and time course of behavioural symptoms, we can begin to propose a causative cascade of changes whereby the mutant gene produces the specific symptomatology. A long term programme within the Brain Repair Group is to provide the comparative analysis of the precise time course and patterns of neuropathological changes at an anatomical level in the target mouse to identify the model that best represent the human form of HD.

Specifically, the principal aims of the thesis are as follows;

- To evaluate mouse models of HD, by producing a detailed characterization of the underlying neuronal pathology in both knock-in ($Hdh^{(CAG)Q150}$ and Hdh^{Q92}) and transgenic (YAC128 and R6/1) mouse models of HD.
- To analyze the progression, location and level of cell death present in these brains and also the possible role that aggregation and inclusion formation may have on the brain pathology.
- To assess the distribution, numbers and form of huntingtin aggregates in the brain tissues from the $Hdh^{(CAG)Q150}$ knock-in mouse line, Hdh^{Q92} knock-in mouse line and R6/1 transgenic and YAC128 transgenic mouse model of HD and compare with human HD.
- To assess whether one of these models represent the human condition more accurately than the others and can we identify a representative model of the human condition.

Chapter 2

Material and methods

2.1 Animals

In this study, two transgenic and knock-in models were used. Animal numbers and their backgrounds were described in detailed in each models of each chapters.

For all experiments the mice were housed together under standard conditions with ad libitum access to water and food. They were kept in a holding room with 12h light: dark cycle and an ambient room temperature of 20°/±1°C. The cages contained sawdust bedding and a cardboard tube for environmental enrichment. Each cage contained 1 to 6 animals.

All genetic mice and their controls have been through behavioural characterization for two years. This study was carried out in accordance with the UK Animals (Scientific Procedures) Act, 1986.

2.2 Histology

The animals were anaesthetized with a 0.2ml intraperitoneal injection of Euthatal (Merial, UK). Mice were perfused intracardially with approximately 100ml of phosphate buffered saline (PBS, pH 7.4) solution for 3 min, followed by another approximately 100ml of 4% paraformaldehyde (PFA) (Fisher Scientific, UK) in a 0.1M PBS solution, pH 7.4, for a further 5min. The brains were carefully removed and placed in 4% PFA in for 4 hours for post fixation at room temperature on a shaker and then transferred to a 25% sucrose in PBS at 4°C until they sank. Brains were sectioned at 40µm intervals in the coronal plane using a freezing sledge microtome (Leitz Bright Series 8000, Germany). The sections were then placed into 96 well plates containing a cryoprotective solution and were stored at -20°C.

2.3 *Cresyl Fast Violet (CV)*

One of six series was stained using the standard Nissl stain, cresyl fast violet for morphological and stereological analysis. Briefly, sections were mounted on the gelatine-coated glass slides (Thermo Scientific, Menzel-glaser, Germany) and then air-dried to allow better preservation of morphology at 37°C for 24 hours. The sections were then dehydrated using a series of ascending ethanol solution (5 min each, 70%, 95%, and 100%) and delipidized in a mixture of chloroform and ethanol (1:1, v/v) for 20 minutes. Following delipidization, the sections were hydrated in a series of descending ethanol solution (5 min each 100%, 95% and 70%) and immersed in distilled water for 5 minutes and stained with cresyl violet (0.7 % in distilled water with 0.5 % sodium acetate, Sigma, UK) for 5 minutes. After rinsing in distilled water for 1 minute, the sections were dehydrated in a graded series of ethanol (5 min each, 70%, 95%, and 100%), cleared in xylene (VWR, Germany) for at least for 10 minutes and then cover-slipped with DPX mounting medium (RA Lamb, UK) and analysed under a Leica DMRBE microscope (Leica, Germany).

2.4 *Immunohistochemisty (IHC)*

All stains were carried out on a one in six series of sections. Free-floating sections were processed for IHC using the sheep anti-S830 (a kind gift from Prof. Gill Bates, King College, London, UK) and rabbit GFAP (DAKO, UK) primary antibodies. The S830 antibody was raised against the product of the N-terminal region to 53 glutamine residues of exon 1 of human gene and selectively recognizes the aggregated form of the mutated htt protein (Milnerwood et al., 2006). The GFAP antibody labels astrocytes and measures reactive astrogliosis (Reiner et al., 2007).

The sections were placed in TRIS Buffered Saline (TBS), (pH 7.4) and washed twice for 5min. The endogenous peroxidise activity was inhibited by incubation in methanol containing 3% H_2O_2 (VWR, Germany) for 5min and then placed in TBS. Non-specific binding sites were blocked with 3 % horse serum in TBS for one hour and the sections were incubated with S830

antibody (diluted 1:25000) and GFAP antibody (1:2000) overnight at room temperature. After several washes in TBS, sections were incubated with a horse anti-goat or horse anti-rabbit secondary antibody, respectively (diluted 1:200, Vector Laboratories, Burlingame, CA, USA) for two hours at room temperature. After several washes in TBS, the sections were incubated with a biotin-streptavidin kit (according to the manufacturer's instructions, Vector Laboratories). After each incubation, the sections were rinsed in TBS. The peroxidise activity was visualized with 3,3'-diaminobenzidine (DAB). Finally, the sections were mounted on gelatine-coated slides, dehydrated in a graded series of ethanol (5 min each, 70%, 95%, and 100%), cleared in xylene and cover-slipped.

The S830 staining was also scored in a semi-quantitative fashion that included the intensity of specific staining in sections: 0 = absent, (+) = nucleus staining; ++ = Diffuse staining; +++ = minimum inclusions; ++++ = Dense inclusions in 3 of mouse models (*Hdh*Q150, *Hdh*Q92 and YAC128), but not in R6/1 mice due to dense and variability between mice.

Light microscopic pictures were taken using a Leica DMRBE microscope fitted with a digital camera (Optronics, California, USA) and imaging Software MagnaFire 1.2C (California, USA). All images captured using the same parameters and saved on a computer for further analysis.

2.5 *S830 / CV Stereology*

All quantification assessed blindly to the genotype of mice. A PC-based image analysis software (Olympus C.A.S.T. grid system v1.6.) on an Olympus BX50 microscope (Japan) was used to quantify the number of CV and S830 + cells. Sections through the striatum were sampled in a systematic random manner using 1: 6 series. On each section, the striatum was outlined under a 4X objective and the enclosed area was calculated by the C.A.S.T grid software. Sections within a defined volume of the striatum were then sampled at random and cells were counted under a 100X objective. The size of the counting window was 265 μm^2 (Figure 2.1).

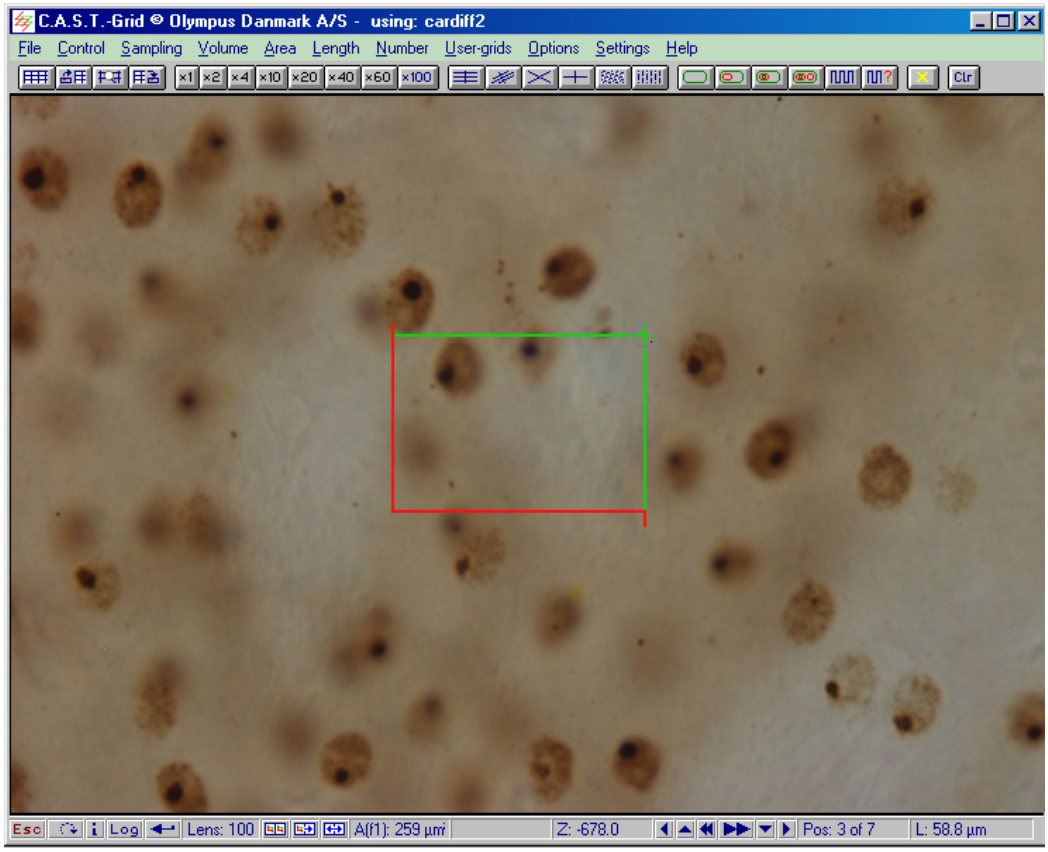

Figure 2. 1.: A schematic view of Olympus C.A.S.T. grid system on a computer screen. A red and green rectangle is counting window of 265 μm^2.

In this window, the cells are touching the green line were included, however cells are touching the red line excluded. And then using the following formula the total number of cells in the structure per section was calculated.

$C = \sum c \times (\sum A / \sum a) \times f$

C: The total number of cells

$\sum c$: The total number of cells counted

$\sum A$: The sum of all the inclusion areas

$\sum a$: The sum of all the sample areas

f: The frequency of sectioning

2.6 Transmission Electron Microscopy (TEM) for morphological study

For electron microscopy mice were anaesthetized by intraperitoneal injection of 0.1 ml of Euthatal and then perfused with 0.9% NaCl for 3min, followed by 2% PFA and 2% glutaraldehyde in 0.1M PBS solution at pH 7.4, for 5min. After perfusion, the brains were carefully removed and washed in PBS. The striatum were selected according to a mouse brain atlas (Paxinos and Franklin 2001) and transferred into PBS. The striatum was cut into small cubes using a razor blade in PBS and transferred into 1% osmium tetroxide in distilled water for 2h at +4°C for the post fixation. After washing with distilled water 4 X 15min, the samples were stained overnight in 0.5% uranyl acetate at 4°C. All tissues used for electron microscopy were dehydrated in ascending concentrations of ethanol and fresh propylene oxide, and then infiltrated overnight in a mixture of propylene oxide and araldite resin (1:1, v/v) on a rotator at room temperature. Following the resin infiltration, the tissues were embedded in fresh resin for 48h at 60°C. Ultrathin sections (60nm) were cut with a diamond knife on an ultracut-microtome (Reichert-Jung, Leica, UK). Thin sections were collected on copper mesh grids, counterstained with 2% uranyl acetate for 10min followed by Reynold's lead citrate for 5min and examined under a Philips transmission electron microscope (Philips EM 208, The Netherlands).

2.7 Transmission Electron Microscopy for immunogold labelling

For electron microscopy mice were anaesthetized by intraperitoneal injection of Euthatal and then perfused with 0.9% NaCl for 3min, followed by 3% PFA and 0.2% glutaraldehyde in 0.1M PBS solution, pH 7.4, for 5min, and then with 3 % PFA alone at a rate of 15ml/min. After perfusion the brains were carefully removed and the striatum were dissected according to a mouse brain atlas (Paxinos and Franklin 2001) and washed in PBS. The striatum tissue was cut into small cubes using a sharp razor blade in PBS and transferred into a cryoprotective solution (0.05M PBS, pH 7.4, containing 25% sucrose and 30% glycerol) for 15min. The tissue was then transferred into

methanol in an automated freeze substitution chamber at -80°C for 48h. The methanol was replaced with fresh methanol during the first two hours at -80°C. The chamber temperature was then allowed to increase -50°C for 88h. Tissues was then infiltrated by a mixture of Lowicryl HM20 resin and methanol (1:1, v/v) for 90min at -50°C, then infiltrated with a mixtures of Lowicryl HM20 resin and methanol (2:1, v/v) for a further 90min at -50°C, then transferred into pure Lowicryl HM20 resin overnight at -50°C. The tissue was then embedded in fresh Lowicryl HM20 resin under UV light for 48h at -50°C. The temperature was then increased to the room temperature for 24h a causing the UV light to polymerised the resin block. Ultrathin sections (60nm) were cut with a diamond knife on an ultracut-microtome (Reichert-Jung, Leica, UK). Thin sections were collected on pioloform-coated nickel mesh grids and were blocked with drops of PBS containing 3% normal donkey serum, 1% bovine serum albumin (BSA), 0.2% Triton-X and 0.1% sodium azide for 45min at room temperature. The sections were then incubated on drops of sheep polyclonal S830 primary antibody (1:500) overnight at 4°C. After rinsing in PBS and distilled water, the sections were incubated again in donkey anti-sheep IgG conjugated gold (10nm, 1:20; BB International) for overnight at 4°C. After washing in PBS, the grids were counterstained with 2% uranyl acetate for 10min followed by Reynold's lead citrate for 5min and examined using a Philips transmission electron microscope.

Experimental Papers

Experimental Papers - Supplementary Information

S.B. Dunnett, S Brooks and Lesley Jones were involved in the planning of experiments and provided valuable advice and input throughout all papers.

Eduardo M Torres has contributed valuable advice on the stereology technique. Alison Baird, former laboratory manager was involved in all mice transactions and all their paperwork. *Hdh*Q150 and *Hdh*Q92 mice were bred and genotype within the laboratory of Dr Lesley Jones, Yac128 and R6/1 mice were bred by Gemma Higgs and Nari Janghra, former research assistants within the Brain Repair Group. Ifor Bowen and Anthony Hann contributed expertise in the electron microscopic analysis throughout all papers.

The all experiments were carried out by the candidate.

Chapter 3

Paper 1

Light and electron microscopic characterization of the evolution of cellular pathology in the R6/1 Huntington's disease transgenic mice.

Bayram-Weston Z., Jones L., Dunnett S.B. and Brooks S.P.

Brain Res Bull. 2011, In press.

Brain Research Bulletin xxx (2011) xxx–xxx

Contents lists available at ScienceDirect

Brain Research Bulletin

journal homepage: www.elsevier.com/locate/brainresbull

Research report

Light and electron microscopic characterization of the evolution of cellular pathology in the R6/1 Huntington's disease transgenic mice☆

Zubeyde Bayram-Weston[a,*], Lesley Jones[b], Stephen B. Dunnett[a], Simon P. Brooks[a]

[a] School of Bioscience, Cardiff University, Museum Avenue, Cardiff CF10 3AX, Wales, UK
[b] Department of Psychological Medicine, 2nd Floor, Henry Wellcome Building, School of Medicine, Cardiff University, Cardiff CF14 4XN, Wales, UK

ARTICLE INFO

Article history:
Received 21 March 2011
Received in revised form 19 June 2011
Accepted 12 July 2011
Available online xxx

Keywords:
Huntington's disease
Aggregations
Inclusions
R6/1
Transgenic mice
Transmission electron microscope (TEM)

ABSTRACT

Huntington's disease (HD) is an inherited neurodegenerative disorder caused by an expansion of CAG repeats in the *Htt* gene. Examination of the post-mortem brains of HD patients shows the presence of diffuse nuclear htt immunoreactivity and intra-nuclear inclusions. The aim of this study was to produce a detailed characterization of the neuronal pathology in the R6/1 transgenic mouse model. The R6/1 carrier mice demonstrate intra-nuclear and extra-nuclear inclusions with the S830 htt antibody at 2–11 months of age. The distribution pattern of neuronal intra-nuclear inclusions (NIIs) was irregular in several brain regions including the striatum, cortex and hippocampus. A greater number of NIIs were found in the ventral striatum than in the dorsal striatum. In the globus pallidus, cerebellum and thalamus the pattern of inclusion formation was relatively consistent over time. At 4 and 6 months of age, the R6/1 mice showed increased glial fibrillary acid protein (GFAP) immunoreactivity in the cortex compared to their wildtype littermates, yet no difference was found in the striatum. Analysis by electron microscopy found that neurons from the R6/1 carriers contained a densely packed cytoplasm at 1.5 months of age, with some neurons displaying structural abnormalities including vacuolization and nuclear membrane folding. No NIIs were detected at this age, but by 7 months of age, NIIs were present with severe cellular vacuolization. The present study indicates that a decrease in striatal volume with cell loss is present in young (2 months) R6/1 mice, and the distribution of NIIs is robust and widespread, with considerably temporal and spatial variation in NII development between mice.

1. Introduction

Huntington's disease (HD) is an autosomal dominant neurodegenerative disease caused by a mutation on the *Htt* gene, which encodes the protein huntingtin [76]. Polyglutamine repeat lengths of greater than 36 are responsible for the disease [68] which manifests symptoms of progressive cognitive, psychiatric and motor impairment [3]. The onset of symptoms usually occurs between 35 and 50 years of age, and ultimately results in death around 15–20 years after the onset of symptoms. However, onset can vary from early childhood to old age depending on repeat length and environmental modification of the disease [19,24]. Polyglutamine repeat lengths of ~65 and above instigate the juvenile form of HD [30]. Cognitive deficits are present in HD gene carriers and early-stage patients well before the onset of the motor symptoms that define the disease [29,37,38,41].

The pathological hallmark of HD is the selective loss of GABAergic medium-sized spiny neurons (MSNs) of the striatum [22,82]. Although the neuropathology is most prominent in the neostriatum and the cerebral cortex [22], other brain areas such as the amygdala and hippocampus are also affected in the early stages of the disease [64]. Other characterising markers of the disease are the presence of protein aggregates and neuronal intra-nuclear inclusions (NIIs), in both HD patients and transgenic mouse models of the disease [15,17]. The role of the aggregates and NIIs is unknown, although three hypotheses have been suggested for the potential role of NIIs, which are (i) they are toxic to cells and initiate the pathology [65–67,69], (ii) they are protective to cells [2,53,61,72], (iii) they are a result of an unknown mechanism with no function in cells [74] and it is generally believed that they contribute to cell death, but it is less accepted that NIIs are directly toxic [15,17,40,84].

As HD is caused by a single gene mutation, it is relatively easy to model in mice. Several genetic rodent models have been generated to help determine the nature and time-course of the disease development in animals [43,50,52,62,83]. The R6 mouse lines were the first transgenic models of HD [50]. The R6/2 mice show a rapidly progressive phenotype which includes motor and cognitive abnormalities, and death by 13–18 weeks of age [13,44,50]. However,

☆ This article is part of a Special Issue entitled 'HD Transgenic Mouse'.

* Corresponding author. Tel.: +44 29 208 74684; fax: +44 29 208 76749.
E-mail address: Bayram-WestonZ@cardiff.ac.uk (Z. Bayram-Weston).

0361-9230/$ – see front matter © 2011 Elsevier Inc. All rights reserved.
doi:10.1016/j.brainresbull.2011.07.009

fewer studies have been carried out on the R6/1 mouse line, in part because of the later onset and slower progression of pathology and symptoms. The R6/1 mice express exon 1 of the human *htt* gene and carry approximately 116 CAG repeats. The endogenous level expression of the R6/2 mice is 75%, whereas, the endogenous level expression of the R6/1 mice is 31% [50]. These mice show somatic instability starting at ~6 weeks of age which progressively increases with age [4,49]. The first sign of motor deficits became apparent with hyperactivity at 4 weeks of age [9]. As the disease progresses, a deficit with feet clasping is pronounced at 14 weeks of age and the mice demonstrate a decline in body weight from 22 weeks of age [56]. These mice exhibit early spatial learning deficits at 12 weeks of age [12]. By 15 weeks of age, cognitive [31] and behavioural [56] impairments become more apparent. Bolivar et al. have shown that overt neuronal pathology only emerges well after the behaviour abnormalities in these mice [8]. Moreover, in R6/1 mice, the degree of motor impairments coincide with in the number of striatal neurons containing NIIs [26]. Intra-nuclear inclusions were first observed in the hippocampus, coinciding with hyperactivity [54], and were most noticeable in the striatum by 9 weeks of age [56]. No cell death has been reported at 30 weeks of age although a decreased DARPP-32 immunostaining has been found [56]. Extracellular striatal dopamine levels are also decreased by 70% in these mice compared to their wildtype littermates and it has been reported that the R6/1 mice are resistant to excitotoxic lesions produced by malonate [60] and quinolinic acid [59].

The present study aimed to characterize anatomically the disease progression in the R6/1 mouse line in animals of between 2 and 11 months of age, in parallel with the longitudinal behavioural study, reported elsewhere [12]. Disease progression was measured by determining the onset, and temporal and spatial pattern of protein aggregation and NII formation throughout the brains of the mice. The present study aims to define developmentally sensitive, disease-related time points in the R6/1 mouse line, to optimise therapeutic potential and identify the suitability of this mouse line for specific therapeutic interventions.

2. Materials and methods

2.1. Animals

In total, 24 male (M) and 30 female (F) R6/1 transgenic mice were used in the following groups: 2 months = 5 wildtype (3M, 2F) and 3 carriers (2F, 1M); 4 months = 5 wildtype (3M, 2F) and 5 carriers (3M, 2F); 6 months = 5 wildtype (2M, 3F) and 5 carriers (5M); 7 months = 5 wildtype (2M, 3F) and 5 carriers (5M); 10 months = 3 wildtype (3F) and 5 carriers (5F) and 11 months = 3 wildtype (3F) and 5 carriers (5F). The R6/1 mice were obtained from Jackson Laboratory (Maine, USA), and maintained on the males, and backcrossed on to C57BL/6j wildtype females with the F1 animals being used for this study. All mice were genotyped on weaning by tail tip samples which were processed by a commercial company (Laragen Inc., Los Angeles). The carrier mice used in the present study carried on average 124 CAG repeats with a range of 118–126. Animals were housed in groups of up to 4 mice under a 12 h:12 h light-dark cycle (lights on 07:00 h) with *ad libitum* access to food and water and an ambient room temperature of 21 ± 1 °C. All experiments were conducted in accordance with the UK Animals (Scientific Procedures) Act 1986, and local ethical review.

2.2. Histology

The animals were deeply anaesthetised with Euthatal (Merial, Essex, UK), pre-washed with 0.1 M phosphate-buffered saline (PBS) and perfused with 4% paraformaldehyde (PFA) (Fisher Scientific, Loughborough, UK) in PBS. The brains were then removed and post-fixed for 4 h and left to saturate with 25% sucrose PBS. The brains were sectioned coronally to a thickness of 40 μm on a freezing sledge

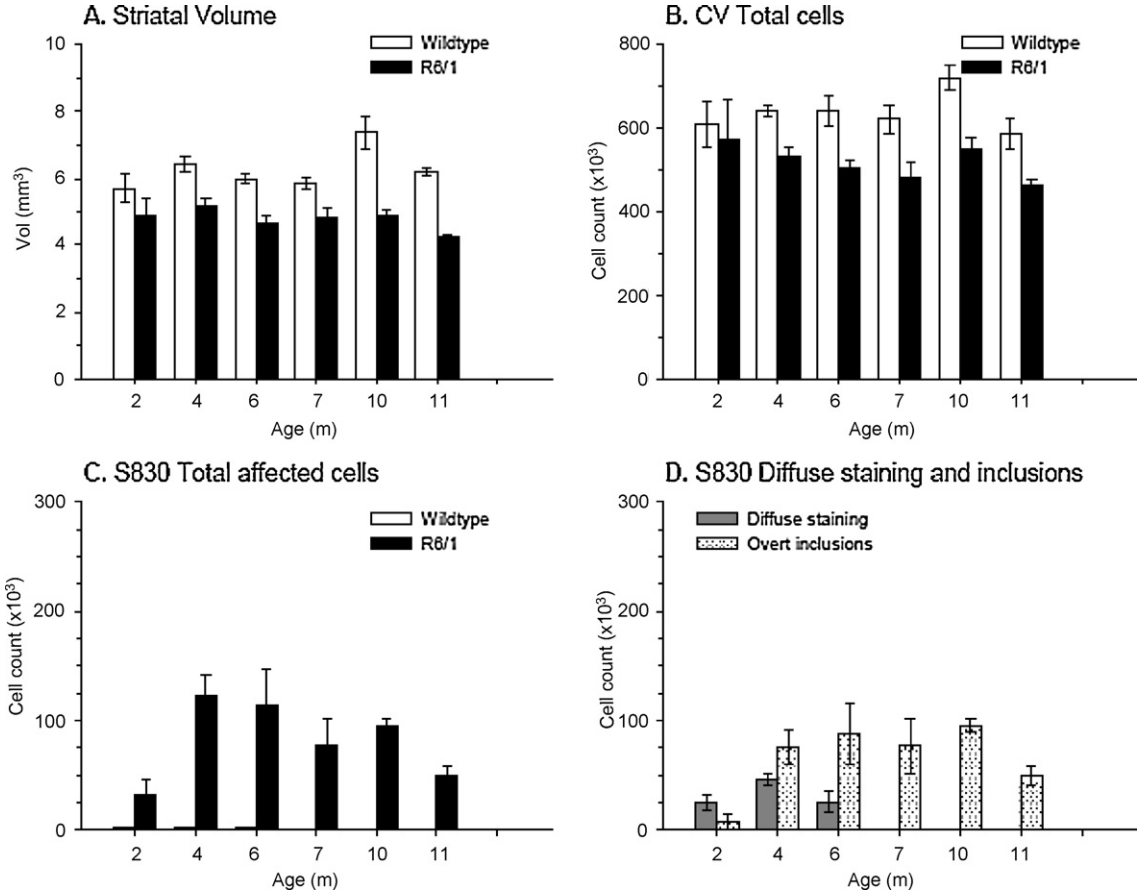

Fig. 1. Striatal volume in R6/1 mice. R6/1 mice demonstrated a decrease in striatal volume with age compared with their wildtype littermates (A). Neuronal cell loss in the striatum in R6/1 mice is also apparent compared with their control (B). The total number of affected cells (cells constitute of both diffuse staining and inclusions) was highest at 4 months of age, after which point the number of affected cells fell (C). Diffuse nuclear staining peaked at 4 months of age and was not detectable by 7 months of age, whereas nuclear inclusions were present in all age groups from 2 months of age with their number peaking at 10 months of age (D).

Please cite this article in press as: Z. Bayram-Weston, et al., Light and electron microscopic characterization of the evolution of cellular pathology in the R6/1 Huntington's disease transgenic mice, Brain Res. Bull. (2011), doi:10.1016/j.brainresbull.2011.07.009

microtome (Leitz Bright Series 8000, Germany) and the sections were stored in antifreeze in the freezer at −20 °C.

2.3. Cresyl fast violet (CV)

Cresyl violet was used for anatomical and stereological analysis of the sections in a one in six series. The sections were mounted on double-coated gelatin slides, dried overnight and then dehydrated in increasing concentrations of ethanol (70%, 95% and 100%) for 5 min each, before being delipidized in a mixture of chloroform and ethanol for 20 min. They were then bathed for 5 min each in 100%, 95%, 70% ethanol and distilled water before the slides were submerged in a solution of cresyl violet acetate, 0.7% in distilled water with 0.5% sodium acetate (Sigma, Hertfordshire, UK) for 5 min. After a rinse in distilled water, the sections were differentiated and dehydrated for 5 min each in 70%, 95% ethanol and finally 100% ethanol before being cover-slipped using DPX mounting medium (RA Lamb, Hambridge, Somerset, UK). The sections were analysed under a Leica DMRBE microscope (Leica, Wetzlar, Germany).

2.4. Immunohistochemistry

Immunohistochemistry was performed as described by Bayram-Weston et al. [7]. The staining was carried out on a one in six series of sections from each brain. The sections were collected in 96 well plates to undergo immunohistochemical reactions while free floating. Sheep anti-S830 primary antibody (a kind gift from Prof. Gillian Bates, King's College, London, UK) which recognizes the N-terminal region to 53Q of exon 1 of the human gene [54], and rabbit anti-glial fibrillary acid protein primary antibody (GFAP; DAKO, Cambridge, UK) which measures reactive astrogliosis, were applied to free floating sections. Reactive astrogliosis was measured by the intensity of GFAP immunoreactivity at 2, 4 and 6 months, based on the average staining of animals at each time point.

The sections were washed in TRIS-buffered saline (TBS) and quenched in distilled water with methanol containing 3% H_2O_2 (VWR) for 5 min. After three washes in TBS, the sections were immersed in a blocking solution containing TBS and 3% horse serum for 1 h. Subsequently they were incubated with S830 antibody (diluted 1:25,000) and GFAP antibody (1:2000) overnight at room temperature, before three washes. Sections were then incubated with horse anti-goat or horse anti-rabbit secondary antibodies (diluted 1:200, Vector Laboratories, Burlingame, CA, USA) for 2 h. To further amplify the signal, a biotin-streptavidin kit was administered according to the manufacturer's instructions (Vector Laboratories) for 2 h. After additional washes in TBS, the peroxidase activity was visualized with 3,3′-diaminobenzidine (DAB) reaction (Sigma–Aldrich, Poole, Dorset, UK). The sections were mounted on gelatine-coated slides, dehydrated and cover-slipped.

Light microscopic pictures were taken using a Leica DMRBE microscope fitted with a digital camera (Optronics, Goleta, California, USA) and MagnaFire 1.2C imaging Software (Goleta, California, USA). All images were captured using the same parameters and saved on computer for further analysis. Images were adjusted in contrast and brightness only for optimal display with Adobe Photoshop 6.0.

2.5. S830/CV stereology

Two dimensional stereology was performed on an Olympus BX50 microscope (Olympus Optical Co. Ltd., Tokyo, Japan) with a PC-based image analysis software (Olympus C.A.S.T. grid system v1.6.). Cell counts were performed on a one in six series of S830-stained and CV sections throughout the entire left striatum and then evaluated blindly to the experimental groups. Briefly, the striatum was outlined under a 4× objective and the enclosed area was calculated by the C.A.S.T. grid software. Sections within a defined volume of the striatum were then sampled at random and cells were counted under a 100× objective using a 265 μm^2 2D optical dissector counting frame. The total number of cells in the structure per section was calculated using the following formula [1]:

$$C = \sum c \times \left(\frac{\sum A}{\sum a} \right) \times f$$

C: the total number of cells; $\sum c$: the total number of cells counted; $\sum A$: the sum of all the inclusion areas; $\sum a$: the sum of all the sample area; f: the frequency of sectioning.

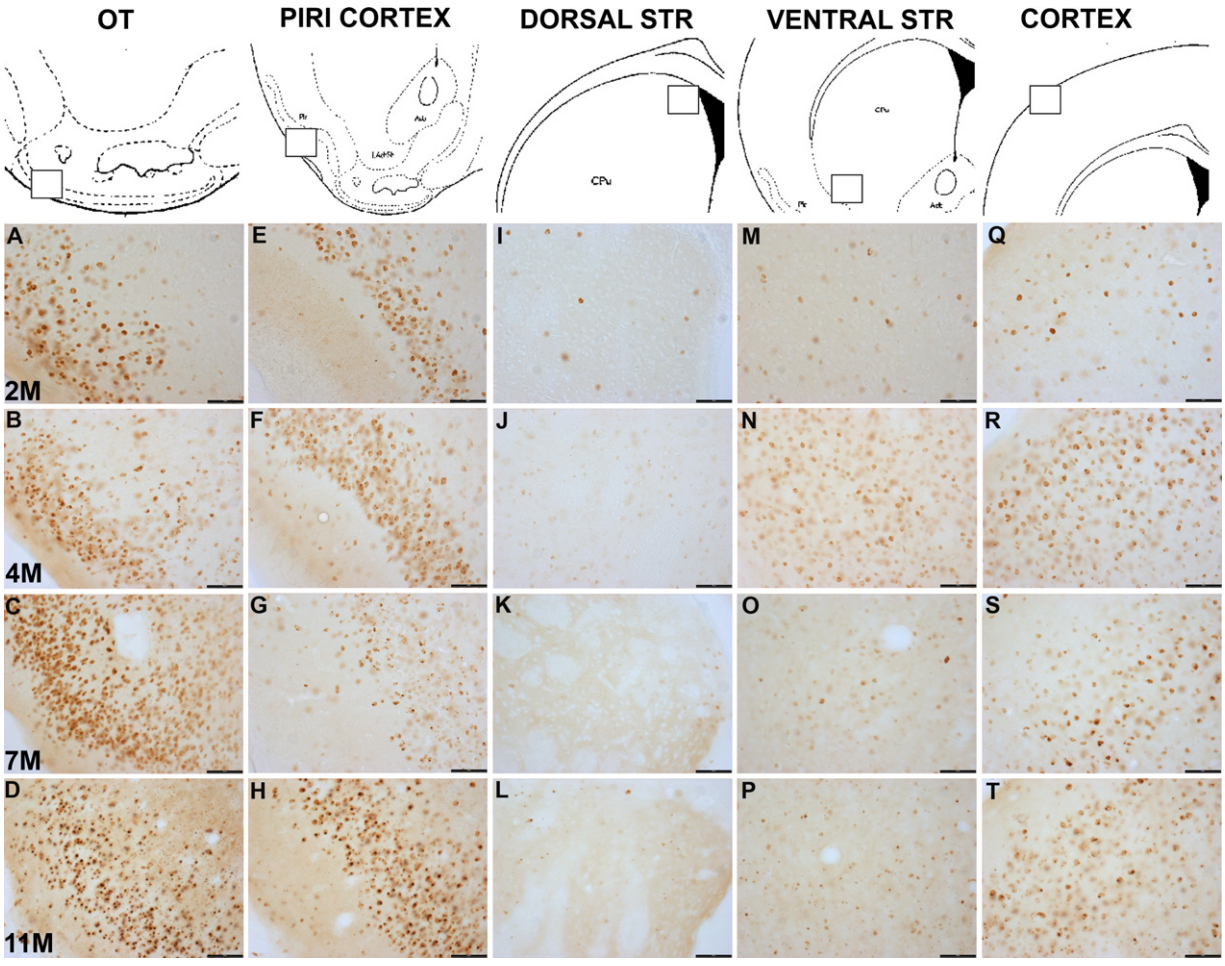

Fig. 2. Temporal progress of S830 immunoreactivity in R6/1 mouse brain. Columns 1: olfactory tubercle (A–D), Columns 2: piriform cortex (E–H), Columns 3: dorsal striatum (I–K), Columns 4: ventral striatum (M–P), Columns 5: cortex (Q–T) at 2, 4, 7 and 11 months of age. The presence of NIIs is clearly visible in all areas of R6/1 mouse brain.

Please cite this article in press as: Z. Bayram-Weston, et al., Light and electron microscopic characterization of the evolution of cellular pathology in the R6/1 Huntington's disease transgenic mice, Brain Res. Bull. (2011), doi:10.1016/j.brainresbull.2011.07.009

Affected cells were identified and the total numbers estimated in terms of positive S830-labelling; affected cells were further categorized in terms of whether they expressed either diffuse nuclear staining alone or exhibited overt inclusions in their nuclei (NIIs) with diffuse nuclear staining. Extra-nuclear neuronal inclusions (ENNIs) have been excluded from counting because they are not within the nuclei of cells.

2.6. Transmission electron microscopy (TEM) for morphological assessment

An additional 8 mice were sacrificed at 1.5 months and 7 months (n: 8; 2 wild-type and 2 carriers at each age) for electron microscopic analysis. The animals were deeply anaesthetised with Euthatal and then perfused with 0.9% NaCl, followed by a mix of 2% PFA and 2% glutaraldehyde, made in a phosphate buffer of 0.1 M (pH 7.4) for 5 min. The striatum was dissected into five random specimens under Leica Wild M3Z (Leica, Wetzlar, Germany) microscope according to the Paxinos and Franklin Atlas [58]. The striatum were then washed several times with PBS, and were cut into small cubes and post-fixed in 1% osmium tetraoxide for 2 h at 4 °C. After several washes in distilled water they were stained overnight in 0.5% uranyl acetate. The following day, specimens were dehydrated in ascending concentrations of ethanol and fresh propylene oxide, and then infiltrated overnight in a mixture of propylene oxide and araldite resin at room temperature. Following resin infiltration, the specimens were embedded in fresh resin. The ultrathin sections of 60 nm thickness were produced in an ultramicrotome (Reichert-Jung, Leica UK Ltd., Milton Keynes, UK) and collected on copper mesh grids. The grids were stained with 2% uranyl acetate for 10 min followed by Reynold's lead citrate for 5 min and examined with a transmission electron microscope (Philips EM 208, Eindhoven, The Netherlands).

2.7. Statistical analyses

Statistical analyses were performed using one- and two-way analyses of variance using the Genstat statistical package (v13.2; VSN International, Hemel Hempsted, UK) with genotype and age as between subject factors.

3. Results

3.1. Striatal atrophy and neuronal cell counts in the R6/1 mice

Striatal volume in the R6/1 transgenic mice and their wild-type littermates was studied between 2 and 11 months of age using CV stained sections. For striatal size measurements a statistically significant main effect of age was returned (Fig. 1A: Age, $F_{5,42} = 4.97$, $p < 0.001$), however, this is likely to be due to fluctuations within the samples, most notably at 10 months of age in the wild type mice. A significant difference between the two genotypes was demonstrated in that the size of the striatum of the R6/1 carriers was smaller than that of the their wildtype littermates (Fig. 1A: Genotype, $F_{1,42} = 122.42$, $p < 0.001$), with this difference between the groups widening with age, probably reflecting fluctuations in the volume estimates in the wild type animals at later time points (Age × Genotype, $F_{5,42} = 3.19$, $p < 0.05$).

In the cresyl violet stained cells, stereological analyses demonstrated a significant reduction in neuronal numbers found for the mice generally as they aged (Fig. 1B: Age, $F_{5,42} = 2.50$, $p < 0.05$), but within this cell loss the R6/1 mice lost more cells compared with their wildtype littermates (Genotype, $F_{1,42} = 37.00$, $p < 0.001$). No interaction effect was found (Age × Genotype, $F_{5,42} = 0.88$, n.s.).

3.2. Aggregation and inclusion pathology in the R6/1 mice

Diffuse nuclear staining (homogeneous staining with no evidence of inclusions) and NIIs (homogeneous staining with an

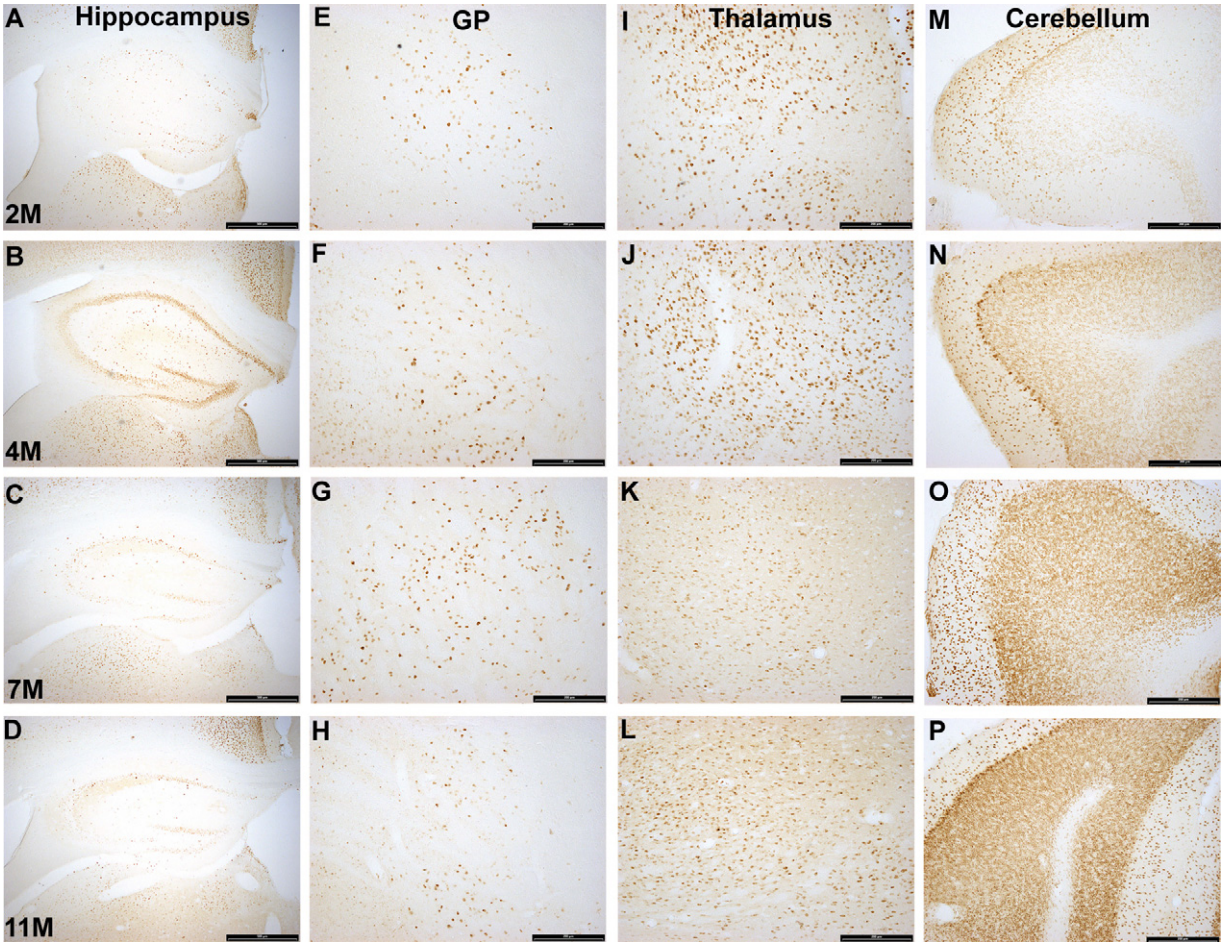

Fig. 3. S830 immunoreactivity in the R6/1 mouse brains. Light micrograph images showing S830 immunoreactivity in the hippocampus (A–D), globus pallidus (E–H), thalamus (I–L), and cerebellum (M–P) at 2, 4, 7 and 11 months of age.

Please cite this article in press as: Z. Bayram-Weston, et al., Light and electron microscopic characterization of the evolution of cellular pathology in the R6/1 Huntington's disease transgenic mice, Brain Res. Bull. (2011), doi:10.1016/j.brainresbull.2011.07.009

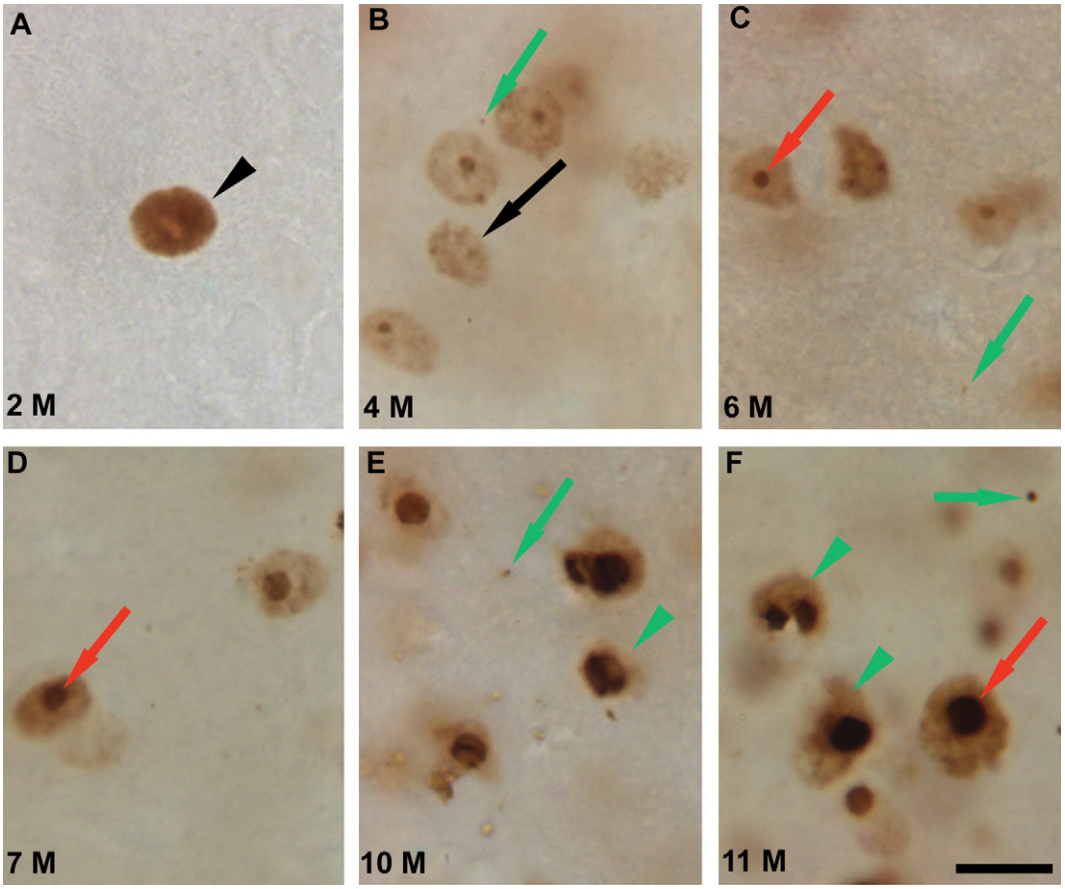

Fig. 4. High power images of nuclear S830 immunoreactivity in the ventral striatum of R6/1 mice. The diffuse nuclear staining was present at 2 and 4 months of age (A–B). 7, 10 and 11 months of age animals exhibit no diffuse nuclear staining but nuclear inclusions (D–F). Neuronal degeneration and enlarged nuclear inclusions were clearly identified at 11 months of age by the light microscope (F). Black arrow shows weak nuclear staining; black arrow head shows diffuse nuclear staining; red arrows denote inclusions; green arrow denote extra-nuclear inclusions; green arrow heads indicate degenerating neurons showing lost of nucleus membrane integrity. Scale bar = 10 μm.

overt inclusion) were detected with S830 immunohistochemistry in the R6/1 transgenic mice. The mice also exhibited an extensive expression of intra- and extra-nuclear neuronal inclusions (ENNIs) across all age groups. The total number of affected cells (diffuse nuclear staining and NIIs) increased from 4 to 6 months of age, after which point the number of affected cells decreased (Fig. 1C: Age, $F_{5,21} = 3.66$, $p < 0.05$). Both diffuse nuclear staining and NIIs were present in 2 month old mice onwards. After 6 months of age, the ratio of diffuse nuclear staining and NIIs had changed and we observed more NIIs in most brain regions examined such as olfactory tubercle (Fig. 2A–D), piriform cortex (Fig. 2E–H), dorsal (Fig. 2I–L), ventral striatum (Fig. 2M–P) and cerebellum (Fig. 3M–P). Diffuse nuclear staining in the striatum peaked at 4 months of age, and was persistent until 6 months of age and then disappeared (Fig. 1D: Age, $F_{5,21} = 19.40$, $p < 0.001$). However, NIIs were present in the striatum at 2 months of age, and up to, and including the 11 month time point (Fig. 2). The numbers of inclusions increased from 2 to 4 months of age and remained high until 10 months of age, before dropping (Fig. 1D: Intra-nuclear inclusions, $F_{5,21} = 3.77$, $p < 0.05$). By 11 months of age, NIIs were distributed widely throughout the striatum, olfactory tubercle, nucleus accumbens, amygdala and piriform cortex. Uniform S830 immunoreactivity was present at 2 months of age and increased with age in the olfactory tubercle and piriform cortex. The striatum showed a scattered distribution of mutant htt in the striatum, and the ventral striatum (Fig. 2M–P) generally had a greater number of inclusions than the dorsal striatum (Fig. 2I–L). The hippocampus (Fig. 3A–D), thalamus (Fig. 3I–L) and cerebellum (Fig. 3M–P) contained NIIs, the globus pallidus (Fig. 3E–H), amygdala (data not shown), medial septum (data not shown) and motor cortex (Fig. 2Q–T), contained a few diffuse nuclear staining and NIIs inclusions. However, the distribution of NIIs in the hippocampus showed uneven localization and were not layer specific in all age groups (Fig. 3). The globus pallidus and thalamus showed increased immunoreactivity at 2 and 4 months of age, but the cerebellum had a consistent increase in S830 staining through to 11 months of age (Fig. 3). Cytosolic and nuclear inclusions progressed with age to form dense and larger inclusions in some areas of the brain including the striatum (Fig. 4), olfactory tubercle and piriform cortex. Many neurons showed nuclear staining that looks similar to diffuse along with an over inclusion (Fig. 4C–F).

The ENNIs were observed at 2 months of age onwards in all brain regions. However, the density and distribution was very low and varied depending on the region of the brain.

3.3. GFAP immunostaining

GFAP immunoreactivity was intense in most regions of the brain including striatum and cortex. The intensity of GFAP staining within the carriers did not change in the striatum when compared to age matched control animals (Fig. 5). However, the cortex contained more intense GFAP-positive astrocytes than their wildtype at 4 and 6 months of age.

3.4. Transmission electron microscopy (TEM)

Transmission electron microscopy observations demonstrated that 1.5-month-old wildtype animals contained a preserved cell

Please cite this article in press as: Z. Bayram-Weston, et al., Light and electron microscopic characterization of the evolution of cellular pathology in the R6/1 Huntington's disease transgenic mice, Brain Res. Bull. (2011), doi:10.1016/j.brainresbull.2011.07.009

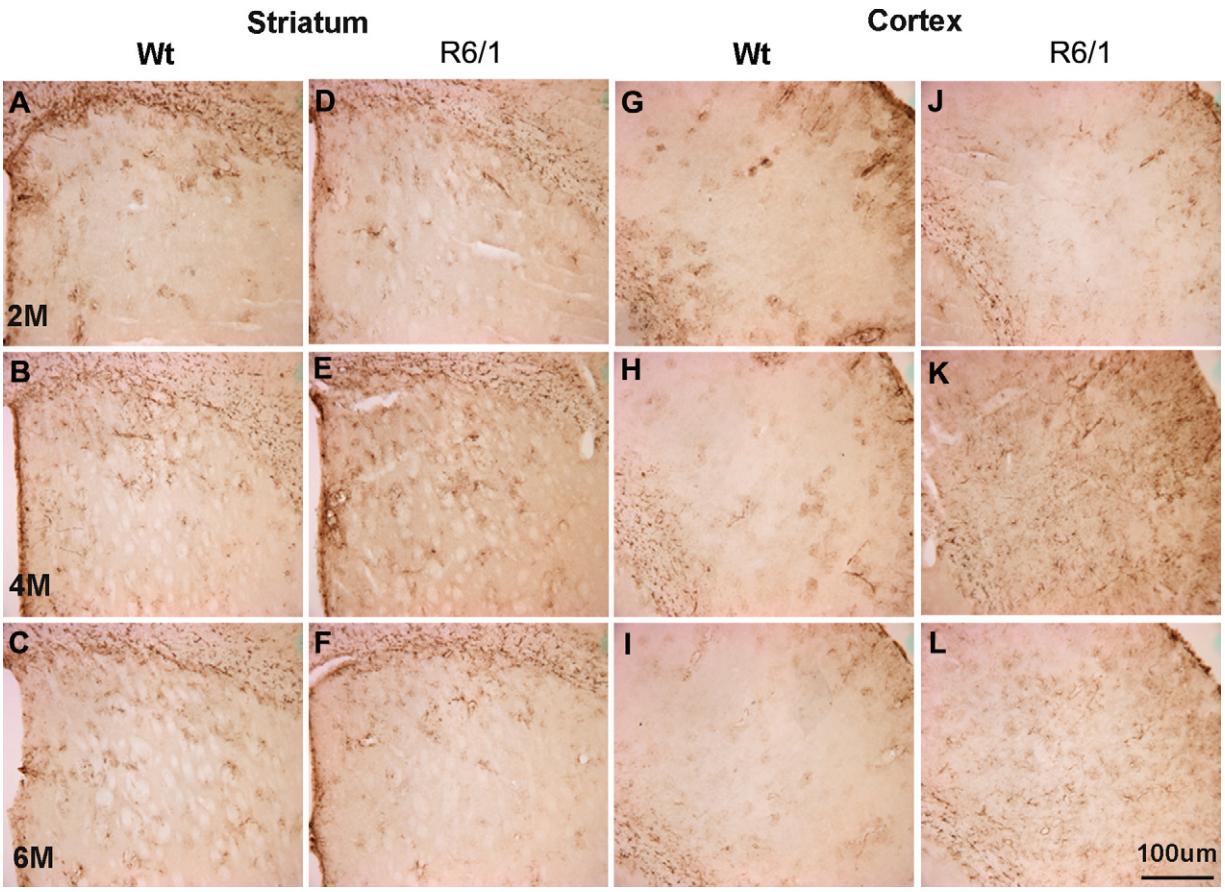

Fig. 5. Light microscopic images showing GFAP immunoreactivity in the striatum (A–F) and cortex (G–L) of wildtype and R6/1 mice. The first row designates 2 months of age, the second row designates 4 months of age and the third row designates 6 months of age. The reactive astrogliosis with GFAP staining is detected in the striatum of both wildtype and carriers. However, the cortex of the 4 and 6-month animals are showing increased GFAP activity in comparison to control animals. Scale bar = 100 μm.

morphology. The mitochondria (green arrows) and synaptic junctions (black arrow) were normal (Fig. 6A). The striatum of the carriers did not contain NIIs at 1.5 months of age and some cells exhibited normal morphology with compact cytoplasm containing organelles (Fig. 6B), whereas others showed signs of necrotic cell death with the loss of membrane integrity, vacuolated cytoplasm and uneven nuclear membrane (Fig. 6C). Again, the striatum of the 7 months of age wildtype mouse exhibited a relatively more preserved morphology (Fig. 6D), than that of the comparable carrier animal (Fig. 6E). The 7-month-old carriers showed degenerative neurons with a number of necrotic features such as angular shape and uneven nuclear membrane and most cytoplasmic organelles were largely destroyed and contained severe vascularisation (Fig. 6F). In addition, the 7-month-old carriers exhibited NIIs (black arrow) within their nuclei (Fig. 6F). These inclusions again appeared as large circular structures with no membrane as reported previously [15,17], but they were again clearly distinguishable from their surroundings.

4. Discussion

From the first time point examined (2 months of age), diffuse nuclear staining and NIIs were distributed widely throughout the striatum, olfactory tubercle, nucleus accumbens, piriform cortex, globus pallidus, thalamus and cerebellum in the R6/1 mice. The distribution of mutant htt found with S830 immunohistochemistry was uneven in the cortex, striatum and hippocampus, in contrast to previous reports of a uniform distribution of mutant htt with EM48 antibody in these areas at 10 months of age [80]. Our findings in the cortex are broadly in agreement with a previous study [54] that demonstrated S830 staining in the cortex of 3-month-old R6/1s. The distribution of NIIs in the hippocampus showed a scattered pattern of S830 immunoreactivity in all age groups which was not layer specific, in disagreement with an earlier study with the S830 antibody that found the localization of mutant htt within the hippocampus to be layer specific and progressive with age [54]. The presence of S830 immunoreactivity in the hippocampus of this mouse line may reflect the cognitive dysfunction in spatial learning tasks in this line [12,57]. Other studies have also confirmed that hippocampal neurons are impaired in the R6/1 mice [23,39,78]. However, our results are in contrast to the van der Borght and Brundin study that failed to detect any NIIs in the hippocampus of this mouse line using the EM48 antibody [78], suggesting that S830 may be the more sensitive of the two antibodies for identifying NIIs.

We also observed NIIs in the cerebellum of R6/1 mice. Interestingly, it has been reported that the cerebellum was spared in the adult onset form of HD [64,70], although, this was not found to be the case in other studies [28,32,63]. Some studies also report the absence of NIIs in the cerebellum of HD patients [17,21,46], yet, one study did report them [25]. The results from the human studies suggest that there is cerebellar pathology, but that is highly variable across individuals. In the R6/1 mice of the present study, cerebellar pathology was present in each of the mice examined.

In the present study, we found a decrease in the striatal volume and cell loss in the carrier animals in comparison to their wildtype littermates by 4 months of age. This is in contrast to a study using R6/1 mice where there was no reported cell loss by 7.5 months of age [56], although this was not measured quantitatively. Our finding is also in contrast with another study which showed a decrease

Please cite this article in press as: Z. Bayram-Weston, et al., Light and electron microscopic characterization of the evolution of cellular pathology in the R6/1 Huntington's disease transgenic mice, Brain Res. Bull. (2011), doi:10.1016/j.brainresbull.2011.07.009

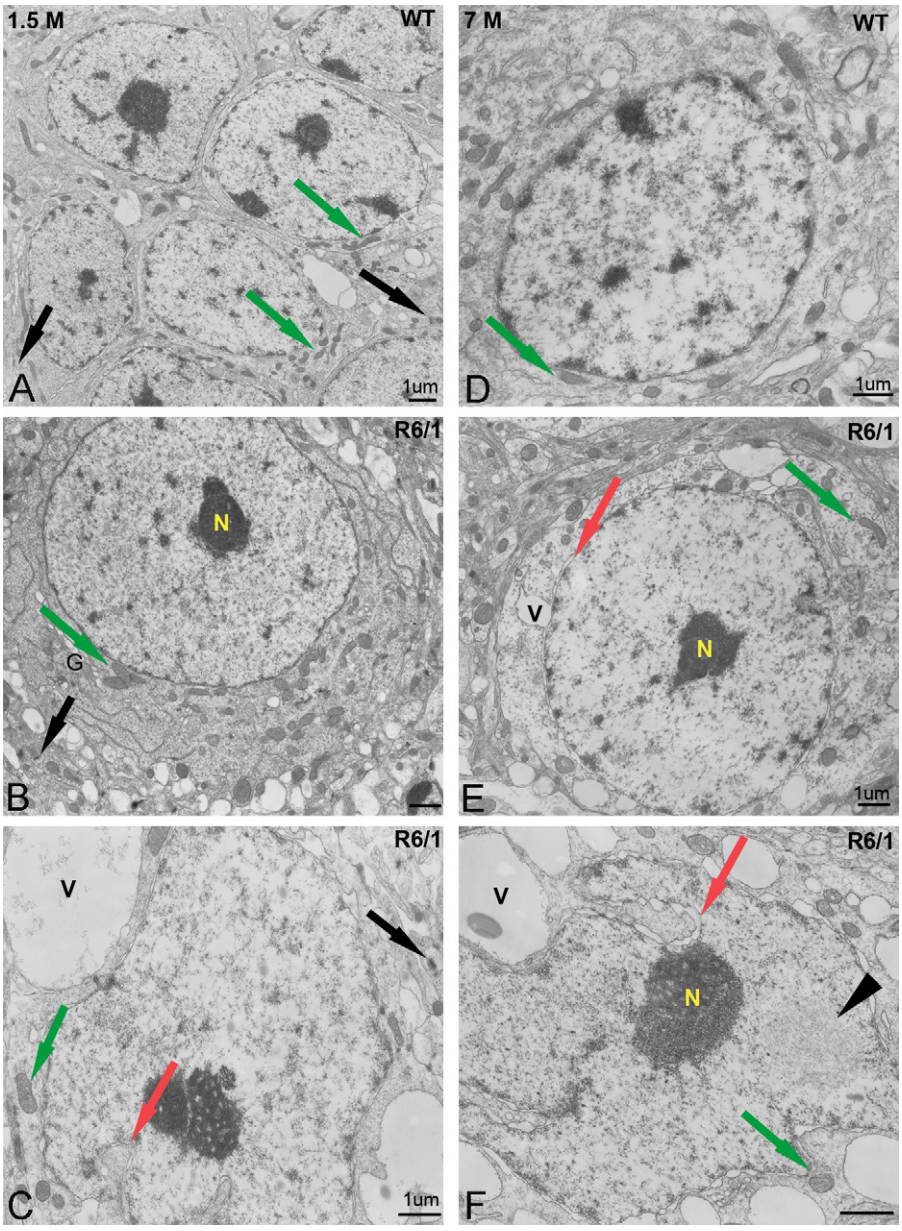

Fig. 6. Electron microscopic images showing striatal cells from 1.5 (left panel) and 7 (right panel) months of age. A morphologically normal cells with synapses, containing mitochondria (green arrows) and synaptic junctions (black arrows) in wildtypes (A and D). In R6/1 mice, a striatal cell exhibits also a well preserved cell morphology containing mitochondria (green arrows), golgi apparatus and synaptic junctions (black arrows) (B), a necrotic cell with uneven nuclear membrane (red arrows) and vacuolated cytoplasm (C). InR6/1 mice, degenerative neurons showed necrotic features such as uneven nuclear membrane contained vascularisation (E) and visible NIIs (black arrow head) in the nucleus (F) at 7 months of age. N, nucleolus; G, golgi apparatus; v, vesicles. Scale bars = 1 μm. (For interpretation of the references to color in this figure legend, the reader is referred to the web version of the article.)

in volume only apparent at 10 months of age [80], however, in this study only a single time point was examined.

Cell death is generally categorized as necrotic or apoptotic. However, to date, the definition of the apoptosis morphologically differs from one study to another [10,11,20,48,81]. For example, the neuronal death found in HD and the R6/1 transgenic mice has been described not as apoptotic cell death, but as dark cell degeneration [77]. Kerr and colleagues have ultrastructurally described apoptosis as the formation of apoptotic cell bodies, cellular shrinkage, condensed chromatin and cytoplasm [33,34]. However, in addition and conversely to these observations, it has been shown that apoptotic cells do not necessarily exhibit all of these criteria, such as the appearance of apoptotic bodies [10]. In our ultrastructural analysis in the YAC128 transgenic [6] and $Hdh^{Q92/Q92}$ knock-in mouse lines [5], we have observed cellular shrinkage, condensed chromatin and cytoplasm, but not the apoptotic cell bodies. Interestingly, the R6/1 mice model shows signs of necrotic cell death, with cell swelling, vacuolization and dissolution of plasma [11]. We have observed the appearance of empty vacuoles in the striatal cells, a component of the degeneration process, by transmission electron microscopy.

Similarly, a recent study has also shown empty vacuoles and suggested that the autophagic system is affected and responsible for the delayed cytosilic turnover in HD [51], but the precise cell death mechanism that underlies the disease is at present still unknown, and may be due to a number of causes [14,16,35,36,73].

In the R6/1 mouse, mutant htt can be seen in axonal terminals by TEM examination [42]. Morton and colleagues have highlighted novel ENNIs in the R6/2 mouse, which are easily identified without immunogold labelling, by TEM examination [55]. Unlike their findings, we were not able to observe ENNIs at the ultrastructural level in the current mouse line, which is in agreement with our previous studies in other transgenic and knock-in HD lines [5–7].

Please cite this article in press as: Z. Bayram-Weston, et al., Light and electron microscopic characterization of the evolution of cellular pathology in the R6/1 Huntington's disease transgenic mice, Brain Res. Bull. (2011), doi:10.1016/j.brainresbull.2011.07.009

Another feature in the brains of HD patients is astrogliosis [18,47]. Glial response has been observed in several genetic models including HdhQ150 knock-in, HdhQ200 knock-in [27,43] and HD89 transgenic mouse lines [62]. However, to our knowledge, it has not been reported in R6/2 transgenic mice [50]. In the present study, we did not demonstrate increased intensity of GFAP immunoreactivity in the striatum when compared to age matched control animals. However, there was a slight increase in the intensity of GFAP in the cortex from 4 months of age when compared to age matched control animals.

Some of the discrepancies observed in the timing and distribution of NIIs may be due to the different antibodies used between studies and technical discrepancies between laboratories. Additionally, variation in background strain has been reported to alter the accumulation of mutant htt and the development of NIIs in the striatal neurons of Hdh^{Q111} mice, the mice on the C57BL/6 background exhibiting the early onset of inclusion formation, which was slowest on 129 Sv background [45]. Similarly, Van Raamsdonk and colleagues have shown that the HD-like phenotypes are modulated by background strain [79]. The pathology we have observed may, therefore, depend on the C57BL/6 background strain we used.

Generally, our results are consistent with those of the R6/2 and other mouse models of HD [5–7,75], and demonstrate the typical neuropathological differences between the human condition and the HD mouse models: widespread deposition of NIIs with limited cell loss. In the post mortem examinations of HD patients, NIIs were more abundant in the cortex than striatum [17,21,25,47,71], and found to be lower in the globus pallidus, hippocampus and thalamus, and absent in the cerebellum [21,25]. Why there should be such differences between the mouse models and the human condition is open to question, but it is nevertheless a striking and consistent observation.

In conclusion, the R6/1 mouse model displays a decrease in striatal volume with evidence of cell loss. Intra-nuclear inclusions were apparent from 2 months of age. The distribution of NIIs was robust, widespread and less uniform in comparison with other studies of the R6/1 line, and between other transgenic and knock-in models, and probably reflects the broad functional pathology exhibited by R6 lines. However the distribution of NIIs does not resemble those which have been reported in adult onset human patients.

Conflict of interest

The author has no conflicts of interest.

Acknowledgements

We thank Prof G. Bates (University of London) for the kind gift of the S830 antibody, Prof. Ifor Bowen and Dr. Anthony Hann for advice on the electron microscope and Alison Baird and Nari Janghra for technical support. The study was supported by an MRC studentship to ZBW, and funding from CHDI Inc. and the MRC.

References

[1] M. Abercrombie, Estimation of nuclear population from microtome sections, Anat. Rec. (1946) 239–247.
[2] M. Arrasate, S. Mitra, E.S. Schweitzer, M.R. Segal, S. Finkbeiner, Inclusion body formation reduces levels of mutant huntingtin and the risk of neuronal death, Nature 431 (2004) 805–810.
[3] G.P. Bates, P.S. Harper, L. Jones, in: G.P. Bates, P.S. Harper, L. Jones (Eds.), Huntington's Disease, Oxford University Press, 2002.
[4] G.P. Bates, L. Mangiarini, A. Mahal, S.W. Davies, Transgenic models of Huntington's disease, Hum. Mol. Genet. 6 (1997) 1633–1637.
[5] Z. Bayram-Weston, S. Brooks, Jones L., S.B. Dunnett, Light and electron microscopic characterization of the evolution of cellular pathology in $Hdh^{Q92/Q92}$ Huntington's disease mice, Brain Res. Bull., in this issue.
[6] Z. Bayram-Weston, L. Jones, S.B. Dunnett, S.P. Brooks, Light and electron microscopic characterization of the evolution of cellular pathology in YAC128 transgenic mice, Brain Res. Bull., in this issue.
[7] Z. Bayram-Weston, E.M. Torres, L. Jones, S.B. Dunnett, S.P. Brooks, Light and electron microscopic characterization of the evolution of cellular pathology in the *Hdh*(CAG)150 Huntington's disease knock-in mouse, Brain Res. Bull., in this issue.
[8] V.J. Bolivar, K. Manley, A. Messer, Early exploratory behavior abnormalities in R6/1 Huntington's disease transgenic mice, Brain Res. 1005 (2004) 29–35.
[9] V.J. Bolivar, S.R. Walters, J.L. Phoenix, Assessing autism-like behavior in mice: variations in social interactions among inbred strains, Behav. Brain Res. 176 (2007) 21–26.
[10] I.D. Bowen, Apoptosis or programmed cell death? Cell Biol. Int. 17 (1993) 365–380.
[11] D.E. Bredesen, R.V. Rao, P. Mehlen, Cell death in the nervous system, Nature 443 (2006) 796–802.
[12] S.P. Brooks, N. Janghra, V.L. Workman, Z. Bayram-Weston, L. Jones, S.B. Dunnett, Longitudinal analysis of the behavioural phenotype in R6/1 (C57BL/6J) Huntington's disease transgenic mice, Brain Res. Bull. (2011), doi:10.1016/j.brainresbull.2011.01.010.
[13] R.J. Carter, L.A. Lione, T. Humby, L. Mangiarini, A. Mahal, G.P. Bates, S.B. Dunnett, A.J. Morton, Characterization of progressive motor deficits in mice transgenic for the human Huntington's disease mutation, J. Neurosci. 19 (1999) 3248–3257.
[14] M. Damiano, L. Galvan, N. Deglon, E. Brouillet, Mitochondria in Huntington's disease, Biochim. Biophys. Acta 1802 (2010) 52–61.
[15] S.W. Davies, M. Turmaine, B.A. Cozens, M. DiFiglia, A.H. Sharp, C.A. Ross, E. Scherzinger, E.E. Wanker, L. Mangiarini, G.P. Bates, Formation of neuronal intranuclear inclusions underlies the neurological dysfunction in mice transgenic for the HD mutation, Cell 90 (1997) 537–548.
[16] M. Deschepper, B. Hoogendoorn, S. Brooks, S.B. Dunnett, L. Jones, Proteomic changes in the brains of Huntington's disease mouse models reflect pathology and implicate mitochondrial changes, Brain Res. Bull. (2011), doi:10.1016/j.brainresbull.2011.01.012.
[17] M. DiFiglia, E. Sapp, K.O. Chase, S.W. Davies, G.P. Bates, J.P. Vonsattel, N. Aronin, Aggregation of huntingtin in neuronal intranuclear inclusions and dystrophic neurites in brain, Science 277 (1997) 1990–1993.
[18] S. Galatioto, Immunohistochemical findings in Huntington's Chorea: report of 9 cases, Pathologica 88 (1996) 491–499.
[19] N. Georgiou, J.L. Bradshaw, E. Chiu, A. Tudor, L. O'Gorman, J.G. Phillips, Differential clinical and motor control function in a pair of monozygotic twins with Huntington's disease, Mov. Disord. 14 (1999) 320–325.
[20] A.M. Gorman, Neuronal cell death in neurodegenerative diseases: recurring themes around protein handling, J. Cell Mol. Med. 12 (2008) 2263–2280.
[21] I. Gourfinkel-An, G. Cancel, C. Duyckaerts, B. Faucheux, J.J. Hauw, Y. Trottier, A. Brice, Y. Agid, E.C. Hirsch, Neuronal distribution of intranuclear inclusions in Huntington's disease with adult onset, Neuroreport 9 (1998) 1823–1826.
[22] G.A. Graveland, R.S. Williams, M. DiFiglia, Evidence for degenerative and regenerative changes in neostriatal spiny neurons in Huntington's disease, Science 227 (1985) 770–773.
[23] H.E. Grote, N.D. Bull, M.L. Howard, A. van Dellen, C. Blakemore, P.F. Bartlett, A.J. Hannan, Cognitive disorders and neurogenesis deficits in Huntington's disease mice are rescued by fluoxetine, Eur. J. Neurosci. 22 (2005) 2081–2088.
[24] J.F. Gusella, M.E. MacDonald, Huntington's disease: the case for genetic modifiers, Genome Med. 1 (2009) 80.
[25] C.A. Gutekunst, S.H. Li, H. Yi, J.S. Mulroy, S. Kuemmerle, R. Jones, D. Rye, R.J. Ferrante, S.M. Hersch, X.J. Li, Nuclear and neuropil aggregates in Huntington's disease: relationship to neuropathology, J. Neurosci. 19 (1999) 2522–2534.
[26] O. Hansson, E. Guatteo, N.B. Mercuri, G. Bernardi, X.J. Li, R.F. Castilho, P. Brundin, Resistance to NMDA toxicity correlates with appearance of nuclear inclusions, behavioural deficits and changes in calcium homeostasis in mice transgenic for exon 1 of the huntington gene, Eur. J. Neurosci. 14 (2001) 1492–1504.
[27] M.Y. Heng, D.K. Duong, R.L. Albin, S.J. Tallaksen-Greene, J.M. Hunter, M.J. Lesort, A. Osmand, H.L. Paulson, P.J. Detloff, Early autophagic response in a novel knock-in model of Huntington disease, Hum. Mol. Genet. 19 (2010) 3702–3720.
[28] Y.O. Herishanu, R. Parvari, Y. Pollack, I. Shelef, B. Marom, T. Martino, M. Cannella, F. Squitieri, Huntington disease in subjects from an Israeli Karaite community carrying alleles of intermediate and expanded CAG repeats in the HTT gene: Huntington disease or phenocopy? J. Neurol. Sci. 277 (2009) 143–146.
[29] A.K. Ho, B.J. Sahakian, R.G. Brown, R.A. Barker, J.R. Hodges, M.N. Ane, J. Snowden, J. Thompson, T. Esmonde, R. Gentry, J.W. Moore, T. Bodner, Profile of cognitive progression in early Huntington's disease, Neurology 61 (2003) 1702–1706.
[30] L.W. Ho, J. Carmichael, J. Swartz, A. Wyttenbach, J. Rankin, D.C. Rubinsztein, The molecular biology of Huntington's disease, Psychol. Med. 31 (2001) 3–14.
[31] A. Hodges, G. Hughes, S. Brooks, L. Elliston, P. Holmans, S.B. Dunnett, L. Jones, Brain gene expression correlates with changes in behavior in the R6/1 mouse model of Huntington's disease, Genes Brain Behav. 7 (2008) 288–299.
[32] D.V. Jeste, L. Barban, J. Parisi, Reduced Purkinje cell density in Huntington's disease, Exp. Neurol. 85 (1984) 78–86.
[33] J.F.R. Kerr, G.G. Gobe, C.M. Winterford, B.V. Harmon, Anatomical methods in cell death, in: L.M. Schwartz, B.A. Osborno (Eds.), Methods in Cell Biology, Academic Press Inc., San Diego, 1995, pp. 1–27.
[34] J.F. Kerr, A.H. Wyllie, A.R. Currie, Apoptosis: a basic biological phenomenon with wide-ranging implications in tissue kinetics, Br. J. Cancer 26 (1972) 239–257.

Please cite this article in press as: Z. Bayram-Weston, et al., Light and electron microscopic characterization of the evolution of cellular pathology in the R6/1 Huntington's disease transgenic mice, Brain Res. Bull. (2011), doi:10.1016/j.brainresbull.2011.07.009

[35] J. Kim, J.P. Moody, C.K. Edgerly, O.L. Bordiuk, K. Cormier, K. Smith, M.F. Beal, R.J. Ferrante, Mitochondrial loss, dysfunction and altered dynamics in Huntington's disease, Hum. Mol. Genet. 19 (2010) 3919–3935.
[36] I. Kim, W. Xu, J.C. Reed, Cell death and endoplasmic reticulum stress: disease relevance and therapeutic opportunities, Nat. Rev. Drug Discov. 7 (2008) 1013–1030.
[37] S.C. Kirkwood, E. Siemers, M.E. Hodes, P.M. Conneally, J.C. Christian, T. Foroud, Subtle changes among presymptomatic carriers of the Huntington's disease gene, J. Neurol. Neurosurg. Psychiatry 69 (2000) 773–779.
[38] A.D. Lawrence, J.R. Hodges, A.E. Rosser, A. Kershaw, C. ffrench-Constant, D.C. Rubinsztein, T.W. Robbins, B.J. Sahakian, Evidence for specific cognitive deficits in preclinical Huntington's disease, Brain 121 (Pt 7) (1998) 1329–1341.
[39] S.E. Lazic, H.E. Grote, C. Blakemore, A.J. Hannan, A. van Dellen, W. Phillips, R.A. Barker, Neurogenesis in the R6/1 transgenic mouse model of Huntington's disease: effects of environmental enrichment, Eur. J. Neurosci. 23 (2006) 1829–1838.
[40] J. Legleiter, G.P. Lotz, J. Miller, J. Ko, C. Ng, G.L. Williams, S. Finkbeiner, P.H. Patterson, P.J. Muchowski, Monoclonal antibodies recognize distinct conformational epitopes formed by polyglutamine in a mutant huntingtin fragment, J. Biol. Chem. 284 (2009) 21647–21658.
[41] J. Lemiere, M. Decruyenaere, G. Evers-Kiebooms, E. Vandenbussche, R. Dom, Cognitive changes in patients with Huntington's disease (HD) and asymptomatic carriers of the HD mutation—a longitudinal follow-up study, J. Neurol. 251 (2004) 935–942.
[42] H. Li, T. Wyman, Z.X. Yu, S.H. Li, X.J. Li, Abnormal association of mutant huntingtin with synaptic vesicles inhibits glutamate release, Hum. Mol. Genet. 12 (2003) 2021–2030.
[43] C.H. Lin, S. Tallaksen-Greene, W.M. Chien, J.A. Cearley, W.S. Jackson, A.B. Crouse, S. Ren, X.J. Li, R.L. Albin, P.J. Detloff, Neurological abnormalities in a knock-in mouse model of Huntington's disease, Hum. Mol. Genet. 10 (2001) 137–144.
[44] L.A. Lione, R.J. Carter, M.J. Hunt, G.P. Bates, A.J. Morton, S.B. Dunnett, Selective discrimination learning impairments in mice expressing the human Huntington's disease mutation, J. Neurosci. 19 (1999) 10428–10437.
[45] A. Lloret, E. Dragileva, A. Teed, J. Espinola, E. Fossale, T. Gillis, E. Lopez, R.H. Myers, M.E. MacDonald, V.C. Wheeler, Genetic background modifies nuclear mutant huntingtin accumulation and HD CAG repeat instability in Huntington's disease knock-in mice, Hum. Mol. Genet. 15 (2006) 2015–2024.
[46] M.L. Maat-Schieman, J.C. Dorsman, M.A. Smoor, S. Siesling, S.G. Van Duinen, J.J. Verschuuren, J.T. den Dunnen, G.J. van Ommen, R.A. Roos, Distribution of inclusions in neuronal nuclei and dystrophic neurites in Huntington disease brain, J. Neuropathol. Exp. Neurol. 58 (1999) 129–137.
[47] M. Maat-Schieman, R. Roos, M. Losekoot, J. Dorsman, C. Welling-Graafland, I. Hegeman-Kleinn, F. Broeyer, M. Breuning, S. van Duinen, Neuronal intranuclear and neuropil inclusions for pathological assessment of Huntington's disease, Brain Pathol. 17 (2007) 31–37.
[48] G. Majno, I. Joris, Apoptosis, oncosis, and necrosis: an overview of cell death, Am. J. Pathol. 146 (1995) 3–15.
[49] L. Mangiarini, K. Sathasivam, A. Mahal, R. Mott, M. Seller, G.P. Bates, Instability of highly expanded CAG repeats in mice transgenic for the Huntington's disease mutation, Nat. Genet. 15 (1997) 197–200.
[50] L. Mangiarini, K. Sathasivam, M. Seller, B. Cozens, A. Harper, C. Hetherington, M. Lawton, Y. Trottier, H. Lehrach, S.W. Davies, G.P. Bates, Exon 1 of the HD gene with an expanded CAG repeat is sufficient to cause a progressive neurological phenotype in transgenic mice, Cell 87 (1996) 493–506.
[51] M. Martinez-Vicente, Z. Talloczy, E. Wong, G. Tang, H. Koga, S. Kaushik, R. de Vries, E. Arias, S. Harris, D. Sulzer, A.M. Cuervo, Cargo recognition failure is responsible for inefficient autophagy in Huntington's disease, Nat. Neurosci. 13 (2010) 567–576.
[52] L.B. Menalled, J.D. Sison, Y. Wu, M. Olivieri, X.J. Li, H. Li, S. Zeitlin, M.F. Chesselet, Early motor dysfunction and striosomal distribution of huntingtin microaggregates in Huntington's disease knock-in mice, J. Neurosci. 22 (2002) 8266–8276.
[53] J. Miller, M. Arrasate, B.A. Shaby, S. Mitra, E. Masliah, S. Finkbeiner, Quantitative relationships between huntingtin levels, polyglutamine length, inclusion body formation, and neuronal death provide novel insight into huntington's disease molecular pathogenesis, J. Neurosci. 30 (2010) 10541–10550.
[54] A.J. Milnerwood, D.M. Cummings, G.M. Dallerac, J.Y. Brown, S.C. Vatsavayai, M.C. Hirst, P. Rezaie, K.P. Murphy, Early development of aberrant synaptic plasticity in a mouse model of Huntington's disease, Hum. Mol. Genet. 15 (2006) 1690–1703.
[55] A.J. Morton, D. Glynn, W. Leavens, Z. Zheng, R.L. Faull, J.N. Skepper, J.M. Wight, Paradoxical delay in the onset of disease caused by super-long CAG repeat expansions in R6/2 mice, Neurobiol. Dis. 33 (2009) 331–341.
[56] B. Naver, C. Stub, M. Moller, K. Fenger, A.K. Hansen, L. Hasholt, S.A. Sorensen, Molecular and behavioral analysis of the R6/1 Huntington's disease transgenic mouse, Neuroscience 122 (2003) 1049–1057.
[57] J. Nithianantharajah, C. Barkus, M. Murphy, A.J. Hannan, Gene–environment interactions modulating cognitive function and molecular correlates of synaptic plasticity in Huntington's disease transgenic mice, Neurobiol. Dis. 29 (2008) 490–504.
[58] G. Paxinos, K.B.J. Franklin, The Mouse Brain in Stereotaxic Coordinates, 2nd ed., Academic Press, San Diego, CA, 2001.
[59] A. Petersen, K. Chase, Z. Puschban, M. DiFiglia, P. Brundin, N. Aronin, Maintenance of susceptibility to neurodegeneration following intrastriatal injections of quinolinic acid in a new transgenic mouse model of Huntington's disease, Exp. Neurol. 175 (2002) 297–300.
[60] A. Petersen, Z. Puschban, J. Lotharius, B. NicNiocaill, P. Wiekop, W.T. O'Connor, P. Brundin, Evidence for dysfunction of the nigrostriatal pathway in the R6/1 line of transgenic Huntington's disease mice, Neurobiol. Dis. 11 (2002) 134–146.
[61] B. Ravikumar, C. Vacher, Z. Berger, J.E. Davies, S. Luo, L.G. Oroz, F. Scaravilli, D.F. Easton, R. Duden, C.J. O'Kane, D.C. Rubinsztein, Inhibition of mTOR induces autophagy and reduces toxicity of polyglutamine expansions in fly and mouse models of Huntington disease, Nat. Genet. 36 (2004) 585–595.
[62] P.H. Reddy, M. Williams, V. Charles, L. Garrett, L. Pike-Buchanan, W.O. Whetsell Jr., G. Miller, D.A. Tagle, Behavioural abnormalities and selective neuronal loss in HD transgenic mice expressing mutated full-length HD cDNA, Nat. Genet. 20 (1998) 198–202.
[63] R.A. Rodda, Cerebellar atrophy in Huntington's disease, J. Neurol. Sci. 50 (1981) 147–157.
[64] H.D. Rosas, W.J. Koroshetz, Y.I. Chen, C. Skeuse, M. Vangel, M.E. Cudkowicz, K. Caplan, K. Marek, L.J. Seidman, N. Makris, B.G. Jenkins, J.M. Goldstein, Evidence for more widespread cerebral pathology in early HD: an MRI-based morphometric analysis, Neurology 60 (2003) 1615–1620.
[65] C.A. Ross, Intranuclear neuronal inclusions: a common pathogenic mechanism for glutamine-repeat neurodegenerative diseases? Neuron 19 (1997) 1147–1150.
[66] C.A. Ross, M.W. Becher, V. Colomer, S. Engelender, J.D. Wood, A.H. Sharp, Huntington's disease and dentatorubral-pallidoluysian atrophy: proteins, pathogenesis and pathology, Brain Pathol. 7 (1997) 1003–1016.
[67] D.C. Rubinsztein, The roles of intracellular protein-degradation pathways in neurodegeneration, Nature 443 (2006) 780–786.
[68] D.C. Rubinsztein, J. Leggo, R. Coles, E. Almqvist, V. Biancalana, J.J. Cassiman, K. Chotai, M. Connarty, D. Crauford, A. Curtis, D. Curtis, M.J. Davidson, A.M. Differ, C. Dode, A. Dodge, M. Frontali, N.G. Ranen, O.C. Stine, M. Sherr, M.H. Abbott, M.L. Franz, C.A. Graham, P.S. Harper, J.C. Hedreen, M.R. Hayden, Phenotypic characterization of individuals with 30–40 CAG repeats in the Huntington disease (HD) gene reveals HD cases with 36 repeats and apparently normal elderly individuals with 36–39 repeats, Am. J. Hum. Genet. 59 (1996) 16–22.
[69] D.C. Rubinsztein, A. Wyttenbach, J. Rankin, Intracellular inclusions pathological markers in diseases caused by expanded polyglutamine tracts? J. Med. Genet. 36 (1999) 265–270.
[70] H.H. Ruocco, I. Lopes-Cendes, L.M. Li, M. Santos-Silva, F. Cendes, Striatal and extrastriatal atrophy in Huntington's disease and its relationship with length of the CAG repeat, Braz. J. Med. Biol. Res. 39 (2006) 1129–1136.
[71] E. Sapp, C. Schwarz, K. Chase, P.G. Bhide, A.B. Young, J. Penney, J.P. Vonsattel, N. Aronin, M. DiFiglia, Huntingtin localization in brains of normal and Huntington's disease patients, Ann. Neurol. 42 (1997) 604–612.
[72] F. Saudou, S. Finkbeiner, D. Devys, M.E. Greenberg, Huntingtin acts in the nucleus to induce apoptosis but death does not correlate with the formation of intranuclear inclusions, Cell 95 (1998) 55–66.
[73] U. Shirendeb, A.P. Reddy, M. Manczak, M.J. Calkins, P. Mao, D.A. Tagle, R.P. Hemachandra, Abnormal mitochondrial dynamics, mitochondrial loss and mutant huntingtin oligomers in Huntington's disease: implications for selective neuronal damage, Hum. Mol. Genet. 20 (2011) 1438–1455.
[74] S.S. Sisodia, Nuclear inclusions in glutamine repeat disorders: are they pernicious coincidental, or beneficial? Cell 95 (1998) 1–4.
[75] E.C. Stack, J.K. Kubilus, K. Smith, K. Cormier, S.J. Del Signore, E. Guelin, H. Ryu, S.M. Hersch, R.J. Ferrante, Chronology of behavioral symptoms and neuropathological sequela in R6/2 Huntington's disease transgenic mice, J. Comp. Neurol. 490 (2005) 354–370.
[76] The Huntington's Disease Collaborative Research Group, A novel gene containing a trinucleotide repeat that is expanded and unstable on Huntington's disease chromosomes, Cell 72 (1993) 971–983.
[77] M. Turmaine, A. Raza, A. Mahal, L. Mangiarini, G.P. Bates, S.W. Davies, Nonapoptotic neurodegeneration in a transgenic mouse model of Huntington's disease, Proc. Natl. Acad. Sci. U.S.A. 97 (2000) 8093–8097.
[78] K. van der Borght, P. Brundin, Reduced expression of PSA-NCAM in the hippocampus and piriform cortex of the R6/1 and R6/2 mouse models of Huntington's disease, Exp. Neurol. 204 (2007) 473–478.
[79] J.M. Van Raamsdonk, M. Metzler, E. Slow, J. Pearson, C. Schwab, J. Carroll, R.K. Graham, B.R. Leavitt, M.R. Hayden, Phenotypic abnormalities in the YAC128 mouse model of Huntington disease are penetrant on multiple genetic backgrounds and modulated by strain, Neurobiol. Dis. 26 (2007) 189–200.
[80] J.M. Van Raamsdonk, Z. Murphy, E.J. Slow, B.R. Leavitt, M.R. Hayden, Selective degeneration and nuclear localization of mutant huntingtin in the YAC128 mouse model of Huntington disease, Hum. Mol. Genet. 14 (2005) 3823–3835.
[81] M. Vila, S. Przedborski, Targeting programmed cell death in neurodegenerative diseases, Nat. Rev. Neurosci. 4 (2003) 365–375.
[82] J.P. Vonsattel, R.H. Myers, T.J. Stevens, R.J. Ferrante, E.D. Bird, E.P. Richardson, Neuropathological classification of Huntington's disease, J. Neuropathol. Exp. Neurol. 44 (1985) 559–577.
[83] V.C. Wheeler, J.K. White, C.A. Gutekunst, V. Vrbanac, M. Weaver, X.J. Li, S.H. Li, H. Yi, J.P. Vonsattel, J.F. Gusella, S. Hersch, W. Auerbach, A.L. Joyner, M.E. MacDonald, Long glutamine tracts cause nuclear localization of a novel form of huntingtin in medium spiny striatal neurons in HdhQ92 and HdhQ111 knock-in mice, Hum. Mol. Genet. 9 (2000) 503–513.
[84] A. Yamamoto, J.J. Lucas, R. Hen, Reversal of neuropathology and motor dysfunction in a conditional model of Huntington's disease, Cell 101 (2000) 57–66.

Please cite this article in press as: Z. Bayram-Weston, et al., Light and electron microscopic characterization of the evolution of cellular pathology in the R6/1 Huntington's disease transgenic mice, Brain Res. Bull. (2011), doi:10.1016/j.brainresbull.2011.07.009

Chapter 4

Paper 2

Light and electron microscopic characterization of the evolution of cellular pathology in YAC128 Huntington's disease transgenic mice

Bayram-Weston Z, Jones L., Dunnett S.B., Brooks S.P

Brain Res Bull. 2011, In press.

Brain Research Bulletin xxx (2011) xxx–xxx

Contents lists available at ScienceDirect

Brain Research Bulletin

journal homepage: www.elsevier.com/locate/brainresbull

Research report

Light and electron microscopic characterization of the evolution of cellular pathology in YAC128 Huntington's disease transgenic mice

Zubeyde Bayram-Weston[a,*], Lesley Jones[b], Stephen B. Dunnett[a], Simon P. Brooks[a]

[a] School of Biosciences, Cardiff University, Museum Avenue, Cardiff CF10 3AX, Wales, UK
[b] Department of Psychological Medicine, 2nd Floor, Henry Wellcome Building, Wales School of Medicine, Cardiff University, Cardiff CF14 4XN, Wales, UK

ARTICLE INFO

Article history:
Received 9 February 2011
Received in revised form 21 April 2011
Accepted 8 May 2011
Available online xxx

Keywords:
Huntington's disease
Aggregations
Inclusions
YAC128 transgenic mouse line
Electron microscopy

ABSTRACT

Huntington's disease (HD) is a progressive neurodegenerative disease caused by the insertion of an expanded polyglutamine sequence within the huntingtin protein. This mutation induces the formation of abnormal protein fragment aggregations and intra-nuclear neuronal inclusions in the brain. The present study aimed to produce a detailed longitudinal characterization of the neuronal pathology in the YAC128 transgenic mouse brain, to determine the similarity of this mouse model to other mouse models and the human condition in the spatial and temporal deposition pattern of the mutant protein fragments. Brain samples were taken from mice aged between 4 and 27 months of age, and assessed using S830 and GFAP immunohistochemistry, stereology and electron microscopy.

Four month old mice did not exhibit intra-nuclear or extra-nuclear inclusions using the S830 antibody. Diffuse nuclear staining was present in the cortex, hippocampus and cerebellum from 6 months of age onwards. By 15 months of age, intra-nuclear inclusions were visible in most brain regions including nucleus accumbens, ventral striatum, lateral striatum, motor cortex, sensory cortex and cerebellum. The ventral striatum had a greater density of inclusions than the dorsal striatum. At 15 and 24 months of age, the mice showed increased reactive astrogliosis in the cortex, but no differences were found in the striatum.

Necrotic cell death with vacuolation, uneven cell membrane and degenerated Golgi apparatus were detected ultrastructurally at 14 months of age, with some cells showing signs of apoptosis. By 26 months of age, most cells were degenerated in the transgenic animals, with lipofuscin granules being more abundant and larger in these mice than in their wildtype littermates. Our results demonstrate a progressive and widespread neuropathology in the YAC128 mice line that shares some similarity to the human condition.

This article is part of a Special Issue entitled 'HD Transgenic Mouse'.

1. Introduction

Huntington disease (HD) is a neurodegenerative disorder characterized by progressive cognitive, psychiatric and motor symptoms. The disease progresses to death 15–20 years after the onset of the symptoms [2]. Studies of HD brains have shown that there is a correlation among the age of symptom onset, CAG repeat length and the atrophy of the striatum [6,46]. However, the disease symptoms may be heterogeneously expressed regardless of CAG repeat length [24]. Other factors such as environmental and genetic components also thought to contribute to the age of onset [79]. Neuroimaging techniques have revealed correlations between striatal and cortical atrophy with cognitive impairment [43]. The neocortex and the striatum (caudate nucleus and putamen) are thought to be the first affected brain regions because these regions exhibit the most extensive atrophy and cell loss [22,77,78]. With the pathological changes in the striatum developing in caudo-rostral, dorso-ventral and medio-lateral directions [78].

The presence of protein aggregates/intra-nuclear inclusions (NIIs) is a neuropathological hallmark of the HD brain and has also been widely reported in transgenic mice and knock-in mouse models [16,19,34,44]. The contribution of aggregate formation in disease pathology is still controversial with regards to whether the aggregates are toxic, pro-survival or have no consequence to the cell [52,59,61–63,66]. A study by Yang and colleagues indicated that NIIs are highly toxic to the cell nucleus [81], and inhibition of aggregate formation in R6/2 transgenic mouse model of HD has been shown to have beneficial effects on survival, weight loss and motor function [60]. Further, a study that compared the effects of aggregate localization in polyglutamine peptides with 20 and 42

* Corresponding author. Tel.: +44 02920874684; fax: +44 029 20 876749.
E-mail address: Bayram-WestonZ@cardiff.ac.uk (Z. Bayram-Weston).

0361-9230/$ – see front matter © 2011 Elsevier Inc. All rights reserved.
doi:10.1016/j.brainresbull.2011.05.005

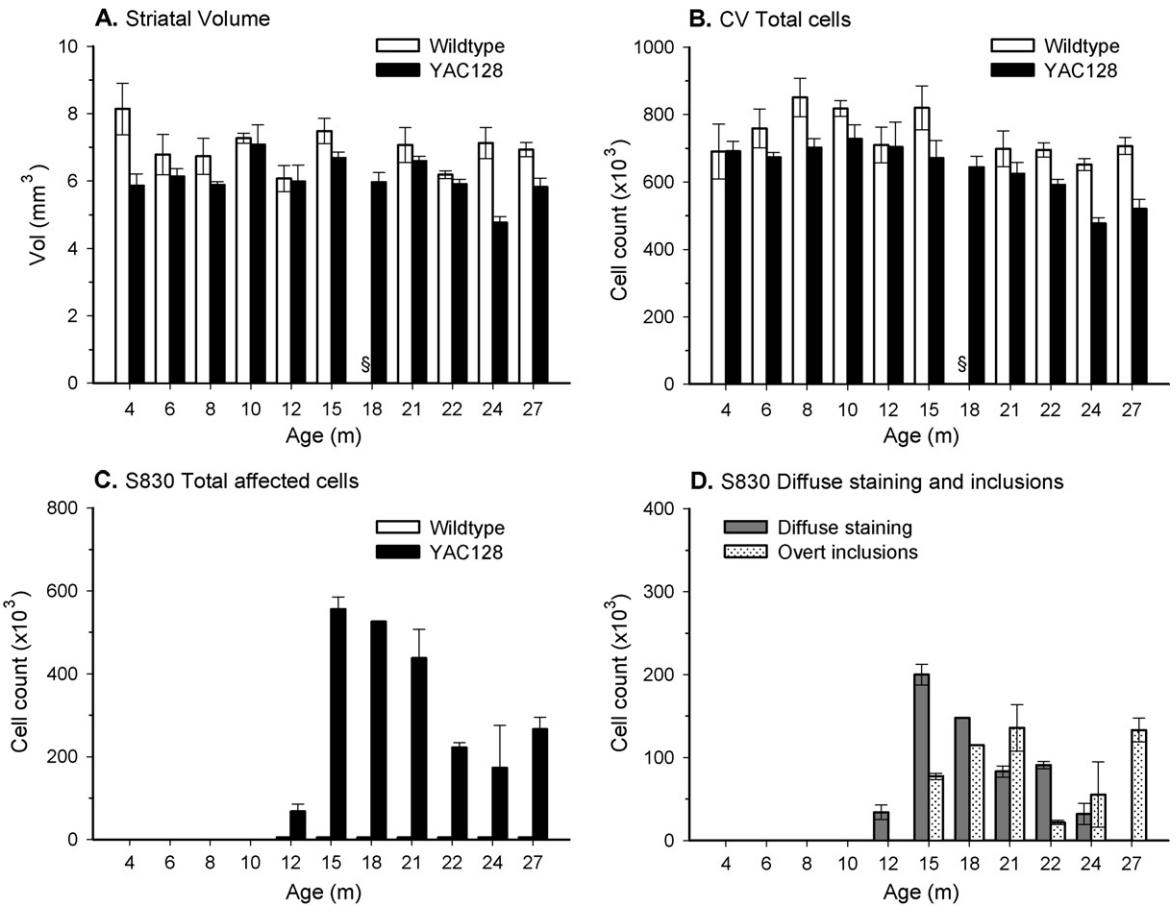

Fig. 1. The striatal volume in YAC128 mouse. The volume of the striatum was decreased in YAC128 mice compared with the wildtype mice (A). Neuronal cell loss in the striatum in YAC128 mice when compared with their controls with age (B). The total number of affected cells was highest at 15 months of age, after which point the number of affected cells decreased (C). The total number of affected cells with the S830 antibody which showed diffuse nuclear staining and inclusions. Nuclear inclusions were present at 15 months, and their number increased until 21 months and decreased by 24 months of age. §Data lost due to failure in tissue processing (D).

CAG repeats demonstrated that the fibrillar forms of both polyglutamine peptides were not toxic in the cytoplasm, however, they lead to cell death when directed to the nucleus [11,12,81].

There is still an incomplete understanding of the cellular and molecular mechanisms underlying neuronal death in HD. Animal models of the disease provide the opportunity to determine the role of protein aggregation and NII formation in the development of the disease. The YAC128 mouse contains the full length human HD gene, including the entire regulatory element [68,74]. These mice develop motor abnormalities from 3 months of age with increased activity in open field test, followed by increased motor impairment by 6 months of age. Some striatal atrophy was present at 9 months of age, by 12 months of age cortical atrophy was also found to be present [68]. In these mice NIIs were not observed until 18 months of age [68], many months after the initial symptom were demonstrated. However, high nuclear immunoreactivity from 2 months onwards was a clear indicator of neuropathology [68,74,75].

In the present study we sought to define the spatial and temporal development of neuronal pathology in the (C57BL/6J) YAC128 mouse, through the examination and quantification of tissue samples taken from mice undergoing a longitudinal behavioural assessment.

2. Materials and methods

2.1. Animals

In the present study, 97 mice were used at 4 months = 9; 6 months = 10; 8 months = 8; 10 months = 10; 12 months = 10; 15 months = 8; 18 months = 5; 21 months = 7; 22 months = 10; 24 months = 10; 27 months = 10 for histology. Fifty-one of these mice (28 male, 23 female) were YAC128 hemizygote transgenic mice with their 46 wildtype (23 male, 23 female). An additional 8 mice were used for the electron microscopic examination at 14 months and 26 months of age (YAC128 = 2 male, 2 female; wildtype = 2 male, 2 female) at 14 months and 26 months of age. The mice were obtained from the Hayden laboratory on a FVB/N background (University of British Columbia, Vancouver, Canada) and subsequently back-crossed onto and maintained on a C57BL/6J (Harlan, UK) background over more than 10 generations. This mouse model has ~128 CAG repeats of human htt randomly inserted into its genome via a yeast artificial chromosome [68]. The mice were housed in cages of up to 6 mice, under a 12 h light–dark cycle (lights on 07:00: lights off 19:00), with access to food and water *ad libitum*. Each mouse had undergone regular behavioural testing for up to two years [8]. All animal experiments were performed in compliance with local ethical review and licences held under the UK Animals (Scientific Procedures) Act 1986.

2.2. Histology

Four to five animals were sacrificed at 2–3 month intervals from 4 months to 27 months of age. The mice were terminally anaesthetized by intraperitoneal administration of 0.2 ml sodium pentobarbital (Euthatal) and transcardially perfused with a prewash solution of approx. 100 ml phosphate-buffered saline (PBS, pH 7.4) for 3 min, followed by approx. 150 ml 4% paraformaldehyde (PFA) solution (Fisher Scientific, Loughborough, UK), pH 7.4 for 5 min. The brains were then removed, post fixed in 4% PFA for 4 h and transferred to 25% sucrose in prewash solution until they sank. The brains were sectioned coronally at 40 μm thickness in series of 1:6 using a freezing-stage microtome (Leitz Bright Series 8000, Germany) and the sections were stored in cryoprotective solution in 96-well plates in the freezer at −20 °C.

2.3. Cresyl fast violet (CV)

Brain sections (one in six series) were stained using the standard Nissl stain, cresyl fast violet for morphological and stereological analysis. The sections were mounted on glass microscope slides (Fisher Scientific), previously double-coated

Please cite this article in press as: Z. Bayram-Weston, et al., Light and electron microscopic characterization of the evolution of cellular pathology in YAC128 Huntington's disease transgenic mice, Brain Res. Bull. (2011), doi:10.1016/j.brainresbull.2011.05.005

Table 1
YAC128 transgenic mice. Formation, progression and distribution of intra-nuclear inclusions (NIIs).

YAC128 brain	Ages										
	4 M	6 M	8 M	10 M	12 M	15 M	18 M	21 M	22 M	24 M	27 M
Olfactory tubercle	0	0	0	0	+/++	++	++	+++	+++	++++	++++
Nucleus accumbens	0	0	0	0	0	+++	++	+++	+	0/+++	+++
Globus pallidus-lateral	0	0	0	0	+	+	0	+	0	+	0/+
Globus pallidus-medial	0	0	0	0	+	+	0	+	0	0	0
Striatum ventral	0	0/+	0	0	+/++	+++	+++	++++	+/+++	+++	+++/++++
Striatum dorsal	0	0	0	0	0/+	++	+	+++	0	0/++	0/+++
Striatum lateral	0	0/+	0	0	+/++	+++	+++	++++	+/+++	0/+++	++++
Striatum medial	0	0/+	0	0	0	++	+	+++	0	0/+/+++	0/+++
Septum lateral	0	0	0	0	+	++	+	+	0	+++	0/+
Septum med	0	0	0	0	+	++	+	+	0	+	0/+
Amygdala BL	0	0/+	0	0	+	++	++	++	+	+	++
Amygdala CL	0	0/+	0	0	+	++	++	++	+	+	++
Thalamus	0	0/+	0	0	+/++	++	+/++	+/++	+	+/++	0/+
Hypothalamus	0	0	0	0	+	+	0/+	+	+/++	+	+
Cerebellum	0	+	+	+	++	++++	++++	++++	++++	++++	++++
Hippocampus	0	0/+	0/+	0/+	0/+	0/++	+/++	0/+++	+/++/+++	0/+/++++	+/++/++++
Motor cortex	0	0/+	0/+	0/+	+/++	+/++/+++	+/++	+/++/+++	+/++/++	+/++/++++	++/+++/++++
Sensory cortex	0	0/+	0/+	0/+	+/++	+/++/+++	+/++	+/++/+++	+/++/+++	+/++/++++	++/+++/++++
Piriform cortex	0	+	+	+	+	++	++	+++	+++	+++	++++

0: absent; +: nuclear staining; ++: diffuse nuclear staining; +++: minimum inclusions; ++++: dense inclusions.

with 1% gelatin, and allowed to dry. The sections were delipidised in increasing levels of alcohol from 70% to 95% and then 100% for 10 min each, followed by 1 h in xylene and then decreasing alcohols for 10 min each from 100% to 95% to 70% and then distilled water, before incubation in the cresyl violet (0.7% in distilled water with 0.5% sodium acetate, Sigma, Hertfordshire, UK) for 5 min. Stained sections were rinsed in distilled water, dehydrated in the graded series of ethanols and then cleared in xylene (VWR, Darmstadt, Germany) before coverslips were mounted using DPX mounting medium (RA Lamb, Hambridge, Somerset, UK). The section were analysed under a Leica DMRBE microscope (Leica, Wetzlar, Germany).

2.4. Immunohistochemistry (IHC)

Immunohistochemistry was carried out following the same protocol as Bayram-Weston et al. [5]. The staining was carried out on a one in six series of sections of each animal. Free-floating sections were processed for IHC using the sheep anti-S830 (a gift from Prof. Gill Bates, Kings College, London, UK) which recognizes the N terminal region to 53Q of exon 1 of mutant huntingtin [34,41], and rabbit anti-GFAP (DAKO, UK) which detects astrocytes and measures reactive astrogliosis [53]. The sections were rinsed in TRIS Buffered Saline (TBS), pH 7.4 and endogenous peroxidase activity was reduced by a 3% H_2O_2 (VWR, Germany) in methanol at room temperature for 5 min. Subsequently, the sections were treated with 3% horse serum in TBS for 1 h, followed by incubation of S830 antibody (diluted 1:25,000) or GFAP antibody (1:2000) overnight. After rinsing in TBS, the sections were incubated with a horse anti-goat or horse anti-rabbit secondary antibody, respectively (diluted 1:200, Vector Laboratories, Burlingame, CA, USA). The sites of antibody biding were detected using a biotin-streptavidin kit, according to the manufacturer's instructions (Vector Laboratories) and the peroxidase activity was visualized with 3,3′-diaminobenzidine (DAB) (Sigma–Aldrich, Poole, Dorset, UK). Thereafter, the sections were mounted on gelatine-coated slides, dehydrated and cover-slipped.

The sections were examined and photographed with a Leica DMRBE microscope fitted with a digital camera (Optronics, Goleta, California, USA) and imaging Software MagnaFire 1.2C (Goleta, CA, USA). All pictures were photographed using the same parameters and saved on computer for further analysis.

A semi-quantitative analysis was used to assess the intensity of specific staining. This included rating the intensity of specific staining in sections: 0 = absent, + = weak nuclear staining; ++ = diffuse nuclear staining; +++ = few/small inclusions; ++++ = many/dense/large inclusions.

2.5. S830/CV stereology

Cell counts were carried out using a PC-based image analysis software (Olympus C.A.S.T. grid system v1.6.) on a Olympus (Denmark) BX50 microscope and 2D counts corrected using the Abercrombie formula [1]. The cells were counted in random regions within a defined volume of the striatum. The counting objective was at 100× and counting frame area was 265 μm^2. Using the formula the total number of cells in the structure per section was calculated. Cell counts were carried out on a 1:6 series of S830-stained, and CV sections, throughout the entire striatum and then assessed blindly to the experimental groups. Total affected cells counted the number of cells displaying positive S830 immunoreactivity. Cell nuclei may also demonstrate diffuse nuclear staining and inclusions, for the purpose of the statistical analyses, these cells are classified as cells with inclusions despite having both.

2.6. Transmission electron microscopy (TEM)

Four mice were sacrificed at 14 months and at 26 months of age and electron microscopy was carried out according to Bayram-Weston et al. [5]. Briefly, animals were anaesthetized with Euthatal and then perfused with 0.9% NaCl, followed by a mixture of 2% PFA and 2% glutaraldehyde solution (pH 7.4). The brains were removed and sectioned into 1–3 mm coronal slides, and then the samples were further dissected into five random specimens from the dorso-lateral striatum under Leica Wild M3Z (Leica, Wetzlar Germany) microscope with razor blade. The tissue samples were post-fixed in 1% osmium tetroxide at +4 °C for 2 h. The samples were then rinsed in distilled water and stained overnight in 0.5% uranyl acetate, dehydrated through a graded series of ethanols and embedded in fresh resin. Ultrathin sections were cut on an ultracut-microtome (Reichert-Jung, Leica UK LTD, Milton Keynes, UK), stained with uranyl acetate followed by Reynold's lead citrate and viewed on a EM 208 transmission electron microscope (Philips, The Netherlands).

2.7. Statistics

Statistical Analyses were performed using one- and two-way ANOVAs using the GenStat statistic programme (VSN International, Hemel Hempsted, UK).

3. Results

3.1. Striatal atrophy and neuronal cell counts

The analyses of the striatal volume in YAC128 transgenic mice and wildtype littermates was calculated from the cresyl violet sections between 4 and 27 months of age. A small but robust reduction in the volume of the striatum in YAC128 mice was demonstrated (Fig. 1A: Genotype; $F_{1,76} = 31.42$, $p < 0.001$). Striatal volume in the YAC128 mice changed with time relatively to the wildtype mice (Genotype × Age; $F_{9,76} = 2.27$, $p < 0.05$), although no clearly progressive pattern of striatal atrophy was observed. In the cresyl violet stained cells, stereological analyses found significant neuronal cell loss in the striatum of the YAC128 mice when compared with their wildtype littermates (Fig. 1B: Genotype, $F_{1,76} = 32.18$, $p < 0.001$). On this measure a decline in cell numbers across age was apparent in both groups (Age; $F_{10,76} = 4.88$, $p < 0.001$) but was not more markedly progressive in the YAC128 mice (Genotype × Age, $F_{9,76} = 1.19$, n.s.).

3.2. Striatal neuronal pathology

The S830 staining showed diffuse nuclear staining and NIIs only in YAC128 mice with the aged matched controls being devoid of immunoreactivity. Intra-nuclear inclusions were absent at 4

Please cite this article in press as: Z. Bayram-Weston, et al., Light and electron microscopic characterization of the evolution of cellular pathology in YAC128 Huntington's disease transgenic mice, Brain Res. Bull. (2011), doi:10.1016/j.brainresbull.2011.05.005

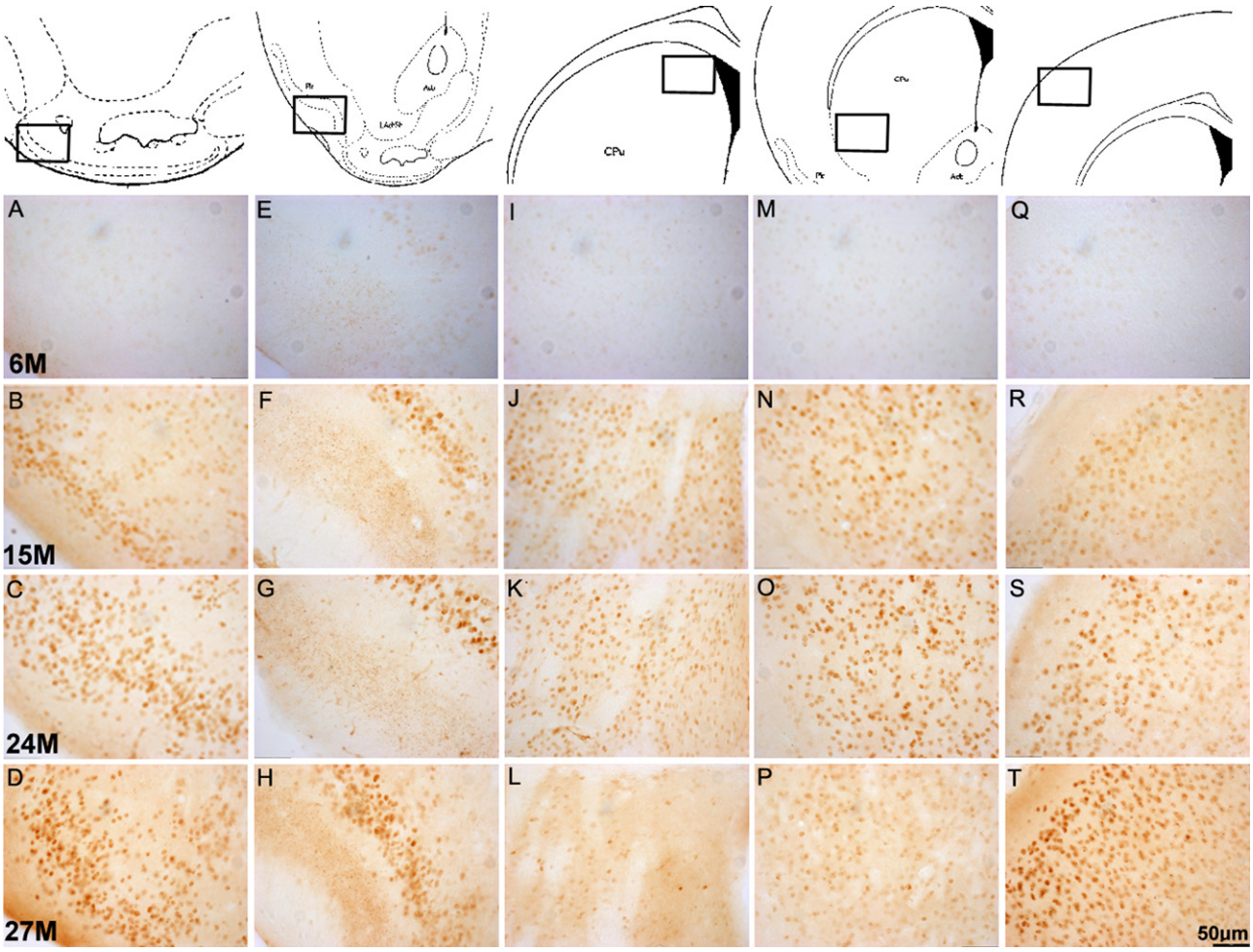

Fig. 2. Temporal progress of S830 immunoreactivity in YAC128 mouse brain. Column 1: olfactory tubercle (A–D), Column 2: piriform cortex (E–H), Column 3: dorsal striatum (I–L), Column 4: ventral striatum (M–P), and Column 5: cortex (Q–T) at 6, 15, 24 and 27 months of age. The development of NIIs is clearly visible in all areas of YAC128 mouse brain.

months of age up to 15 months of age, present at 15 months and abundant at 21 months of age. At 4 months of age we did not observe either diffuse nuclear staining or NIIs in the brain. By 6 months of age, very weak nuclear staining was present but limited to specific brain regions (amygdala, thalamus, cerebellum, hippocampus, cortex and ventral striatum: see Table 1) with some variability between animals. Thus, diffuse nuclear staining first seen in the ventral striatum and amygdala in some animals at 6 months of age was not seen in other animals at 8 and 10 months of age, and only became a stable feature of staining in all animals from 12 months of age. By 12 months of age, the S830 antibody demonstrated diffuse nuclear staining in the majority of the brain regions. By contrast, the aggregation of staining into NIIs was not present until 15 months of age in any of the brain areas. The diffuse nuclear staining appeared in most of the brain regions from this age onwards, including the olfactory tubercle, cortex, thalamus and cerebellum. A minimal number of inclusions were observed in the nucleus accumbens, ventro-lateral striatum and all layers of the cortex. Dense inclusions were limited to the cerebellum at this stage. At 21 months of age, NIIs were distributed widely throughout the striatum, olfactory tubercle, nucleus accumbens, thalamus and piriform cortex along with persistent diffuse nucleus staining. By 24 months of age, the presence of diffuse nuclear staining and NIIs remained region specific (Figs. 2 and 3 and Table 1). The NIIs appeared to be small and round in 21 month old mice. Cell nuclei demonstrating inclusions may also exhibit diffuse nuclear staining (Fig. 4). The results of stereological analyses of the striatum revealed that the total number of affected cells was highest at 15 months of age, after which point the number decreased (Fig. 1C: affected cells, $F_{6,26} = 19.75$, $p < 0.001$). Staining with the S830 antibody indicated that diffuse nuclear staining was present in the striatum at 12 months of age, where the number of affected cells increased up to 15 months of age and then gradually decreased from this point to 24 months of age. The diffuse staining without inclusions was no longer observed in aged animals of 27 month old (Fig. 1D: diffuse nuclear staining, $F_{6,26} = 84.04$, $p < 0.001$). Intra-nuclear inclusions were present at 15 months, and their number increased until 21 months and decreased by 24 months of age, interestingly, by 27 months of age, the number of NIIs was higher again (Fig. 1D: inclusions, $F_{6,26} = 11.68$, $p < 0.001$).

The extra-nuclear inclusions (ENNIs) were not present in the sections of 4 months old YAC128 mice. At 6 months old, ENNIs were present in the thalamus, hypothalamus and cortex and the distribution of ENNIs gradually increased with age. By 27 months, ENNIs were distributed throughout the brain (Table 2).

3.3. GFAP immunostaining

The GFAP immunostaining was increased with age both in carries and control animals, but the distribution of GFAP within transgenic animals did not reveal an increased intensity of GFAP in the striatum when compared to their age matched wildtype litter-

Please cite this article in press as: Z. Bayram-Weston, et al., Light and electron microscopic characterization of the evolution of cellular pathology in YAC128 Huntington's disease transgenic mice, Brain Res. Bull. (2011), doi:10.1016/j.brainresbull.2011.05.005

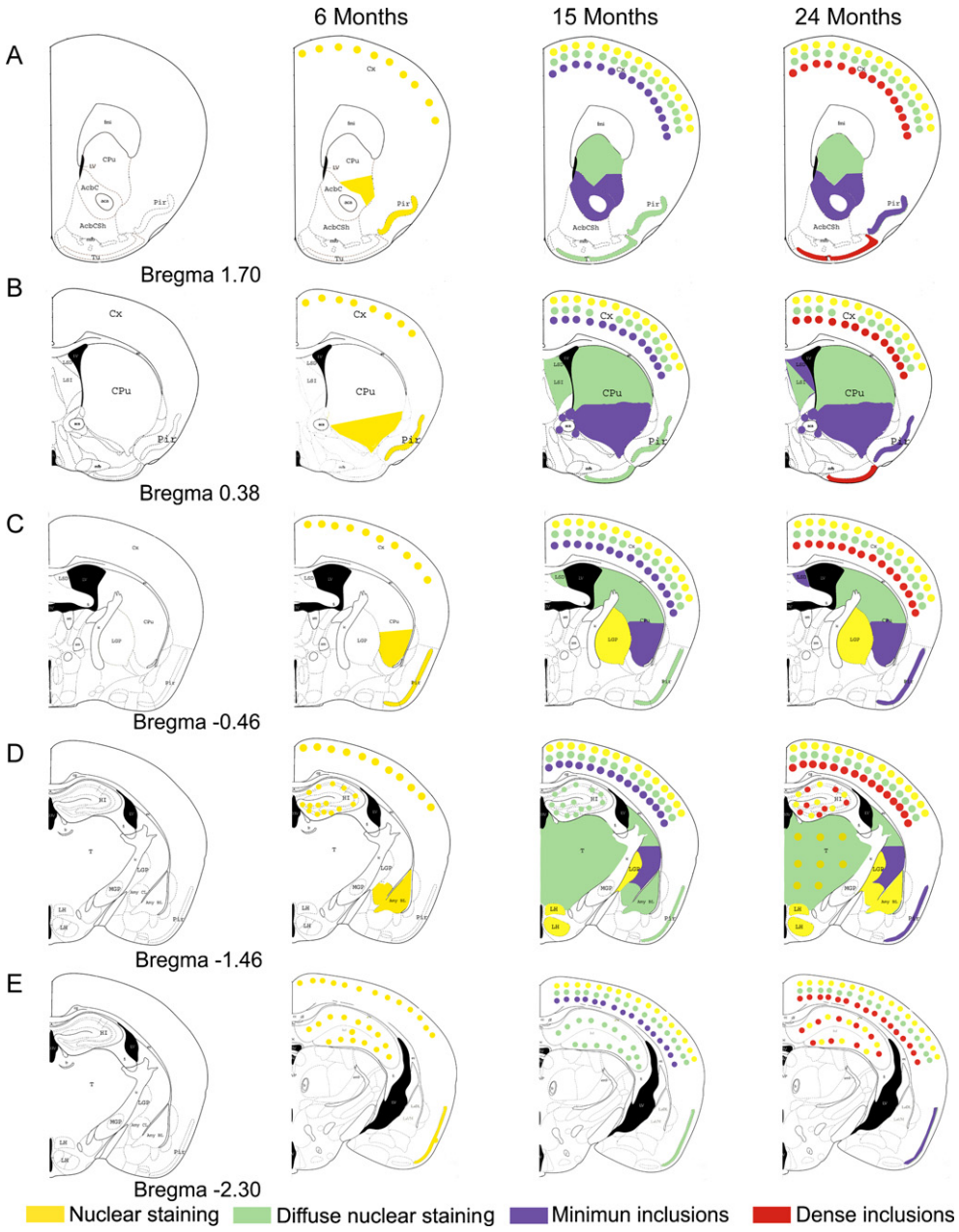

Fig. 3. Illustrative overview of the spatial and temporal evolution of S830 immunostaining in the YAC128 mouse brain at five coronal levels in a rostral-to-caudal sequence. The illustrative diagram is adapted after the atlas of Paxinos and Franklin [49]. Each column shows the expression patterns of S830 immunoreactivity at three time points (6 M, 15 M and 24 M) in different colours. For colour coding see bottom of columns. Overlapping staining is represented by mixed colour.

mates. However, the expression of GFAP was more intense in the cortex of the transgenic animals compared to the wildtype control mice (Fig. 5).

3.4. Electron microscopy

Electron microscopic evaluation revealed that the striatum of 14 months old wild-type animals showed regular medium-sized striatal neuron morphology. The mitochondria and synaptic junctions appeared to be normal (Fig. 6A). Asymmetric synapses were observed between neurons, and had terminals with densely packed small round vesicles with associated mitochondria (Fig. 6B). Conversely, we also observed three different types of cell morphology in the 14 month old YAC128 animals. There were large cholinergic neurons present where the structure appeared to be normal as seen in wildtype animals (Fig. 6C and D). There were also medium-sized striatal neurons that demonstrated the loss of membrane integrity (arrow head), vacuolation, degenerated mitochondria and Golgi apparatus which are features of necrotic cell death (Fig. 6E), and a third cell morphology was present that presented as dark, dense cells, characteristic of cells undergoing apoptosis [7,47] (Fig. 6F).

The rough endoplasmic reticulum, mitochondria, Golgi apparatus and lipofuscin granules were present in medium-sized striatal neurons in 26 month old wildtype animals. However, these animals showed minor degeneration due to their age, this can be characterized as increased lipofuscin granules. Asymmetric synapses showed clearly defined synaptic vesicles containing mitochondria (Fig. 7A and B). In the transgenic mice, degenerated cells were present that were characterized by the presence of condensed cytoplasm, larger lipofuscin granules and vacuolation. Transgenic animals had more and bigger lipofuscin granules than their wildtype littermates (Fig. 7C and E). Nuclear inclusions were also visible at this stage

Please cite this article in press as: Z. Bayram-Weston, et al., Light and electron microscopic characterization of the evolution of cellular pathology in YAC128 Huntington's disease transgenic mice, Brain Res. Bull. (2011), doi:10.1016/j.brainresbull.2011.05.005

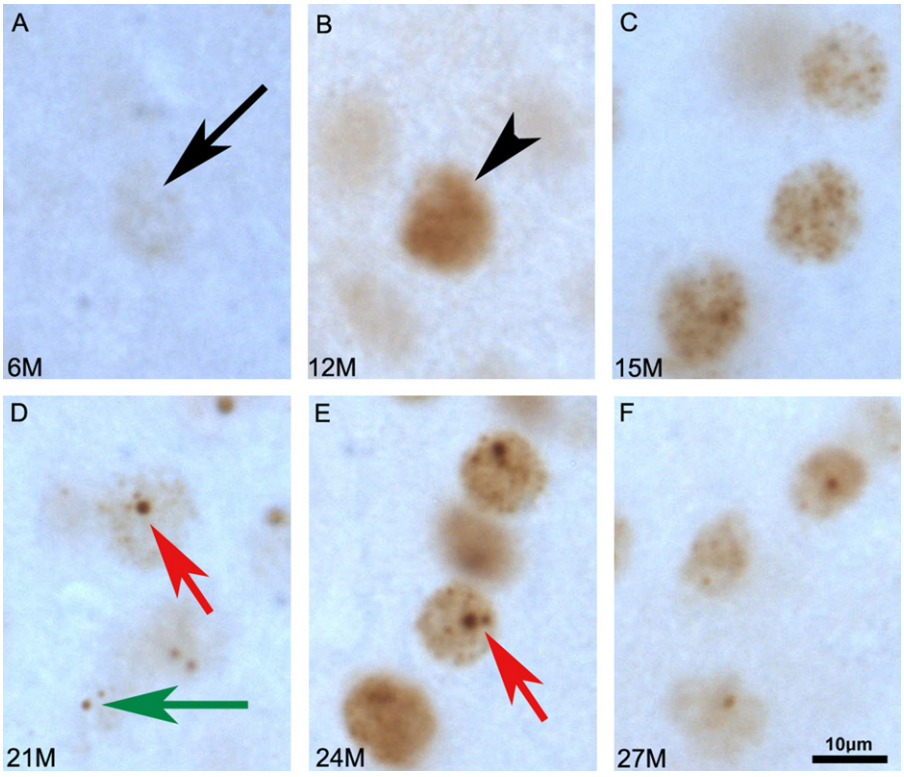

Fig. 4. High magnification images of nuclear S830 immunoreactivity in the ventra-striatal sections of YAC128 mouse brain, ages between 6 and 27 months old (A–F). The diffuse nuclear staining was observed in animals aged between 6 and 24 months (A–E). 27 months old animals display intra-nuclear inclusions with diffuse nuclear staining (E and F). We were not able to identify neuronal degeneration and enlarged nuclear inclusions by the light microscope. Black arrow designates weak nuclear staining; black arrow head designates diffuse nuclear staining; red arrows designate inclusions; green arrow indicates extra-nuclear inclusions. Scale bar = 10 μm.

(Fig. 7E) with many striatal cells being extensively degenerated (Fig. 7F).

4. Discussion

The YAC128 mice displayed regional expression of intra- and extra-nuclear inclusions with the S830 antibody. At 4 months of age we did not observe either diffuse nuclear staining or NIIs in the brain. By 6 months, very weak nuclear staining was observed in some brain regions which included the ventral striatum, piriform cortex and cerebellum. From 12 months of age, the S830 antibody demonstrated diffuse nuclear staining in the majority of the brain regions and this progressed with age, such that by 15 months of age, the NIIs were detectable in the nucleus accumbens, ventra-lateral striatum, cerebellum and motor and sensory cortices. At 21 months of age, both diffuse nuclear staining and overt NIIs were widely distributed throughout the striatum, olfactory tubercle, nucleus accumbens, thalamus and cortex. By 27 months of age, the appearance of diffuse nuclear staining and NIIs were varied depending on the region of the brain. These findings in YAC128 mouse model are

Table 2
YAC128 transgenic mice. Formation, progression and distribution of extra-nuclear inclusions (ENNIs).

YAC128 brain	Ages										
	4 M	6 M	8 M	10 M	12 M	15 M	18 M	21 M	22 M	24 M	27 M
Olfactory tubercle	0	0	0	0	0	++	++	++	+++	+++	+++
Nucleus accumbens	0	0	0	0	0	+	0	0	0	0	+
Globus pallidus-lateral	0	0	0	0	0	+	+	+++	0	+	++
Globus pallidus-medial	0	0	0	0	0	+	+	+++	0	+	+
Striatum ventral	0	0	0	0	0	0	0	0	0	+	++
Striatum dorsal	0	0	0	0	0	0	0	0	0	0	0/+
Striatum lateral	0	0	0	0	0	0	0	0	0	0/+	0/+
Striatum medial	0	0	0	0	0	0	0	0	0	0	0/+
Septum lateral	0	0	0	0	+	+++	0/+	++++	0/+	++++	++++
Septum med	0	0	0	0	+	++	0/+	++++	0	+++	0/+
Amygdala BL	0	0	0	0	0	+	+	+	0	0/+	+
Amygdala CL	0	0	0	0	0	+	+	+	0/+	+	+++
Thalamus	0	0/+	0/+	0	++	+	0	+	0	0	+
Hypothalamus	0	+	0/+	0	+	++	+++	++	+++	++++	++++
Cerebellum	0	0/+	0	0	0/+	+	++	++	++	++++	+++
Hippocampus	0	0	0	0	0	0/+	0/+	0/+	0/+	0/+	+
Motor cortex	0	0/+	0/+	0/+	0/+	+	0/+	0/+	0/+	0/+/++	++/+++
Sensory cortex	0	0/+	0/+	0/+	0/+	+	0/+	0/+	0/+	0/+/++	++/+++
Piriform cortex	0	+	0/+	0/+	+	+++	+++	+++	++++	++++	++++

0: absent; +: very low staining; ++: intermediate staining; +++: dense staining; ++++: very dense staining.

Please cite this article in press as: Z. Bayram-Weston, et al., Light and electron microscopic characterization of the evolution of cellular pathology in YAC128 Huntington's disease transgenic mice, Brain Res. Bull. (2011), doi:10.1016/j.brainresbull.2011.05.005

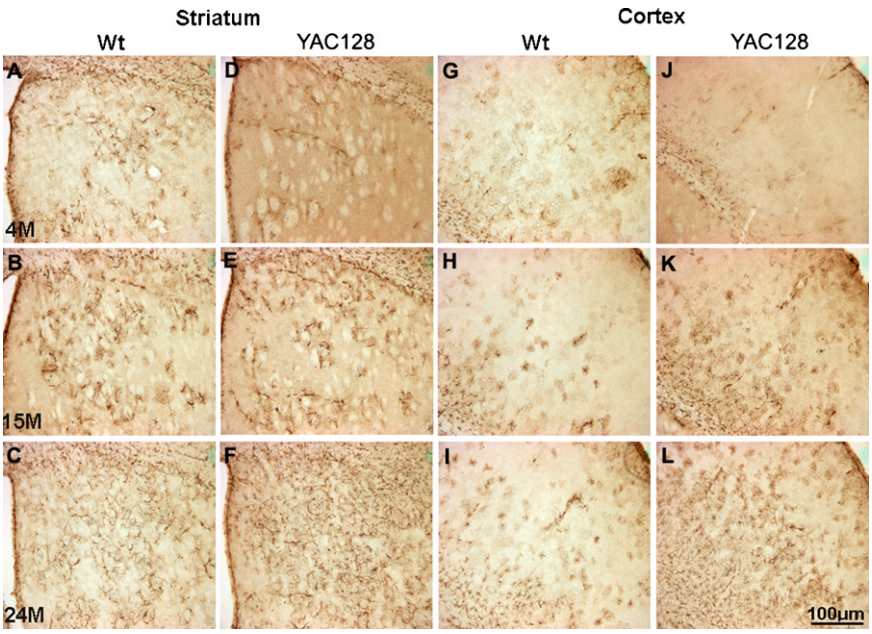

Fig. 5. The distribution of GFAP activity in the striatum and cortex of wildtype (A–C and G–I) and YAC128 mice (D–F and J–L). First row denotes 4 months old YAC128 mice, second row denotes 15 months old and third row denotes 24 months old. The intense expression of GFAP is observed in the striatum of older animals of both wildtype and YAC128 mice. However, the cortex of the older animals (15 M and 24 M) contains increased GFAP activity comparison to control animals. Scale bar = 100 μm.

in agreement with the characteristic neuropathological features in HD [19,21,25,37,61].

In human post-mortem studies more aggregates are found in the cortex than in the striatum [19,21,25,37,61]. Our study demonstrates the same pattern in the YAC128 mouse, where aggregates were abundant throughout the cortex and seen only in the ventrolateral striatum. However, there is variability in the distribution and area of aggregates/NIIs in different studies undertaken on human post-mortem tissues. For example, one study shows aggregates/NIIs present to a lesser extent in the globus pallidus and the thalamus, but were rarely seen in the ventral striatum and absent in the cerebellum [21]. In another study, the small numbers of inclusions in the striatum has been confirmed but they have reported absence of NIIs in the globus pallidus [37]. The density of aggregates was also found to be lower in the caudate, putamen, substantia nigra, hypothalamic nuclei and thalamus than in the cortex and was rarely seen in the globus pallidus, hippocampus and cerebellum by Gutekunst and colleagues [25]. Our results in the YAC128 mouse model partially agree with the Gutekunst study [25], as the density of aggregates was lower in the hypothalamic nuclei, thalamus and globus pallidus, similarly we have found a greater density of aggregates in the cortex than the dorsal striatum. Interestingly, in YAC128 mice, Van Raamsdonk and colleagues reported that the striatum contained more nuclear staining than in any other regions of the brains at 3 month old [74]. This may due to the differences in antibodies used in the two studies, but may also relate to different expression patterns on the different mouse background strains [76]. In HD the aggregates are most prominent in the neostriatum and in the cerebral cortex, the sites of most prominent cell loss. Therefore, not surprisingly, it has been suggested that there is a close relationship between neuronal degeneration and the occurrence of neuronal inclusions [21,25,37], although a precise causative relationship has proved difficult to define.

We have also observed dense NIIs in cerebellum in YAC128 mice, in agreement with another study showing the highest level of mutant huntingtin in the cerebellum [71]. Interestingly, it has been reported that the density of Purkinje cells in the cerebellum was reduced in HD patients [31,54], and cerebellar atrophy has also been observed [54]. A recent study has also reported that there was slight cerebellar atrophy with no caudate atrophy identified by computerized tomographic and magnetic resonance imaging scans [27]. Our observations are consistent with some human studies that demonstrate cerebellar abnormality.

The possible theories regarding the accumulation of the misfolded protein in the neurodegenerative diseases are reviewed by Ross and Poirier [58]. The authors suggest a possibility that in some models of neurodegerative disease, the initial stage of aggregate formation could be stochastic with the time of the death being random in individual neurons [13]. This would be to the process of neurodegeneration being a gradual and graded process. Supporting the former theory, we observe in the present study on the YAC128 mouse and in a previous R6/1 transgenic mouse model study [4], the appearance of S830 staining was stochastic, whereas, our previous studies in HdhQ150 and HdhQ92 knock-in models [3,5] showed more graded appearance of S830 staining. Our data suggest that there may a dichotomy between the transgenic and knock-in models of the disease in this respect. The behavioural data from our laboratory is suggestive that in the YAC128 mouse line, many of the behavioural abnormalities observed are not progressive in nature [8], suggestive of sensitive time periods in the disease development, rather than an ongoing insidious process. However, we have also observed non-progressive behavioural abnormalities in the HdhQ92 knock-in mouse line [73], which does exhibit a gradual and directional advancement of neuropathology.

In addition to nuclear inclusions, we also find moderate neuronal loss in the striatum, although this loss was not as significant as found in human post-mortem studies [25,26,78], even in the aged mice, and more importantly was not markedly progressive. Our results are parallel with Van Raamsdonk and colleagues which have shown the striatal neuronal loss in YAC128 mice [74]. However, it conflicts with other studies, which have reported that in some transgenic and knock-in mouse models of HD the striatal volume is decreased with no evidence of striatal neuronal loss [33,35,38,40].

The YAC72 transgenic mouse model of HD expressing mutant full-length Htt also demonstrated signs of specific striatal degeneration and reactive gliosis by 12 months of age. However, in YAC72 mice, the accumulation of protein aggregates did not correlate with the neurological symptoms [28], suggesting that some changes

Please cite this article in press as: Z. Bayram-Weston, et al., Light and electron microscopic characterization of the evolution of cellular pathology in YAC128 Huntington's disease transgenic mice, Brain Res. Bull. (2011), doi:10.1016/j.brainresbull.2011.05.005

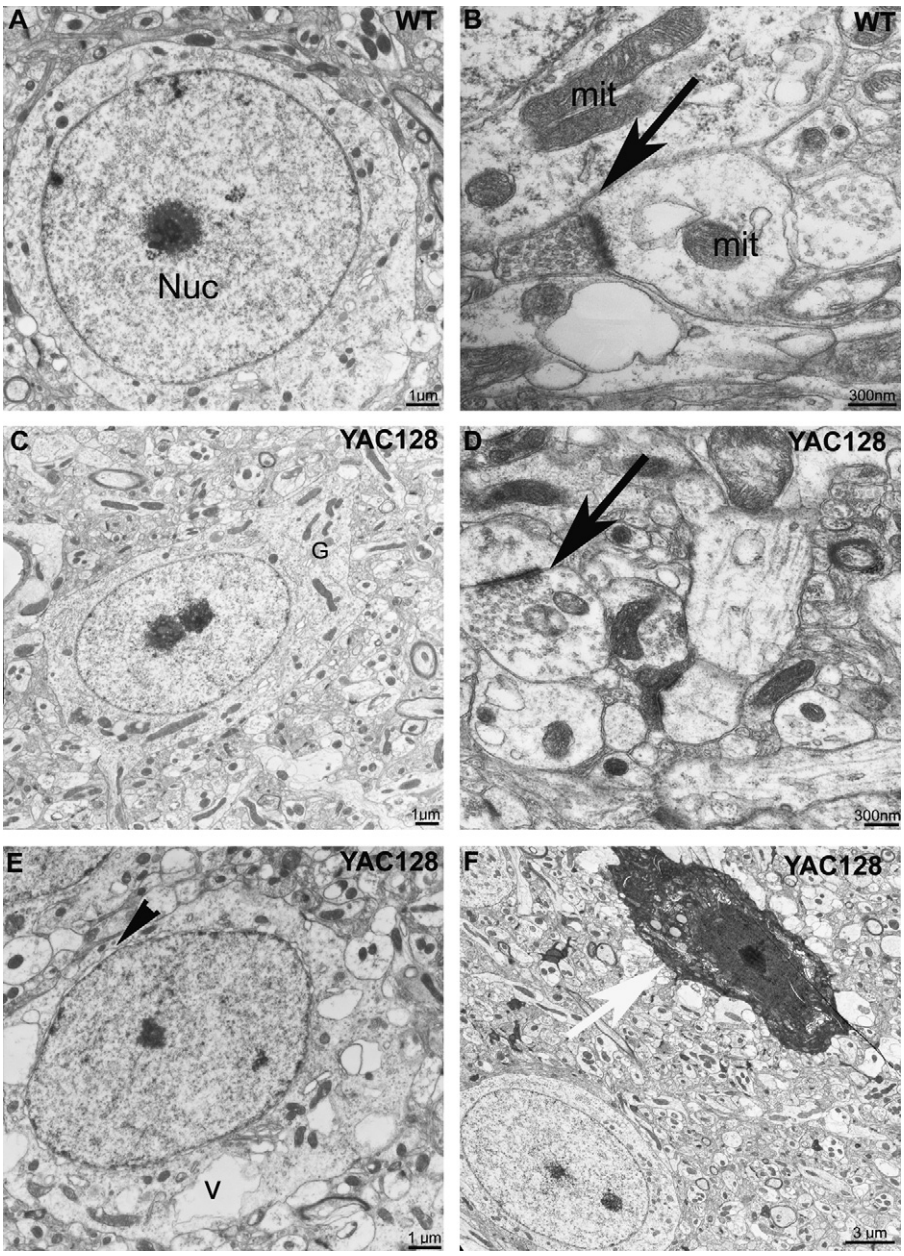

Fig. 6. Electron micrographs showing striatal cells of 14 months old WT and YAC128 mice. A morphologically normal medium-sized striatal neuron (A) containing mitochondria (mit) and axon terminals that form asymmetric synapses (black arrows) with dendritic spine (B). Three cell structures have been observed in transgenic animals. Firstly, a normal cell morphology of transgenic animal (C) with their asymmetric synapse (D). In some cells, the cytoplasm is characterized by the presence of vacuolisation (E), while in some other cells, apoptotic bodies are often observed in close contact with other cells type (F). As the apoptotic process proceeds, the nuclei appear homogenously dark and shrunken and the cytoplasm is condensed and often detached from the surrounding (F). Nuc, nucleus; G, Golgi apparatus; v, vesicles; black arrows, asymmetric synaptic junctions; apoptotic cell, white arrow; arrow head, nuclear membrane integrity. Scale bars are as stated in the figures.

in the affected cells occur before the overt protein accumulation or the cell death. This phenomenon has been widely reported in HD mouse models and has been suggested to be due a synaptic pathology rather than overt cell loss [42]. Thus, live-cell, time-lapse microscopy in transgenic PC12 cells has suggested that aggregates are cytoprotective at some stages and postpone cell death, but may be toxic to the cells at another time. In addition, it has been reported that aggregate size was not a good predictor of cell death [20]. Alternatively, the aggregates may be present in the cells in conformations that are not sensitive to the range of histological stains and antibodies commonly used [34].

A recent study using electron microscopy showed that individuals with HD may also exhibit abnormal cell morphology in peripheral tissues [69]. In this study, we examined ultrastructurally the brain samples of YAC128 mice. Our findings are in agreement with previous reports on post-mortem tissues of individuals with HD and transgenic and knock-in mouse models, where nuclear inclusions contain filamentous structures [16,19,25,48]. Electron microscopic analysis of human HD brain tissues has revealed nuclear membrane indentations, nuclear disorganization, reduction of the ribosomes [55,56], large accumulations of lipofuscin granules, enlarged mitochondria [72] and DNA fragmentation [9,30,50]. Our results show similar characteristic features in this mouse line which agrees our previous findings in the *Hdh*$^{(CAG)150}$ knock-in mouse [5]. By ultrastructural examination, it has been observed that ENNIs were present in the synaptic densities of the neurons in the R6/2 mouse line [44]. We fail to find any ENNIs in the synaptic junctions of the neurons in the YAC128 mice line, which

Please cite this article in press as: Z. Bayram-Weston, et al., Light and electron microscopic characterization of the evolution of cellular pathology in YAC128 Huntington's disease transgenic mice, Brain Res. Bull. (2011), doi:10.1016/j.brainresbull.2011.05.005

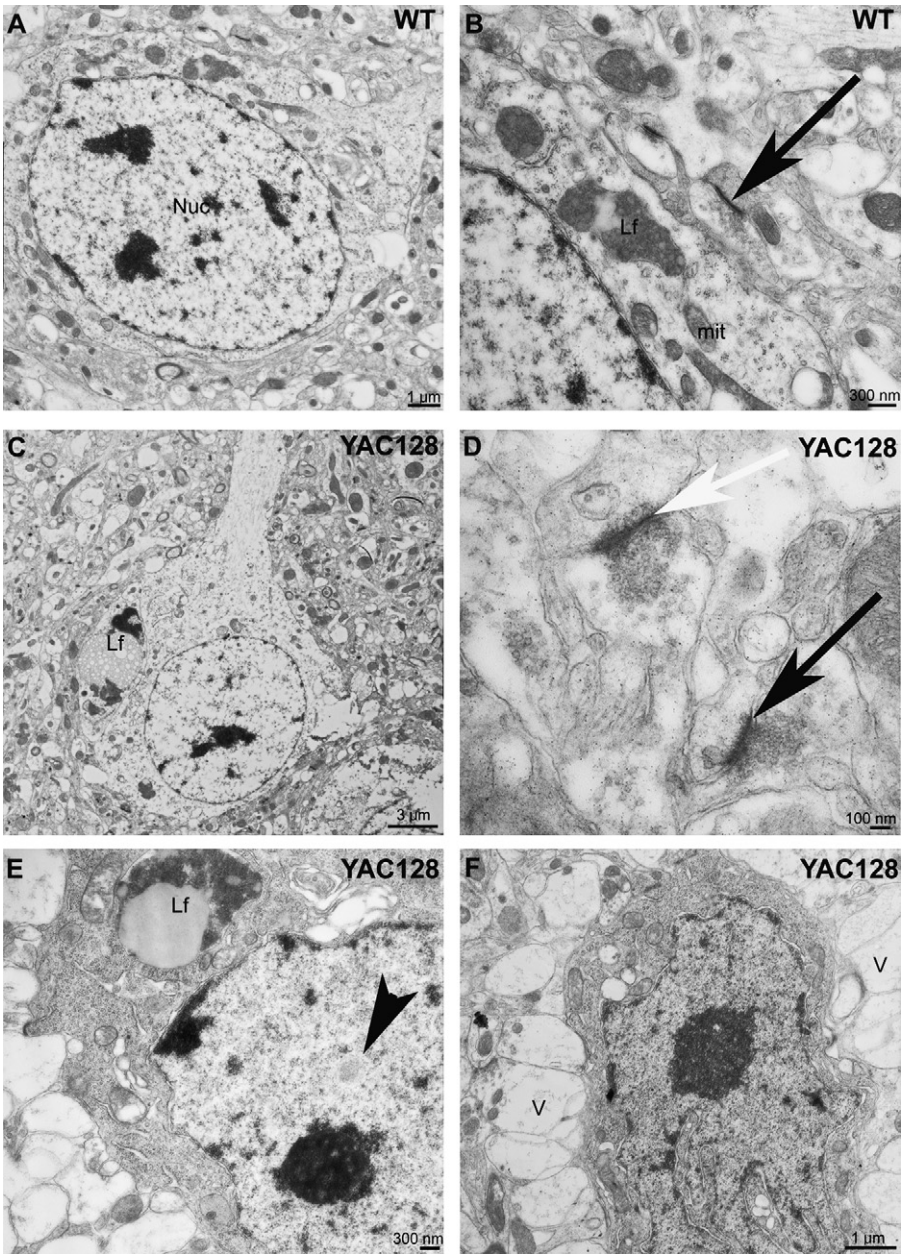

Fig. 7. Electron micrographs showing striatal cells of 26 months old WT and YAC128 mice. Almost morphologically medium-sized striatal neuron (A) containing small lipofuscin granules (Lf) and asymmetric synaptic junction (B). A large cholinergic neurons of transgenic animal shows large lipofuscin granules (C) with their symmetric synapse (white arrow) with a dendritic spine containing pleomorphic vesicles and asymmetric synapse (D). Another cell type had the cytoplasm which is characterized by the presence of vacuolation (E and F). A degenerated cell with uneven nuclear membrane and condensed cytoplasm (F). Nuc, nucleus; mit, mitochondria; v, vesicles; black arrows, asymmetric synaptic junction; white arrow, symmetric synaptic junction; black arrow head, intra nuclear inclusion. Scale bars are as stated in the figures.

is parallel with our previous findings [3–5]. A previous study has shown that there were several increased shrunken, angular, dark neurons with reduced cytoplasm and nucleoplasm in R6/2 mouse brains [70]. Similarly, in BAC-HD transgenic mice, the degenerating dark neurons were present in the striatum at 12 months of age by ultrastructural examination [23]. Consistent with these data, our results show similar morphology with dark degenerating neurons in 14 month old YAC128 transgenic mice. As noted elsewhere [29] the electron microscopic examination of the R6/1 transgenic mouse striatum revealed the presence of striatal neurons with altered ultrastructural features such as condensed chromatin, a heterochromatic mass adjacent to nucleolus and inclusions [29]. Evidence suggests that mitochondrial dysfunction and oxidative stress are important factors for the neurodegeneration observed in the HD brain [14,18,32,36,65]. In the present study we also observed degenerated mitochondria in some cells in 14 and 26 month old animals, but not all cells. In particular mitochondria in dark cells that were undergoing cell death were difficult to identify relative to normal unaffected cells. We are currently looking specifically at mitochondrial dysfunction in several HD mouse lines to determine the role and extent of mitochondria in cell death in these lines.In HD patients, it has been reported that the dorsal putamen exhibited the highest density of apoptotic cells in comparison to the ventral part of the putamen [50]. In the current study the formation of NIIs are more predominant in the ventral striatum rather than the dorsal striatum. These data suggest two possible scenarios: that the majority of vulnerable neurons have already died and therefore they do not contain NIIs, or alternatively, NIIs are playing a protective role in the cell. The role of inclusions still remains to be elucidated. The data from *in vivo* and *in vitro* studies suggests

Please cite this article in press as: Z. Bayram-Weston, et al., Light and electron microscopic characterization of the evolution of cellular pathology in YAC128 Huntington's disease transgenic mice, Brain Res. Bull. (2011), doi:10.1016/j.brainresbull.2011.05.005

three possible hypotheses for their function in HD. The first theory suggests that aggregates are toxic to cells and leads the pathology and secondly, they are protective to cell from toxic proteins. Finally, they are side products with no function in cell death [57,59,62,66]. The present study revealed cells containing NIIs and severely distorted organelles at the ultrastructural level. Results from another study showed that in htt171-82Q-injected rats, the occurrence of NIIs leads to neuronal dysfunction and neuronal degeneration associated with reactive astrogliosis [17]. The study also assessed the impact of htt protein length on the formation of aggregates and conversely found that increased htt protein length postpones the appearance of nuclear inclusions [17]. Hence, the cell death in HD may be associated with expanded glutamine repeats which induce apoptosis and cell death [17,30,64]. It has been suggested that inclusions develop prior to neurological symptoms and overt neurodegeneration [15]. However, in some full-length htt mouse models, motor and cognitive impairment with neuronal loss occur before the appearance of NIIs [39,68,75]. These data indicate that neuronal dysfunction and loss can take place well before visible insoluble protein aggregation. Interestingly, Slow and colleagues state that soluble protein fragments are more difficult to visualize than insoluble forms and they have suggested that the insoluble aggregated proteins may not be toxic, whereas soluble protein fragments are [67], and it has been demonstrated that there is a correlation between aggregate formation and cell death, suggesting that aggregates are ultimately toxic to cells [20]. In agreement with other reports [10,44,45], the present study suggests that aggregates play a role in neuronal dysfunction and neuronal cell death.

We did not observe any changes in the intensity of reactive astrogliosis with GFAP immunostaining in the striatum of YAC128 mice in comparison to their wildtype littermates, which is in agreement with our other studies on the Hdh^{Q92} and $Hdh^{(CAG)150}$ knock-in mice [3,5]. However it conflicts with other studies, which have reported an increase in reactive astrogliosis in transgenic [51,70] and knock-in mice [35,80]. Furthermore, we have observed increased GFAP immunoreactivity in the cortex of the YAC128 mice than when compared with controls. This may suggest that the reactive astrogliosis may not relate with the mutant htt but may be outcome of the cell loss in the striatum.Taken together, the present study indicates that a number of similarities exist between the YAC128 transgenic mouse model and the human disease with respect to the appearance and distribution of NIIs. The general feature of the model is that inclusion development is more prominent in the cortex than the striatum and that striatal cell loss is present but increases with age at a rate that is comparable with the wildtype animals.

Conflict of interest

The authors have no conflicts of interest.

Acknowledgements

We thank Prof G Bates (University of London) for the kind gift of the S830 antibody, Prof Ifor Bowen and Dr Anthony Hann for advice on the electron microscope and Alison Baird, Gemma Higgs and Nari Janghra for technical support. The study was supported by an MRC studentship to ZBW, and funding from CHDI Inc. and the MRC.

References

[1] M. Abercrombie, Estimation of nuclear population from microtome sections, Anat. Rec. 94 (1946) 239–247.
[2] G.P. Bates, P.S. Harper, L. Jones (Eds.), Huntington's Disease, Oxford University Press, 2002.
[3] Z. Bayram-Weston, S. Brooks, L. Jones, S.B. Dunnett, Light and electron microscopic characterization of the evolution of cellular pathology in $Hdh^{Q92/Q92}$ Huntington's disease mice, Brain Res. Bull., in this issue.
[4] Z. Bayram-Weston, L. Jones, S.B. Dunnett, S.P. Brooks, Light and electron microscopic characterization of the evolution of cellular pathology in the R6/1 transgenic mouse, Brain Res. Bull., in this issue.
[5] Z. Bayram-Weston, E.M. Torres, L. Jones, S.B. Dunnett, S.P. Brooks, Light and electron microscopic characterization of the evolution of cellular pathology in the *Hdh*(CAG)150 Huntington's disease knock-in mouse, Brain Res. Bull., in this issue.
[6] M.W. Becher, J.A. Kotzuk, A.H. Sharp, S.W. Davies, G.P. Bates, D.L. Price, C.A. Ross, Intranuclear neuronal inclusions in Huntington's disease and dentatorubral and pallidoluysian atrophy: correlation between the density of inclusions and IT15 CAG triplet repeat length, Neurobiol. Dis. 4 (1998) 387–397.
[7] I.D. Bowen, Apoptosis or programmed cell death? Cell Biol. Int. 17 (1993) 365–380.
[8] S. Brooks, G. Higgs, N. Janghra, L. Jones, S.B. Dunnett, Longitudinal analysis of the behavioural phenotype in YAC128 (C57BL/6J) Huntington's disease transgenic mice, Brain Res. Bull. (2010), doi:10.1016/j.brainresbull.2010.05.005.
[9] N.J. Butterworth, L. Williams, J.Y. Bullock, D.R. Love, R.L. Faull, M. Dragunow, Trinucleotide (CAG) repeat length is positively correlated with the degree of DNA fragmentation in Huntington's disease striatum, Neuroscience 87 (1998) 49–53.
[10] J. Carmichael, J. Chatellier, A. Woolfson, C. Milstein, A.R. Fersht, D.C. Rubinsztein, Bacterial and yeast chaperones reduce both aggregate formation and cell death in mammalian cell models of Huntington's disease, Proc. Natl. Acad. Sci. U.S.A. 97 (2000) 9701–9705.
[11] S. Chen, V. Berthelier, W. Yang, R. Wetzel, Polyglutamine aggregation behavior in vitro supports a recruitment mechanism of cytotoxicity, J. Mol. Biol. 311 (2001) 173–182.
[12] S. Chen, R. Wetzel, Solubilization and disaggregation of polyglutamine peptides, Protein Sci. 10 (2001) 887–891.
[13] G. Clarke, R.A. Collins, B.R. Leavitt, D.F. Andrews, M.R. Hayden, C.J. Lumsden, R.R. McInnes, A one-hit model of cell death in inherited neuronal degenerations, Nature 406 (2000) 195–199.
[14] M. Damiano, L. Galvan, N. Deglon, E. Brouillet, Mitochondria in Huntington's disease, Biochim. Biophys. Acta 1802 (2010) 52–61.
[15] S.W. Davies, K. Beardsall, M. Turmaine, M. DiFiglia, N. Aronin, G.P. Bates, Are neuronal intranuclear inclusions the common neuropathology of triplet-repeat disorders with polyglutamine-repeat expansions? Lancet 351 (1998) 131–133.
[16] S.W. Davies, M. Turmaine, B.A. Cozens, M. DiFiglia, A.H. Sharp, C.A. Ross, E. Scherzinger, E.E. Wanker, L. Mangiarini, G.P. Bates, Formation of neuronal intranuclear inclusions underlies the neurological dysfunction in mice transgenic for the HD mutation, Cell 90 (1997) 537–548.
[17] L.P. de Almeida, C.A. Ross, D. Zala, P. Aebischer, N. Deglon, Lentiviral-mediated delivery of mutant huntingtin in the striatum of rats induces a selective neuropathology modulated by polyglutamine repeat size, huntingtin expression levels, and protein length, J. Neurosci. 22 (2002) 3473–3483.
[18] M. Deschepper, B. Hoogendoorn, S. Brooks, S.B. Dunnett, L. Jones, Proteomic changes in the brains of Huntington's disease mouse models reflect pathology and implicate mitochondrial changes, Brain Res. Bull. (2011), doi:10.1016/j.brainresbull.2011.01.012.
[19] M. DiFiglia, E. Sapp, K.O. Chase, S.W. Davies, G.P. Bates, J.P. Vonsattel, N. Aronin, Aggregation of huntingtin in neuronal intranuclear inclusions and dystrophic neurites in brain, Science 277 (1997) 1990–1993.
[20] B. Gong, M.C. Lim, J. Wanderer, A. Wyttenbach, A.J. Morton, Time-lapse analysis of aggregate formation in an inducible PC12 cell model of Huntington's disease reveals time-dependent aggregate formation that transiently delays cell death, Brain Res. Bull. 75 (2008) 146–157.
[21] I. Gourfinkel-An, G. Cancel, C. Duyckaerts, B. Faucheux, J.J. Hauw, Y. Trottier, A. Brice, Y. Agid, E.C. Hirsch, Neuronal distribution of intranuclear inclusions in Huntington's disease with adult onset, Neuroreport 9 (1998) 1823–1826.
[22] G.A. Graveland, R.S. Williams, M. DiFiglia, Evidence for degenerative and regenerative changes in neostriatal spiny neurons in Huntington's disease, Science 227 (1985) 770–773.
[23] M. Gray, D.I. Shirasaki, C. Cepeda, V.M. Andre, B. Wilburn, X.H. Lu, J. Tao, I. Yamazaki, S.H. Li, Y.E. Sun, X.J. Li, M.S. Levine, X.W. Yang, Full-length human mutant huntingtin with a stable polyglutamine repeat can elicit progressive and selective neuropathogenesis in BACHD mice, J. Neurosci. 28 (2008) 6182–6195.
[24] J.F. Gusella, M.E. MacDonald, Huntington's disease: the case for genetic modifiers, Genome Med. 1 (2009) 80.
[25] C.A. Gutekunst, S.H. Li, H. Yi, J.S. Mulroy, S. Kuemmerle, R. Jones, D. Rye, R.J. Ferrante, S.M. Hersch, X.J. Li, Nuclear and neuropil aggregates in Huntington's disease: relationship to neuropathology, J. Neurosci. 19 (1999) 2522–2534.
[26] J.C. Hedreen, S.E. Folstein, Early loss of neostriatal striosome neurons in Huntington's disease, J. Neuropathol. Exp. Neurol. 54 (1995) 105–120.
[27] Y.O. Herishanu, R. Parvari, Y. Pollack, I. Shelef, B. Marom, T. Martino, M. Cannella, F. Squitieri, Huntington disease in subjects from an Israeli Karaite community carrying alleles of intermediate and expanded CAG repeats in the HTT gene: Huntington disease or phenocopy? J. Neurol. Sci. 277 (2009) 143–146.
[28] J.G. Hodgson, N. Agopyan, C.A. Gutekunst, B.R. Leavitt, F. LePiane, R. Singaraja, D.J. Smith, N. Bissada, K. McCutcheon, J. Nasir, L. Jamot, X.J. Li, M.E. Stevens, E. Rosemond, J.C. Roder, A.G. Phillips, E.M. Rubin, S.M. Hersch, M.R. Hayden, A YAC mouse model for Huntington's disease with full-length mutant hunt-

Please cite this article in press as: Z. Bayram-Weston, et al., Light and electron microscopic characterization of the evolution of cellular pathology in YAC128 Huntington's disease transgenic mice, Brain Res. Bull. (2011), doi:10.1016/j.brainresbull.2011.05.005

ingtin, cytoplasmic toxicity, and selective striatal neurodegeneration, Neuron 23 (1999) 181–192.
[29] C. Iannicola, S. Moreno, S. Oliverio, R. Nardacci, A. Ciofi-Luzzatto, M. Piacentini, Early alterations in gene expression and cell morphology in a mouse model of Huntington's disease, J. Neurochem. 75 (2000) 830–839.
[30] H. Ikeda, M. Yamaguchi, S. Sugai, Y. Aze, S. Narumiya, A. Kakizuka, Expanded polyglutamine in the Machado–Joseph disease protein induces cell death in vitro and in vivo, Nat. Genet. 13 (1996) 196–202.
[31] D.V. Jeste, L. Barban, J. Parisi, Reduced Purkinje cell density in Huntington's disease, Exp. Neurol. 85 (1984) 78–86.
[32] J. Kim, J.P. Moody, C.K. Edgerly, O.L. Bordiuk, K. Cormier, K. Smith, M.F. Beal, R.J. Ferrante, Mitochondrial loss, dysfunction and altered dynamics in Huntington's disease, Hum. Mol. Genet. 19 (2010) 3919–3935.
[33] G.J. Klapstein, R.S. Fisher, H. Zanjani, C. Cepeda, E.S. Jokel, M.F. Chesselet, M.S. Levine, Electrophysiological and morphological changes in striatal spiny neurons in R6/2 Huntington's disease transgenic mice, J. Neurophysiol. 86 (2001) 2667–2677.
[34] C. Landles, K. Sathasivam, A. Weiss, B. Woodman, H. Moffitt, S. Finkbeiner, B. Sun, J. Gafni, L.M. Ellerby, Y. Trottier, W.G. Richards, A. Osmand, P. Paganetti, G.P. Bates, Proteolysis of mutant huntingtin produces an exon 1 fragment that accumulates as an aggregated protein in neuronal nuclei in Huntington disease, J. Biol. Chem. 285 (2010) 8808–8823.
[35] C.H. Lin, S. Tallaksen-Greene, W.M. Chien, J.A. Cearley, W.S. Jackson, A.B. Crouse, S. Ren, X.J. Li, R.L. Albin, P.J. Detloff, Neurological abnormalities in a knock-in mouse model of Huntington's disease, Hum. Mol. Genet. 10 (2001) 137–144.
[36] M.T. Lin, M.F. Beal, Mitochondrial dysfunction and oxidative stress in neurodegenerative diseases, Nature 443 (2006) 787–795.
[37] M.L. Maat-Schieman, J.C. Dorsman, M.A. Smoor, S. Siesling, S.G. Van Duinen, J.J. Verschuuren, J.T. den Dunnen, G.J. van Ommen, R.A. Roos, Distribution of inclusions in neuronal nuclei and dystrophic neurites in Huntington disease brain, J. Neuropathol. Exp. Neurol. 58 (1999) 129–137.
[38] E. Martin-Aparicio, A. Yamamoto, F. Hernandez, R. Hen, J. Avila, J.J. Lucas, Proteasomal-dependent aggregate reversal and absence of cell death in a conditional mouse model of Huntington's disease, J. Neurosci. 21 (2001) 8772–8781.
[39] L.B. Menalled, J.D. Sison, I. Dragatsis, S. Zeitlin, M.F. Chesselet, Time course of early motor and neuropathological anomalies in a knock-in mouse model of Huntington's disease with 140 CAG repeats, J. Comp. Neurol. 465 (2003) 11–26.
[40] L.B. Menalled, J.D. Sison, Y. Wu, M. Olivieri, X.J. Li, H. Li, S. Zeitlin, M.F. Chesselet, Early motor dysfunction and striosomal distribution of huntingtin microaggregates in Huntington's disease knock-in mice, J. Neurosci. 22 (2002) 8266–8276.
[41] A.J. Milnerwood, D.M. Cummings, G.M. Dallerac, J.Y. Brown, S.C. Vatsavayai, M.C. Hirst, P. Rezaie, K.P. Murphy, Early development of aberrant synaptic plasticity in a mouse model of Huntington's disease, Hum. Mol. Genet. 15 (2006) 1690–1703.
[42] A.J. Milnerwood, L.A. Raymond, Early synaptic pathophysiology in neurodegeneration: insights from Huntington's disease, Trends Neurosci. 33 (2010) 513–523.
[43] A. Montoya, B.H. Price, M. Menear, M. Lepage, Brain imaging and cognitive dysfunctions in Huntington's disease, J. Psychiatry Neurosci. 31 (2006) 21–29.
[44] A.J. Morton, M.A. Lagan, J.N. Skepper, S.B. Dunnett, Progressive formation of inclusions in the striatum and hippocampus of mice transgenic for the human Huntington's disease mutation, J. Neurocytol. 29 (2000) 679–702.
[45] K.P. Murphy, R.J. Carter, L.A. Lione, L. Mangiarini, A. Mahal, G.P. Bates, S.B. Dunnett, A.J. Morton, Abnormal synaptic plasticity and impaired spatial cognition in mice transgenic for exon 1 of the human Huntington's disease mutation, J. Neurosci. 20 (2000) 5115–5123.
[46] R.H. Myers, J.P. Vonsattel, T.J. Stevens, L.A. Cupples, E.P. Richardson, J.B. Martin, E.D. Bird, Clinical and neuropathologic assessment of severity in Huntington's disease, Neurology 38 (1988) 341–347.
[47] J.R. O'Kusky, J. Nasir, F. Cicchetti, A. Parent, M.R. Hayden, Neuronal degeneration in the basal ganglia and loss of pallido-subthalamic synapses in mice with targeted disruption of the Huntington's disease gene, Brain Res. 818 (1999) 468–479.
[48] J.M. Ordway, S. Tallaksen-Greene, C.A. Gutekunst, E.M. Bernstein, J.A. Cearley, H.W. Wiener, L.S. Dure, R. Lindsey, S.M. Hersch, R.S. Jope, R.L. Albin, P.J. Detloff, Ectopically expressed CAG repeats cause intranuclear inclusions and a progressive late onset neurological phenotype in the mouse, Cell 91 (1997) 753–763.
[49] G. Paxinos, K.B.J. Franklin, The Mouse Brain in Stereotaxic Coordinates, 2nd ed., Academic Press, San Diego, CA, 2001.
[50] C. Portera-Cailliau, J.C. Hedreen, D.L. Price, V.E. Koliatsos, Evidence for apoptotic cell death in Huntington disease and excitotoxic animal models, J. Neurosci. 15 (1995) 3775–3787.
[51] P.H. Reddy, M. Williams, V. Charles, L. Garrett, L. Pike-Buchanan, W.O. Whetsell Jr., G. Miller, D.A. Tagle, Behavioural abnormalities and selective neuronal loss in HD transgenic mice expressing mutated full-length HD cDNA, Nat. Genet. 20 (1998) 198–202.
[52] P.H. Reddy, M. Williams, D.A. Tagle, Recent advances in understanding the pathogenesis of Huntington's disease, Trends Neurosci. 22 (1999) 248–255.
[53] A. Reiner, N. Del Mar, Y.P. Deng, C.A. Meade, Z. Sun, D. Goldowitz, R6/2 neurons with intranuclear inclusions survive for prolonged periods in the brains of chimeric mice, J. Comp. Neurol. 505 (2007) 603–629.
[54] R.A. Rodda, Cerebellar atrophy in Huntington's disease, J. Neurol. Sci. 50 (1981) 147–157.
[55] R.A. Roos, G.T. Bots, Nuclear membrane indentations in Huntington's chorea, J. Neurol. Sci. 61 (1983) 37–47.
[56] R.A. Roos, J.F. Pruyt, J. de Vries, G.T. Bots, Neuronal distribution in the putamen in Huntington's disease, J. Neurol. Neurosurg. Psychiatry 48 (1985) 422–425.
[57] C.A. Ross, Intranuclear neuronal inclusions: a common pathogenic mechanism for glutamine-repeat neurodegenerative diseases? Neuron 19 (1997) 1147–1150.
[58] C.A. Ross, M.A. Poirier, Protein aggregation and neurodegenerative disease, Nat. Med. 10 (Suppl.) (2004) S10–S17.
[59] D.C. Rubinsztein, A. Wyttenbach, J. Rankin, Intracellular inclusions, pathological markers in diseases caused by expanded polyglutamine tracts? J. Med. Genet. 36 (1999) 265–270.
[60] I. Sanchez, C. Mahlke, J. Yuan, Pivotal role of oligomerization in expanded polyglutamine neurodegenerative disorders, Nature 421 (2003) 373–379.
[61] E. Sapp, C. Schwarz, K. Chase, P.G. Bhide, A.B. Young, J. Penney, J.P. Vonsattel, N. Aronin, M. DiFiglia, Huntingtin localization in brains of normal and Huntington's disease patients, Ann. Neurol. 42 (1997) 604–612.
[62] F. Saudou, S. Finkbeiner, D. Devys, M.E. Greenberg, Huntingtin acts in the nucleus to induce apoptosis but death does not correlate with the formation of intranuclear inclusions, Cell 95 (1998) 55–66.
[63] G. Schilling, M.W. Becher, A.H. Sharp, H.A. Jinnah, K. Duan, J.A. Kotzuk, H.H. Slunt, T. Ratovitski, J.K. Cooper, N.A. Jenkins, N.G. Copeland, D.L. Price, C.A. Ross, D.R. Borchelt, Intranuclear inclusions and neuritic aggregates in transgenic mice expressing a mutant N-terminal fragment of huntingtin, Hum. Mol. Genet. 8 (1999) 397–407.
[64] M.C. Senut, S.T. Suhr, B. Kaspar, F.H. Gage, Intraneuronal aggregate formation and cell death after viral expression of expanded polyglutamine tracts in the adult rat brain, J. Neurosci. 20 (2000) 219–229.
[65] U. Shirendeb, A.P. Reddy, M. Manczak, M.J. Calkins, P. Mao, D.A. Tagle, R.P. Hemachandra, Abnormal mitochondrial dynamics, mitochondrial loss and mutant huntingtin oligomers in Huntington's disease: implications for selective neuronal damage, Hum. Mol. Genet. 20 (2011) 1438–1455.
[66] S.S. Sisodia, Nuclear inclusions in glutamine repeat disorders: are they pernicious, coincidental, or beneficial? Cell 95 (1998) 1–4.
[67] E.J. Slow, R.K. Graham, M.R. Hayden, To be or not to be toxic: aggregations in Huntington and Alzheimer disease, Trends Genet. 22 (2006) 408–411.
[68] E.J. Slow, J. van Raamsdonk, D. Rogers, S.H. Coleman, R.K. Graham, Y. Deng, R. Oh, N. Bissada, S.M. Hossain, Y.Z. Yang, X.J. Li, E.M. Simpson, C.A. Gutekunst, B.R. Leavitt, M.R. Hayden, Selective striatal neuronal loss in a YAC128 mouse model of Huntington disease, Hum. Mol. Genet. 12 (2003) 1555–1567.
[69] F. Squitieri, A. Falleni, M. Cannella, S. Orobello, F. Fulceri, P. Lenzi, F. Fornai, Abnormal morphology of peripheral cell tissues from patients with Huntington disease, J. Neural Transm. 117 (2010) 77–83.
[70] E.C. Stack, J.K. Kubilus, K. Smith, K. Cormier, S.J. Del Signore, E. Guelin, H. Ryu, S.M. Hersch, R.J. Ferrante, Chronology of behavioral symptoms and neuropathological sequela in R6/2 Huntington's disease transgenic mice, J. Comp. Neurol. 490 (2005) 354–370.
[71] T.V. Strong, D.A. Tagle, J.M. Valdes, L.W. Elmer, K. Boehm, M. Swaroop, K.W. Kaatz, F.S. Collins, R.L. Albin, Widespread expression of the human and rat Huntington's disease gene in brain and nonneural tissues, Nat. Genet. 5 (1993) 259–265.
[72] I. Tellez-Nagel, A.B. Johnson, R.D. Terry, Studies on brain biopsies of patients with Huntington's chorea, J. Neuropathol. Exp. Neurol. 33 (1974) 308–332.
[73] R.C. Trueman, S.P. Brooks, L. Jones, S.B. Dunnett, Time course of choice reaction time deficits in the Hdh(Q92) knock-in mouse model of Huntington's disease in the operant serial implicit learning task (SILT), Behav. Brain Res. 189 (2008) 317–324.
[74] J.M. Van Raamsdonk, Z. Murphy, E.J. Slow, B.R. Leavitt, M.R. Hayden, Selective degeneration and nuclear localization of mutant huntingtin in the YAC128 mouse model of Huntington disease, Hum. Mol. Genet. 14 (2005) 3823–3835.
[75] J.M. Van Raamsdonk, J. Pearson, E.J. Slow, S.M. Hossain, B.R. Leavitt, M.R. Hayden, Cognitive dysfunction precedes neuropathology and motor abnormalities in the YAC128 mouse model of Huntington's disease, J. Neurosci. 25 (2005) 4169–4180.
[76] J.M. Van Raamsdonk, S.C. Warby, M.R. Hayden, Selective degeneration in YAC mouse models of Huntington disease, Brain Res. Bull. 72 (2007) 124–131.
[77] J.P. Vonsattel, M. DiFiglia, Huntington disease, J. Neuropathol. Exp. Neurol. 57 (1998) 369–384.
[78] J.P. Vonsattel, R.H. Myers, T.J. Stevens, R.J. Ferrante, E.D. Bird, E.P. Richardson Jr., Neuropathological classification of Huntington's disease, J. Neuropathol. Exp. Neurol. 44 (1985) 559–577.
[79] N.S. Wexler, J. Lorimer, J. Porter, F. Gomez, C. Moskowitz, E. Shackell, K. Marder, G. Penchaszadeh, S.A. Roberts, J. Gayan, D. Brocklebank, S.S. Cherny, L.R. Cardon, J. Gray, S.R. Dlouhy, S. Wiktorski, M.E. Hodes, P.M. Conneally, J.B. Penney, J. Gusella, J.H. Cha, M. Irizarry, D. Rosas, S. Hersch, Z. Hollingsworth, M. MacDonald, A.B. Young, J.M. Andresen, D.E. Housman, M.M. De Young, E. Bonilla, T. Stillings, A. Negrette, S.R. Snodgrass, M.D. Martinez-Jaurrieta, M.A. Ramos-Arroyo, J. Bickham, J.S. Ramos, F. Marshall, I. Shoulson, G.J. Rey, A. Feigin, N. Arnheim, A. Acevedo-Cruz, L. Acosta, J. Alvir, K. Fischbeck, L.M. Thompson, A. Young, L. Dure, C.J. O'Brien, J. Paulsen, A. Brickman, D. Krch, S. Peery, P. Hogarth, D.S. Higgins Jr., B. Landwehrmeyer, Venezuelan kindreds reveal that genetic and environmental factors modulate Huntington's disease age of onset, Proc. Natl. Acad. Sci. U.S.A. 101 (2004) 3498–3503.
[80] A. Yamamoto, J.J. Lucas, R. Hen, Reversal of neuropathology and motor dysfunction in a conditional model of Huntington's disease, Cell 101 (2000) 57–66.
[81] W. Yang, J.R. Dunlap, R.B. Andrews, R. Wetzel, Aggregated polyglutamine peptides delivered to nuclei are toxic to mammalian cells, Hum. Mol. Genet. 11 (2002) 2905–2917.

Please cite this article in press as: Z. Bayram-Weston, et al., Light and electron microscopic characterization of the evolution of cellular pathology in YAC128 Huntington's disease transgenic mice, Brain Res. Bull. (2011), doi:10.1016/j.brainresbull.2011.05.005

Chapter 5

Paper 3

Light and electron microscopic characterization of the evolution of cellular pathology in Hdh(Q92) Huntington's disease knock-in mice.

Bayram-Weston Z., Jones L., Dunnett S.B. and Brooks S.P.

Brain Res Bull. 2011, in press.

Brain Research Bulletin xxx (2011) xxx–xxx

Contents lists available at ScienceDirect

Brain Research Bulletin

journal homepage: www.elsevier.com/locate/brainresbull

Research report

Light and electron microscopic characterization of the evolution of cellular pathology in Hdh^{Q92} Huntington's disease knock-in mice

Zubeyde Bayram-Weston[a,*], Lesley Jones[b], Stephen B. Dunnett[a], Simon P. Brooks[a]

[a] School of Biosciences, Cardiff University, Museum Avenue, Cardiff CF10 3AX, Wales, UK
[b] Dept of Psychological Medicine, 2nd Floor, Henry Wellcome Building, Wales School of Medicine, Cardiff University, Cardiff CF14 4XN, Wales, UK

ARTICLE INFO

Article history:
Received 16 September 2010
Received in revised form 15 March 2011
Accepted 18 March 2011
Available online xxx

Keywords:
Huntington's disease
Aggregations
Inclusions
HdhQ92/Q92 knock-in mouse line
Electron microscopy

ABSTRACT

Huntington's disease (HD) is a fatally progressive neurodegenerative disease that is characterized anatomically by the abnormal accumulation of fragments of mutant huntingtin protein, within the glia and neurons of the brain. Several genetic (transgenic and knock-in) animal models have been established to mimic human HD. None of these models represent all of the elements of the human disease, but they provide an opportunity to understand the processes of the disease and aid in the development of therapeutic strategies. In this study, the Hdh^{Q92} mouse model of Huntington's disease was analysed at different time points across the lifespan of the animal. At 4 months of age, Hdh$^{Q92/Q92}$ mice showed dense nuclear staining and nuclear inclusions in the olfactory tubercle and striatum with the mutant N-terminal antibody S830. Widespread formation of mutant huntingtin aggregates in the neuronal nuclei and cytosol increased in number with age and disease progression. Electron microscopy revealed that at 14 and at 21 months of age neurons showed the features of both necrotic and apoptotic cell death, such as irregular nuclear and cytoplasmic membranes, dark condensed nuclei, vacuolated cytoplasm, and swollen mitochondria. The spatial spread of NIIs progressed along the anterior-posterior and ventral-dorsal planes. Our detailed analyses of the Hdh^{Q92} mouse line demonstrated a progressive and marked early focal striatal pathology with later widespread neuronal changes, including cellular degeneration, mutant protein aggregation and inclusion formation. We have demonstrated that the distribution of intra- and extra nuclear inclusions in this animal model expresses many features similar to the human pathology.

1. Introduction

Huntington's disease (HD) is a neurodegenerative disorder caused by the expansion of a trinucleotide CAG repeat in the gene that encodes the huntingtin protein (Htt) [49]. Emerging evidence has suggested that normal htt plays a role in membrane trafficking in the cytoplasm and interacts with many other proteins some of which are involved in transcriptional regulation and cytoskeletal organization [24,45]. Within the brain, this protein is prevalent in the cytoplasm, but less abundant in the nucleus [9,11,18,44].

Mutant htt contains an abnormal CAG repeat expansion and is associated with the neurodegeneration of the basal ganglia and cerebral cortex [56]. The neocortex and striatum are thought to be the first areas to be affected in the HD brain, and these regions exhibit the most extensive atrophy as the disease progresses. Within the striatum, early pathology is characterised by selective loss of striatal medium spiny neurons (MSNs) accompanied by reactive astrogliosis [57]. As MSNs are the major target of extra-striatal afferents from the neocortex and thalamus, loss of these projection neurons may be attributed to the cortical atrophy [13,36]. There is a noticeable decrease in the striatal volume and a corresponding enlargement of the lateral ventricles [2], with these pathological changes in the striatum of patients spreading along the caudo-rostral, dorso-ventral and medio-lateral planes [57]. Neuronal loss also extends to other regions of the brain as the disease progresses, particularly the globus pallidus (GP), thalamus, substantia nigra (SN) and hippocampus [56]. Rosas and colleagues demonstrated with MRI that widespread degeneration is not just a feature of advanced disease, but may occur even in the early to mid-stages of the disease process [40].

According to Davies and DiFiglia, when Htt contains 37 or more CAG repeats mutant htt misfolds and accumulates as large insoluble aggregates/neuronal inclusions (NIIs). Aggregates are a neuropathological feature of HD and mouse models of the disease [8,10], and they are believed to confer a toxic gain of function to the carrier, however, loss of wild type Htt may also have a role in HD pathology [7,35,41,43,46]. *In vitro* studies postulate the possibility that the toxicity of mutant htt is induced by the aggregates [53,58,59], but the mechanisms of the toxicity are still unknown. Inclusions have been found in the cortex of HD brains, while many

* Corresponding author. Tel.: +44 02920874684; fax: +44 029 20 876749.
E-mail address: Bayram-WestonZ@cardiff.ac.uk (Z. Bayram-Weston).

0361-9230/$ – see front matter © 2011 Elsevier Inc. All rights reserved.
doi:10.1016/j.brainresbull.2011.03.013

MSNs are devoid of these inclusions despite the presence of neuronal loss [15]. It has also been reported that N-terminal fragments of mutant htt are localized in dystrophic neurites in the cortex and striatum and occasionally in astrocytes [54] of post mortem HD brains [10]. Extra-nuclear inclusions (ENNIs) are also present in both HD and mouse model brains [10,22,31]. ENNIs may be precursors of intra-nuclear inclusions [27,42].

After discovery of the HD gene in 1993, a number of genetic mouse models of HD have been created to better understand the disease and the development of the disease pathology [14,17,21,25,29,34,47,60,62]. The Hdh^{Q92} knock-in mouse model has ~90 CAG repeats inserted into exon 1 of the mouse *HD* gene [60]. This mouse line demonstrates mild motor-learning impairments from 4 months of age [6,50–52] but otherwise demonstrates little behavioural pathology until the mice are in the latter stages of life. As part of an ongoing programme to provide a comparative characterisation of different HD mouse lines [3–5], the present study evaluated the nature and the spatial and temporal distribution of neuropathology in the Hdh^{Q92} mouse line. Brains were taken at regular time points from 4 to 24 months of age and assessed with immunohistochemical, stereological and transmission electron microscope (TEM), to determine the development of striatal cell loss, mutant huntingtin aggregation and inclusion formation, and whether there was an accompanying inflammatory response as determined by a glial fibrillary acid protein (GFAP) marker.

2. Materials and methods

2.1. Animals

Fifty one (26 Female, 25 male) $Hdh^{Q92/Q92}$ homozygotes knock-in mice and their 50 wildtype litter mates (26 Female, 25 male), were backcrossed for six generations in-house, onto a C57BL/6J (Harlan, UK) background. This mouse model has 90 CAG repeats inserted into exon 1 of the mouse *HD* gene [60]. The mice were housed together under standard conditions with *ad libitum* access to water and food under a 12 h:12 h light–dark cycle (07:00 lights on: 19:00 lights off) and an ambient room temperature of $20 \pm 1\,^{\circ}C$. The cages contained sawdust bedding and a cardboard tube for environmental enrichment. Each cage contained 1–6 animals. The animals were sampled from the same cohort as was subjected to longitudinal behavioural analysis presented in the accompanying report [6]. This study was carried out in accordance with local ethical review and personal, project and facilities licences issued under the UK Animals (Scientific Procedures) Act, 1986.

2.2. Histology

The animals were sacrificed at 2–3 month intervals between 4 months and 24 months of age. They were anaesthetized with Euthetal and perfused trans-cardially. The brains were then removed, post-fixed in 4% PFA for 4 h, and cryoprotected in 25% sucrose in PBS at 4 °C. Coronal sections (40 μm) of the brain were cut in series of 1:6 using a freezing sledge microtome (Leitz Bright Series 8000, Germany) and the sections were stored in cryoprotective solution at −20 °C until required.

2.3. Cresyl fast violet (CV)

A one in 6 series was stained using the standard Nissl stain cresyl fast violet. Briefly, the sections were mounted on gelatine-coated slides and air-dried at 37 °C for 24 h. The sections were then dehydrated in a graded series of ethanol, and delipidised in a mixture of chloroform and ethanol (1:1, v/v). Following delipidisation, the sections were hydrated in a gradually decreasing series of ethanol and immersed in distilled water and stained with cresyl violet (0.7% in distilled water with 0.5% sodium acetate, Sigma, UK) for 5 min. After rinsing with the distilled water, the sections were dehydrated in a graded series of ethanol, cleared in xylene, cover-slipped with DPX mounting medium (RA Lamb, UK), and analysed under a Leica DMRBE microscope (Leica, Germany).

2.4. Immunohistochemistry

Immunohistochemistry (IHC) was undertaken according to Trueman et al. [50]. Briefly, all stains were applied on a one in six series of sections. Free-floating sections were processed for IHC using the sheep anti-S830 (Prof. G. Bates, Kings College, London, UK) and rabbit GFAP (DAKO, UK) primary antibodies. The S830 antibody selectively recognizes the aggregated form of the mutated htt protein [30]. The GFAP antibody was used for detecting astrocytes and measuring reactive astrogliosis [37].

The sections were then placed in TRIS Buffered Saline (TBS), washed x3, and then the endogenous peroxidise activity was quenched in methanol containing 3% H_2O_2 (VWR, Germany). This process was followed by 1 h incubation with 3% horse serum in TBS. Alternate series of sections were then incubated with S830 antibody (diluted 1:25000) or GFAP antibody (1:2000) overnight. After thorough washing in TBS, the sections were incubated with a horse anti-goat or horse anti-rabbit secondary antibody, respectively (diluted 1:200, Vector Laboratories, Burlingame, CA, USA). A biotin–streptavidin kit was used according to the manufacturer's instructions (Vector Laboratories) and the peroxidise activity was visualized with 3,3′-diaminobenzidine (DAB) (Sigma–Aldrich, Poole, Dorset, UK). The sections were mounted on gelatine-coated slides, dehydrated and cover-slipped.

A Leica DMRBE microscope fitted with a digital camera (Optronics, Goleta, California, USA) and imaging Software MagnaFire 1.2C (Goleta, California, USA) were used for light microscopic images. All pictures were captured using the same parameters and saved on computer for further analysis. A semi-quantitative analysis was used to assess the intensity of specific staining. This included the intensity of specific staining in sections: 0 = absent, + = week nuclear staining; + + = diffuse nuclear staining; + + + = few/minimum inclusions; + + + + = many/dense inclusions.

2.5. S830/CV stereology

2 dimensional cell counts were carried out using a PC-based image analysis software (Olympus C.A.S.T. grid system v1.6.) on a Olympus BX50 microscope (Olympus Corporation, Tokyo, Japan) and corrected using the Abercrombie formula [1]. Total cell counts were estimated by unbiased sampling through the striatum, using the automated microscope stage to select 265 μm^2 counting frames (viewed under a 100× counting objective and 10× eyepiece) at regular intervals throughout the striatum, Total striatal cell numbers (C) of each defined cell type were calculated according to the following formula:

$$C = \sum c \times \left(\frac{\sum A}{\sum a} \right) \times f$$

where $\sum c$ is the total number of cells counted; $\sum A$ is the sum of all the inclusion areas; $\sum a$ is the sum of all sample areas; and f is the frequency of sectioning. Cell counts were carried out on 1:6 series of S830-stained and of CV sections, throughout the entire striatum. All quantitative microscopy was undertaken and analysed blind to the experimental group and mouse age.

Please cite this article in press as: Z. Bayram-Weston, et al., Light and electron microscopic characterization of the evolution of cellular pathology in Hdh^{Q92} Huntington's disease knock-in mice, Brain Res. Bull. (2011), doi:10.1016/j.brainresbull.2011.03.013

2.6. Transmission electron microscopy (TEM)

For electron microscopy, four mice aged 14 months and 21 months were anaesthetized with Euthetal and perfused with 0.9% NaCl, followed by a mixture of 2% PFA and 2% glutaraldehyde in 0.1 M PBS solution (pH 7.4). The striatum of the brains were carefully dissected and post-fixed with 1% osmium tetroxide for 2 h at +4 °C. After washing with distilled water, the samples were stained overnight in 0.5% uranyl acetate at 4 °C and dehydrated in ascending series of ethanol and fresh propylene oxide, and then infiltrated overnight in a mixture of propylene oxide and araldite resin (1:1, v/v) and were embedded in fresh resin. Ultrathin sections (60 nm) were cut with a diamond knife on an ultracut-microtome (Reichert-Jung, Leica UK LTD, Milton Keynes, UK), collected on copper mesh grids and contrasted with uranyl acetate and Reynold's lead citrate. The prepared sections were examined with a Philips transmission electron microscope (Philips EM 208, The Netherlands).

2.7. Statistics

Statistical analyses were performed using one- and two-way ANOVA, using Genstat statistic programme (VSN International, Hemel Hempstead, UK).

3. Results

3.1. Striatal atrophy and neuronal cell counts pathology in the Hdh^{Q92} mice

We examined the volume of the striatum in $Hdh^{Q92/Q92}$ mice and wildtype littermates between 4 and 24 months of age in CV stained sections. The total striatal volume (Fig. 1A: Ages, $F_{8,70} = 12.98$, $p < 0.001$) and the total number of striatal neurons stained with CV (Fig. 1B: Ages, $F_{8,70} = 18.57$, $p < 0.001$) were relatively constant between 4 and 15 months of age, but then declined significantly over 15–24 months, towards the end of the lifespan. The decline of the striatal volume was similar between knock-in and wild type mice, however that there was a significant disease-dependent effects (Fig. 1A: Genotype, $F_{1,70} = 14.48$ $p < 0.001$). There was also significant effect on the total number of neurons (Fig. 1B: Genotype, $F_{1,70} = 10.96$ $p < 0.001$). There were no interaction effect on the striatal volume (Ages X Genotype, $F_{8,70} = 1.51$, n.s.), but the number of neurons decreased differentially with age for the two genotypes (Ages X Genotype, $F_{8,70} = 4.39$, $p < 0.001$), with the wildtype mice demonstrating a greater number of neurons relative to the knock-in animals as the mice aged.

3.2. Striatal neuronal pathology in the Hdh^{Q92} mice

The S830 staining demonstrated diffuse nuclear staining and nuclear inclusions in the homozygous mice. These mice exhibited distinctive regional expression of intra- and extra-nuclear inclusions. Intra-nuclear inclusions were not present in 4 month old homozygous mice, but diffuse nuclear staining in neurons within both the striatum and olfactory tubercle was seen from 4 to 12 months (Figs. 2D and E and 3A–C, Table 1). Both diffuse nuclear staining and minimum inclusions were focused in the olfactory tubercle and striatum at 6 months (Fig. 2H, K and N). By 8 months of age, diffuse nuclear staining appeared in the piriform cortex with few inclusions present in the olfactory tubercle and nucleus accumbens. By 10 months of age, nuclear inclusions were distributed widely throughout the striatum, olfactory tubercle, nucleus accumbens, central amygdala and piriform cortex with persistent diffuse nucleus staining throughout these areas (Table 1 and graphical summary in Fig. 4). This pattern of deposition did not change until 24 months of age where the presence of diffuse nuclear staining and inclusions varied depending on the brain region. The hypothalamus, cerebellum, and hippocampus all contained nuclear staining, and the medial septum and motor cortex contained diffuse nuclear staining, whereas there was no immunoreactivity in the globus pallidus or basolateral amygdala at this age (Fig. 4, Table 1). The total number of S830 affected cells gradually increased up to18 months of age, after which point the number of affected cells fell (Fig. 1C: Age, $F_{8,34} = 7.69$, $p < 0.001$). When separated to diffusely stained cells which were present at 4 months and peaked at 10 months of age, before dropping, an affect of age was found (Fig. 1D:Age, $F_{8,34} = 9.12$, $p < 0.001$). Similarly, the number of inclusions present also changed with time (Fig. 1D: inclusions, $F_{8,34} = 15.19$, $p < 0.001$), from being present at 10 months of age, peaking at 18 months of age before declining again. The extra-nuclear inclusions were first identified at 6 months old, in the olfactory tubercle, nucleus accumbens and striatum (Fig. 3F). At 24 months, the density and distribution varied depending on the region of the brain (Table 2), with the spread of pathology generally being along the anterior–posterior and ventral–dorsal planes. Cytosolic and nuclear inclusions progressed with age to more dense and larger inclusions (Figs. 3D–F and 4).

3.3. GFAP immunostaining

The homozygous $Hdh^{Q92/Q92}$ mice in the present experiment did not reveal any detectable increase in GFAP activity in comparison with the wildtype controls at any age. Although, GFAP activity increased with age in both homozygotes and control animals and was intense in several regions of the brain including striatum and cortex, neither the density nor the distribution of activity differed between the two experimental groups (Fig. 5).

3.4. Electron microscopy

Ultrastructural analysis revealed that the organelles found in the cell bodies of the striatum of 14 months old wild-type animal had preserved morphology including mitochondria, single strands of rough endoplasmic reticulum, polyribosomes and Golgi apparatus. The mitochondria and synaptic junctions appeared to be normal (Fig. 6A). Medium spiny neurons within the striatum of the homozygote animals exhibited intra-nuclear inclusions with small circular filamentous structures that could be easily identified and clearly distinguishable from their surrounding structures (NII in Fig. 6C) as seen before [8,10]. The loss of membrane integrity, a symptom usually associated with necrosis, was identified within cells exhibiting vacuolated cytoplasm, swollen mitochondria and uneven nuclear membrane (Fig. 6C). The majority of cells appeared unusually dark showing signs of apoptosis with dark cytoplasmic and nuclear contents. The cytoplasm also showed condensation and shrinkage, and the cell membrane was usually detached from the surrounding cells (Fig. 6E). MSNs within the striatum of the 21 months old wild type mouse revealed a more compact structure, and a preserved morphology, than that of the homozygote animal (Fig. 6B). The 21 month old homozygotes showed degenerative neurons with a number of apoptotic features (Fig. 6F). These neurons showed structural abnormalities such as angular shape and uneven nuclear membrane. The cytoplasm appeared severely vacuolated and contained swollen mitochondria. Most of the other cytoplasmic organelles were largely destroyed. Moreover, the 21 months old homozygotes displayed neuronal inclusions in the cytoplasm. These inclusions again appeared as large circular filamentous structures with no membrane (NII in Fig. 6D and F), but they were again clearly distinguishable from their surrounding as a result of their high electron density.

Please cite this article in press as: Z. Bayram-Weston, et al., Light and electron microscopic characterization of the evolution of cellular pathology in Hdh^{Q92} Huntington's disease knock-in mice, Brain Res. Bull. (2011), doi:10.1016/j.brainresbull.2011.03.013

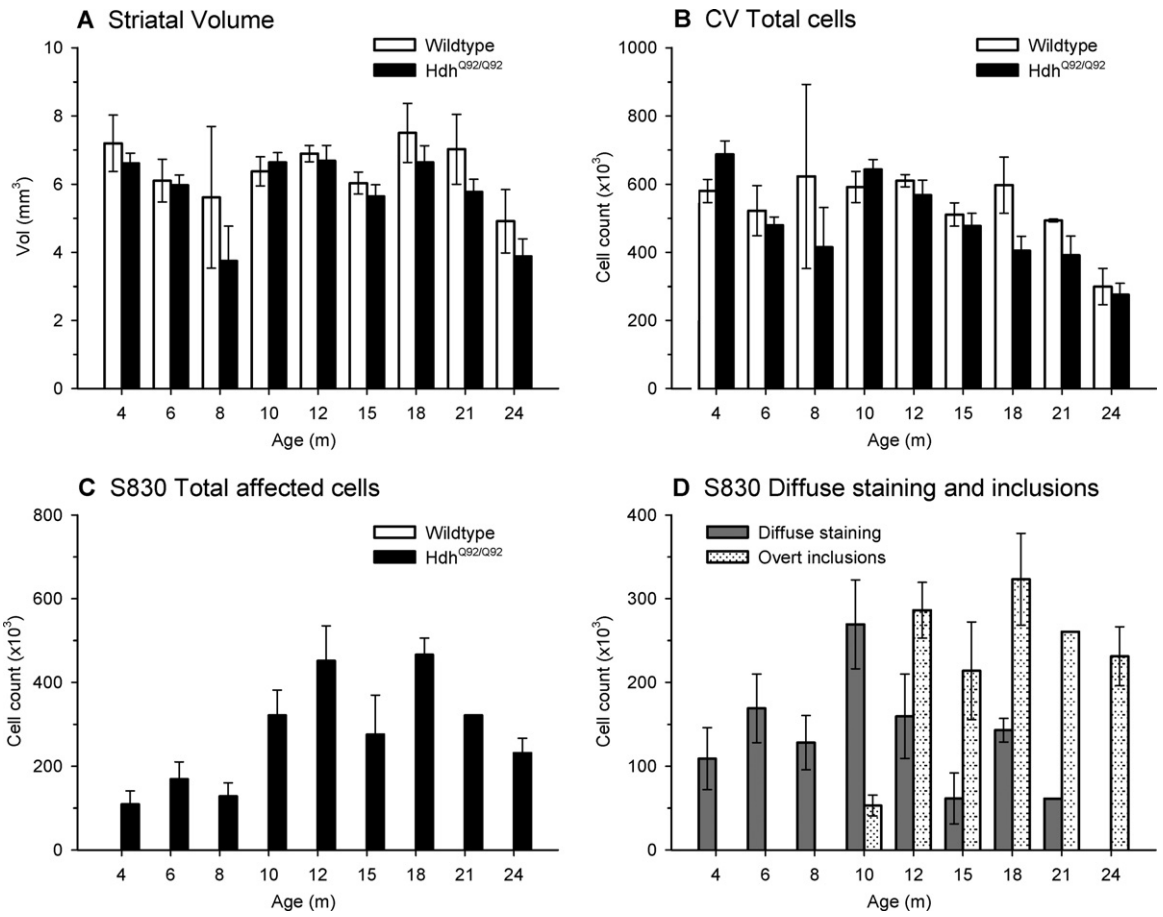

Fig. 1. The volume of the striatum in *Hdh*$^{Q92/Q92}$ mice and wildtype littermates between 4 and 24 months of age. The total neuron numbers of Cresyl violet – stained neurons in both wildtype and homozygote animals (A). The number of neurons in the wildtype mice is greater than that of the homozygous animals regardless of age (B). The number of affected cells increased with age from 4 months old peaks at 18 months and gradually decreased thereafter (C). Diffuse nuclear staining increased in number from 4 months to 10 months of age before decreasing steadily over the remaining 14 months. By contrast, intra-nuclear inclusions increased from 10 months to peak 18 months of age (D).

4. Discussion

The Hdh$^{Q92/Q92}$ mice exhibited a distinctive expression of intra- and extra-nuclear inclusions as revealed by the S830 huntingtin antibody staining which was both age- and region-dependent. We did not detect any intra-nuclear inclusions in 4 month old homozygous mice. However, even at this young age, diffuse nuclear staining was present in both the striatum and olfactory tubercle. Both diffuse nuclear staining and neuronal inclusions progressed with age, and by 10 months of age, nuclear inclusions were distributed extensively within the striatum, olfactory tubercle, nucleus accumbens, central amygdala and piriform cortex, in the presence of persistent diffuse nucleus staining. This deposition did not change up to 24 months of age when the mice exhibited diffuse nuclear staining

Table 1
Hdh$^{Q92/Q92}$ knock-in mice. Formation, progression and distribution of neuronal intra-nuclear inclusions (NIIs).

Hdh$^{Q92/Q92}$ brain/ages	4	6	8	10	12	15	18	21	24
Olfactory tubercle	++	++	+++	+++	++++	++++	++++	++++	++++
Nucleus accumbens	++	+++	+++	+++	++++	++++	++++	++++	++++
Globus pallidus-lateral	0	0	0	0	0	0	0	0	0
Globus pallidus-medial	0	0	0	0	0	0	0	0	0
Striatum ventral	+	+/++	+/++	++/+++	++++	++++	++++	++++	++++
Striatum dorsal	+	+/++	+/++	++/+++	++++	++++	++++	++++	++++
Striatum posterior	++	++	++	++/+++	++++	++++	++++	++++	++++
Septum lateral	0	+	+	+/++	++++	++++	++++	++++	++++
Septum med	0	0	0	0	+	+	++	++	++
Amygdala BL	0	0	0	0	0	0	0	0	0
Amygdala CL	0	++	++	+++	++++	++++	++++	++++	++++
Thalamus	0	0	0	0	0	0	+	+	0
Hypothalamus	0	0	0	0	0	0	+	+	+
Cerebellum	0	0	0	0	0	0	N/A	+	+
Hippocampus	0	0	0	0	0	0	+	+	+
Motor cortex	0	0	0	0	0	0	0/+	0/+	++
Sensory cortex	0	0	0	0	0	0	0/+	0/+	+++
Piriform cortex	0	0	+/++	++/+++	++/+++	++++	++++	+++	++++

0: absent, +: nuclear staining, ++: diffuse nuclear staining, +++: minimum inclusions, ++++: dense inclusions, N/A: not available.

Please cite this article in press as: Z. Bayram-Weston, et al., Light and electron microscopic characterization of the evolution of cellular pathology in Hdh^{Q92} Huntington's disease knock-in mice, Brain Res. Bull. (2011), doi:10.1016/j.brainresbull.2011.03.013

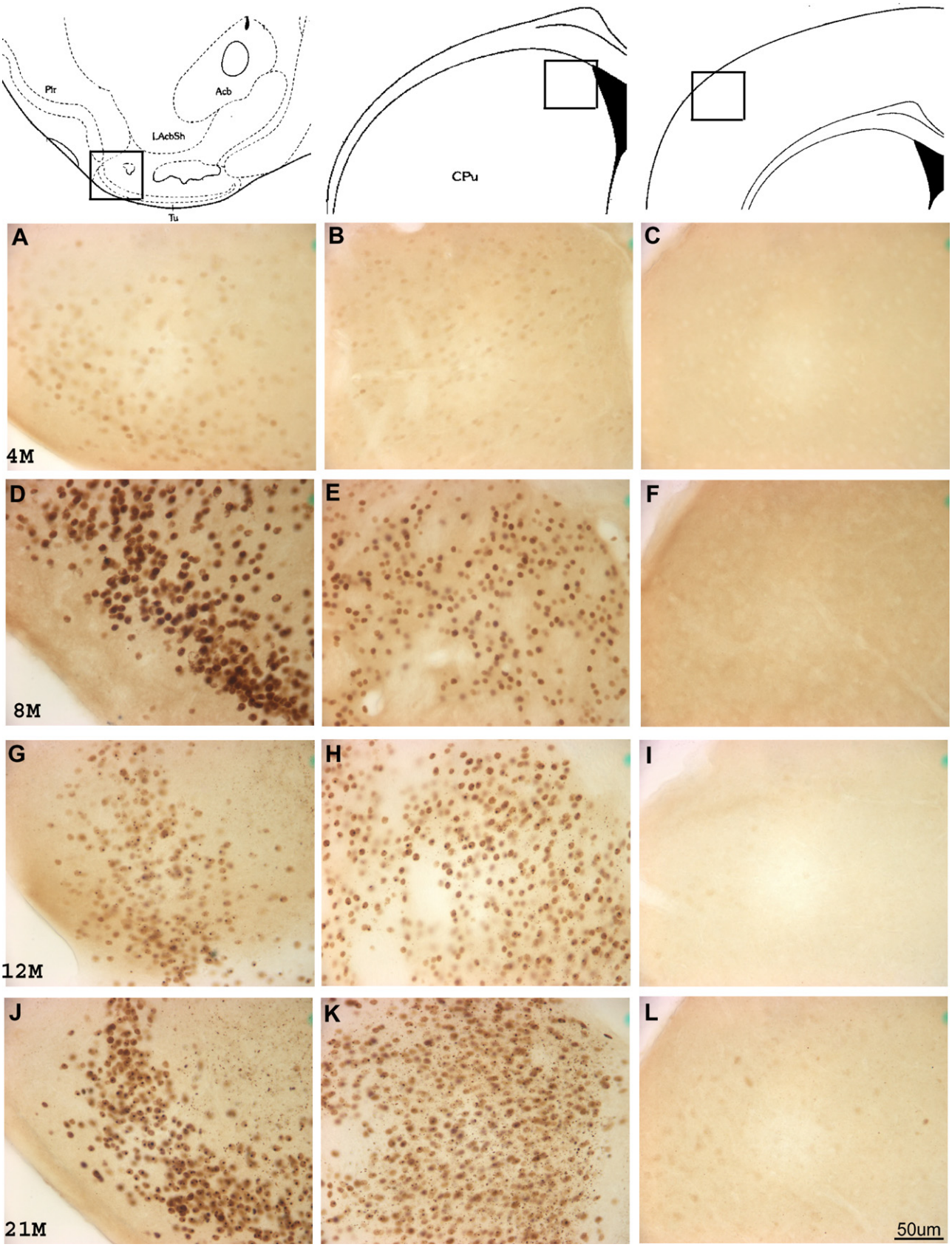

Fig. 2. Temporal evolution of S830 immunostaining of $Hdh^{Q92/Q92}$ brain in olfactory tubercle. (A,D,G,J), striatum (B,E,H,K), and cortex (C,F,I,L) at 4 (A–C), 8(D–F), 12 (G–I) and 21 (J–L) months of age. The development of NIIs is clearly visible in olfactory tubercle and striatal cells. Pir: piriform cortex, Tu: olfactory tubercle, CPu: striatum, Acb: nucleus accumbens, AcbSh: nucleus accumbens, shell. Scale bar = 50 μm.

Please cite this article in press as: Z. Bayram-Weston, et al., Light and electron microscopic characterization of the evolution of cellular pathology in Hdh^{Q92} Huntington's disease knock-in mice, Brain Res. Bull. (2011), doi:10.1016/j.brainresbull.2011.03.013

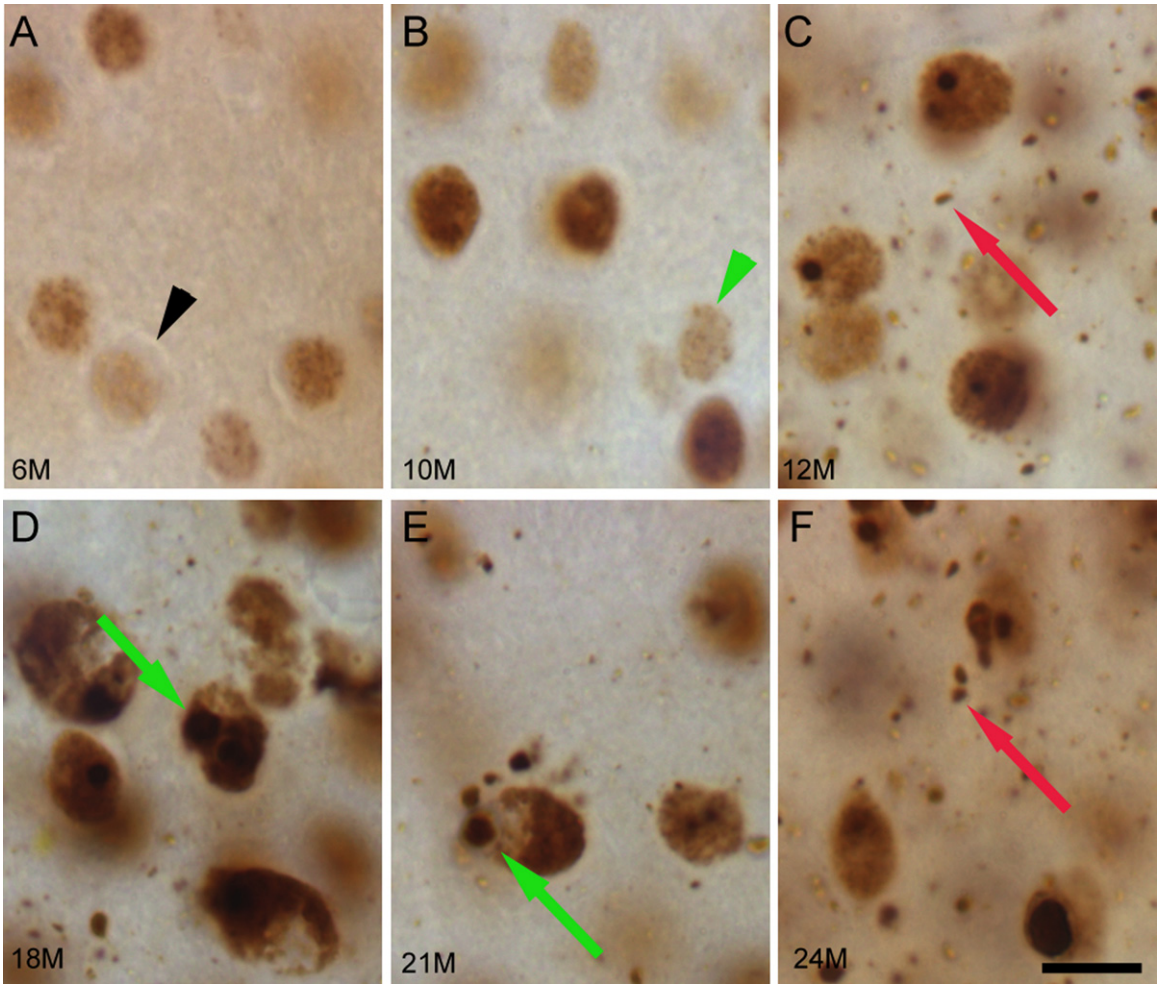

Fig. 3. High magnification images of striatal sections of $Hdh^{Q92/Q92}$ brain, showing age-dependent nuclear S830 immunoreactivity in 6 to 24 months old mice (A–F). Both diffuse nucleus staining and nuclear inclusions are observed in animals aged between 6 and 12 months (A–C). Older animals display no diffuse nucleus staining but widespread nuclear inclusions (D–F) and at 21 months of age (E), show neuronal degeneration with uneven nuclear membrane, vacuolisation around NIIs, and enlarged nuclear inclusions. Black arrow head denotes nuclear staining; green arrows indicate inclusions; red arrows indicate extra nuclear inclusions. Scale bar = 10 μm.

and inclusions the size and density of which varied depending on the region of the brain (Fig. 4 and Table 1). This work supports the hypothesis that the aggregation process begins with diffuse accumulation of protein in the nucleus, and as the phenotype progresses, they undergo an aggregation process and probable conformational changes resulting in progressively larger NII aggregates [19].

Wheeler et al. [61] previously reported that striatal neurons in homozygous $Hdh^{Q92/Q92}$ mice expressed diffuse nuclear staining from 4.5 to 5 months old. Our study confirmed that diffuse

Table 2
$Hdh^{Q92/Q92}$ knock-in mouse. Formation, progression and distribution of extra-nuclear inclusions (ENNIs).

$Hdh^{Q92/Q92}$ brain/ages	4	6	8	10	12	15	18	21	24
Olfactory tubercle	0	+	+	++	++++	++++	++++	++++	++++
Nucleus accumbens	0	+	+	+++	++++	++++	++++	++++	++++
Globus pallidus-lateral	0	0	+	++	+++	+++	+++	+++	+++
Globus pallidus-medial	0	0	+	+	++	++	+++	+++	++
Striatum ventral	0	+	+	+/++	+/++	0/+/++	++/+++	+++	+++
Striatum dorsal	0	+	+	+/++	+/++	0/+/++	++/+++	++/+++	+++
Striatum posterior	0	+	+	+/++	+/++	0/+/++	++/+++	++/+++	+++
Septum lateral	0	0	+	++	+++	+++	+++	+++	+++
Septum med	0	0	+	+	++	++	++	++	++
Amygdala BL	0	0	0	0	+	+	+	+	++
Amygdala CL	0	+	+	+	+++	+++	+++	+++	++++
Thalamus	0	0	0	+	+	+	+	+	++
Hypothalamus	0	0	0	+	+	+	+	+	+++
Cerebellum	0	0	0	+	+	++	N/A	+	+++
Hippocampus	0	0	0	+	+	+	+	+	++
Motor cortex	0	0	0	0	+	+	+	+	+++
Sensory cortex	0	0	0	0	+	+	+	++	+++
Piriform cortex	0	0	+	+	+++	+++	+++	+	++++

0: absent, +: very low staining, ++: intermediate staining, +++: dense staining, ++++: very dense staining, N/A: not available.

Please cite this article in press as: Z. Bayram-Weston, et al., Light and electron microscopic characterization of the evolution of cellular pathology in Hdh^{Q92} Huntington's disease knock-in mice, Brain Res. Bull. (2011), doi:10.1016/j.brainresbull.2011.03.013

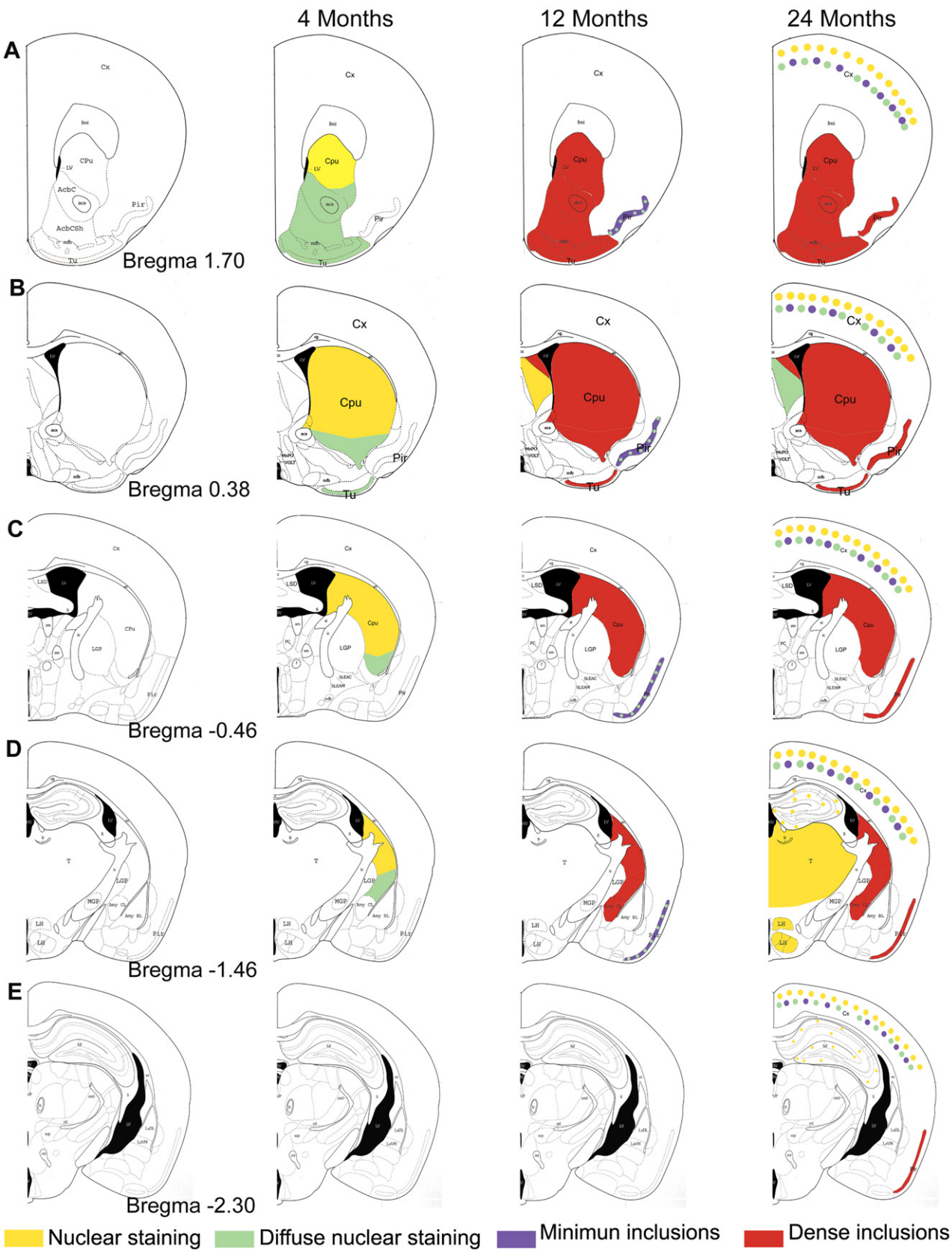

Fig. 4. Schematic overview of the spatial and temporal evolution of S830 immunostaining in Hdh$^{Q92/Q92}$ mouse brain at five coronal levels from anterior to posterior. The schematic diagram is modified after the atlas of Paxinos and Franklin, 1997 [33]. Each column shows the S830 expression patterns for three time points (4 M, 12 M and 24 M) in different colours. For colour coding see bottom of columns. Overlapping staining is represented by mixed colour.

Please cite this article in press as: Z. Bayram-Weston, et al., Light and electron microscopic characterization of the evolution of cellular pathology in Hdh^{Q92} Huntington's disease knock-in mice, Brain Res. Bull. (2011), doi:10.1016/j.brainresbull.2011.03.013

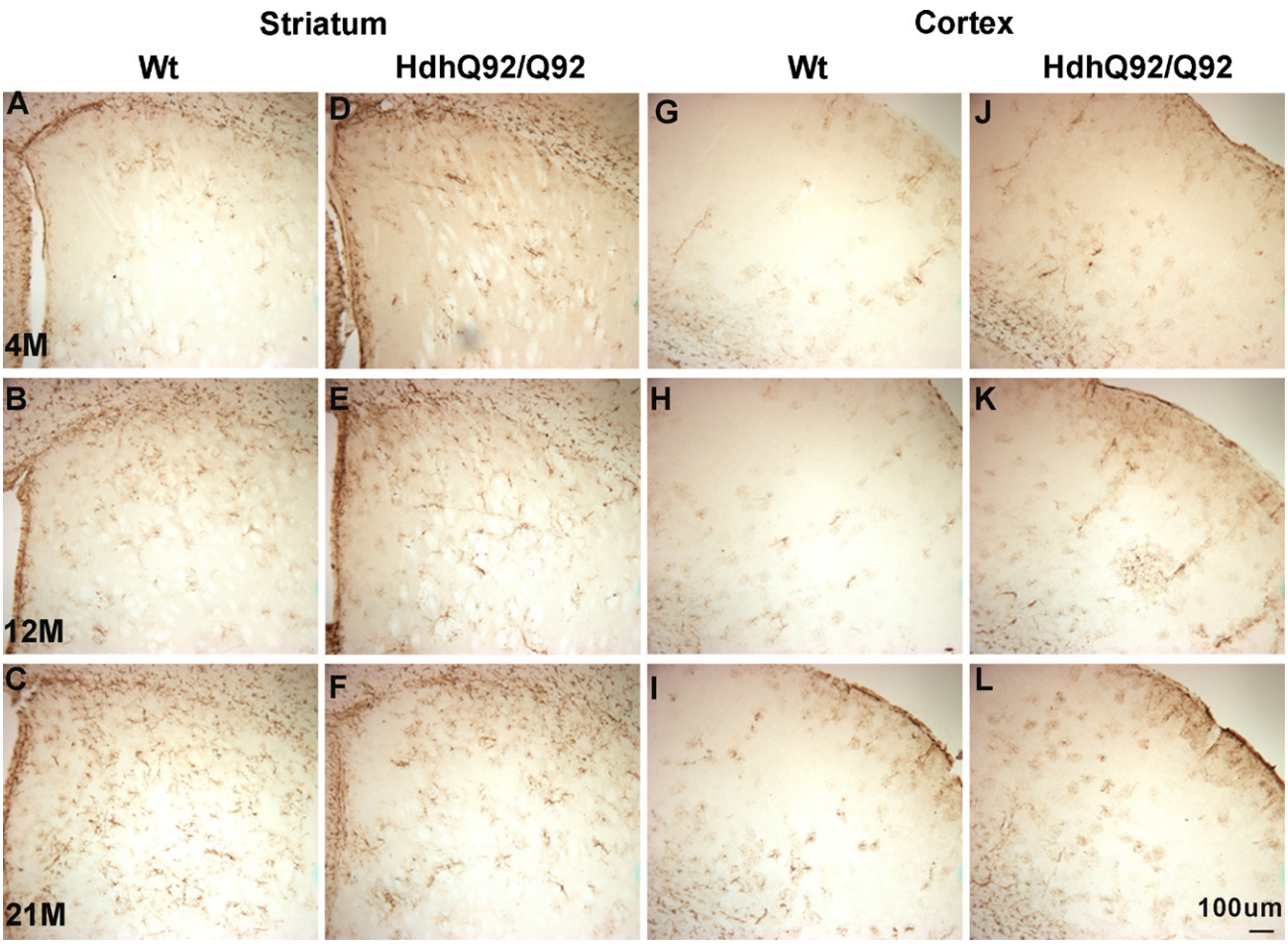

Fig. 5. GFAP immunolabelling in the striatum and cortex of wildtype and $Hdh^{Q92/Q92}$ mice. First row represent 4 months old wildtype and *Hdh*$^{Q92/Q92}$ mice, second row represents 12 months old and third row represents 21 months old. Strong intensity of GFAP immunostaining is observed in the striatum and the cortex of older animals of both wildtype and $Hdh^{Q92/Q92}$ mice. Wildtype animals showed increased GFAP activity with age, however, it did not differ from $Hdh^{Q92/Q92}$ mice. Scale bar = 100 μm.

nuclear staining was distributed throughout the striatum at this age. In addition, we also detected the diffuse immunoreaction in other regions, especially olfactory tubercle and nucleus accumbens of 4 months old homozygous mice. This finding was consistent with that of Trueman et al. [50] who showed that diffuse nuclear staining within the striatum and the olfactory tubercle was also observed from 4 months of age in the same mouse model. Wheeler et al. [61] reported the presence of intra-nuclear inclusions in 12–15 months old mice, whereas our study revealed that the inclusions together with persistent diffuse nuclear staining were first clearly detectable as early as 8 months of age, especially in the olfactory tubercle, striatum and nucleus accumbens. The former study [61] also described a progressive glutamine-dependent process whereby the major population of EM48 affected neurones were found in the striatum. They reported that this process also occurs in a small proportion of cells in other regions of the brain, in a gradient from youngest to oldest (1.5–10 months) and that the piriform cortex and cerebral cortex were equally affected. We did not observe the presence of intra-nuclear inclusions in 12 month old cerebral cortex. The earlier appearance of pathology that we report in comparison with the previous study [61] is less likely to be attributable to a drift in phenotype, as the repeat length is believed to have remained relatively stable in this strain, and is more likely to be due to differences in the sensitivity of the S830 over the EM48 antibodies. It has been recently shown that the different antibodies are sensitive to different confirmations of the protein, or that the protein reveals the relevant epitopes at different stages in the aggregation process [20].

In the current study, our primary focus was on characterising the distribution of the extra nuclear inclusions in $Hdh^{Q92/Q92}$ mice. Sections of 4 month old homozygous mice did not express any detectable extra-nuclear inclusions. However, by 6 months old mice began to show small extra-nuclear neuronal inclusions in some regions of the brain, including the olfactory tubercle, nucleus accumbens and striatum. The distribution of extra-nuclear inclusions was found to increase gradually with the age of mice. At 24 months, the density of the distribution varied depending on the region of the brain (Table 2). Li and colleagues [23] found that other brain regions (cortex, cerebellum, hippocampus) showed weak staining in the cytoplasm with EM48 antibody in mice of 27 months [23]. This observation is not consistent with our findings, in that our 24 month old animals did not display any cytoplasmic staining. On the contrary, our 24 month old $Hdh^{Q92/Q92}$ mice exhibited dense inclusions in the piriform cortex, minimum inclusions in the sensory cortex, and diffuse nucleus staining in the motor cortex. We also did not observe any nuclear inclusion formation in the globus pallidus. However we did detect modest levels of extra-nuclear inclusions in this region from 8 months and onwards. Furthermore, Yamamoto et al. [63] reported that the diffuse nuclear staining were present at 2 months in the HD94 mice striatum with lesser extent than extra-nuclear aggregates. In our studies, the diffuse nuclear staining was observed at 4 months of age in the $Hdh^{Q92/Q92}$ mice with no extra-nuclear aggregates. Again, this small difference in precise timing may be due to the different antibodies and mouse lines used in both studies. Lloret et al. have shown that

Please cite this article in press as: Z. Bayram-Weston, et al., Light and electron microscopic characterization of the evolution of cellular pathology in Hdh^{Q92} Huntington's disease knock-in mice, Brain Res. Bull. (2011), doi:10.1016/j.brainresbull.2011.03.013

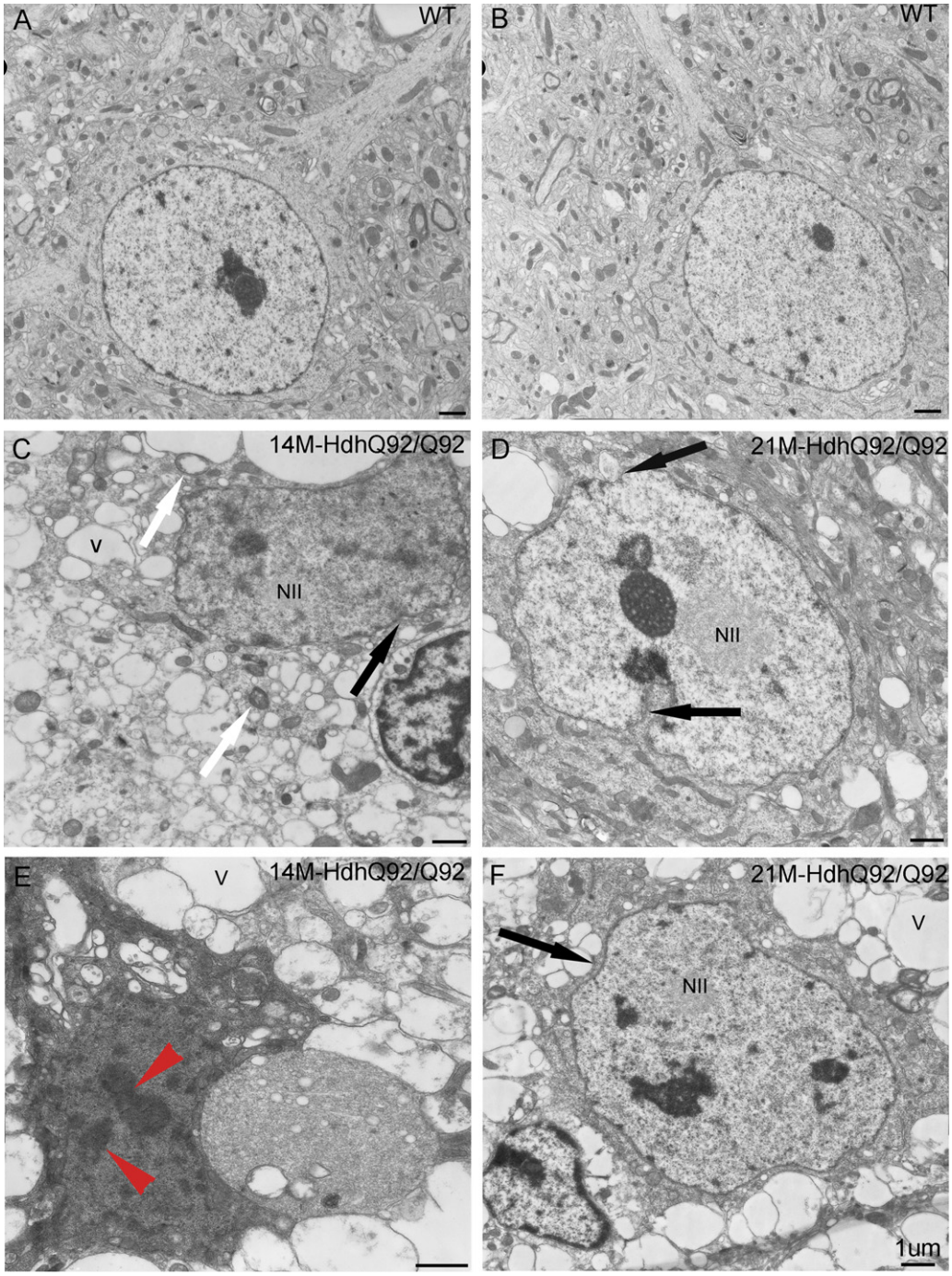

Fig. 6. Morphological characterization of the striatal cells in wildtypes (A,B) and $Hdh^{Q92/Q92}$ mice (C,D) at 14 and 21 months of age. Left panel indicates 14 months; right panel indicates 21 months of age. In wildtype animals, the cells were closely packed together (A,B). In $Hdh^{Q92/Q92}$ mice, necrotic changes such as vacuolization and membrane disintegration are noticeable (C,D). Some neurons showed apoptotic cell death features such as chromatin fragmentation, red arrow heads (E). Nuclear inclusions (NIIs) were clearly discernible from their surroundings with their pale appearance in both 14 months (C) and 21 months (D,F) with electron microscope. Neuronal degeneration as shown by loss of cytoplasmic contents noted in both age (C-F). NII: intra-nuclear inclusion, v: vacuole, black arrows indicate: uneven nuclear membrane, white arrows shows: swollen mitochondria. Magnifications are as described in figures. (For interpretation of the references to color in this figure legend, the reader is referred to the web version of the article.)

genetic background alters accumulation of mutant htt and NIIs in striatal neurons [26]. Similarly, Van Raamsdonk et al. have shown that the HD-like phenotypes are modulated by background strain [55], therefore the pathology may vary depending on the mouse background strain used in both studies.

The characteristic neuropathological features in HD patients are most prominent in the neostriatum and in the cerebral cortex, but are also observed in other brain areas, including accumbens, globus pallidus, amygdala and hippocampus, which are affected in the early stages of the disease [40]. Several studies have tried to correlate the existence and distribution of NIIs with neuronal degeneration in HD patients [12,15,28]. Maat-Schieman et al. have shown that there is a similar pattern between the distribution of NIIs and affected layers of the cortex [28]. Similarly, Gourfinkel-An et al. [12] have indicated that there was a close relationship between neuronal degeneration and the existence of neuronal

Please cite this article in press as: Z. Bayram-Weston, et al., Light and electron microscopic characterization of the evolution of cellular pathology in Hdh^{Q92} Huntington's disease knock-in mice, Brain Res. Bull. (2011), doi:10.1016/j.brainresbull.2011.03.013

inclusions. Inclusions were more abundant in all layers of the cerebral cortex and the dorsal striatum. However, they were less evident in the globus pallidus and the thalamus, and were rarely seen in the ventral striatum and absent in the cerebellum [12]. These results were partially confirmed by Maat-Schieman et al., who have shown that NIIs were absent in the cerebellum, less abundant in the neostriatum and more abundant in all layers of neocortex, however, they were not observed in globus pallidus and substantia nigra [28]. Gutekunst et al. [15] also reported many more aggregates in the cortex than in the striatum. However, they identified dorso-striatal neuronal loss, while no cortical degeneration was described. Higher-grade cases on the Vonsattel scale [57] had fewer aggregates, suggesting that the lower levels of inclusions typically reported in the human brain may be a result of a greater level of overt neuronal loss than in the mouse, in particular in the striatum, over time. Moreover, aggregates were not distributed in the mouse brain in the same way as the pattern of either cellular pathology or neuronal loss seen in HD. Thus, Gutekunst et al. found that the density of aggregates was lower in the caudate, putamen, substantia nigra, hypothalamic nuclei and thalamus than in the cortex in human HD, and in the globus pallidus, hippocampus and cerebellum, aggregates were rarely seen [15]. Our findings in the $Hdh^{Q92/Q92}$ partially agree with Gutekunst results, as the density of aggregates was relatively low in the hypothalamic nuclei, thalamus, globus pallidus and hippocampus of the $Hdh^{Q92/Q92}$ mouse also. However we have found greater density of aggregates in the striatum. Additionally, Gutekunst et al. found larger punctate aggregates in later grade cases [15], as in the $Hdh^{Q92/Q92}$ mouse model. Although we have observed NIIs in the $Hdh^{Q92/Q92}$ mouse line, we have also found the same degree of overt neuronal loss as in the human studies [15,16,57].

In the current study, we also used electron microscopy to examine fixed brain tissue, an approach not previously used in the Hdh^{Q92} mice line. Our analysis agrees with previous reports of post-mortem tissue from HD patients brains and transgenic mouse models, where intra-nuclear inclusions consist of filamentous structures [8,10,15,32]. At the ultrastructural level, it has been shown that human HD brain tissues exhibit nuclear membrane indentations, nuclear disorganization, reduction of the ribosomes [38,39], large accumulations of lipofucsin granules and enlarged mitochondria [48]. Our results show characteristic features in this mouse line similar both to the descriptions in the human brain [8,10,15,38] and to our previous findings in the $Hdh^{(CAG)Q150}$ knock-in mouse [5] and YAC128 transgenic mouse [4]. Morton et al. have reported that ENNIs were present in the synaptic densities of the neurons by electron microscopy using immunogold labelling in the R6/2 mouse line [31]. Although we identified ENNIs with S830 immunohistochemistry in the light microscope, we were not able to identify ENNIs in the synaptic junctions of the neurons in the Hdh^{Q92} mice line by conventional, non-immunogold TEM, which is in agreement with our previous studies [3–5]. This suggests that ENNIs may be a soluble form of aggregate and thus require antibodies to enhance the visualization with electron microscopy.

Furthermore, we did not find any alteration in the intensity of GFAP immunostaining between Hdh^{Q92} homozygous and their littermates. This finding is at variance with the reports of Yamamoto et al. [63] who found increased GFAP activity in the striatum at 4.5 months of age in the related HD94 mouse line. Similarly, Reddy et al. [34] also observed increased reactive astrogliosis in their transgenic HD89 mice [34], in agreement with our other studies on the $Hdh^{(CAG)Q150}$, YAC128 and R6/1 mouse models [3–5]. This may indicate that astroglial reaction was not associated with the expanded CAG repeat length.

In summary, the present study found a progressive and spatially circumscribed development of neuropathology in the Hdh^{Q92} knock-in mouse line, that developed in a ventro-dorsal, medial–lateral, and anterior–posterior fashion, as described in man. The areas most affected were the olfactory tubercle, nucleus accumbens, striatum, lateral septum, the central amygdala and piriform cortex with the regions that were affected earliest being the olfactory tubercle, nucleus accumbens and striatum. Furthermore, our study indicated that motor and sensory cortices were affected with NIIs at the later stage, consistent with HD patients. This mouse line also demonstrated a brain atrophy and striatal cell loss that underlies the advanced disease in man.

Acknowledgements

We thank Prof Gillian Bates (King College London) for the generous gift of S830 antibody, Prof Ifor Bowen and Dr Anthony Hann (Cardiff University) for their helpful advice on the EM studies and Alison Baird, Jane Heath and Linda Elisston for technical support. This study was funded a MRC studentship to ZBW, and project funding by Cure Huntington's Disease Intuitive (CHDI) Foundation Inc.

References

[1] M. Abercrombie, Estimation of nuclear population from microtome sections, Anatomical Records (1946) 239–247.
[2] G.P. Bates, P.S. Harper, L. Jones 2, in: G.P. Bates, P.S. Harper, L. Jones (Eds.), Huntington's Disease, Oxford University Press, 2002.
[3] Z. Bayram-Weston, L. Jones, S.B. Dunnett, S.P. Brooks, Light and electron microscopic characterization of the evolution of cellular pathology in the R6/1 transgenic mouse., Brain Res. Bull., in this issue (2010).
[4] Z. Bayram-Weston, L. Jones, S.B. Dunnett, S.P. Brooks, Light and electron microscopic characterization of the evolution of cellular pathology in YAC128 transgenic mice, Brain Res. Bull., in this issue.
[5] Z. Bayram-Weston, E.M. Torres, L. Jones, S.B. Dunnett, Brooks S.P. Light and electron microscopic characterization of the evolution of cellular pathology in the *Hdh*(CAG)150 Huntington's disease knock-in mouse, Brain Res. Bull., in this issue.
[6] S. Brooks, G. Higgs, L. Jones, S.B. Dunnett, Longitudinal analysis of the behavioural phenotype in Hdh(Q92) Huntington's disease knock-in mice, Brain Res. Bull. (2010), doi:10.1016/j.brainresbull.2010.05.003.
[7] E. Cattaneo, P. Calabresi, Mutant huntingtin goes straight to the heart, Nat. Neurosci. 5 (2002) 711–712.
[8] S.W. Davies, M. Turmaine, B.A. Cozens, M. DiFiglia, A.H. Sharp, C.A. Ross, E. Scherzinger, E.E. Wanker, L. Mangiarini, G.P. Bates, Formation of neuronal intranuclear inclusions underlies the neurological dysfunction in mice transgenic for the HD mutation, Cell 90 (1997) 537–548.
[9] M. DiFiglia, E. Sapp, K. Chase, C. Schwarz, A. Meloni, C. Young, E. Martin, J.P. Vonsattel, R. Carraway, S.A. Reeves, Huntingtin is a cytoplasmic protein associated with vesicles in human and rat brain neurons, Neuron 14 (1995) 1075–1081.
[10] M. DiFiglia, E. Sapp, K.O. Chase, S.W. Davies, G.P. Bates, J.P. Vonsattel, N. Aronin, Aggregation of huntingtin in neuronal intranuclear inclusions and dystrophic neurites in brain, Science 277 (1997) 1990–1993.
[11] R.J. Ferrante, C.A. Gutekunst, F. Persichetti, S.M. McNeil, N.W. Kowall, J.F. Gusella, M.E. MacDonald, M.F. Beal, S.M. Hersch, Heterogeneous topographic and cellular distribution of huntingtin expression in the normal human neostriatum, J. Neurosci. 17 (1997) 3052–3063.
[12] I. Gourfinkel-An, G. Cancel, C. Duyckaerts, B. Faucheux, J.J. Hauw, Y. Trottier, A. Brice, Y. Agid, E.C. Hirsch, Neuronal distribution of intranuclear inclusions in Huntington's disease with adult onset, Neuroreport 9 (1998) 1823–1826.
[13] G.A. Graveland, R.S. Williams, M. DiFiglia, Evidence for degenerative and regenerative changes in neostriatal spiny neurons in Huntington's disease, Science 227 (1985) 770–773.
[14] M. Gray, D.I. Shirasaki, C. Cepeda, V.M. Andre, B. Wilburn, X.H. Lu, J. Tao, I. Yamazaki, S.H. Li, Y.E. Sun, X.J. Li, M.S. Levine, X.W. Yang, Full-length human mutant huntingtin with a stable polyglutamine repeat can elicit progressive and selective neuropathogenesis in BACHD mice, J. Neurosci. 28 (2008) 6182–6195.
[15] C.A. Gutekunst, S.H. Li, H. Yi, J.S. Mulroy, S. Kuemmerle, R. Jones, D. Rye, R.J. Ferrante, S.M. Hersch, X.J. Li, Nuclear and neuropil aggregates in Huntington's disease: relationship to neuropathology, J. Neurosci. 19 (1999) 2522–2534.
[16] J.C. Hedreen, S.E. Folstein, Early loss of neostriatal striosome neurons in Huntington's disease, J. Neuropathol. Exp. Neurol. 54 (1995) 105–120.
[17] J.G. Hodgson, N. Agopyan, C.A. Gutekunst, B.R. Leavitt, F. LePiane, R. Singaraja, D.J. Smith, N. Bissada, K. McCutcheon, J. Nasir, L. Jamot, X.J. Li, M.E. Stevens, E. Rosemond, J.C. Roder, A.G. Phillips, E.M. Rubin, S.M. Hersch, M.R. Hayden, A YAC mouse model for Huntington's disease with full-length mutant huntingtin, cytoplasmic toxicity, and selective striatal neurodegeneration, Neuron 23 (1999) 181–192.
[18] A.T Hoogeveen, R. Willemsen, N. Meyer, K.E. de Rooij, R.A. Roos, G.J. van Ommen, H. Galjaard, Characterization and localization of the Huntington disease gene product, Hum. Mol. Genet. 2 (1993) 2069–2073.

Please cite this article in press as: Z. Bayram-Weston, et al., Light and electron microscopic characterization of the evolution of cellular pathology in Hdh^{Q92} Huntington's disease knock-in mice, Brain Res. Bull. (2011), doi:10.1016/j.brainresbull.2011.03.013

[19] C. Landles, G.P. Bates, Huntingtin and the molecular pathogenesis of Huntington's disease – fourth in molecular medicine review series 1, Embo Rep. 5 (2004) 958–963.
[20] C. Landles, K. Sathasivam, A. Weiss, B. Woodman, H. Moffitt, S. Finkbeiner, B. Sun, J. Gafni, L.M. Ellerby, Y. Trottier, W.G. Richards, A. Osmand, P. Paganetti, G.P. Bates, Proteolysis of mutant huntingtin produces an exon 1 fragment that accumulates as an aggregated protein in neuronal nuclei in Huntington disease, J. Biol. Chem. 285 (2010) 8808–8823.
[21] M.S. Levine, G.J. Klapstein, A. Koppel, E. Gruen, C. Cepeda, M.E. Vargas, E.S. Jokel, E.M. Carpenter, H. Zanjani, R.S. Hurst, A. Efstratiadis, S. Zeitlin, M.F. Chesselet, Enhanced sensitivity to N-methyl-D-aspartate receptor activation in transgenic and knockin mouse models of Huntington's disease, J. Neurosci. Res. 58 (1999) 515–532.
[22] H. Li, S.H. Li, A.L. Cheng, L. Mangiarini, G.P. Bates, X.J. Li, Ultrastructural localization and progressive formation of neuropil aggregates in Huntington's disease transgenic mice, Hum. Mol. Genet. 8 (1999) 1227–1236.
[23] H. Li, S.H. Li, H. Johnston, P.F. Shelbourne, X.J. Li, Amino-terminal fragments of mutant huntingtin show selective accumulation in striatal neurons and synaptic toxicity, Nat. Genet. 25 (2000) 385–389.
[24] J.Y. Li, M. Plomann, P. Brundin, Huntington's disease: a synaptopathy? Trends Mol. Med. 9 (2003) 414–420.
[25] C.H. Lin, S. Tallaksen-Greene, W.M. Chien, J.A. Cearley, W.S. Jackson, A.B. Crouse, S. Ren, X.J. Li, R.L. Albin, P.J. Detloff, Neurological abnormalities in a knock-in mouse model of Huntington's disease, Hum. Mol. Genet. 10 (2001) 137–144.
[26] A. Lloret, E. Dragileva, A. Teed, J. Espinola, E. Fossale, T. Gillis, E. Lopez, R.H. Myers, M.E. MacDonald, V.C. Wheeler, Genetic background modifies nuclear mutant huntingtin accumulation and HD CAG repeat instability in Huntington's disease knock-in mice, Hum. Mol. Genet. 15 (2006) 2015–2024.
[27] A. Lunkes, J.L. Mandel, A cellular model that recapitulates major pathogenic steps of Huntington's disease, Hum. Mol. Genet. 7 (1998) 1355–1361.
[28] M.L. Maat-Schieman, J.C. Dorsman, M.A. Smoor, S. Siesling, S.G. Van Duinen, J.J. Verschuuren, J.T. den Dunnen, G.J. van Ommen, R.A. Roos, Distribution of inclusions in neuronal nuclei and dystrophic neurites in Huntington disease brain, J. Neuropathol. Exp. Neurol. 58 (1999) 129–137.
[29] L.B. Menalled, J.D. Sison, I. Dragatsis, S. Zeitlin, M.F. Chesselet, Time course of early motor and neuropathological anomalies in a knock-in mouse model of Huntington's disease with 140 CAG repeats, J. Comp. Neurol. 465 (2003) 11–26.
[30] A.J. Milnerwood, D.M. Cummings, G.M. Dallerac, J.Y. Brown, S.C. Vatsavayai, M.C. Hirst, P. Rezaie, K.P. Murphy, Early development of aberrant synaptic plasticity in a mouse model of Huntington's disease, Hum. Mol. Genet. 15 (2006) 1690–1703.
[31] A.J. Morton, M.A. Lagan, J.N. Skepper, S.B. Dunnett, Progressive formation of inclusions in the striatum and hippocampus of mice transgenic for the human Huntington's disease mutation, J. Neurocytol. 29 (2000) 679–702.
[32] J.M. Ordway, S. Tallaksen-Greene, C.A. Gutekunst, E.M. Bernstein, J.A. Cearley, H.W. Wiener, L.S. Dure, R. Lindsey, S.M. Hersch, R.S. Jope, R.L. Albin, P.J. Detloff, Ectopically expressed CAG repeats cause intranuclear inclusions and a progressive late onset neurological phenotype in the mouse, Cell 91 (1997) 753–763.
[33] G. Paxinos, K.B.J. Franklin, The Mouse Brain in Stereotaxic Coordinates, 2nd ed., Academic Press, San Diego, CA, 2001.
[34] P.H. Reddy, M. Williams, V. Charles, L. Garrett, L. Pike-Buchanan, W.O. Whetsell Jr., G. Miller, D.A. Tagle, Behavioural abnormalities and selective neuronal loss in HD transgenic mice expressing mutated full-length HD cDNA, Nat. Genet. 20 (1998) 198–202.
[35] P.H. Reddy, M. Williams, D.A. Tagle, Recent advances in understanding the pathogenesis of Huntington's disease, Trends Neurosci. 22 (1999) 248–255.
[36] A. Reiner, R.L. Albin, K.D. Anderson, C.J. D'Amato, J.B. Penney, A.B. Young, Differential loss of striatal projection neurons in Huntington disease, Proc. Natl. Acad. Sci. U. S. A. 85 (1988) 5733–5737.
[37] A. Reiner, N. Del Mar, Y.P. Deng, C.A. Meade, Z. Sun, D. Goldowitz, R6/2 neurons with intranuclear inclusions survive for prolonged periods in the brains of chimeric mice, J. Comp. Neurol. 505 (2007) 603–629.
[38] R.A. Roos, G.T. Bots, Nuclear membrane indentations in Huntington's chorea, J. Neurol. Sci. 61 (1983) 37–47.
[39] R.A. Roos, J.F. Pruyt, J. de Vries, G.T. Bots, Neuronal distribution in the putamen in Huntington's disease, J. Neurol. Neurosurg. Psychiatry 48 (1985) 422–425.
[40] H.D. Rosas, W.J. Koroshetz, Y.I. Chen, C. Skeuse, M. Vangel, M.E. Cudkowicz, K. Caplan, K. Marek, L.J. Seidman, N. Makris, B.G. Jenkins, J.M. Goldstein, Evidence for more widespread cerebral pathology in early HD: an MRI-based morphometric analysis, Neurology 60 (2003) 1615–1620.
[41] C.A. Ross, Intranuclear neuronal inclusions: a common pathogenic mechanism for glutamine-repeat neurodegenerative diseases? Neuron 19 (1997) 1147–1150.
[42] E. Sapp, C. Schwarz, K. Chase, P.G. Bhide, A.B. Young, J. Penney, J.P. Vonsattel, N. Aronin, M. DiFiglia, Huntingtin localization in brains of normal and Huntington's disease patients, Ann. Neurol. 42 (1997) 604–612.
[43] F. Saudou, S. Finkbeiner, D. Devys, M.E. Greenberg, Huntingtin acts in the nucleus to induce apoptosis but death does not correlate with the formation of intranuclear inclusions, Cell 95 (1998) 55–66.
[44] A.H. Sharp, S.J. Loev, G. Schilling, S.H. Li, X.J. Li, J. Bao, M.V. Wagster, J.A. Kotzuk, J.P. Steiner, A. Lo, Widespread expression of Huntington's disease gene (IT15) protein product, Neuron 14 (1995) 1065–1074.
[45] R.R. Singaraja, S. Hadano, M. Metzler, S. Givan, C.L. Wellington, S. Warby, A. Yanai, C.A. Gutekunst, B.R. Leavitt, H. Yi, K. Fichter, L. Gan, K. McCutcheon, V. Chopra, J. Michel, S.M. Hersch, J.E. Ikeda, M.R. Hayden, HIP14, a novel ankyrin domain-containing protein, links huntingtin to intracellular trafficking and endocytosis, Hum. Mol. Genet. 11 (2002) 2815–2828.
[46] S.S. Sisodia, Nuclear inclusions in glutamine repeat disorders: are they pernicious, coincidental, or beneficial? Cell 95 (1998) 1–4.
[47] E.J Slow, J. van Raamsdonk, D. Rogers, S.H. Coleman, R.K. Graham, Y. Deng, R. Oh, N. Bissada, S.M. Hossain, Y.Z. Yang, X.J. Li, E.M. Simpson, C.A. Gutekunst, B.R. Leavitt, M.R. Hayden, Selective striatal neuronal loss in a YAC128 mouse model of Huntington disease, Hum. Mol. Genet. 12 (2003) 1555–1567.
[48] I. Tellez-Nagel, A.B. Johnson, R.D. Terry, Studies on brain biopsies of patients with Huntington's chorea, J. Neuropathol. Exp. Neurol. 33 (1974) 308–332.
[49] The Huntington's Disease Collaborative Research Group, A novel gene containing a trinucleotide repeat that is expanded and unstable on Huntington's disease chromosomes, Cell 72 (1993) 971–983.
[50] R.C. Trueman, S.P. Brooks, L. Jones, S.B. Dunnett, The operant serial implicit learning task reveals early onset motor learning deficits in the Hdh knock-in mouse model of Huntington's disease, Eur. J. Neurosci. 25 (2007) 551–558.
[51] R.C. Trueman, S.P. Brooks, L. Jones, S.B. Dunnett, Time course of choice reaction time deficits in the Hdh(Q92) knock-in mouse model of Huntington's disease in the operant serial implicit learning task (SILT), Behav. Brain Res. 189 (2008) 317–324.
[52] R.C. Trueman, S.P. Brooks, L. Jones, S.B. Dunnett, Rule learning, visuospatial function and motor performance in the Hdh(Q92) knock-in mouse model of Huntington's disease, Behav. Brain Res. 203 (2009) 215–222.
[53] E. Trushina, R.B. Dyer, J.D. Badger, D. Ure, L. Eide, D.D. Tran, B.T. Vrieze, V. Legendre-Guillemin, P.S. McPherson, B.S. Mandavilli, B. Van Houten, S. Zeitlin, M. McNiven, R. Aebersold, M. Hayden, J.E. Parisi, E. Seeberg, I. Dragatsis, K. Doyle, A. Bender, C. Chacko, C.T. McMurray, Mutant huntingtin impairs axonal trafficking in mammalian neurons in vivo and in vitro, Mol. Cell Biol. 24 (2004) 8195–8209.
[54] M. Turmaine, A. Raza, A. Mahal, L. Mangiarini, G.P. Bates, S.W. Davies, Nonapoptotic neurodegeneration in a transgenic mouse model of Huntington's disease, Proc. Natl. Acad. Sci. U. S. A. 97 (2000) 8093–8097.
[55] J.M. Van Raamsdonk, M. Metzler, E. Slow, J. Pearson, C. Schwab, J. Carroll, R.K. Graham, B.R. Leavitt, M.R. Hayden, Phenotypic abnormalities in the YAC128 mouse model of Huntington disease are penetrant on multiple genetic backgrounds and modulated by strain, Neurobiol. Dis. 26 (2007) 189–200.
[56] J.P. Vonsattel, M. DiFiglia, Huntington disease, J. Neuropathol. Exp. Neurol. 57 (1998) 369–384.
[57] J.P. Vonsattel, R.H. Myers, T.J. Stevens, R.J. Ferrante, E.D. Bird, E.P. Richardson Jr., Neuropathological classification of Huntington's disease, J. Neuropathol. Exp. Neurol. 44 (1985) 559–577.
[58] S. Waelter, A. Boeddrich, R. Lurz, E. Scherzinger, G. Lueder, H. Lehrach, E.E. Wanker, Accumulation of mutant huntingtin fragments in aggresome-like inclusion bodies as a result of insufficient protein degradation, Mol. Biol. Cell 12 (2001) 1393–1407.
[59] A. Weiss, A. Roscic, P. Paganetti, Inducible mutant huntingtin expression in HN10 cells reproduces Huntington's disease-like neuronal dysfunction, Mol. Neurodegener. 4 (2009) 11.
[60] V.C. Wheeler, W. Auerbach, J.K. White, J. Srinidhi, A. Auerbach, A. Ryan, M.P. Duyao, V. Vrbanac, M. Weaver, J.F. Gusella, A.L. Joyner, M.E. MacDonald, Length-dependent gametic CAG repeat instability in the Huntington's disease knock-in mouse, Hum. Mol. Genet. 8 (1999) 115–122.
[61] V.C. Wheeler, J.K. White, C.A. Gutekunst, V. Vrbanac, M. Weaver, X.J. Li, S.H. Li, H. Yi, J.P. Vonsattel, J.F. Gusella, S. Hersch, W. Auerbach, A.L. Joyner, M.E. MacDonald, Long glutamine tracts cause nuclear localization of a novel form of huntingtin in medium spiny striatal neurons in HdhQ92 and HdhQ111 knock-in mice, Hum. Mol. Genet. 9 (2000) 503–513.
[62] J.K. White, W. Auerbach, M.P. Duyao, J.P. Vonsattel, J.F. Gusella, A.L. Joyner, M.E. MacDonald, Huntingtin is required for neurogenesis and is not impaired by the Huntington's disease CAG expansion, Nat. Genet. 17 (1997) 404–410.
[63] A. Yamamoto, J.J. Lucas, R. Hen, Reversal of neuropathology and motor dysfunction in a conditional model of Huntington's disease, Cell 101 (2000) 57–66.

Please cite this article in press as: Z. Bayram-Weston, et al., Light and electron microscopic characterization of the evolution of cellular pathology in Hdh^{Q92} Huntington's disease knock-in mice, Brain Res. Bull. (2011), doi:10.1016/j.brainresbull.2011.03.013

Chapter 6

Paper 4

Light and electron microscopic characterization of the evolution of cellular pathology in the Hdh(CAG)150 Huntington's disease knock-in mouse.

Bayram-Weston Z., Torres E.M., Jones L., Dunnett S.B., and Brooks S.P.

Brain Res Bull. 2011, in press.

Brain Research Bulletin xxx (2011) xxx–xxx

Contents lists available at ScienceDirect

Brain Research Bulletin

journal homepage: www.elsevier.com/locate/brainresbull

Research report

Light and electron microscopic characterization of the evolution of cellular pathology in the Hdh$^{(CAG)150}$ Huntington's disease knock-in mouse☆

Zubeyde Bayram-Weston[a,*], Eduardo M. Torres[a], Lesley Jones[b], Stephen B. Dunnett[a], Simon P. Brooks[a]

[a] School of Biosciences, Cardiff University, Museum Avenue, Cardiff CF10 3AX, Wales, UK
[b] Department of Psychological Medicine, 2nd Floor, Henry Wellcome Building, Wales School of Medicine, Cardiff University, Cardiff CF14 4XN, Wales, UK

ARTICLE INFO

Article history:
Received 29 July 2010
Received in revised form 15 March 2011
Accepted 18 March 2011
Available online xxx

Keywords:
Huntington's disease
Aggregations
Inclusions
HdhQ150/Q150
Knock-in
Transmission electron microscope (TEM)

ABSTRACT

Huntington's disease is an autosomal dominant, progressive neurodegenerative disease in which a single mutation in the gene responsible for the protein huntingtin leads to a primarily striatal and cortical neuronal loss, resulting progressive motor, cognitive and psychiatric disability and ultimately death. The mutation induces an abnormal protein accumulation within cells, although the precise role of this accumulation in the disease process is unknown. Several animal models have been created to model the disease. In the present study, the pathology of the *Hdh*$^{CAG(150)}$ mouse model was analyzed longitudinally over 24 months. At 5 months of age, the mutant N-terminal antibody S830 found dense nuclear staining and nuclear inclusions in the olfactory tubercle and striatum of the *Hdh*$^{Q150/Q150}$ mice. Nuclear inclusions increased in number and size with age and disease progression, and spread in ventral to dorsal, and anterior to posterior pattern. Electron microscopy observations at 14 months of age revealed that the neurons showed a normal nucleus having a circular shape and regular membranes in a densely packed cytoplasm, whereas by 21 months the cytoplasm was vacuolated and contained swollen mitochondria with many degenerated cytoplasmic organelles. Immunogold labelling of the S830 antibody was found to be specifically localised to the inner area of the neuronal intra-nuclear inclusions.

Our data demonstrate a marked and progressive cellular phenotype that begins at 5 months of age and progresses with time. The pathology the *Hdh*$^{Q150/Q150}$ line was focused on the striatum and cortex until the late stage of the disease, consistent with the human condition.

1. Introduction

Huntington's disease (HD) is an adult-onset neurodegenerative disorder characterized by progressive cognitive, psychiatric and motor symptoms. It is associated with a mutation in the *htt gene*, which codes for the huntingtin protein (Htt). The gene contains a polymorphic stretch of repeated CAG trinucleotides which encodes polyglutamine (polyQ) [40]. Mutant htt contains an abnormal CAG repeat expansion responsible for the neurodegeneration, primary focus on the basal ganglia and cerebral cortex [45], which may be preceded by neuronal dysfunction. The most noticeable neurodegenerative changes are found in the medium spiny neurons (MSNs) of striatum (caudate nucleus and putamen) with neuronal loss and astrogliosis being a feature [2,44,45]. In addition to this severe loss of the MSNs, some atrophy is also present in the cerebral cortex [19,31]. As the disease progresses, neuronal loss becomes widespread and effects other regions of the brain linked to corticostriatal circuits, including the globus pallidus (GP), thalamus, substantia nigra (SN) and hippocampus [9,44,45]. How the mutated huntingtin protein causes this cell death is still a matter of speculation.

In HD, mutant huntingtin misfolds and accumulates as large insoluble aggregates/neuronal intra-nuclear inclusions (NIIs). These NIIs are a pathological marker of the disease both in mice and humans [7,8]. The expanded CAG sequence of mutant huntingtin causes protein misfolding and promotes the recruiting of a variety of proteins which then form aggregates [7,8,14]. Although, the genetics of HD are well documented, the functional role of protein aggregation in neuronal cell death remains unclear. It is still unknown as to whether aggregates are toxic to neurons, protective against cell degeneration, or simply a side-product markers of other ongoing cellular processes causing cell death [27,32,34,37].

In addition to the NII pathology within the cell soma, it has also been observed that N-terminal fragments of mutant huntingtin accumulate in dystrophic neurites in the cortex, the striatum and in astrocytes in the R6/2 transgenic mice [35,42], and in post mortem HD brains [32,36]. Extra-nuclear neuronal inclusions (ENNIs) have been identified in both human and mouse brain [8,15,22]. These ENNIs may be the precursors of intra-nuclear inclusions [18].

☆ This article is part of a Special issue entitled 'HD Transgenic Mouse'.

* Corresponding author. Tel.: +44 29 20 874684; fax: +44 29 20 876749.
E-mail address: bayram-westonZ@cardiff.ac.uk (Z. Bayram-Weston).

0361-9230/$ – see front matter © 2011 Elsevier Inc. All rights reserved.
doi:10.1016/j.brainresbull.2011.03.014

Gutekunst et al. [11] found that neuropil aggregates were much more common than nuclear aggregates and they were present before the onset of clinical symptoms in post mortem HD brains.

A third key sign of cellular pathology is the astrocyte-mediated inflammatory response to cell insult. Glial fibrillary acidic protein (GFAP) is expressed primarily by astroglia and is an indicator of astroglial activation [3,6,28]. The brain reacts to neuronal injuries with an increase in number and size of cells expressing GFAP [48]. Astrogliosis is observed in human HD [10,43] and in the HD mouse lines including *Hdh*$^{CAG(150)}$ [17] and HD89 [26]. By contrast, other mouse lines, such as R6/2 mice, do not show any reactive astrogliosis, although they do exhibit modest cell death, striatal atrophy, and reduced brain size [20].

The present study sought to characterise the development of disease neuropathology in the *Hdh*$^{(CAG)150}$ mouse line. We used histology and immunohistochemistry with stereological quantitation, and transmission electron microscopy (TEM) to investigate aggregate formation in more detail in an attempt to better understand the development of neuronal pathology in this mouse model of HD. The present study focused on the progression, distribution, number and form of huntingtin aggregates in the different regions of the brain, and also assessed brain atrophy and neuronal cell loss within the same brain sections from tissue taken at regular intervals between 5 and 24 months of age.

2. Materials and methods

2.1. Animals

In total 99 mice were used in the present study, spread across 9 time points (5 months = 7; 6 months = 11; 8 months = 5; 10 months = 16; 12 months = 12; 15 months = 12; 18 months = 15; 21 months = 10; 24 months = 10). Fifty one of these mice (29 female and 22 male) were *Hdh*$^{Q150/Q150}$ knock-in mice with 48 wildtype litter mates (29 female and 19 male). The mice were bred in-house from the original line, imported to our laboratory on a mixed 129/Ola × C57BL/6 J background and backcrossed onto C57BL/6 J background (Harlan, UK) over six generations. This mouse has had the normal length CAG repeat in exon 1 of the mouse *Hdh* gene replaced with a 150 CAG repeats [17]. These mice had on average 132 ± 2.65 CAG repeats (range 120–143 repeats). The mice were housed together under standard conditions with *ad libitum* access to water and food. The mice were housed in a holding room under a 12 h:12 h light/dark cycle (lights on 0700 h) and an ambient room temperature of 21 ± 1 °C. The cages contained sawdust bedding and a cardboard tube for environmental enrichment. Each cage contained 2–6 animals. Each mouse had undergone periodic behavioural testing for up to two years [4]. This study was carried out in accordance with the UK Animals (Scientific Procedures) Act, 1986.

2.2. Histology

The animals were sacrificed at 3 months = 3, 5 months = 7; 6 months = 11; 8 months = 5; 10 months = 16; 12 months = 12; 15 months = 12; 18 months = 15; 21 months = 10; 24 months = 10. They were anaesthetized by intraperitoneal injection of 0.2 ml of Euthetal (Merial, Essex, UK) and then perfused intracardially with phosphate-buffered saline (PBS, pH 7.4) for 3 min. Followed by 4% paraformaldehyde (PFA) (Fisher Scientific, Loughborough, UK) in a 0.1 M PBS solution, pH 7.4, for a further 5 min. The brains were carefully removed, post fixed in 4% PFA for 4 h, and then transferred in 25% sucrose in PBS, until they sank. For striatal analysis coronal sections (40 μm) of the brain were cut in series of 1:6 using a freezing sledge microtome (Leitz Bright Series 8000, Germany). The sections were stored in cryoprotective solution at −20 °C.

2.3. Cresyl fast violet (CV)

A one in six series was stained using the standard Nissl stain, cresyl fast violet for morphological and stereological analysis. The sections were mounted on gelatine-coated glass slides (Fisher Scientific), and allowed to dry at 37 °C for 24 h. The sections were then dehydrated in a graded series of ethanol (5 min each, 70%, 95%, and 100%) and delipidised in a mixture of chloroform and ethanol (1:1, v/v) for 20 min. Following delipidisation, the sections were hydrated in a gradually decreasing series of ethanol (5 min each 100%, 95% and 70%) and immersed in distilled water for 5 min and stained with cresyl violet (0.7% in distilled water with 0.5% sodium acetate, Sigma, Hertfordshire, UK) for 5 min. After rinsing in distilled water for 1 min, the sections were dehydrated in a graded series of ethanol (5 min each, 70%, 95%, and 100%), cleared in xylene (VWR, Darmstadt, Germany) for at least for 10 min, cover-slipped with DPX mounting medium (RA Lamb, Hambridge, Somerset, UK) and analyzed under a Leica DMRBE microscope (Leica, Wetzlar, Germany).

2.4. Immunohistochemistry

Immunohistochemistry was carried out according to Trueman et al. [41]. Briefly, all stains were performed on a 1:6 series of sections. Free-floating sections were processed immunohistochemically using the sheep anti-S830 (a kind gift from Prof. Gillian Bates, King's College, London, UK) and rabbit GFAP (DAKO, Cambridge, UK) primary antibodies. The S830 antibody was raised against the product of the N-terminal region to 53 glutamine residues of exon 1 and selectively recognizes the aggregated form of the mutated htt protein [21].

The sections were placed in (pH 7.4) TRIS buffered saline (TBS), and washed twice for 5 min. The endogenous peroxidise activity was inhibited by incubation in methanol containing 3% H_2O_2 (VWR) for 5 min, and then placed in TBS. Non-specific binding sites were blocked with 3% horse serum in TBS for 1 h, and the sections were incubated with S830 antibody (diluted 1:25,000) and GFAP antibody (1:2000) overnight at room temperature. After several washes in TBS, sections were incubated with a horse anti-goat or horse anti-rabbit secondary antibody (diluted 1:200, Vector Laboratories, Burlingame, CA, USA) for 2 h at room temperature. After several washes in TBS, the sections were incubated with a biotin–streptavidin kit according to the manufacturer's instructions (Vector Laboratories). After each incubation, the sections were rinsed in TBS. The peroxidase activity was visualized with 3,3′-diaminobenzidine (DAB) (Sigma–Aldrich, Poole, Dorset, UK). Finally, the sections were mounted on gelatine-coated slides, dehydrated and cover-slipped.

Light microscopic pictures were taken using a Leica DMRBE microscope fitted with a digital camera (Optronics, Goleta, CA, USA) and MagnaFire 1.2 C imaging Software (Goleta, CA, USA). All images were captured using the same parameters and saved on computer for further analysis. Images were adjusted in contrast and brightness only for optimal display with Adobe Photoshop 6.0.

The staining in the homozygote mice was also scored in a semi-quantitative fashion that included the intensity of specific staining in sections: 0 = absent, + = weak nuclear staining present; ++ = diffuse nuclear staining; +++ = few/minimum inclusions; ++++ = many/dense inclusions. Animal numbers each time point was as follows: 5 months = 4; 6 months = 7; 8 months = 4; 10 months = 7; 12 months = 7; 15 months = 6; 18 months = 4; 21 months = 5; 24 months = 7.

2.5. S830/CV stereology

For the stereological assessment 98 animals were used as follows: 5months = 7; 6 months = 11; 8 months = 5; 10 months = 16; 12 months = 12; 15 months = 12; 18 months = 15; 21 months = 10; 24 months = 10. Two dimensional stereology was carried out using a PC-based image analysis software (Olympus C.A.S.T. grid system v1.6.) on a Olympus BX50 microscope (Olympus Optical Co., Ltd., Tokyo, Japan). Cell counts were carried out on a 1:6 series of GFAP, S830-stained, and CV sections, throughout the entire left striatum and then assessed blindly to the experimental groups. Cell counts were performed on a Leica DMRB microscope with the counting objective was at 100× and counting frame area was 265 μm^2 and corrected using the Abercrombie formula [1].

2.6. Transmission electron microscopy (TEM) for morphological study

For the electron microscopy, four mice for each group (aged 14 months and 21 months) were anaesthetized by intraperitoneal injection of 0.2 ml of Euthetal and then perfused with 0.9% NaCl for 3 min, followed by 2% PFA and 2% glutaraldehyde in 0.1 M PBS solution at pH 7.4, for 5 min. After perfusion, the brains were carefully removed and washed in PBS. Tissues were cut into small cubes and transferred into 1% osmium tetroxide for 2 h at +4 °C. After washing with distilled water 4 × 15 min, the samples were stained overnight in 0.5% uranyl acetate at +4 °C. All tissues used for electron microscopy were dehydrated in ascending concentrations of ethanol and fresh propylene oxide, and then infiltrated overnight in a mixture of propylene oxide and araldite resin (1:1, v/v) on a rotary shaker at room temperature. Following resin infiltration, the tissues were embedded in fresh resin for 48 h at 60 °C. Ultrathin sections (60 nm) were cut with a diamond knife on an ultracut-microtome (Reichert-Jung, Leica UK LTD, Milton Keynes, UK). Thin sections were collected on copper mesh grids, counterstained with 2% uranyl acetate for 10 min followed by Reynold's lead citrate for 5 min and examined under a Philips transmission electron microscope (Philips EM 208, Eindhoven, The Netherlands).

2.7. Transmission electron microscopy for immunogold labelling

Two mice for each group (aged 14 months and 21 months) were anaesthetized by intraperitoneal injection 0.2 ml of Euthetal and then perfused with 0.9% NaCl for 3 min. This was followed by 3% PFA and 0.2% glutaraldehyde in 0.1 M PBS solution, pH 7.4, for 5 min, and then with 3% PFA alone at a rate of 15 ml/min. After perfusion the brains were carefully removed and washed in PBS. Relevant region of the brain was cut into small cubes and transferred into a cryoprotective solution (0.05 M PBS, pH 7.4, containing 25% sucrose and 30% glycerol) for 15 min. The tissue was then transferred into methanol in an automated freeze substitution chamber at −80 °C for 48 h (Reichest *EM*AFS, Leica mikrosysteme, Wien, Austria). The methanol was replaced with fresh methanol during the first 2 h at −80 °C. The chamber temperature was then allowed to increase to −50 °C for 88 h. The tissue was then infiltrated by a mixture of Lowicryl HM20 resin and methanol (1:1, v/v) for 90 min at −50 °C,

Please cite this article in press as: Z. Bayram-Weston, et al., Light and electron microscopic characterization of the evolution of cellular pathology in the Hdh$^{(CAG)150}$ Huntington's disease knock-in mouse, Brain Res. Bull. (2011), doi:10.1016/j.brainresbull.2011.03.014

then infiltrated with a mixture of Lowicryl HM20 resin and methanol (2:1, v/v) for a further 90 min at −50 °C, then transferred into pure Lowicryl HM20 resin overnight at −50 °C. The tissue was then embedded in fresh Lowicryl HM20 resin under UV light for 48 h at −50 °C. The temperature was then increased to 20 °C for 24 h to complete resin polymerisation. Ultra-thin sections (60 nm) were cut with a diamond knife on the ultracut-microtome. Thin sections were collected on pioloform-coated nickel mesh grids and were blocked with drops of PBS containing 3% normal donkey serum, 1% bovine serum albumine, 0.2% Triton-X and 0.1% sodium azide for 45 min at room temperature. The sections were then incubated on drops of sheep polyclonal S830 primary antibody (1:500) overnight at +4 °C. After rinsing in PBS and distilled water, the sections were incubated again in donkey anti-sheep IgG conjugated gold (10 nm, 1:20; BB International, Cardiff, UK) for overnight at +4 °C. After washing in PBS, the grids were counterstained with 2% uranyl acetate for 10 min followed by Reynold's lead citrate for 5 min and examined using a Philips transmission electron microscope.

2.8. Statistical analysis

Statistical analyses were undertaken using two-way ANOVA (Genstat v13.2; VSN International, Hemel Hempstead, UK), in all cases with age as a between-subjects factor. Striatal volume and total striatal cell counts compared Genotype (wildtype vs. $Hdh^{150/150}$) as a second between-subjects factor, whereas cell counts of striatal cells bearing inclusion pathology used type of pathology (diffuse vs. inclusion) as a second within-subjects factor. In view of the large number of age groups with relatively few animals of each genotype at each age, a subsequent analysis was undertaken to determine the age at which overt pathology was significant by repeating the analyses of variance with data blocked into three age bands: young (4, 6 and 8 month), mature (10, 12 and 15 month) and aged (18, 21 and 24 month). Comparisons between different ages and age ranges were corrected for multiple comparisons by the Newman–Keuls test.

3. Results

3.1. Striatal atrophy and neuronal cell counts in the $Hdh^{(CAG)150}$ mouse

We examined the volume of the striatum in $Hdh^{Q150/Q150}$ mice and wildtype littermates from 5 months to 24 months of age. The volume of the striatum was significantly reduced in the $Hdh^{Q150/Q150}$ mice compared with the wildtype mice irrespective of age (Fig. 1A: genotype, $F_{1,74} = 32.44$, $p < 0.001$). There was also a significant age effect (age, $F_{8,74} = 15.93$, $p < 0.01$) and a significant interaction effect between the groups over time (genotype × age, $F_{8,74} = 3.30$, $p < 0.01$), suggesting that $Hdh^{Q150/Q150}$ mice had reduced striatal volume from 6 months of age which remained lower then that of wildtypes from this point onwards. However, in the *post hoc* analysis with mice blocked into three age bands, the two main effects remained highly significant but the interaction term was no longer so ($F_{2,86} = 0.20$,n.s.), suggesting that the above interaction is associated with random variation between a large number of independent small groups.

In the cresyl violet stained sections, stereological analyses revealed a significant increase in striatal cell numbers from 4 months of age until 8 months which then remained stable (Fig. 1B: age, $F_{8,74} = 12.16$, $p < 0.001$). Furthermore, statistical analysis revealed a significant genotype effect (Fig. 1B: genotype, $F_{1,74} = 6.50$, $p < 0.05$) with $Hdh^{Q150/Q150}$ mice showing reduced cell number throughout. However, no interaction effects was found (genotype × age, $F_{8,74} = 0.92$, n.s.). The main effect of genotype remained significant in the blocked *post hoc* analysis.

3.2. Striatal neuronal pathology in the $Hdh^{Q150/Q150}$ mouse

Within the $Hdh^{Q150/Q150}$ brain, S830 staining showed diffuse nuclear staining and nuclear inclusions only in the homozygous mice. There was no S830 staining found in the control animals, indicating that nuclear inclusion formation was dependent on the mutation. In order to establish the onset age, a small sample of 3 mice was examined at 3 months of age. In this sample, no intra-nuclear inclusions were observed in any region of the brain, however, faint nuclear staining was seen throughout the brain. By 5 months of age the S830 antibody demonstrated diffuse nuclear staining and inclusions, the presence of which varied depending on the brain region. A this early age, diffuse nuclear staining and a low density of inclusions (minimum inclusions) were observed in the olfactory tubercle, central amygdala and striatum (Figs. 2 and 3), but were not apparent in other regions of the brain (Fig. 2 and Table 1). At 15 month of age, nuclear inclusions were distributed widely throughout the brain. At this age persistent diffuse nuclear staining was still present but had disappeared completely by 18 months of age (Fig. 2 and Table 1). In aged homozygous mice (21 and 24 months old), the spatial distribution pattern of inclusions persisted. Analyses of this pathology found that the total number of affected neurons, which was comprised of the collective number of cells with diffuse *htt* staining or inclusions (Fig. 1C: affected neurons, $F_{8,43} = 8.35$, $p < 0.001$) increased up to 18 months of age, before dropping. The number of diffusely stained cells were maximal at the earliest time point investigated at 5 months, and declined thereafter to almost 0 by 18 months of age (Fig. 1D: diffuse staining, $F_{8,43} = 73.00$, $p < 0.001$).

By contrast, the numbers of intra-nuclear inclusions increased to a peak at 18 months of age, before dropping (Fig. 1D: inclusions, $F_{8,43} = 19.54$, $p < 0.001$). Nuclear inclusions appeared to be large, singular and round in one year old mice (Fig. 4C). Inclusions were usually localised in close proximity to the nuclear membrane in older mice (Fig. 4E).

Both the decline of early onset diffuse staining (young > mature > aged) and the increase in the numbers of cells bearing overt inclusions with age (young < mature = aged) remained significant in the blocked analyses ($F_{2,49} = 145.26$ and 29.48, respectively, both $p < 0.001$).

Extra-nuclear inclusions existed in all age groups except 3 month old mice. The distribution of extra-nuclear inclusions was consistent at low levels throughout the brain up to 10 months old. However, by 12 months of age the density of the distribution varied depending on the region of the brain. At this point, the extra-nuclear inclusions increased in the globus pallidus, amygdala and piriform cortex, whereas other area of the brain remained unchanged. In very old homozygous mice (21 and 24 months old), the extra-nuclear inclusions were present throughout the brain (Table 2). Hence, cytosolic and nuclear inclusions increased in number and size with age and disease progression.

3.3. Assessment of neuronal cell death

3.3.1. GFAP immunostaining

GFAP is the main intermediate filament in astrocytes and defines the astrocytic morphology. Since one of the main features of astroglial reaction is the increased size of cellular projections, it is possible to assess the astroglial reaction that is identifiable by the increased expression of GFAP [3]. The expression of GFAP was intense in several regions of the brain including the striatum and cortex (Fig. 5) and increased in the striatum with age in both mouse groups (age, $F_{2,21} = 14.78$, $p < 0.001$), but no differences in expression levels between the groups was identified in either brain region (genotype, $F_{2,21} = 0.69$, n.s.). No interaction effects (genotype × age, $F_{2,21} = 0.95$, n.s.) were found for the expression levels in the striatum (data not shown).

3.4. Electron microscopy

The neurodegeneration of $Hdh^{Q150/Q150}$ knock-in mice at different time points was studied using electron microscopy. Observations of the earlier time point (14 months) revealed that the neurons had a normal circular nucleus with regular membranes, and a densely packed cytoplasm (Fig. 6A). Mitochondria also appeared normal and there was no evidence of vacuolisation,

Please cite this article in press as: Z. Bayram-Weston, et al., Light and electron microscopic characterization of the evolution of cellular pathology in the $Hdh^{(CAG)150}$ Huntington's disease knock-in mouse, Brain Res. Bull. (2011), doi:10.1016/j.brainresbull.2011.03.014

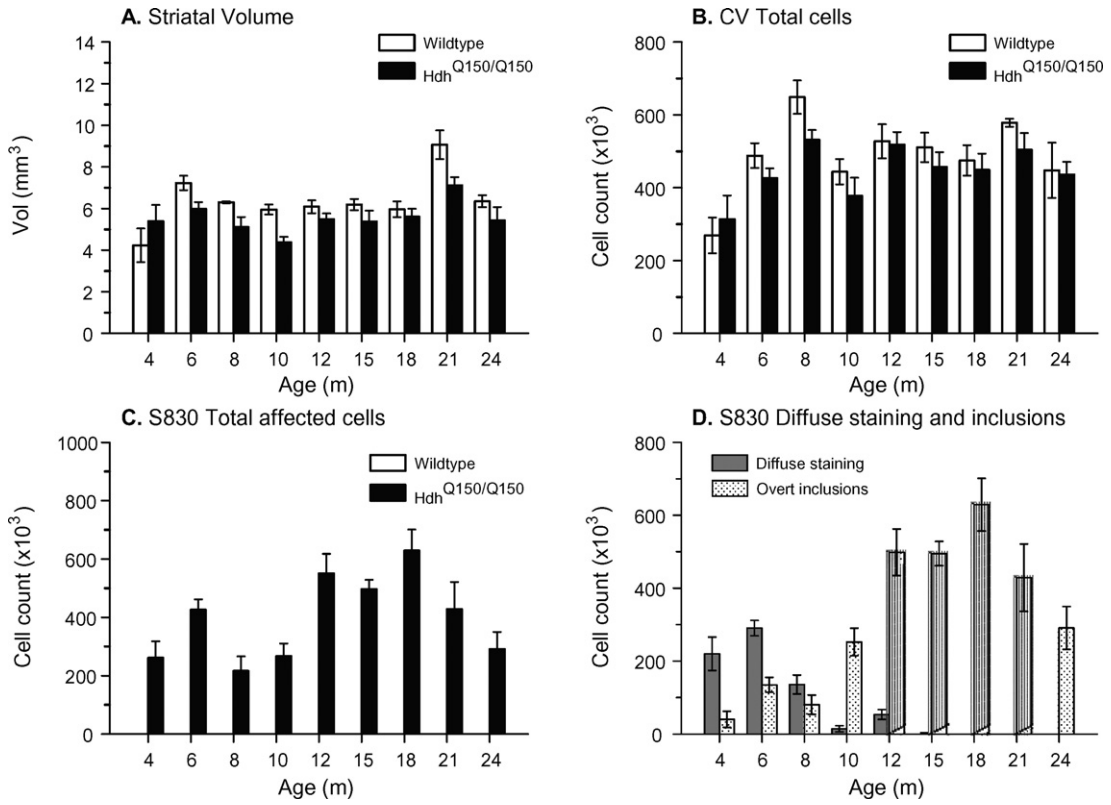

Fig. 1. Age-dependent distribution of cresyl violet – stained neurons and S830 affected cells in striatum of Wt and homozygote. (A) The comparison of the total volume of the striatum in *Hdh*$^{Q150/Q150}$ animals and wildtype mice. In 10 months and 24 months old animals, the volume of the striatum in *Hdh*$^{Q150/Q150}$ animals were less than in wildtype mice. (B) Cresyl violet-stained neurons in both wildtype and homozygote animals. The number of neurons in wildtype is relatively higher than that in homozygotes regardless of age. (C) Age related distribution of S830 affected neurons in striatum of *Hdh*$^{Q150/Q150}$ mice. The number of affected cells increased as age progress from 5 months, peaks at 18 months and gradually decreased thereafter. Affected cells (D) showing diffuse nucleus staining and/or intra-nuclear inclusions. Affected cells showing diffuse nucleus staining decreased in number from 5 months to 12 months, whereas those with intra-nuclear inclusions increased gradually up to age of 18 months and then slowly decreased. Bars indicate means ± s.e.m.

dilation or membrane degeneration. In the *Hdh*$^{Q150/Q150}$ mice, the striatum showed NIIs with a small circular filamentous structure that could be easily identified and clearly distinguishable from the surrounding structures (Fig. 6B). The striatum of the 21 month old wildtype mouse revealed a more compact structure than that of the homozygote animal. That of the 21 month old homozygote showed hypertrophic degenerative neurons with a number of necrotic features (Fig. 6E). These neurons showed structural abnormalities such as angular shape and uneven nuclear membranes. The cytoplasm appeared severely vacuolated and contained swollen mitochondria. Most of the other cytoplasmic organelles were largely deformed. Electron dense bodies were also found in the cytoplasm which may be the degenerated lysosomal structures. However, it is noteworthy that the wildtype mice also showed these bodies but their numbers were reduced from those in the aged matched homozygote mouse. Moreover, the 21 month old homozy-

Table 1
Hdh$^{Q150/Q150}$ knock-in mice. Formation, progression and distribution of neuronal intra-nuclear inclusions (NIIs).

Q150 brain/ages	5M	6M	8M	10M	12M	15M	18M	21M	24M
Olfactory tubercle	++/+++	+++	++	++++	++++	++++	++++	++++	++++
Nucleus accumbens	++/+++	+++	++	++++	++++	++++	++++	++++	++++
Globus pallidus-lateral	+/++	+/++	++	+/++	+++	+++	+++	++++	++++
Globus pallidus-medial	+/++	+/++	++	+/++	+++	+++	+++	++++	++++
Striatum ventral	++/+++	+++	+++	++++	++++	++++	++++	++++	++++
Striatum dorsal	++/+++	+++	+++	++++	++++	++++	++++	++++	++++
Striatum posterior	++/+++	+++	+++	++++	++++	++++	++++	++++	++++
Septum lateral	+/++	++	++	++	++	++	+++	++++	+++
Septum med	+/++	++	++	+++	+++	+++	++++	++++	+++
Amygdala BL	+	+	+	+	++	++	+++	+++	+++
Amygdala CL	++/+++	++/+++	++/+++	+++	++++	++++	++++	++++	++++
Thalamus	+/++	++	+/++	++/+++	+++	+++	+++	+++	++++
Hypothalamus	++	++	+/++	++/+++	+++	+++	+++	+++	++++
Cerebellum	+/++	+/++	+/++	+/++/+++	+/++/+++	++++	++++	++++	++++
Hippocampus	++	+/++	+/++	+/++/+++	+/++/+++	++/++++	+++/++++	+++/++++	++++
Motor cortex	+/++	+/++/+++	+/++/+++	+/++/+++	+/++/+++	++/+++/++++	+++/++++	+++/++++	+++/++++
Sensory cortex	+/++	+/++/+++	+/++/+++	+/++/+++	+/++/+++	++/+++/++++	+++/++++	+++/++++	+++/++++
Piriform cortex	++	++	+/++	++/+++	++++	++++	++++	++++	++++

0: absent, +: nuclear staining, ++: diffuse nuclear staining, +++: minimum inclusions, ++++: dense inclusions.

Please cite this article in press as: Z. Bayram-Weston, et al., Light and electron microscopic characterization of the evolution of cellular pathology in the Hdh$^{(CAG)150}$ Huntington's disease knock-in mouse, Brain Res. Bull. (2011), doi:10.1016/j.brainresbull.2011.03.014

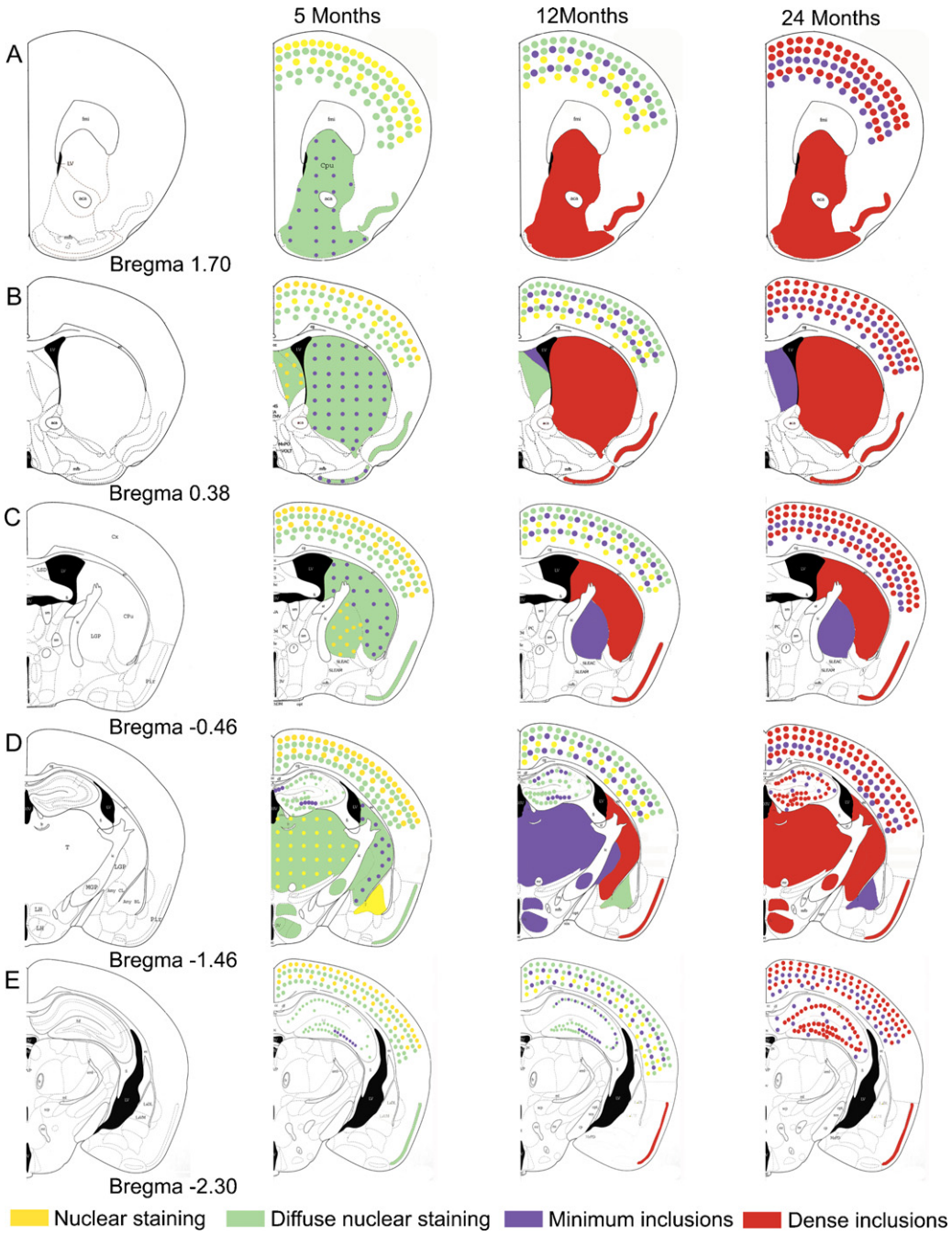

Fig. 2. Schematic overview of the spatial and temporal evolution of S830 immunostaining in *Hdh*$^{Q150/Q150}$ mouse brain at five coronal levels from anterior to posterior based on the atlas of Paxinos and Franklin (1997) [25] shown in the left column. Each subsequent column shows the S830 expression patterns for three time points 5, 12 and 24 months, respectively, using different colours. To indicate types of cellular pathology (see legend). Overlapping staining is represented by mixed colour. Abbreviations; Aca: anterior commissure, Amy BL: basolateral amygdale, Amy CL: central amygdala, cc: corpus callosum, CPu: caudate putamen, Cx: cortex, fmi: corpus callosum, GP: globus pallidus, LS: lateral septum, LSD: dorsal lateral septum, LGP: lateral globus pallidus, LV: lateral ventricle, Mfb: medial forebrain bundle, MGP: medial globus pallidus, Pir: piriform cortex, T: thalamus, Tu: olfactory tubercle.

gote mouse exhibited neuronal inclusions in the cytoplasm. These inclusions appeared as large circular filamentous structures with no membrane, but they were clearly distinguishable from their surrounding as a result of their high electron density (Fig. 6E). We were unable to determine small neuritic aggregates (ENNIs) by electron microscopy.

We also performed immunogold labelling of S830 antibody on the 14 month old and 21 month old homozygote knock-in mice. The immuno-reaction of mutant huntingtin was found to be specifically localised to the inside of the nuclear inclusion. The immunogold reactivity was confined to the filamentous bodies in the inside of nucleus and appeared as clusters of immunogold particles (Fig. 6C and F). No gold particles were seen in the negative control sections to which the application of primary antibody was omitted.

4. Discussion

All of the regions of the *Hdh*$^{Q150/Q150}$ brain examined showed diffuse nuclear staining and nuclear inclusions when immunolabelled with S830 antibody at 5 month of age. Low levels of both diffuse nuclear staining and NIIs were observed in the olfac-

Please cite this article in press as: Z. Bayram-Weston, et al., Light and electron microscopic characterization of the evolution of cellular pathology in the Hdh$^{(CAG)150}$ Huntington's disease knock-in mouse, Brain Res. Bull. (2011), doi:10.1016/j.brainresbull.2011.03.014

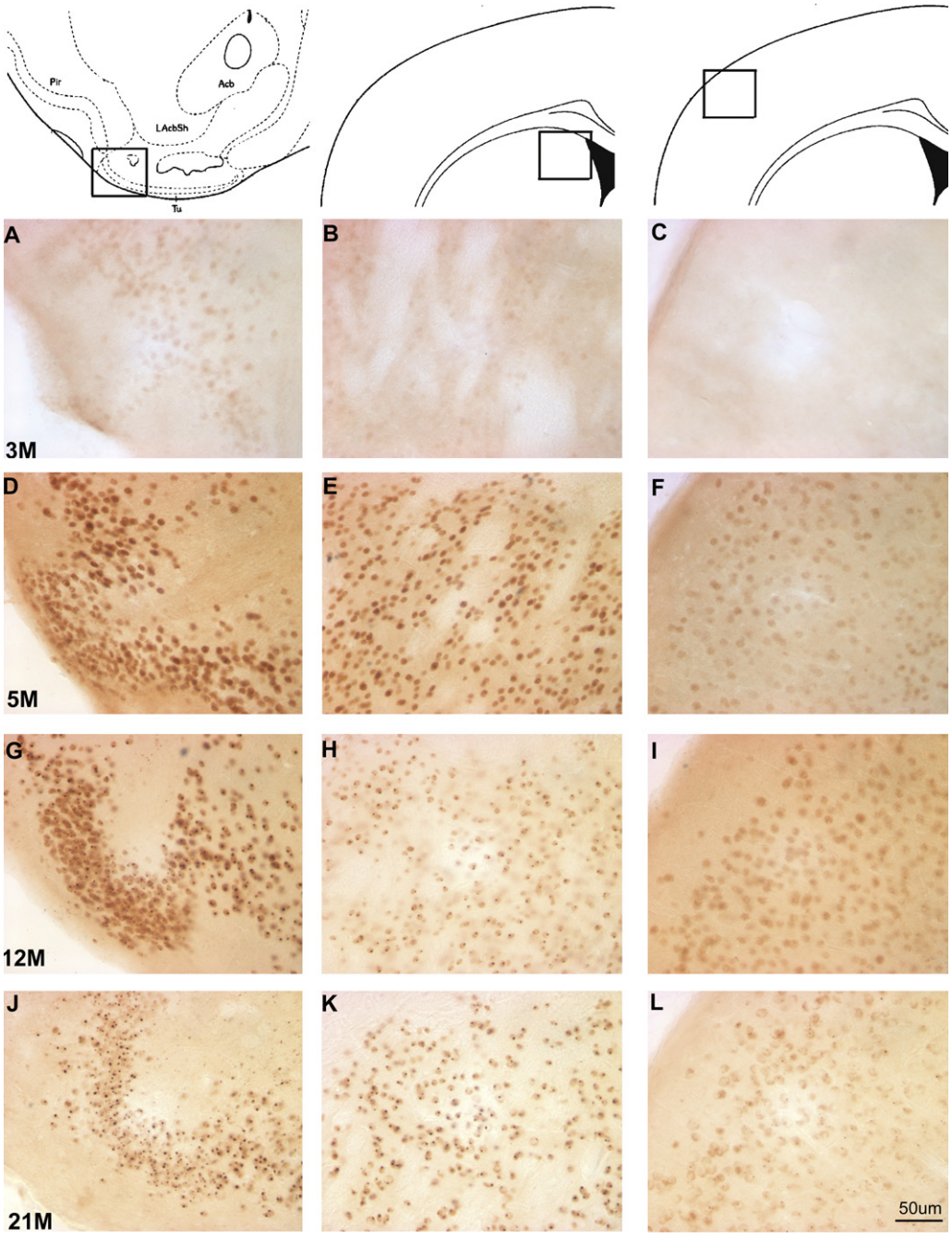

Fig. 3. Temporal evolution of S830 immunostaining of *Hdh*$^{Q150/Q150}$ brain in olfactory tubercle (left panels), striatum (middle panels), and cortex (right panels) at 3, 5, 12 and 21 months of age, in successive rows. The development of NIIs is clearly visible in olfactory tubercle and striatal cells.

tory tubercle, nucleus accumbens and striatum of young animals (5–12M). The 15 month old homozygote animals displayed NIIs in all regions of the brain with persistent diffuse nuclear staining, whereas by 18 months of age the mice no longer expressed diffuse nuclear immunoreactivity. This data suggests that the aggregation commences with the diffuse accumulation of protein in the nucleus, and as the phenotype progresses, these small diffuse concentrations are replaced by larger NII aggregates. Previous studies suggest mutant huntingtin may accumulate first in degenerating neurites and which then appear as a neuronal inclusion [33], or that they merge from individual aggregates into a single or several nuclear inclusions [14]. The latter description is more consistent with our study, which demonstrates that as the number of cells with inclusions increases, the number of cells with aggregations decreases. Consequently we report an inverse relationship between diffuse nuclear staining and inclusion number that is age dependant.

Tallaksen-Greene et al. [38] found in their histological studies on the *Hdh*$^{Q150/Q150}$ mice that huntingtin-associated NIIs were largely restricted to the striatum, with no evidence of gross neurodegeneration. The results of our study indicated that the nuclear inclusions can be present in all regions of the brain but that the distribution is age-dependent. The inclusions were found predominantly in the olfactory tubercle, nucleus accumbens, the striatum and central amygdala. Our study also demonstrated that nuclear inclusions were distributed widely in the striatum with persistent diffuse nuclear staining at 15 months old. This finding was consistent with that of Tallaksen-Greene et al. [38] who demonstrated that within the striatum, intra-nuclear huntingtin immunoreactiv-

Please cite this article in press as: Z. Bayram-Weston, et al., Light and electron microscopic characterization of the evolution of cellular pathology in the Hdh$^{(CAG)150}$ Huntington's disease knock-in mouse, Brain Res. Bull. (2011), doi:10.1016/j.brainresbull.2011.03.014

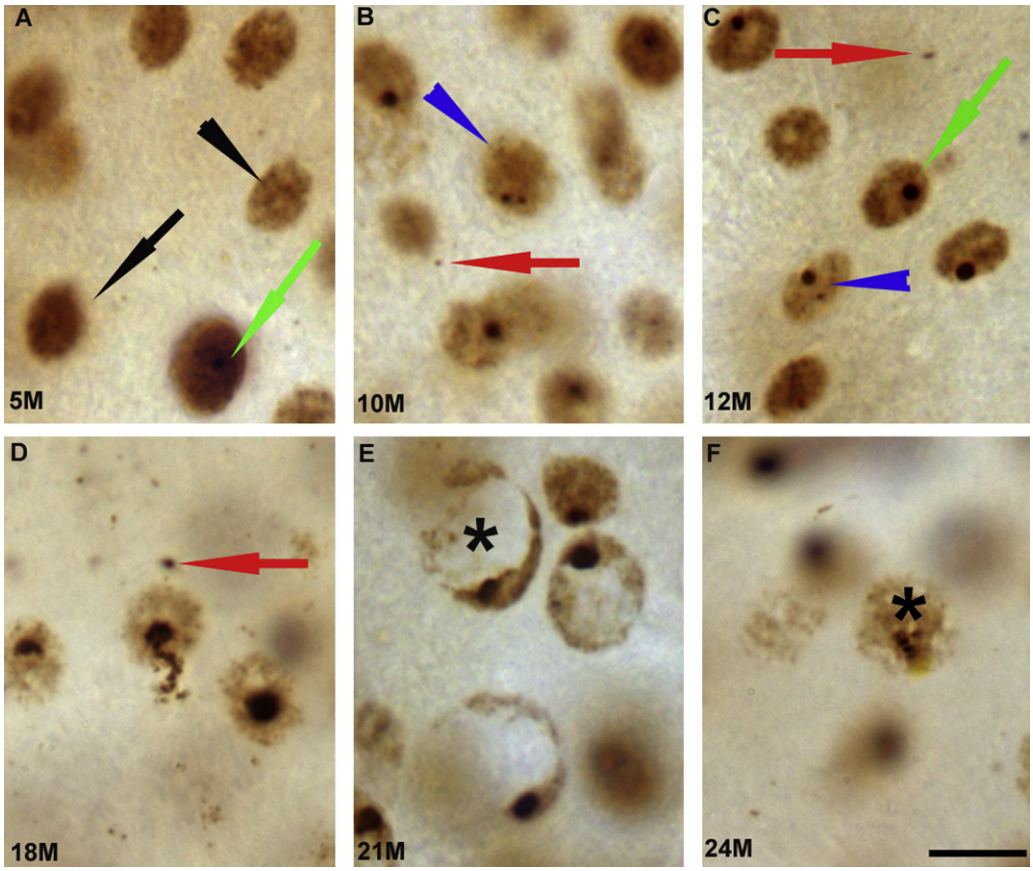

Fig. 4. High magnification images of striatal sections of *Hdh*$^{Q150/Q150}$ brain, showing age-dependent nuclear S830 immunoreactivity in 5 months through 24 months old mice (A–F). Both diffuse nucleus staining and nuclear inclusions are observed in animals aged 5, 10 and 12 months (A–C). Older animals display cells with diffuse nuclear staining together with nuclear inclusions (D–F), and these cells were widespread throughout the striatum at 21 months of age (E). The blue arrowheads denote cells with more than a single inclusion and the black arrow denotes diffuse nuclear staining. The green arrows indicate inclusions and the red arrows indicate extra nuclear inclusions. Scale bar = 10 μm. (For interpretation of the references to colour in this figure legend, the reader is referred to the web version of the article.)

ity was also observed from 6 months of age and that the diffuse staining persisted until 8 months [38]. We also observed diffuse nuclear staining in animals up to 12 months of age. With regard to the nuclear inclusions, the results of our study are consistent with those obtained by Tallaksen-Greene et al. [38] that showed nuclear inclusions were distributed widely throughout the striatum. By contrast, we did not find diffuse nuclear staining in aged animals. Another study by Woodman et al. [47] found evidence of NIIs in the striatum and hippocampus by 6 months of age and in the cortex by 8 months of age in the*Hdh*$^{Q150/Q150}$ mice, which may be due to the differences in the penetrance of the background strains used [47]. In contrast, we were able to observe NIIs in the olfactory tubercle, nucleus accumbens and striatum of 5 months old *Hdh*$^{Q150/Q150}$ mice. It has been reported that *Hdh*$^{(CAG)Q150}$ mice exhibits a reduction in striatal neuron numbers and in striatal volume at approximately 23 months of age [13]. A recent paper found

Table 2
Hdh$^{Q150/Q150}$ knock-in mice. Formation, progression and distribution of extra-nuclear inclusions (ENNIs).

Q150 brain/ages	5M	6M	8M	10M	12M	15M	18M	21M	24M
Olfactory tubercle	+	+/++	+	+/++	+++	++++	++++	++++	++++
Nucleus accumbens	+	+/++	+	+/++	++	+++	++++	++++	++++
Globus pallidus-lateral	+	+/++	+	+/++	+++	+++	++++	++++	++++
Globus pallidus-medial	+	+/++	+	+/++	+++	+++	++++	++++	++++
Striatum ventral	+	+/++	+	+/++	++	+++	+++	++++	++++
Striatum dorsal	+	+/++	+	+/++	++	+++	+++	++++	++++
Striatum posterior	+	+/++	+	+/++	++	+++	+++	++++	++++
Septum lateral	+	+/++	+	+/++	++	+++	+++	+++	+++
Septum med	+	+/++	+	+/++	+++	+++	+++	+++	+++
Amygdala BL	+	+/++	+	+/++	++	++	++	++	++
Amygdala CL	+	+/++	+	+/++	+++	+++	+++	++++	+++
Thalamus	+	+/++	+	+/++	++	++	+++	+++	++++
Hypothalamus	+	+/++	+	+/++	++	++	+++	+++	++++
Cerebellum	+	+/++	+	+/++	+++	++++	++++	++++	++++
Hippocampus	+	+/++	+	+/++	++	++	++	++	++
Motor cortex	+	+/++	+	+/++	++	++	+++	+++	+++
Sensory cortex	+	+/++	+	+/++	++	++	+++	+++	+++
Piriform cortex	+	+/++	+	+/++	+++	+++	++++	++++	++++

0: absent, +: very low staining, ++: intermediate staining, +++: dense staining, ++++: very dense staining.

Please cite this article in press as: Z. Bayram-Weston, et al., Light and electron microscopic characterization of the evolution of cellular pathology in the Hdh$^{(CAG)150}$ Huntington's disease knock-in mouse, Brain Res. Bull. (2011), doi:10.1016/j.brainresbull.2011.03.014

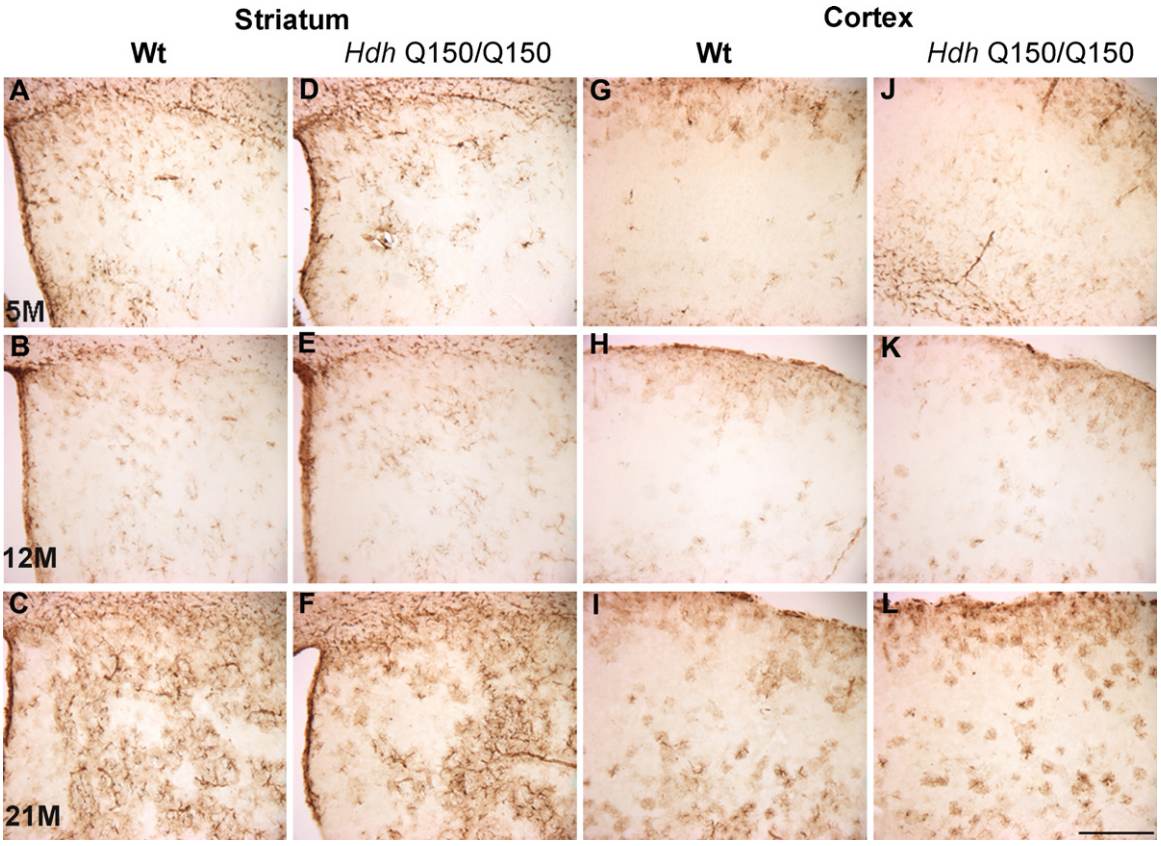

Fig. 5. Photomicrographs show the GFAP immunoreactive astrocytes in the striatum and cortex of the wildtype and *Hdh*$^{Q150/Q150}$ animals. (A–C) and (G–I) represent wildtype mice; (D–F) and (J–L) represent the *Hdh*$^{Q150/Q150}$ mouse. First row embody: 5 months old age; second row, 12 months old and third row, 21 months old, respectively. Scale bar = 100 μm.

no decrease in striatal volume or striatal neurons in the HdhQ200 mice [12], however, in the current study we have observed reduced striatal volume and striatal neuron numbers at 6 months of age. This may be due to the differences in the background.

Gutekunst et al. [11] have used the EM48 antibody which was raised against the first 256 amino acids of huntingtin and selectively recognizes aggregated huntingtin, to reveal more aggregates in the cortex than in striatum in the post mortem human HD brain. This observation is not reflected in our findings, in the *Hdh*$^{Q150/Q150}$ knock-in mouse line, where the striatum exhibited a greater number of aggregates than in the cortex. Our findings are consistent with other neuropathological studies in the HD mouse models [16,17,46] and represents one of the key differences between the human condition and the genetic mouse models. The light microscopy presented in the present study however, does reflect the pattern of aggregate distribution in different regions of HD human brain, for example in the caudate, putamen, substantia nigra, hypothalamic nuclei, thalamus, where aggregates are found in the human but at lower densities than in the cortex. At a cellular level, Gutekunst et al. [11] also described different localization of EM48-labelling in the HD cortical neurons. The EM48-labelled aggregates were found in the neuropil, in neuronal nuclei and perikarya, conversely we did not observe S830-labelling in the perikarya in the *Hdh*$^{Q150/Q150}$ mouse line, which may reflect differences in the antibodies.

Based on the results of our investigation, we further reveal that the extra-nuclear inclusions existed in all age groups from 5 months of age onwards. The ENNIs were found to be distributed throughout the brain in animals up to 10 months old. At 12 month the distribution of the immunoreaction products varied depending on the region of the brain. The globus pallidus, amygdala and piriform cortex, show increased intensity of extra-nuclear inclusions whereas other areas of the brain remained the same. Older homozygous mice of 21 and 24 months of age show the presence of these inclusions in all regions of the brain, but more densely than seen prior to 10 months of age. Morton et al. [22] showed that there is a progressive appearance of NIIs and ENNIs in striatum, cortex and hippocampus of R6/2 transgenic mice, with ubiquitin antibody [22]. In these R/2 mice there were two distinctly separate populations of inclusions, NIIs and ENNIs. We have also observed extra diffuse nuclear staining in the present study. Unlike Morton et al., we were not able to detect any ENNIs in the synaptic dendrites of the neurons by electron microscopy at any age. This may due to different antibodies used to detect inclusions, methodological differences between laboratories or differences in the mouse lines, as the R6/2 transgenic mice have a more rapidly progressing and severe phenotype than that seen in the *Hdh*$^{Q150/Q150}$ knock-in line.

In the present study, our TEM data in the *Hdh*$^{Q150/Q150}$ mouse line is in broad agreement with previous reports in the post-mortem of HD brains and transgenic mouse models, where intra-nuclear inclusions consist of filamentous structures [7,8,11,23]. In early studies, HD patient brains show nuclear membrane indentations, nuclear disorganization, reduction of the ribosomes [29,30], large accumulations of lipofucsin granules and enlarged mitochondria [39] at the ultrastructural level. Our findings show similar characteristic features in the *Hdh*$^{Q150/Q150}$ mouse. Yu et al. [48] found that the striatal neurons of 14 month *Hdh*$^{Q150/Q150}$ mice showed markers of cytoplasmic degeneration such as cytoplasmic swelling, vacuolization, enlargement and degenerated mitochondria. In the present study these were absent in 14 month old animals. However, they were present in the 21 month old *Hdh*$^{Q150/Q150}$ mice. Moreover, our results revealed that immuno-

Please cite this article in press as: Z. Bayram-Weston, et al., Light and electron microscopic characterization of the evolution of cellular pathology in the Hdh$^{(CAG)150}$ Huntington's disease knock-in mouse, Brain Res. Bull. (2011), doi:10.1016/j.brainresbull.2011.03.014

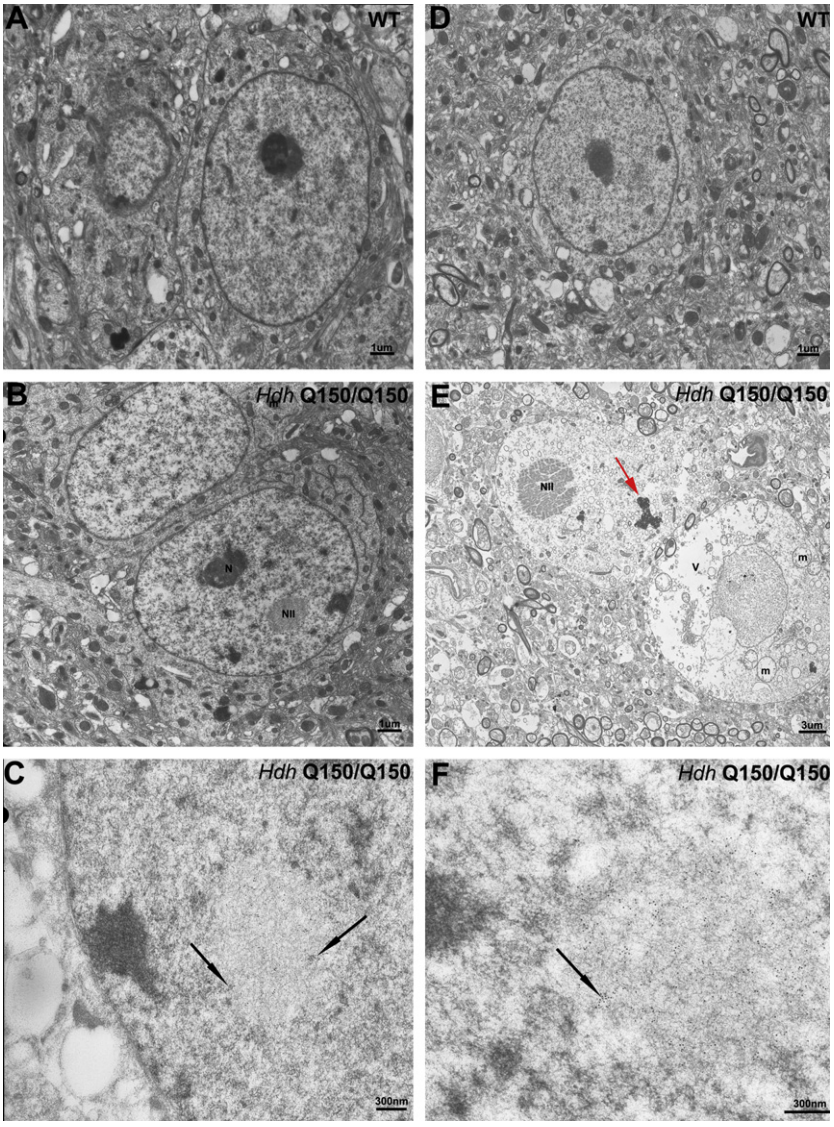

Fig. 6. TEM and immunogold images of the striatum of $Hdh^{Q150/Q150}$ (B, C, E and F) and wildtype mice (A and D) at 14 and 21 months of age. Left panel represents 14 months; right panel represents 21 months of age. Nuclear inclusions are observed in both 14 months (B) and 21 months (E) with electron microscope. Hypertrophic neuronal degeneration as shown by loss of cytoplasmic contents such as mitochondria (m) and large vacuolization (v) in noted in older $Hdh^{Q150/Q150}$ (E). S830 immunogold labelled particles are localised in intra-nuclear inclusions as shown by black arrows in 14 months (C) and 21 months old (F) animals. WT: wildtype, Hdh CAG (150): $Hdh^{Q150/Q150}$, N: nucleolus, NII: intra-nuclear inclusion, red arrow: electron dense body. Magnifications are as described in figures. (For interpretation of the references to colour in this figure legend, the reader is referred to the web version of the article.)

gold particles were only confined to the intra-nuclear inclusions. In contrast to our finding, Yu et al. [48] detected immunogold particles that were either clustered within the degenerating mitochondria or associated with the mitochondrial membrane [48]. Similarly Panov et al. [24] showed with electron microscopy, that mutant huntingtin is also localized on the mitochondrial membrane of the cells in YAC72 transgenic mice [24]. The differences in location of immunogold particles may be due to the antibody used, the precise histochemical and ultrastructural methods and/or the mouse strain. Mutant huntingtin aggregates were also observed in hypertrophic and dark glial cells with no visible cytoplasmic organelles in the striatum of R6/2 mice at 12 weeks with EM48 antibody by TEM [35]. In agreement, we have found hypertrophic cells with no visible cytoplasmic organelles also in the $Hdh^{Q150/Q150}$ mice. A recent study found that nuclear pore complexes deteriorate in aged mice. In old neurons, this progression leads to an increased nuclear permeability and causes a leakage of cytoplasmic proteins into the nucleus. It has also been revealed that cytoplasmic proteins such as intra-nuclear tubulin aggregates into large filamentous structures which caused severe morphological chromatin abnormalities [5]. This supports the idea, that the $Hdh^{Q150/Q150}$ mice had uneven nuclear membrane suggesting a possible deterioration of the nuclear pore complexes in HD.

Interestingly, we did not find any alteration in the intensity of GFAP immunostaining between $Hdh^{Q150/Q150}$ homozygous and their littermates. This finding contradicts the result of Lin et al. [17] and Yu et al. [48], who studied the same $Hdh^{Q150/Q150}$ knock-in mouse line and found increased GFAP activity at 14 months of age. This may indicate that astroglial reaction was not associated with the expanded CAG repeat length.

In running longitudinal studies of this nature several technical difficulties arose, most notably regarding the consistency of staining. At the 8 month time point we lost some consistency of the S830 staining which impacted on our S830 cell counts but also on our 8 month cresyl violet counts. We also had a tissue processing failure in 5 months of age which may have resulted in artificially low cell

Please cite this article in press as: Z. Bayram-Weston, et al., Light and electron microscopic characterization of the evolution of cellular pathology in the $Hdh^{(CAG)150}$ Huntington's disease knock-in mouse, Brain Res. Bull. (2011), doi:10.1016/j.brainresbull.2011.03.014

counts. These problems resulted in slightly disproportionate counts compared with adjacent date sets, but we included counts in the final data sets, as they are still representative of the animals used.

Here, we have shown that a marked and progressive cellular phenotype is present in the *Hdh*$^{Q150/Q150}$ mouse model. Diffuse nuclear staining and inclusions are first observed at 5 months and progress with age. The *Hdh*$^{Q150/Q150}$ mice show reduced striatal volume compared to the wildtypes. Our data confirms that the *Hdh*$^{Q150/Q150}$ mice show cell pathology similar to those obtained from post-mortem brains of HD patients.

Acknowledgements

We thank Prof Gillian Bates (King College London) for the generous gift of S830 antibody. We also thank Prof I for Bowen and Dr Antony Hann (Cardiff University) for helpful advice on implementation of the EM studies and Ali Baird, Jane Heath and Linda Elliston for technical support. This work was funded by the Medical Research Council of the UK and Cure Huntington's Disease Intuitive (CHDI) Foundation Inc..

References

[1] M. Abercrombie, Estimation of nuclear population from microtome sections, Anat. Rec. (1946) 239–247.
[2] G.P. Bates, P.S. Harper, L. Jones, in: G.P. Bates, P.S. Harper, L. Jones (Eds.), Huntington's Disease, vol. 5, Oxford University Press, 2002.
[3] A. Bignami, L.F. Eng, D. Dahl, C.T. Uyeda, Localization of the glial fibrillary acidic protein in astrocytes by immunofluorescence, Brain Res. 43 (1972) 429–435.
[4] S. Brooks, G. Higgs, L. Jones, S.B. Dunnett, Longitudinal analysis of the behavioural phenotype in Hdh((CAG)150) Huntington's disease knock-in mice, Brain Res. Bull. (2010).
[5] M.A. D'Angelo, M. Raices, S.H. Panowski, M.W. Hetzer, Age-dependent deterioration of nuclear pore complexes causes a loss of nuclear integrity in postmitotic cells, Cell 136 (2009) 284–295.
[6] D. Dahl, A. Bignami, K. Weber, M. Osborn, Filament proteins in rat optic nerves undergoing Wallerian degeneration: localization of vimentin, the fibroblastic 100-A filament protein, in normal and reactive astrocytes, Exp. Neurol. 73 (1981) 496–506.
[7] S.W. Davies, M. Turmaine, B.A. Cozens, M. DiFiglia, A.H. Sharp, C.A. Ross, E. Scherzinger, E.E. Wanker, L. Mangiarini, G.P. Bates, Formation of neuronal intranuclear inclusions underlies the neurological dysfunction in mice transgenic for the HD mutation, Cell 90 (1997) 537–548.
[8] M. DiFiglia, E. Sapp, K.O. Chase, S.W. Davies, G.P. Bates, J.P. Vonsattel, N. Aronin, Aggregation of huntingtin in neuronal intranuclear inclusions and dystrophic neurites in brain, Science 277 (1997) 1990–1993.
[9] R.J. Ferrante, N.W. Kowall, M.F. Beal, E.P. Richardson Jr., E.D. Bird, J.B. Martin, Selective sparing of a class of striatal neurons in Huntington's disease, Science 230 (1985) 561–563.
[10] S. Galatioto, Immunohistochemical findings in Huntington's Chorea: report of 9 cases, Pathologica 88 (1996) 491–499.
[11] C.A. Gutekunst, S.H. Li, H. Yi, J.S. Mulroy, S. Kuemmerle, R. Jones, D. Rye, R.J. Ferrante, S.M. Hersch, X.J. Li, Nuclear and neuropil aggregates in Huntington's disease: relationship to neuropathology, J. Neurosci. 19 (1999) 2522–2534.
[12] M.Y. Heng, D.K. Duong, R.L. Albin, S.J. Tallaksen-Greene, J.M. Hunter, M.J. Lesort, A. Osmand, H.L. Paulson, P.J. Detloff, Early autophagic response in a novel knock-in model of Huntington disease, Hum. Mol. Genet. 19 (2010) 3702–3720.
[13] M.Y. Heng, S.J. Tallaksen-Greene, P.J. Detloff, R.L. Albin, Longitudinal evaluation of the Hdh(CAG)150 knock-in murine model of Huntington's disease, J. Neurosci. 27 (2007) 8989–8998.
[14] R.R. Kopito, Aggresomes, inclusion bodies and protein aggregation, Trends Cell Biol. 10 (2000) 524–530.
[15] H. Li, S.H. Li, A.L. Cheng, L. Mangiarini, G.P. Bates, X.J. Li, Ultrastructural localization and progressive formation of neuropil aggregates in Huntington's disease transgenic mice, Hum. Mol. Genet. 8 (1999) 1227–1236.
[16] H. Li, S.H. Li, H. Johnston, P.F. Shelbourne, X.J. Li, Amino-terminal fragments of mutant huntingtin show selective accumulation in striatal neurons and synaptic toxicity, Nat. Genet. 25 (2000) 385–389.
[17] C.H. Lin, S. Tallaksen-Greene, W.M. Chien, J.A. Cearley, W.S. Jackson, A.B. Crouse, S. Ren, X.J. Li, R.L. Albin, P.J. Detloff, Neurological abnormalities in a knock-in mouse model of Huntington's disease, Hum. Mol. Genet. 10 (2001) 137–144.
[18] A. Lunkes, J.L. Mandel, A cellular model that recapitulates major pathogenic steps of Huntington's disease, Hum. Mol. Genet. 7 (1998) 1355–1361.
[19] V. Macdonald, G. Halliday, Pyramidal cell loss in motor cortices in Huntington's disease, Neurobiol. Dis. 10 (2002) 378–386.
[20] L. Mangiarini, K. Sathasivam, M. Seller, B. Cozens, A. Harper, C. Hetherington, M. Lawton, Y. Trottier, H. Lehrach, S.W. Davies, G.P. Bates, Exon 1 of the HD gene with an expanded CAG repeat is sufficient to cause a progressive neurological phenotype in transgenic mice, Cell 87 (1996) 493–506.
[21] A.J. Milnerwood, D.M. Cummings, G.M. Dallerac, J.Y. Brown, S.C. Vatsavayai, M.C. Hirst, P. Rezaie, K.P. Murphy, Early development of aberrant synaptic plasticity in a mouse model of Huntington's disease, Hum. Mol. Genet. 15 (2006) 1690–1703.
[22] A.J. Morton, M.A. Lagan, J.N. Skepper, S.B. Dunnett, Progressive formation of inclusions in the striatum and hippocampus of mice transgenic for the human Huntington's disease mutation, J. Neurocytol. 29 (2000) 679–702.
[23] J.M. Ordway, S. Tallaksen-Greene, C.A. Gutekunst, E.M. Bernstein, J.A. Cearley, H.W. Wiener, L.S. Dure, R. Lindsey, S.M. Hersch, R.S. Jope, R.L. Albin, P.J. Detloff, Ectopically expressed CAG repeats cause intranuclear inclusions and a progressive late onset neurological phenotype in the mouse, Cell 91 (1997) 753–763.
[24] A.V. Panov, C.A. Gutekunst, B.R. Leavitt, M.R. Hayden, J.R. Burke, W.J. Strittmatter, J.T. Greenamyre, Early mitochondrial calcium defects in Huntington's disease are a direct effect of polyglutamines, Nat. Neurosci. 5 (2002) 731–736.
[25] G. Paxinos, K.B.J. Franklin, The Mouse Brain in Stereotaxic Coordinates, 2nd ed., Academic Press, San Diego CA, 2001.
[26] P.H. Reddy, M. Williams, V. Charles, L. Garrett, L. Pike-Buchanan, W.O. Whetsell Jr., G. Miller, D.A. Tagle, Behavioural abnormalities and selective neuronal loss in HD transgenic mice expressing mutated full-length HD cDNA, Nat. Genet. 20 (1998) 198–202.
[27] P.H. Reddy, M. Williams, D.A. Tagle, Recent advances in understanding the pathogenesis of Huntington's disease, Trends Neurosci. 22 (1999) 248–255.
[28] A. Reiner, N. Del Mar, Y.P. Deng, C.A. Meade, Z. Sun, D. Goldowitz, R6/2 neurons with intranuclear inclusions survive for prolonged periods in the brains of chimeric mice, J. Comp. Neurol. 505 (2007) 603–629.
[29] R.A. Roos, G.T. Bots, Nuclear membrane indentations in Huntington's chorea, J. Neurol. Sci. 61 (1983) 37–47.
[30] R.A. Roos, J.F. Pruyt, J. de Vries, G.T. Bots, Neuronal distribution in the putamen in Huntington's disease, J. Neurol. Neurosurg. Psychiatry 48 (1985) 422–425.
[31] H.D. Rosas, A.K. Liu, S. Hersch, M. Glessner, R.J. Ferrante, D.H. Salat, K.A. van der, B.G. Jenkins, A.M. Dale, B. Fischl, Regional and progressive thinning of the cortical ribbon in Huntington's disease, Neurology 58 (2002) 695–701.
[32] C.A. Ross, Intranuclear neuronal inclusions: a common pathogenic mechanism for glutamine-repeat neurodegenerative diseases? Neuron 19 (1997) 1147–1150.
[33] E. Sapp, C. Schwarz, K. Chase, P.G. Bhide, A.B. Young, J. Penney, J.P. Vonsattel, N. Aronin, M. DiFiglia, Huntingtin localization in brains of normal and Huntington's disease patients, Ann. Neurol. 42 (1997) 604–612.
[34] F. Saudou, S. Finkbeiner, D. Devys, M.E. Greenberg, Huntingtin acts in the nucleus to induce apoptosis but death does not correlate with the formation of intranuclear inclusions, Cell 95 (1998) 55–66.
[35] J.Y. Shin, Z.H. Fang, Z.X. Yu, C.E. Wang, S.H. Li, X.J. Li, Expression of mutant huntingtin in glial cells contributes to neuronal excitotoxicity, J. Cell Biol. 171 (2005) 1001–1012.
[36] S.K. Singhrao, P. Thomas, J.D. Wood, J.C. MacMillan, J.W. Neal, P.S. Harper, A.L. Jones, Huntingtin protein colocalizes with lesions of neurodegenerative diseases: an investigation in Huntington's, Alzheimer's, and Pick's diseases, Exp. Neurol. 150 (1998) 213–222.
[37] S.S. Sisodia, Nuclear inclusions in glutamine repeat disorders: are they pernicious, coincidental, or beneficial? Cell 95 (1998) 1–4.
[38] S.J Tallaksen-Greene, A.B. Crouse, J.M. Hunter, P.J. Detloff, R.L. Albin, Neuronal intranuclear inclusions and neuropil aggregates in HdhCAG(150) knockin mice, Neuroscience 131 (2005) 843–852.
[39] I. Tellez-Nagel, A.B. Johnson, R.D. Terry, Studies on brain biopsies of patients with Huntington's chorea, J. Neuropathol. Exp. Neurol. 33 (1974) 308–332.
[40] The Huntington's Disease Collaborative Research Group, A novel gene containing a trinucleotide repeat that is expanded and unstable on Huntington's disease chromosomes, Cell 72 (1993) 971–983.
[41] R.C. Trueman, S.P. Brooks, L. Jones, S.B. Dunnett, The operant serial implicit learning task reveals early onset motor learning deficits in the Hdh knock-in mouse model of Huntington's disease, Eur. J. Neurosci. 25 (2007) 551–558.
[42] M. Turmaine, A. Raza, A. Mahal, L. Mangiarini, G.P. Bates, S.W. Davies, Nonapoptotic neurodegeneration in a transgenic mouse model of Huntington's disease, Proc. Natl. Acad. Sci. U.S.A. 97 (2000) 8093–8097.
[43] J.C. Vis, L.F. Nicholson, R.L. Faull, W.H. Evans, N.J. Severs, C.R. Green, Connexin expression in Huntington's diseased human brain, Cell Biol. Int. 22 (1998) 837–847.
[44] J.P. Vonsattel, M. DiFiglia, Huntington disease, J. Neuropathol. Exp. Neurol. 57 (1998) 369–384.
[45] J.P. Vonsattel, R.H. Myers, T.J. Stevens, R.J. Ferrante, E.D. Bird, E.P. Richardson Jr., Neuropathological classification of Huntington's disease, J. Neuropathol. Exp. Neurol. 44 (1985) 559–577.
[46] V.C. Wheeler, J.K. White, C.A. Gutekunst, V. Vrbanac, M. Weaver, X.J. Li, S.H. Li, H. Yi, J.P. Vonsattel, J.F. Gusella, S. Hersch, W. Auerbach, A.L. Joyner, M.E. MacDonald, Long glutamine tracts cause nuclear localization of a novel form of huntingtin in medium spiny striatal neurons in HdhQ92 and HdhQ111 knock-in mice, Hum. Mol. Genet. 9 (2000) 503–513.
[47] B. Woodman, R. Butler, C. Landles, M.K. Lupton, J. Tse, E. Hockly, H. Moffitt, K. Sathasivam, G.P. Bates, The Hdh(Q150/Q150) knock-in mouse model of HD and the R6/2 exon 1 model develop comparable and widespread molecular phenotypes, Brain Res. Bull. 72 (2007) 83–97.
[48] Z.X. Yu, S.H. Li, J. Evans, A. Pillarisetti, H. Li, X.J. Li, Mutant huntingtin causes context-dependent neurodegeneration in mice with Huntington's disease, J. Neurosci. 23 (2003) 2193–2202.

Please cite this article in press as: Z. Bayram-Weston, et al., Light and electron microscopic characterization of the evolution of cellular pathology in the Hdh$^{(CAG)150}$ Huntington's disease knock-in mouse, Brain Res. Bull. (2011), doi:10.1016/j.brainresbull.2011.03.014

Chapter 7

General Discussion

General Discussion

A variety of rodent genetic models have been created in an attempt to reproduce the human condition (Gray et al., 2008; Heng et al., 2007; Hodgson et al., 1996; Hodgson et al., 1999; Lin et al., 2001; Lloret et al., 2006; Mangiarini et al., 1996; Reddy et al., 1998; Schilling et al., 1999; Slow et al., 2003; Von Horsten et al., 2003; White et al., 1997; Yamamoto et al., 2000). Such models not only provide us with the opportunity to study the pathological process underling the disease, but also provide a platform for the testing of novel therapeutic interventions, however, no animal model fully replicates all of the key elements of the disease consequently each model must be apprised to determine their validity as a model of the disease.

In this thesis, a comprehensive investigation has been carried out to study the distribution of polyQ aggregates and NIIs in the brains of four different mouse models of HD. It has been observed that the distribution of aggregates and inclusions differs between each mouse model with minor similarities in the spatial and temporal distribution of aggregate pathology between each line. Briefly, in the YAC128 mice, aggregates were present from 6 months of age, again limited to specific brain regions such as the ventral striatum, amygdala and cortex with some variability between animals. However, at 15 months of age, inclusions were present in the ventro-lateral striatum, cortex and cerebellum. The R6/1 transgenic mice exhibited an extensive expression of aggregates and inclusions across all age groups with S830 immunohistochemistry, from 3.5 weeks of age (unpublished observations Bayram-Weston Z, *Appendix, Figure 1*). Regionally restricted distribution of NIIs were observed in the *Hdh*Q92 mice, which exhibited aggregates from 4 months of age in the olfactory tubercle, nucleus accumbens and striatum. The *Hdh*Q150 mice displayed a widespread distribution of inclusions throughout their lives from 5 months of age, which began in the olfactory tubercle, nucleus accumbens and striatum and was present in all brain regions at 24 months of age. As would be expected, aggregation and NII formation increased with advancing age in each of the mouse lines.

Summary Table of Results in the transgenic and knock-in mice

Strain Name	YAC128 (~ 128CAG)	R6/1 (~ 124CAG)	*Hdh*Q92 (~ 90CAG)	*Hdh*Q150 (~ 132CAG)
Striatal volume loss	21M	10M	24M	21M
Striatal cell loss	22M	11M	18M	24M
Appearance of diffuse nuclear staining	6M (Striatum, amygdala, cerebellum, hippocampus motor cortex, sensory cortex, piriform cortex)	3.5 weeks (All brain regions)	4M (Olfactory tubercle, nucleus accumbens, striatum)	5M (Olfactory tubercle, nucleus accumbens, striatum, globus pallidus, amygdala, thalamus, hypothalamus, cerebellum, hippocampus, motor cortex, sensory cortex, piriform cortex)
Appearance of NIIs	15M (Nucleus accumbens, ventral striatum, lateral striatum, cerebellum, motor and sensory cortex	3.5 weeks (All brain regions)	6M (Nucleus accumbens)	5M (Olfactory tubercle, nucleus accumbens, striatum, amygdala CL)
Spread of the pathology	Widespread specific to structures	Widespread	Ventral-dorsal anterior -posterior	Ventral-dorsal anterior- posterior
Reactive gliosis	Negative (striatum)	Negative (striatum)	Negative (striatum)	Negative (striatum)
	15M (slightly positive cortex)	4M (slightly positive cortex)	Negative (cortex)	Negative (cortex)
Ultrastructure of striatal cells	14M and 26M (Apoptotic and necrotic)	1.5 M and 7M (Necrotic)	14M and 21M (Apoptotic and necrotic)	14M and 21M (Necrotic)

a)Striatal atrophy

A profound atrophy of the striatum and the cortex has been reported in post-mortem brain analysis (Halliday et al., 1998; Vonsattel et al., 1985). It has been shown that striatal volume is decreased with no evidence of striatal neuronal loss in some transgenic (Klapstein et al., 2001; Martin-Aparicio et al., 2001; van Dellen et al., 2000) and knock-in mouse models of HD (Levine et al., 1999; Menalled et al., 2002). However, in this thesis, the results have shown that striatal volume loss is present in late time points in the YAC128, R6/1, *Hdh*Q92 and *Hdh*Q150 mice in comparison to their wildtype littermates.

b) Striatal cell loss

Not all animal models of HD that express mutant huntingtin show signs of the striatal cell loss (Levine et al., 1999; Shelbourne et al., 1999; Stack et al., 2005), although some models do (Carroll et al., 2011; Diaz-Hernandez et al., 2005; Kantor et al., 2006; Lin et al., 2001; McBride et al., 2006; Reddy et al., 1998). The cell loss is minimal compared with that observed in post-mortem human brains. In agreement, the results from this thesis have shown that there is evidence of striatal neuronal loss in these mouse models but not as robust as seen in the human condition. This finding may suggest that the cells of HD mouse models are more resistant to the disease process than human cells.

c-) Ultrastructural comparison of cell death in the HD mouse lines

Cell death is categorized as apoptotic, necrotic or autophagic depending on the morphological appearance of the cells. Apoptosis is characterized by cell volume loss, membrane blebbing, chromatin condensation, DNA fragmentation and appearance of apoptotic bodies (Kerr et al., 1972; Kerr et al., 1995; Koh et al., 1995) although all apoptotic cells necessarily do not exhibit apoptotic cell bodies (Bowen, 1993). Apoptosis causes cell shrinkage and is not related to cell lysis or inflammation (Gorman,

2008). However, necrosis includes swelling of ER and mitochondria, does not have apoptotic bodies and nuclear fragmentation. It causes cell swelling and loss of ATP which leads to cell lysis. Necrosis triggers inflammation in the surrounding environment, as a result of releasing cellular contents into the extracellular space (Gorman, 2008). Autophagic cell death is characterized by autophagic vacuoles and has been suggested that it is triggered by amino-acid starvation and protein aggregation (Bredesen et al., 2006; Kim et al., 2008).

Ultrastructural analysis of YAC128 transgenic and *Hdh*Q92 knock-in mice showed signs of apoptosis with cellular shrinkage, condensed chromatin and cytoplasmic contents without any apoptotic bodies. However, R6/1 transgenic and *Hdh*Q150 knock-in mice displayed more necrotic cell death such as vacuolated cytoplasm, uneven nuclear membrane, loss of membrane integrity and did not show cellular shrinkage, suggesting in the pathology is different in each mouse line and may be due to the differences in the genetic construct. Interestingly, In all these models, there was a degree of vacuolation in the cells supporting recent evidence that the autophagic system may be responsible for HD (Kim et al., 2008; Martinez-Vicente et al., 2010). However, the molecular mechanism of neuronal cell death in HD is not well understood, especially in relation to apoptosis, necrotic and autophagic mechanisms. This is partly due to a lack of consensus as to what apoptotic cells should look like at the ultrastructural level. Demonstrating cell death with TEM is also technically challenging due to the sporadic incidence of the phenomena and the small tissue sample used, in addition tissue samples are often not optimal for use with TEM due to a range of factors such as post-mortem delay time and related fixation problems.

Is astrogliosis present in these mouse models?

GFAP is the main intermediate filament in astrocytes and defines the astrocytic morphology. The astroglial reaction is assessed by the morphology of the astrocytes and the increased expression of GFAP (Bignami et al., 1972). The astroglial reaction is reported in HD post-mortem brains (Galatioto,

1996; Hedreen and Folstein, 1995; Maat-Schieman et al., 2007; Vonsattel et al., 1985) and has been reported in several genetic models such as the Hdh^{Q150} (Heng et al., 2007; Lin et al., 2001), Hdh^{Q200} (Heng et al., 2010) and HD89 (Reddy et al., 1998) mouse lines but not in R6/2 mice (Mangiarini et al., 1996). However, in all mice models examined in this thesis, there was no strong evidence of astroglial reaction with anti-GFAP immunohistochemistry. None of the mouse lines studied demonstrated any increase in GFAP activity in the striatum in comparison to control animals at any age. GFAP activity increased with age in both genetically modified animals and control animals, although, the cortex of transgenic animals (R6/1 and YAC128 mice) contained increased GFAP activity compared to their wildtypes at older ages. As all models did not consistently show GFAP activity, this may suggest that astroglial reaction is not associated with the expanded CAG repeat length.

Is cell death associated with NIIs?

From autopsy tissues it can be seen that neuronal loss progresses in a dorso to ventral striatum direction (Hedreen and Folstein, 1995; Mitchell et al., 1999). The frequency of cortical neurons containing NIIs is increased in juvenile patients (DiFiglia et al., 1997), however, striatal NIIs are less abundant in these patients (Kuemmerle et al., 1999), showing a dissociation between the aggregation and selective pattern of striatal neuronal loss. The precise role of NIIs in cell death is still unknown. Three possible scenarios have been hypothesised for their role in HD pathology. There is evidence that NIIs are not toxic, particularly as several mouse lines demonstrate functional pathology in the absence of NIIs (Hodgson et al., 1999; Menalled et al., 2003; Slow et al., 2003; Slow et al., 2005; Van Raamsdonk et al., 2005b), suggesting that neuronal dysfunction and loss might occur well before the visible NIIs, and cell loss is not related with NIIs load. However, recent studies have indicated that aggregates might be present in conformations that are more difficult to visualise than insoluble forms, with commonly used antibodies (Landles et al., 2010; Sathasivam et al., 2010; Slow et al., 2006), suggesting

these confirmations are present from the start, even if we do not seen them they may still be toxic to the cells.

Interestingly, the results from this thesis show that the distribution of inclusion formation in the striatum of the HD mouse line was different. In The YAC128 mice, NIIs seems more dominant in the ventral striatum than the dorsal striatum. Similarly, in the R6/1 mice showed the same patterns which inclusions were more in the ventral striatum than the dorsal striatum, whereas, the *Hdh*Q150 and *Hdh*Q92 mice displayed dense the aggregates and NIIs in the entire striatum. The distribution of aggregates/ NIIs in the cortex of HD mouse line was also different. The YAC128 and R6/1 mice have shown more aggregates and NIIs in the cortex than the striatum, whilst, the *Hdh*Q92 mice showed more aggregates in the striatum than the cortex, however, the *Hdh*Q150 mice displayed widespread distribution of NIIs which did not differ in the regions of the striatum and the cortex. In post-mortem HD brains, many studies agree that the cortex contains more inclusions than the striatum (DiFiglia et al., 1997; Gourfinkel-An et al., 1998; Gutekunst et al., 1999; Maat-Schieman et al., 1999; Sapp et al., 1997). All layers of neocortex of post-mortem tissue contained NIIs, however, they were widespread in layers III, V and VI, and in juvenile-onset patients, layer II also contained NIIs (Maat-Schieman et al., 1999). When considered together, the striatum receives excitatory glutamatergic inputs from the entire cerebral cortex, therefore, the selective striatal vulnerability in HD may be due to the vast glutamatergic inputs they receive into these cells (Mathai and Smith, 2011). It has been emphasised that brains of HD patients undergo neurophysiological alterations as revealed by electrophysiological studies (Ghiglieri et al., 2011). A recent study shows that the variable symptomatology in HD is correlated with the variable compartmental pattern of GABA receptor and cell loss in the striatum and the cortex (Thu et al., 2010). When considered together these findings support the hypothesis that intracellular dysfunction may be induced by aggregates/NIIs and suggesting the aggregation process is toxic to the cells. More studies need to be carried out to link any neuronal dysfunction and the formation of NIIs in these areas.

Although, the neuropathology is most prominent in the neostriatum and the cerebral cortex, other brain areas such as amygdala, hippocampus

(Rosas et al., 2003), GP and the nucleus accumbens (van den Bogaard et al., 2011) are also affected. There is little concordance with regards to other regions of the brain. For example, Gutekunst et al have observed rare appearance of NIIs in the cerebellum (Gutekunst et al., 1999), while others did not find NIIs in the cerebellum (DiFiglia et al., 1997; Gourfinkel-An et al., 1998; Maat-Schieman et al., 1999). The results of this thesis show that there NIIs initially appeared in the olfactory tubercle in each mouse line. It has been hypothesised that PD begins in the myenteric plexus and olfactory system (Braak et al., 2006). Interestingly, one recent study has shown that individuals in presymptomatic HD showed odour recognition impairment (Paulsen et al., 2008), similar to those seen PD patients (Chahine and Stern, 2011), supporting the idea that olfactory system may be involved in the HD pathology. Therefore, further investigation into other regions of the brain in addition to the striatum and cortex, is required.

In the human study, it has been observed that the cerebellum is abnormally small, but the result of the neuropathological assessment showed cerebellar density is unaffected in early HD (Vonsattel et al., 1985). However, more recent studies indicate cerebellar atrophy in HD (Fennema-Notestine et al., 2004; Henley et al., 2006; Herishanu et al., 2009; Jeste et al., 1984; Rodda, 1981; Vonsattel and DiFiglia, 1998). Again, NIIs were present in the cerebellum of YAC128, R6/1 and *Hdh*Q150 mice, but not in the *Hdh*Q92 mice at late stage. The cortex was the one of the regions affected less with NIIs in the *Hdh*Q92 mice. This result is interesting because, *Hdh*Q92 mice showed late motor deficit in rotarod at 27 months of age, overlapping the late appearance of NIIs in the cerebellum. This supports the involvement of NIIs in motor impairment and the cerebellar involvement in motor coordination and suggests the cerebellum is involved in motor deficit seen HD patients and mouse models. It would be interesting to apply S830 antibody to different regions of the human post-mortem brains such as olfactory tubercle, piriform cortex and cerebellum.

Is the genetic construct predictive of the neuropathology?

All of the animal models studied in this thesis have a different genetic construct. The YAC128 mice have yeast artificial chromosome expressing the entire human protein with 128 CAG repeats. However, the R6/1 mice contain the N terminal fragment of human gene with ~ 124 CAG repeats. While, *Hdh*Q92 and *Hdh*Q150 mice include ~ 90 CAG and ~ 134 CAG repeats which inserted into murine *Hdh* locus, respectively. The CAG repeat length was relatively similar, suggesting the NIIs pathology in these mouse is not entirely related with CAG repeat length. The R6/1 mice have a relatively shorter life span comparison to the YAC128, *Hdh*Q92 and *Hdh*Q150 mice which have lived up to 2.5 years and contained NIIs at an early age, supporting the hypothesis that the fragment of human huntingtin gene is more toxic than the full length huntingtin mutation, despite having a shorter repeat length. These results also suggest that inserting human huntingtin gene into the mouse genome triggers other gene's interference in transgenic mice and CAG repeat length does not affect on the distribution of aggregates and NIIs.

It should be acknowledged that a number of gene expression studies have been carried on HD patients and HD models which are detailed in (Seredenina and Luthi-Carter, 2011). Briefly, the results from these studies have shown that the regional and cellular gene expression changes in human HD brain and are more pronounced in the striatum and the cortex (Hodges et al., 2006; Kuhn et al., 2007). Similarly, the striatal gene expression changes have been observed in some genetic models of HD including the R6/1, R6/2, YAC128, *HdhQ150* and *Hdh*Q92 mice. Significantly, all these mice had correlations with human striatal gene expression changes and the highest correlations were reported in *Hdh*Q150 and R6/2 mice (Kuhn et al., 2007). Similarly, the expression of specific gene has been found to correlate well with behavioural end points in R6/1 mice (Hodges et al., 2008). Similarly, in YAC128 mice, changes in the gene expression levels have been reported as early as 3 months of age (Becanovic et al., 2010) supporting the gene expression levels and the genetic construct contribute the pathology seen in these models.

The results from this thesis also show that the aggregation process coincides with the behavioural deficits observed in these mice. YAC128 mice showed that nuclear staining was present in the ventral striatum and cortex at 6 months of age, in parallel, cognitive impairments were present in this mouse line on the C57BL/6J background at 6 months old (Brooks et al., 2010a; Brooks et al., 2011). Similarly, the appearance of diffuse nuclear staining and NIIs in the hippocampus (Milnerwood et al., 2006) and in most of the brain regions at 3.5 weeks of age (unpublished observations, Bayram-Weston Z), overlapping with motor deficit were detected at 4 weeks of age in the R6/1 mice (Bolivar et al., 2004). The appearance of inclusion in the *Hdh*Q150 mice coincided with motor impairments at 3 months of age (Lin et al., 2001), and cognitive impairment at 6 months of age (Brooks et al., 2006; Woodman et al., 2007). Yet again, a similar pattern has been observed in the *Hdh*Q92 mouse line, where the presence of diffuse nuclear staining but not with inclusions coinciding with the cognitive deficit was present at 4 months of age (Trueman et al., 2007; Trueman et al., 2008), suggesting that the deposition of mutant huntingtin protein may be toxic and cause neopathological changes in the cell.

Although atrophy occurs in the brain, it is important to note the mutant huntingtin protein is ubiquitously expressed throughout the whole organism. A number of peripheral abnormalities have been reported in HD patients such as increased corticosteroid level (Bjorkqvist et al., 2006; Heuser et al., 1991), reduced testosterone level (Markianos et al., 2005) and gastrointestinal dysfunction (van der Burg et al., 2011), indicating the importance of peripheral defects in HD pathology. Similarly, in the HdhQ150 and R6/2 mice, peripheral pathology has been reported including muscle pathology (Moffitt et al., 2009), making it difficult to assess, because motor symptoms may be due to the fact that peripheral pathology exists alongside brain pathology.

Is there a faithful representative animal model?

A representative animal model should recapitulate motor, cognitive and behavioural disturbances, alongside the neuropathology which has been observed in individuals affected with HD. Data from presymptomatic HD

patients show behavioural and cognitive changes occur well before the onset of motor symptoms (Duff et al., 2007; Johnson et al., 2007; Solomon et al., 2007). However, determining exact cognitive and psychiatric abnormalities is challenging in the rodent models. The behavioural phenotypes and pathological features of some animal models were summarised in chapter 1, however many of these models still need to be characterized fully.

Taken into account when analysing the above traits, the R6/1 mice have a more severe phenotype than other models studied here, showing the early and widespread appearance of aggregates. R6/1 mice do not replicate an accurate picture of the neuropathological features of adult-onset HD, but may be more representative of juvenile HD. The behavioural features of the *Hdh*Q92 and *Hdh*Q150 knock-in mice appear to replicate adult-onset HD best due to their early onset of cognitive and psychiatric deficits. However, NIIs are more striatal than cortical unlike post mortem human brains, so they do not fully represent human HD. The YAC128 mouse line is a more representative model of HD, in terms of aggregate formation as the neuropathology is more cortical in nature.

Future work

Many brain disorders such as Huntington's disease, Alzheimer's disease, amyotrophic lateral sclerosis (ALS), PD, stroke, head trauma and infection, are associated with inflammation that is involved in neuropathogenesis (Heneka and O'Banion, 2007). Microglia and astrocytes act as immune cells in the inflamed brain. Both cell types, but especially microglia, are thought to contribute to the onset of inflammation in many brain diseases by producing a range of proinflammatory mediators including cytokines, reactive oxygen species, complement factors, neurotoxic secretory products, free radical species and nitric oxide, all of which can contribute to neuronal dysfunction and cell death. The cytokine-induced neuronal insults can activate microglia (Griffin et al., 1998). An impairment of microglial performance with genetic or environmental insults could worsen neuronal dysfunction. The next phase of this study will assess the inflammation processes at these models in more detail.

Conclusions

The results presented in this thesis are as follows;

- There is cell loss with reduced striatal volume in the striatum of each mouse line.
- The features of apoptotic cell death are present in the YAC128 and *Hdh*Q92 lines, whereas necrotic cell death was more evident in the R6/1 and *Hdh*Q150 lines.
- R6/1 mice do not replicate an accurate picture of the neuropathological features of adult-onset HD, but may be more representative of juvenile HD.
- In *Hdh*Q92 and *Hdh*Q150 knock-in mice, NIIs are more striatal than cortical unlike post mortem human HD brains.
- The YAC128 mouse line is a more representative model of HD, in terms of aggregate formation, resembling the human HD pathology.

In this thesis, the results demonstrate that each of the mouse lines has an incomparable pattern of development of neuropathology and distribution of NIIs, and this may be representative of the neuronal dysfunction in each of these mouse lines.

Appendix

Fig.1 : Photomicrographs of S830 staining in the different regions of the R6/1 mice at 3.5 weeks of age. The aggregates and NIIs were present in the olfactory tubercle (OT), piriform cortex, ventral striatum, dorsal striatum, cortex, Amydala, Thamus, cerebellum and hippocampus.

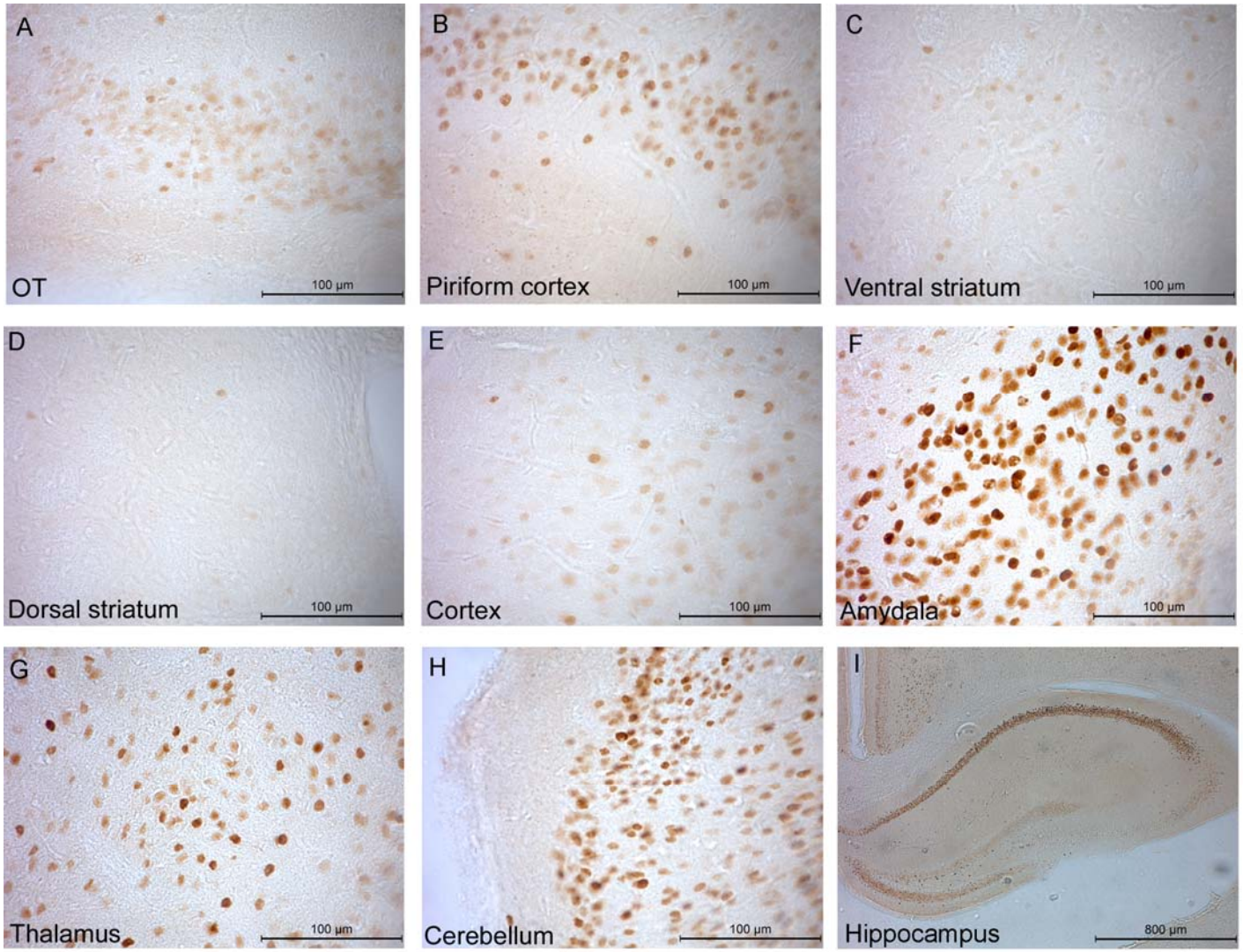

BUFFERS AND SOLUTIONS

TRIS BUFFRED SALINE I (Concentrated stock solution)

TRIS base	48g
Sodium chloride	36g
Distilled water	1000ml

Adjusted to pH7.3 with concentrated HCl and stored at $+4C^0$

TRIS BUFFRED SALINE II-0.1M (Working solution)

250 ml of stock solution (above) +750 ml Distilled water Adjusted to pH 7.3 with concentrated HCl and stored at $+4C^0$

0.05 M TRIS NON SALINE (TNS) for DAB demonstration for HPR

TRIS base	6.0g
Distilled water	1000ml

Adjusted to pH7.6 with concentrated HCl and prepare as needed

DAB stock solution

DAB	1g
TNS Buffer solution(above)	100ml

Dissolved and divided into 2ml aliquots in small bijou pots. Freeze the aliquots as quickly as possible.

DAB Solution A:

DAB	20mg
TNS Buffer solution(above)	40ml

Mixed very well and aliquot 2ml and kept in $4C^0$ until needed

DAB working solution B:

DAB	2ml aliquot DAB (above)
Buffer solution	40 ml
30% H_2O_2	12µm

PHOSPHATE BUFFERED SALINE (PRE-WASH) FOR PERFUSION

Di-Sodium hydrogen orthophosphate	90g
Sodium chloride	45g
Distilled water	5000ml

Adjusted to pH 7.3 with orthophosphoric acid

4% Paraformaldehyde solution

40 g Paraformaldehyde dissolved with heat on the stirrer (50-60C^0) in 1000ml Prewash (above) for 3h, then turned the heat and left stirring overnight at room temperature. Adjusted to pH 7.3 with sodiumhydoxidase or orthophosphoric acid.

25% sucrose

Sucrose	25g
TBS	Make up to 100ml

Antifreeze Solution

Na_2HPO_4 (dibasic)	4.36g
NaH_2PO_4 (monobasic)	1.256g

Fully dissolved in 320 ml distilled water and then added

Ethylene glycol (sigma E-9129)	240 ml
Glycerol (sigma G-7893)	240ml

Everything mixed very well and stored in the +4C^0.

Cresyl violet working solution;

Cresyl violet	7g
Sodium Acetate (anhydrous)	5g
Distilled water.	600ml

Adjusted to pH 3.5 with glacial acetic acid. Made up to a final volume of 1000ml and left stirring overnight. Stored at room temperature (up to 1 year) Filtered before use.

Acid Alcohol;

Glacial Acetic Acid	5ml
95% alcohol	200ml

PHOSPHATE BUFFERED SALINE (SORENSEN) FOR TEM

Solution A

Sodium phosphate ($Na_2HPO_4.2H_2O$)	11.876g
Distilled water	1000ml

Solution B

Potassium phosphate (KH_2PO_4)	9.8g
Distilled water	1000ml

818 ml *Solution A* +182ml *Solution B* (pH 7.4)

ARALDITE RESIN

Araldite CY212 (AGAR)	10g
DDSA (AGAR)	10g
BDMA (AGAR)	10g

LOWICRYLS HM20 RESIN (AGAR Kit)

Crosslinker D	2.98g
Monomer E	17.02g
Initiator C	0.10g

REYNOLD'S LEAD CITRATE

Lead nitrate (Sigma)	1.33g
Sodium citrate	1.76g
Distilled water	30ml

Adjusted pH 12 with aprox. 8 ml NaOH

Reference List

Reference List

1. The Huntington's Disease Collaborative Research Group (1993). A novel gene containing a trinucleotide repeat that is expanded and unstable on Huntington's disease chromosomes. Cell *72*, 971-983.

2. Albin,R.L., Reiner,A., Anderson,K.D., Dure,L.S., Handelin,B., Balfour,R., Whetsell,W.O., Jr., Penney,J.B., and Young,A.B. (1992). Preferential loss of striato-external pallidal projection neurons in presymptomatic Huntington's disease. Ann. Neurol. *31*, 425-430.

3. Alexander,G.E. and Crutcher,M.D. (1990). Functional architecture of basal ganglia circuits: neural substrates of parallel processing. Trends Neurosci. *13*, 266-271.

4. Alexander,G.E., Crutcher,M.D., and DeLong,M.R. (1990). Basal ganglia-thalamocortical circuits: parallel substrates for motor, oculomotor, "prefrontal" and "limbic" functions. Prog. Brain Res. *85*, 119-146.

5. Alexander,G.E., DeLong,M.R., and Strick,P.L. (1986). Parallel organization of functionally segregated circuits linking basal ganglia and cortex. Annu. Rev. Neurosci. *9*, 357-381.

6. Ambrose,C.M., Duyao,M.P., Barnes,G., Bates,G.P., Lin,C.S., Srinidhi,J., Baxendale,S., Hummerich,H., Lehrach,H., Altherr,M., and . (1994). Structure and expression of the Huntington's disease gene: evidence against simple inactivation due to an expanded CAG repeat. Somat. Cell Mol. Genet. *20*, 27-38.

7. Andrew,S.E., Goldberg,Y.P., Kremer,B., Telenius,H., Theilmann,J., Adam,S., Starr,E., Squitieri,F., Lin,B., Kalchman,M.A., and . (1993). The relationship between trinucleotide (CAG) repeat length and clinical features of Huntington's disease. Nat. Genet. *4*, 398-403.

8. Arrasate,M., Mitra,S., Schweitzer,E.S., Segal,M.R., and Finkbeiner,S. (2004). Inclusion body formation reduces levels of mutant huntingtin and the risk of neuronal death. Nature *431*, 805-810.

9. Aylward,E.H., Nopoulos,P.C., Ross,C.A., Langbehn,D.R., Pierson,R.K., Mills,J.A., Johnson,H.J., Magnotta,V.A., Juhl,A.R., and Paulsen,J.S. (2011). Longitudinal change in regional brain volumes in prodromal Huntington disease. J. Neurol. Neurosurg. Psychiatry *82*, 405-410.

10. Aylward,E.H., Sparks,B.F., Field,K.M., Yallapragada,V., Shpritz,B.D., Rosenblatt,A., Brandt,J., Gourley,L.M., Liang,K., Zhou,H., Margolis,R.L., and Ross,C.A. (2004). Onset and rate of striatal atrophy in preclinical Huntington disease. Neurology *63*, 66-72.

11. Bates,G.P., Harper,P.S., and Jones,L. (2002). 5. In Huntington's Disease, G.P.Bates, P.S.Harper, and L.Jones, eds. Oxford university Press).

12. Bates,G.P., Mangiarini,L., Mahal,A., and Davies,S.W. (1997). Transgenic models of Huntington's disease. Hum. Mol. Genet. *6*, 1633-1637.

13. Bear M.F., Paradiso M.A, and Connors B.W. (2006). Neurons and Glia. In Neuroscience Exploring the brain, Bear M.F.Connors B.W.Paradiso M.A., ed. Williams&Wilkins), pp. 23-48.

14. Becanovic,K., Pouladi,M.A., Lim,R.S., Kuhn,A., Pavlidis,P., Luthi-Carter,R., Hayden,M.R., and Leavitt,B.R. (2010). Transcriptional changes in Huntington disease identified using genome-wide expression profiling and cross-platform analysis. Hum. Mol. Genet. *19*, 1438-1452.

15. Becher,M.W., Kotzuk,J.A., Sharp,A.H., Davies,S.W., Bates,G.P., Price,D.L., and Ross,C.A. (1998). Intranuclear neuronal inclusions in Huntington's disease and dentatorubral and pallidoluysian atrophy: correlation between the density of inclusions and IT15 CAG triplet repeat length. Neurobiol. Dis. *4*, 387-397.

16. Bence,N.F., Sampat,R.M., and Kopito,R.R. (2001). Impairment of the ubiquitin-proteasome system by protein aggregation. Science *292*, 1552-1555.

17. Benn,C.L., Luthi-Carter,R., Kuhn,A., Sadri-Vakili,G., Blankson,K.L., Dalai,S.C., Goldstein,D.R., Spires,T.L., Pritchard,J., Olson,J.M., van Dellen,A., Hannan,A.J., and Cha,J.H. (2010). Environmental enrichment reduces neuronal intranuclear inclusion load but has no effect on messenger RNA expression in a mouse model of Huntington disease. J. Neuropathol. Exp. Neurol. *69*, 817-827.

18. Bennett,E.J., Shaler,T.A., Woodman,B., Ryu,K.Y., Zaitseva,T.S., Becker,C.H., Bates,G.P., Schulman,H., and Kopito,R.R. (2007). Global changes to the ubiquitin system in Huntington's disease. Nature *448*, 704-708.

19. Bhide,P.G., Day,M., Sapp,E., Schwarz,C., Sheth,A., Kim,J., Young,A.B., Penney,J., Golden,J., Aronin,N., and DiFiglia,M. (1996). Expression of normal and mutant huntingtin in the developing brain. J. Neurosci. *16*, 5523-5535.

20. Bignami,A., Eng,L.F., Dahl,D., and Uyeda,C.T. (1972). Localization of the glial fibrillary acidic protein in astrocytes by immunofluorescence. Brain Res. *43*, 429-435.

21. Bjorkqvist,M., Petersen,A., Bacos,K., Isaacs,J., Norlen,P., Gil,J., Popovic,N., Sundler,F., Bates,G.P., Tabrizi,S.J., Brundin,P., and Mulder,H. (2006). Progressive alterations in the hypothalamic-pituitary-adrenal axis in the R6/2 transgenic mouse model of Huntington's disease. Hum. Mol. Genet. *15*, 1713-1721.

22. Bolivar,V.J., Manley,K., and Messer,A. (2004). Early exploratory behavior abnormalities in R6/1 Huntington's disease transgenic mice. Brain Res. *1005*, 29-35.

23. Borlongan,C.V., Koutouzis,T.K., and Sanberg,P.R. (1997). 3-Nitropropionic acid animal model and Huntington's disease. Neurosci. Biobehav. Rev. *21*, 289-293.

24. Bowen,I.D. (1993). Apoptosis or programmed cell death? Cell Biol. Int. *17*, 365-380.

25. Braak,H., de Vos,R.A., Bohl,J., and Del Tredici,K. (2006). Gastric alpha-synuclein immunoreactive inclusions in Meissner's and Auerbach's plexuses in cases staged for Parkinson's disease-related brain pathology. Neurosci. Lett. *396*, 67-72.

26. Bredesen,D.E., Rao,R.V., and Mehlen,P. (2006). Cell death in the nervous system. Nature *443*, 796-802.

27. Brooks,S., Higgs,G., Janghra,N., Jones,L., and Dunnett,S.B. (2010a). Longitudinal analysis of the behavioural phenotype in YAC128 (C57BL/6J) Huntington's disease transgenic mice. Brain Res. Bull.

28. Brooks,S., Higgs,G., Jones,L., and Dunnett,S.B. (2010b). Longitudinal analysis of the behavioural phenotype in Hdh((CAG)150) Huntington's disease knock-in mice. Brain Res. Bull.

29. Brooks,S., Higgs,G., Jones,L., and Dunnett,S.B. (2010c). Longitudinal analysis of the behavioural phenotype in Hdh(Q92) Huntington's disease knock-in mice. Brain Res. Bull.

30. Brooks,S.P., Betteridge,H., Trueman,R.C., Jones,L., and Dunnett,S.B. (2006). Selective extra-dimensional set shifting deficit in a knock-in mouse model of Huntington's disease. Brain Res. Bull. *69*, 452-457.

31. Brooks,S.P., Janghra,N., Higgs,G.V., Bayram-Weston,Z., Heuer,A., Jones,L., and Dunnett,S.B. (2011). Selective cognitive impairment in the YAC128 Huntington's disease mouse. Brain Res. Bull.

32. Butterworth,N.J., Williams,L., Bullock,J.Y., Love,D.R., Faull,R.L., and Dragunow,M. (1998). Trinucleotide (CAG) repeat length is positively correlated with the degree of DNA fragmentation in Huntington's disease striatum. Neuroscience *87*, 49-53.

33. Campodonico,J.R., Codori,A.M., and Brandt,J. (1996). Neuropsychological stability over two years in asymptomatic carriers of the Huntington's disease mutation. J. Neurol. Neurosurg. Psychiatry *61*, 621-624.

34. Carroll,J.B., Lerch,J.P., Franciosi,S., Spreeuw,A., Bissada,N., Henkelman,R.M., and Hayden,M.R. (2011). Natural history of disease

in the YAC128 mouse reveals a discrete signature of pathology in Huntington disease. Neurobiol. Dis. *43*, 257-265.

35. Carter,R.J., Lione,L.A., Humby,T., Mangiarini,L., Mahal,A., Bates,G.P., Dunnett,S.B., and Morton,A.J. (1999). Characterization of progressive motor deficits in mice transgenic for the human Huntington's disease mutation. J. Neurosci. *19*, 3248-3257.

36. Cattaneo,E. and Calabresi,P. (2002). Mutant huntingtin goes straight to the heart. Nat. Neurosci. *5*, 711-712.

37. Cha,J.H., Kosinski,C.M., Kerner,J.A., Alsdorf,S.A., Mangiarini,L., Davies,S.W., Penney,J.B., Bates,G.P., and Young,A.B. (1998). Altered brain neurotransmitter receptors in transgenic mice expressing a portion of an abnormal human huntington disease gene. Proc. Natl. Acad. Sci. U. S. A *95*, 6480-6485.

38. Chahine,L.M. and Stern,M.B. (2011). Diagnostic markers for Parkinson's disease. Curr. Opin. Neurol. *24*, 309-317.

39. Chang,D.T., Rintoul,G.L., Pandipati,S., and Reynolds,I.J. (2006). Mutant huntingtin aggregates impair mitochondrial movement and trafficking in cortical neurons. Neurobiol. Dis. *22*, 388-400.

40. Chen,S., Berthelier,V., Yang,W., and Wetzel,R. (2001). Polyglutamine aggregation behavior in vitro supports a recruitment mechanism of cytotoxicity. J. Mol. Biol. *311*, 173-182.

41. Chen,S. and Wetzel,R. (2001). Solubilization and disaggregation of polyglutamine peptides. Protein Sci. *10*, 887-891.

42. Chenery,H.J., Angwin,A.J., and Copland,D.A. (2008). The basal ganglia circuits, dopamine, and ambiguous word processing: a neurobiological account of priming studies in Parkinson's disease. J. Int. Neuropsychol. Soc. *14*, 351-364.

43. Ciechanover,A. (1994). The ubiquitin-proteasome proteolytic pathway. Cell *79*, 13-21.

44. Clabough,E.B. and Zeitlin,S.O. (2006). Deletion of the triplet repeat encoding polyglutamine within the mouse Huntington's disease gene results in subtle behavioral/motor phenotypes in vivo and elevated levels of ATP with cellular senescence in vitro. Hum. Mol. Genet. *15*, 607-623.

45. Clark,J.I. and Muchowski,P.J. (2000). Small heat-shock proteins and their potential role in human disease. Curr. Opin. Struct. Biol. *10*, 52-59.

46. Cornett,J., Cao,F., Wang,C.E., Ross,C.A., Bates,G.P., Li,S.H., and Li,X.J. (2005). Polyglutamine expansion of huntingtin impairs its nuclear export. Nat. Genet. *37*, 198-204.

47. Coyle,J.T. and Schwarcz,R. (1976). Lesion of striatal neurones with kainic acid provides a model for Huntington's chorea. Nature *263*, 244-246.

48. Cudkowicz,M. and Kowall,N.W. (1990). Degeneration of pyramidal projection neurons in Huntington's disease cortex. Ann. Neurol. *27*, 200-204.

49. D'Angelo,M.A., Raices,M., Panowski,S.H., and Hetzer,M.W. (2009). Age-dependent deterioration of nuclear pore complexes causes a loss of nuclear integrity in postmitotic cells. Cell *136*, 284-295.

50. Dahl,D., Bignami,A., Weber,K., and Osborn,M. (1981). Filament proteins in rat optic nerves undergoing Wallerian degeneration: localization of vimentin, the fibroblastic 100-A filament protein, in normal and reactive astrocytes. Exp. Neurol. *73*, 496-506.

51. Damiano,M., Galvan,L., Deglon,N., and Brouillet,E. (2010). Mitochondria in Huntington's disease. Biochim. Biophys. Acta *1802*, 52-61.

52. Davies,S.W., Beardsall,K., Turmaine,M., DiFiglia,M., Aronin,N., and Bates,G.P. (1998). Are neuronal intranuclear inclusions the common neuropathology of triplet-repeat disorders with polyglutamine-repeat expansions? Lancet *351*, 131-133.

53. Davies,S.W., Turmaine,M., Cozens,B.A., DiFiglia,M., Sharp,A.H., Ross,C.A., Scherzinger,E., Wanker,E.E., Mangiarini,L., and Bates,G.P. (1997). Formation of neuronal intranuclear inclusions underlies the neurological dysfunction in mice transgenic for the HD mutation. Cell *90*, 537-548.

54. de la Monte,S.M., Vonsattel,J.P., and Richardson,E.P., Jr. (1988). Morphometric demonstration of atrophic changes in the cerebral cortex, white matter, and neostriatum in Huntington's disease. J. Neuropathol. Exp. Neurol. *47*, 516-525.

55. Deschepper,M., Hoogendoorn,B., Brooks,S., Dunnett,S.B., and Jones,L. (2011). Proteomic changes in the brains of Huntington's disease mouse models reflect pathology and implicate mitochondrial changes. Brain Res. Bull.

56. Diaz-Hernandez,M., Torres-Peraza,J., Salvatori-Abarca,A., Moran,M.A., Gomez-Ramos,P., Alberch,J., and Lucas,J.J. (2005). Full motor recovery despite striatal neuron loss and formation of irreversible amyloid-like inclusions in a conditional mouse model of Huntington's disease. J. Neurosci. *25*, 9773-9781.

57. DiFiglia,M., Sapp,E., Chase,K., Schwarz,C., Meloni,A., Young,C., Martin,E., Vonsattel,J.P., Carraway,R., Reeves,S.A., and . (1995).

Huntingtin is a cytoplasmic protein associated with vesicles in human and rat brain neurons. Neuron *14*, 1075-1081.

58. DiFiglia,M., Sapp,E., Chase,K.O., Davies,S.W., Bates,G.P., Vonsattel,J.P., and Aronin,N. (1997). Aggregation of huntingtin in neuronal intranuclear inclusions and dystrophic neurites in brain. Science *277*, 1990-1993.

59. Djousse,L., Knowlton,B., Hayden,M., Almqvist,E.W., Brinkman,R., Ross,C., Margolis,R., Rosenblatt,A., Durr,A., Dode,C., Morrison,P.J., Novelletto,A., Frontali,M., Trent,R.J., McCusker,E., Gomez-Tortosa,E., Mayo,D., Jones,R., Zanko,A., Nance,M., Abramson,R., Suchowersky,O., Paulsen,J., Harrison,M., Yang,Q., Cupples,L.A., Gusella,J.F., MacDonald,M.E., and Myers,R.H. (2003). Interaction of normal and expanded CAG repeat sizes influences age at onset of Huntington disease. Am. J. Med. Genet. A *119A*, 279-282.

60. Djousse,L., Knowlton,B., Hayden,M.R., Almqvist,E.W., Brinkman,R.R., Ross,C.A., Margolis,R.L., Rosenblatt,A., Durr,A., Dode,C., Morrison,P.J., Novelletto,A., Frontali,M., Trent,R.J., McCusker,E., Gomez-Tortosa,E., Mayo,C.D., Jones,R., Zanko,A., Nance,M., Abramson,R.K., Suchowersky,O., Paulsen,J.S., Harrison,M.B., Yang,Q., Cupples,L.A., Mysore,J., Gusella,J.F., MacDonald,M.E., and Myers,R.H. (2004). Evidence for a modifier of onset age in Huntington disease linked to the HD gene in 4p16. Neurogenetics. *5*, 109-114.

61. Dragatsis,I., Levine,M.S., and Zeitlin,S. (2000). Inactivation of Hdh in the brain and testis results in progressive neurodegeneration and sterility in mice. Nat. Genet. *26*, 300-306.

62. Duff,K., Paulsen,J.S., Beglinger,L.J., Langbehn,D.R., and Stout,J.C. (2007). Psychiatric symptoms in Huntington's disease before diagnosis: the predict-HD study. Biol. Psychiatry *62*, 1341-1346.

63. Dunah,A.W., Jeong,H., Griffin,A., Kim,Y.M., Standaert,D.G., Hersch,S.M., Mouradian,M.M., Young,A.B., Tanese,N., and Krainc,D. (2002). Sp1 and TAFII130 transcriptional activity disrupted in early Huntington's disease. Science *296*, 2238-2243.

64. Dunnett,S.B. and Rosser,A.E. (2004). Cell therapy in Huntington's disease. NeuroRx. *1*, 394-405.

65. Duyao,M.P., Auerbach,A.B., Ryan,A., Persichetti,F., Barnes,G.T., McNeil,S.M., Ge,P., Vonsattel,J.P., Gusella,J.F., Joyner,A.L., and . (1995). Inactivation of the mouse Huntington's disease gene homolog Hdh. Science *269*, 407-410.

66. Eddleston,M. and Mucke,L. (1993). Molecular profile of reactive astrocytes--implications for their role in neurologic disease. Neuroscience *54*, 15-36.

67. Faber,P.W., Voisine,C., King,D.C., Bates,E.A., and Hart,A.C. (2002). Glutamine/proline-rich PQE-1 proteins protect Caenorhabditis elegans neurons from huntingtin polyglutamine neurotoxicity. Proc. Natl. Acad. Sci. U. S. A *99*, 17131-17136.

68. Fennema-Notestine,C., Archibald,S.L., Jacobson,M.W., Corey-Bloom,J., Paulsen,J.S., Peavy,G.M., Gamst,A.C., Hamilton,J.M., Salmon,D.P., and Jernigan,T.L. (2004). In vivo evidence of cerebellar atrophy and cerebral white matter loss in Huntington disease. Neurology *63*, 989-995.

69. Ferrante,R.J. (2009). Mouse models of Huntington's disease and methodological considerations for therapeutic trials. Biochim. Biophys. Acta *1792*, 506-520.

70. Ferrante,R.J., Beal,M.F., Kowall,N.W., Richardson,E.P., Jr., and Martin,J.B. (1987a). Sparing of acetylcholinesterase-containing striatal neurons in Huntington's disease. Brain Res. *411*, 162-166.

71. Ferrante,R.J. and Kowall,N.W. (1987). Tyrosine hydroxylase-like immunoreactivity is distributed in the matrix compartment of normal human and Huntington's disease striatum. Brain Res. *416*, 141-146.

72. Ferrante,R.J., Kowall,N.W., Beal,M.F., Martin,J.B., Bird,E.D., and Richardson,E.P., Jr. (1987b). Morphologic and histochemical characteristics of a spared subset of striatal neurons in Huntington's disease. J. Neuropathol. Exp. Neurol. *46*, 12-27.

73. Ferrante,R.J., Kowall,N.W., Beal,M.F., Richardson,E.P., Jr., Bird,E.D., and Martin,J.B. (1985). Selective sparing of a class of striatal neurons in Huntington's disease. Science *230*, 561-563.

74. Fortune,M.T., Vassilopoulos,C., Coolbaugh,M.I., Siciliano,M.J., and Monckton,D.G. (2000). Dramatic, expansion-biased, age-dependent, tissue-specific somatic mosaicism in a transgenic mouse model of triplet repeat instability. Hum. Mol. Genet. *9*, 439-445.

75. Galatioto,S. (1996). [Immunohistochemical findings in Huntington's Chorea: report of 9 cases]. Pathologica *88*, 491-499.

76. Georgiou,N., Bradshaw,J.L., Chiu,E., Tudor,A., O'Gorman,L., and Phillips,J.G. (1999). Differential clinical and motor control function in a pair of monozygotic twins with Huntington's disease. Mov Disord. *14*, 320-325.

77. Gerfen,C.R. (1984). The neostriatal mosaic: compartmentalization of corticostriatal input and striatonigral output systems. Nature *311*, 461-464.

78. Gerfen,C.R., Baimbridge,K.G., and Miller,J.J. (1985). The neostriatal mosaic: compartmental distribution of calcium-binding protein and

parvalbumin in the basal ganglia of the rat and monkey. Proc. Natl. Acad. Sci. U. S. A *82*, 8780-8784.

79. Gerfen,C.R., Engber,T.M., Mahan,L.C., Susel,Z., Chase,T.N., Monsma,F.J., Jr., and Sibley,D.R. (1990). D1 and D2 dopamine receptor-regulated gene expression of striatonigral and striatopallidal neurons. Science *250*, 1429-1432.

80. Gerfen,C.R. and Surmeier,D.J. (2010). Modulation of Striatal Projection Systems by Dopamine. Annu. Rev. Neurosci.

81. Gerfen,C.R. and Young,W.S., III (1988). Distribution of striatonigral and striatopallidal peptidergic neurons in both patch and matrix compartments: an in situ hybridization histochemistry and fluorescent retrograde tracing study. Brain Res. *460*, 161-167.

82. Gertler,T.S., Chan,C.S., and Surmeier,D.J. (2008). Dichotomous anatomical properties of adult striatal medium spiny neurons. J. Neurosci. *28*, 10814-10824.

83. Ghiglieri,V., Bagetta,V., Calabresi,P., and Picconi,B. (2011). Functional interactions within striatal microcircuit in animal models of huntington's disease. Neuroscience.

84. Gil,J.M., Mohapel,P., Araujo,I.M., Popovic,N., Li,J.Y., Brundin,P., and Petersen,A. (2005). Reduced hippocampal neurogenesis in R6/2 transgenic Huntington's disease mice. Neurobiol. Dis. *20*, 744-751.

85. Gil,J.M. and Rego,A.C. (2008). Mechanisms of neurodegeneration in Huntington's disease. Eur. J. Neurosci. *27*, 2803-2820.

86. Ginovart,N., Lundin,A., Farde,L., Halldin,C., Backman,L., Swahn,C.G., Pauli,S., and Sedvall,G. (1997). PET study of the pre- and post-synaptic dopaminergic markers for the neurodegenerative process in Huntington's disease. Brain *120 (Pt 3)*, 503-514.

87. Goebel,H.H., Heipertz,R., Scholz,W., Iqbal,K., and Tellez-Nagel,I. (1978). Juvenile Huntington chorea: clinical, ultrastructural, and biochemical studies. Neurology *28*, 23-31.

88. Goldberg,Y.P., Nicholson,D.W., Rasper,D.M., Kalchman,M.A., Koide,H.B., Graham,R.K., Bromm,M., Kazemi-Esfarjani,P., Thornberry,N.A., Vaillancourt,J.P., and Hayden,M.R. (1996). Cleavage of huntingtin by apopain, a proapoptotic cysteine protease, is modulated by the polyglutamine tract. Nat. Genet. *13*, 442-449.

89. Gomez-Esteban,J.C., Lezcano,E., Zarranz,J.J., Velasco,F., Garamendi,I., Perez,T., and Tijero,B. (2007). Monozygotic twins suffering from Huntington's disease show different cognitive and behavioural symptoms. Eur. Neurol. *57*, 26-30.

90. Gomez-Tortosa,E., MacDonald,M.E., Friend,J.C., Taylor,S.A., Weiler,L.J., Cupples,L.A., Srinidhi,J., Gusella,J.F., Bird,E.D., Vonsattel,J.P., and Myers,R.H. (2001). Quantitative neuropathological changes in presymptomatic Huntington's disease. Ann. Neurol. *49*, 29-34.

91. Gonitel,R., Moffitt,H., Sathasivam,K., Woodman,B., Detloff,P.J., Faull,R.L., and Bates,G.P. (2008). DNA instability in postmitotic neurons. Proc. Natl. Acad. Sci. U. S. A *105*, 3467-3472.

92. Gorman,A.M. (2008). Neuronal cell death in neurodegenerative diseases: recurring themes around protein handling. J. Cell Mol. Med. *12*, 2263-2280.

93. Gourfinkel-An,I., Cancel,G., Duyckaerts,C., Faucheux,B., Hauw,J.J., Trottier,Y., Brice,A., Agid,Y., and Hirsch,E.C. (1998). Neuronal distribution of intranuclear inclusions in Huntington's disease with adult onset. Neuroreport *9*, 1823-1826.

94. Graveland,G.A., Williams,R.S., and DiFiglia,M. (1985). Evidence for degenerative and regenerative changes in neostriatal spiny neurons in Huntington's disease. Science *227*, 770-773.

95. Gray,M., Shirasaki,D.I., Cepeda,C., Andre,V.M., Wilburn,B., Lu,X.H., Tao,J., Yamazaki,I., Li,S.H., Sun,Y.E., Li,X.J., Levine,M.S., and Yang,X.W. (2008). Full-length human mutant huntingtin with a stable polyglutamine repeat can elicit progressive and selective neuropathogenesis in BACHD mice. J. Neurosci. *28*, 6182-6195.

96. Graybiel,A.M. (1990). Neurotransmitters and neuromodulators in the basal ganglia. Trends Neurosci. *13*, 244-254.

97. Griffin,W.S., Sheng,J.G., Royston,M.C., Gentleman,S.M., McKenzie,J.E., Graham,D.I., Roberts,G.W., and Mrak,R.E. (1998). Glial-neuronal interactions in Alzheimer's disease: the potential role of a 'cytokine cycle' in disease progression. Brain Pathol. *8*, 65-72.

98. Grote,H.E., Bull,N.D., Howard,M.L., van Dellen,A., Blakemore,C., Bartlett,P.F., and Hannan,A.J. (2005). Cognitive disorders and neurogenesis deficits in Huntington's disease mice are rescued by fluoxetine. Eur. J. Neurosci. *22*, 2081-2088.

99. Guidetti,P., Bates,G.P., Graham,R.K., Hayden,M.R., Leavitt,B.R., MacDonald,M.E., Slow,E.J., Wheeler,V.C., Woodman,B., and Schwarcz,R. (2006). Elevated brain 3-hydroxykynurenine and quinolinate levels in Huntington disease mice. Neurobiol. Dis. *23*, 190-197.

100. Gunawardena,S., Her,L.S., Brusch,R.G., Laymon,R.A., Niesman,I.R., Gordesky-Gold,B., Sintasath,L., Bonini,N.M., and Goldstein,L.S. (2003). Disruption of axonal transport by loss of huntingtin or

expression of pathogenic polyQ proteins in Drosophila. Neuron *40*, 25-40.

101. Gusella,J.F. and MacDonald,M.E. (2006). Huntington's disease: seeing the pathogenic process through a genetic lens. Trends Biochem. Sci. *31*, 533-540.

102. Gusella,J.F. and MacDonald,M.E. (2009). Huntington's disease: the case for genetic modifiers. Genome Med. *1*, 80.

103. Gusella,J.F., Wexler,N.S., Conneally,P.M., Naylor,S.L., Anderson,M.A., Tanzi,R.E., Watkins,P.C., Ottina,K., Wallace,M.R., Sakaguchi,A.Y., and . (1983). A polymorphic DNA marker genetically linked to Huntington's disease. Nature *306*, 234-238.

104. Gutekunst,C.A., Li,S.H., Yi,H., Mulroy,J.S., Kuemmerle,S., Jones,R., Rye,D., Ferrante,R.J., Hersch,S.M., and Li,X.J. (1999). Nuclear and neuropil aggregates in Huntington's disease: relationship to neuropathology. J. Neurosci. *19*, 2522-2534.

105. Halliday,G.M., McRitchie,D.A., Macdonald,V., Double,K.L., Trent,R.J., and McCusker,E. (1998). Regional specificity of brain atrophy in Huntington's disease. Exp. Neurol. *154*, 663-672.

106. Hansson,O., Guatteo,E., Mercuri,N.B., Bernardi,G., Li,X.J., Castilho,R.F., and Brundin,P. (2001). Resistance to NMDA toxicity correlates with appearance of nuclear inclusions, behavioural deficits and changes in calcium homeostasis in mice transgenic for exon 1 of the huntington gene. Eur. J. Neurosci. *14*, 1492-1504.

107. Harper,P.S. (1992). The epidemiology of Huntington's disease. Hum. Genet. *89*, 365-376.

108. Harper,P.S. (2002). *Huntington's Disease:Historical background*. Huntington's Disease, Oxford Universy Press, Third Edition 3-27.

109. Harris,E.C. and Barraclough,B.M. (1994). Suicide as an outcome for medical disorders. Medicine (Baltimore) *73*, 281-296.

110. Hartl,F.U. and Hayer-Hartl,M. (2002). Molecular chaperones in the cytosol: from nascent chain to folded protein. Science *295*, 1852-1858.

111. Hedreen,J.C. and Folstein,S.E. (1995). Early loss of neostriatal striosome neurons in Huntington's disease. J. Neuropathol. Exp. Neurol. *54*, 105-120.

112. Heneka,M.T. and O'Banion,M.K. (2007). Inflammatory processes in Alzheimer's disease. J. Neuroimmunol. *184*, 69-91.

113. Heng,M.Y., Duong,D.K., Albin,R.L., Tallaksen-Greene,S.J., Hunter,J.M., Lesort,M.J., Osmand,A., Paulson,H.L., and Detloff,P.J.

(2010). Early autophagic response in a novel knock-in model of Huntington disease. Hum. Mol. Genet. *19*, 3702-3720.

114. Heng,M.Y., Tallaksen-Greene,S.J., Detloff,P.J., and Albin,R.L. (2007). Longitudinal evaluation of the Hdh(CAG)150 knock-in murine model of Huntington's disease. J. Neurosci. *27*, 8989-8998.

115. Henley,S.M., Frost,C., MacManus,D.G., Warner,T.T., Fox,N.C., and Tabrizi,S.J. (2006). Increased rate of whole-brain atrophy over 6 months in early Huntington disease. Neurology *67*, 694-696.

116. Herishanu,Y.O., Parvari,R., Pollack,Y., Shelef,I., Marom,B., Martino,T., Cannella,M., and Squitieri,F. (2009). Huntington disease in subjects from an Israeli Karaite community carrying alleles of intermediate and expanded CAG repeats in the HTT gene: Huntington disease or phenocopy? J. Neurol. Sci. *277*, 143-146.

117. Hershko,A. and Ciechanover,A. (1998). The ubiquitin system. Annu. Rev. Biochem. *67*, 425-479.

118. Heuser,I.J., Chase,T.N., and Mouradian,M.M. (1991). The limbic-hypothalamic-pituitary-adrenal axis in Huntington's disease. Biol. Psychiatry *30*, 943-952.

119. Hickey,M.A., Kosmalska,A., Enayati,J., Cohen,R., Zeitlin,S., Levine,M.S., and Chesselet,M.F. (2008). Extensive early motor and non-motor behavioral deficits are followed by striatal neuronal loss in knock-in Huntington's disease mice. Neuroscience.

120. Ho,A.K., Sahakian,B.J., Brown,R.G., Barker,R.A., Hodges,J.R., Ane,M.N., Snowden,J., Thompson,J., Esmonde,T., Gentry,R., Moore,J.W., and Bodner,T. (2003). Profile of cognitive progression in early Huntington's disease. Neurology *61*, 1702-1706.

121. Ho,L.W., Brown,R., Maxwell,M., Wyttenbach,A., and Rubinsztein,D.C. (2001a). Wild type Huntingtin reduces the cellular toxicity of mutant Huntingtin in mammalian cell models of Huntington's disease. J. Med. Genet. *38*, 450-452.

122. Ho,L.W., Carmichael,J., Swartz,J., Wyttenbach,A., Rankin,J., and Rubinsztein,D.C. (2001b). The molecular biology of Huntington's disease. Psychol. Med. *31*, 3-14.

123. Hobbs,N.Z., Henley,S.M., Ridgway,G.R., Wild,E.J., Barker,R.A., Scahill,R.I., Barnes,J., Fox,N.C., and Tabrizi,S.J. (2010). The progression of regional atrophy in premanifest and early Huntington's disease: a longitudinal voxel-based morphometry study. J. Neurol. Neurosurg. Psychiatry *81*, 756-763.

124. Hodges,A., Hughes,G., Brooks,S., Elliston,L., Holmans,P., Dunnett,S.B., and Jones,L. (2008). Brain gene expression correlates

with changes in behavior in the R6/1 mouse model of Huntington's disease. Genes Brain Behav. *7*, 288-299.

125. Hodges,A., Strand,A.D., Aragaki,A.K., Kuhn,A., Sengstag,T., Hughes,G., Elliston,L.A., Hartog,C., Goldstein,D.R., Thu,D., Hollingsworth,Z.R., Collin,F., Synek,B., Holmans,P.A., Young,A.B., Wexler,N.S., Delorenzi,M., Kooperberg,C., Augood,S.J., Faull,R.L., Olson,J.M., Jones,L., and Luthi-Carter,R. (2006). Regional and cellular gene expression changes in human Huntington's disease brain. Hum. Mol. Genet. *15*, 965-977.

126. Hodgson,J.G., Agopyan,N., Gutekunst,C.A., Leavitt,B.R., LePiane,F., Singaraja,R., Smith,D.J., Bissada,N., McCutcheon,K., Nasir,J., Jamot,L., Li,X.J., Stevens,M.E., Rosemond,E., Roder,J.C., Phillips,A.G., Rubin,E.M., Hersch,S.M., and Hayden,M.R. (1999). A YAC mouse model for Huntington's disease with full-length mutant huntingtin, cytoplasmic toxicity, and selective striatal neurodegeneration. Neuron *23*, 181-192.

127. Hodgson,J.G., Smith,D.J., McCutcheon,K., Koide,H.B., Nishiyama,K., Dinulos,M.B., Stevens,M.E., Bissada,N., Nasir,J., Kanazawa,I., Disteche,C.M., Rubin,E.M., and Hayden,M.R. (1996). Human huntingtin derived from YAC transgenes compensates for loss of murine huntingtin by rescue of the embryonic lethal phenotype. Hum. Mol. Genet. *5*, 1875-1885.

128. Hoogeveen,A.T., Willemsen,R., Meyer,N., de Rooij,K.E., Roos,R.A., van Ommen,G.J., and Galjaard,H. (1993). Characterization and localization of the Huntington disease gene product. Hum. Mol. Genet. *2*, 2069-2073.

129. Howeler,C.J., Busch,H.F., Geraedts,J.P., Niermeijer,M.F., and Staal,A. (1989). Anticipation in myotonic dystrophy: fact or fiction? Brain *112 (Pt 3)*, 779-797.

130. Huntington,G. (2003). On chorea. George Huntington, M.D. J. Neuropsychiatry Clin. Neurosci. *15*, 109-112.

131. Huot,P., Levesque,M., and Parent,A. (2007). The fate of striatal dopaminergic neurons in Parkinson's disease and Huntington's chorea. Brain *130*, 222-232.

132. Iannicola,C., Moreno,S., Oliverio,S., Nardacci,R., Ciofi-Luzzatto,A., and Piacentini,M. (2000). Early alterations in gene expression and cell morphology in a mouse model of Huntington's disease. J. Neurochem. *75*, 830-839.

133. Ikeda,H., Yamaguchi,M., Sugai,S., Aze,Y., Narumiya,S., and Kakizuka,A. (1996). Expanded polyglutamine in the Machado-Joseph disease protein induces cell death in vitro and in vivo. Nat. Genet. *13*, 196-202.

134. Jeste,D.V., Barban,L., and Parisi,J. (1984). Reduced Purkinje cell density in Huntington's disease. Exp. Neurol. *85*, 78-86.

135. Johnson,S.A., Stout,J.C., Solomon,A.C., Langbehn,D.R., Aylward,E.H., Cruce,C.B., Ross,C.A., Nance,M., Kayson,E., Julian-Baros,E., Hayden,M.R., Kieburtz,K., Guttman,M., Oakes,D., Shoulson,I., Beglinger,L., Duff,K., Penziner,E., and Paulsen,J.S. (2007). Beyond disgust: impaired recognition of negative emotions prior to diagnosis in Huntington's disease. Brain *130*, 1732-1744.

136. Johnston,J.A., Ward,C.L., and Kopito,R.R. (1998). Aggresomes: a cellular response to misfolded proteins. J. Cell Biol. *143*, 1883-1898.

137. Kaltenbach,L.S., Romero,E., Becklin,R.R., Chettier,R., Bell,R., Phansalkar,A., Strand,A., Torcassi,C., Savage,J., Hurlburt,A., Cha,G.H., Ukani,L., Chepanoske,C.L., Zhen,Y., Sahasrabudhe,S., Olson,J., Kurschner,C., Ellerby,L.M., Peltier,J.M., Botas,J., and Hughes,R.E. (2007). Huntingtin interacting proteins are genetic modifiers of neurodegeneration. PLoS. Genet. *3*, e82.

138. Kantor,O., Temel,Y., Holzmann,C., Raber,K., Nguyen,H.P., Cao,C., Turkoglu,H.O., Rutten,B.P., Visser-Vandewalle,V., Steinbusch,H.W., Blokland,A., Korr,H., Riess,O., Von Horsten,S., and Schmitz,C. (2006). Selective striatal neuron loss and alterations in behavior correlate with impaired striatal function in Huntington's disease transgenic rats. Neurobiol. Dis. *22*, 538-547.

139. Kaplan,S., Itzkovitz,S., and Shapiro,E. (2007). A universal mechanism ties genotype to phenotype in trinucleotide diseases. PLoS. Comput. Biol. *3*, e235.

140. Kassubek,J., Juengling,F.D., Kioschies,T., Henkel,K., Karitzky,J., Kramer,B., Ecker,D., Andrich,J., Saft,C., Kraus,P., Aschoff,A.J., Ludolph,A.C., and Landwehrmeyer,G.B. (2004). Topography of cerebral atrophy in early Huntington's disease: a voxel based morphometric MRI study. J. Neurol. Neurosurg. Psychiatry *75*, 213-220.

141. Kawaguchi,Y. (1997). Neostriatal cell subtypes and their functional roles. Neurosci. Res. *27*, 1-8.

142. Kawaguchi,Y., Wilson,C.J., Augood,S.J., and Emson,P.C. (1995). Striatal interneurones: chemical, physiological and morphological characterization. Trends Neurosci. *18*, 527-535.

143. Kegel,K.B., Meloni,A.R., Yi,Y., Kim,Y.J., Doyle,E., Cuiffo,B.G., Sapp,E., Wang,Y., Qin,Z.H., Chen,J.D., Nevins,J.R., Aronin,N., and DiFiglia,M. (2002). Huntingtin is present in the nucleus, interacts with the transcriptional corepressor C-terminal binding protein, and represses transcription. J. Biol. Chem. *277*, 7466-7476.

144. Kegel,K.B., Sapp,E., Yoder,J., Cuiffo,B., Sobin,L., Kim,Y.J., Qin,Z.H., Hayden,M.R., Aronin,N., Scott,D.L., Isenberg,G., Goldmann,W.H., and DiFiglia,M. (2005). Huntingtin associates with acidic phospholipids at the plasma membrane. J. Biol. Chem. *280*, 36464-36473.

145. Kennedy,L., Evans,E., Chen,C.M., Craven,L., Detloff,P.J., Ennis,M., and Shelbourne,P.F. (2003). Dramatic tissue-specific mutation length increases are an early molecular event in Huntington disease pathogenesis. Hum. Mol. Genet. *12*, 3359-3367.

146. Kennedy,L. and Shelbourne,P.F. (2000). Dramatic mutation instability in HD mouse striatum: does polyglutamine load contribute to cell-specific vulnerability in Huntington's disease? Hum. Mol. Genet. *9*, 2539-2544.

147. Kerr,J.F., Wyllie,A.H., and Currie,A.R. (1972). Apoptosis: a basic biological phenomenon with wide-ranging implications in tissue kinetics. Br. J. Cancer *26*, 239-257.

148. Kerr,J.F.R., Gobe,G.G., Winterford,C.M., and Harmon,B.V. (1995). Anatomical Methods in Cell Death. In Methods In Cell Biology, L.M.Schwartz and B.A.Osborno, eds. (San Diego: Academic Press, Inc.), pp. 1-27.

149. Kim,I., Xu,W., and Reed,J.C. (2008). Cell death and endoplasmic reticulum stress: disease relevance and therapeutic opportunities. Nat. Rev. Drug Discov. *7*, 1013-1030.

150. Kim,J., Moody,J.P., Edgerly,C.K., Bordiuk,O.L., Cormier,K., Smith,K., Beal,M.F., and Ferrante,R.J. (2010). Mitochondrial loss, dysfunction and altered dynamics in Huntington's disease. Hum. Mol. Genet. *19*, 3919-3935.

151. Kipps,C.M., Duggins,A.J., Mahant,N., Gomes,L., Ashburner,J., and McCusker,E.A. (2005). Progression of structural neuropathology in preclinical Huntington's disease: a tensor based morphometry study. J. Neurol. Neurosurg. Psychiatry *76*, 650-655.

152. Kirkwood,S.C., Siemers,E., Hodes,M.E., Conneally,P.M., Christian,J.C., and Foroud,T. (2000). Subtle changes among presymptomatic carriers of the Huntington's disease gene. J. Neurol. Neurosurg. Psychiatry *69*, 773-779.

153. Kirkwood,S.C., Su,J.L., Conneally,P., and Foroud,T. (2001). Progression of symptoms in the early and middle stages of Huntington disease. Arch. Neurol. *58*, 273-278.

154. Klapstein,G.J., Fisher,R.S., Zanjani,H., Cepeda,C., Jokel,E.S., Chesselet,M.F., and Levine,M.S. (2001). Electrophysiological and morphological changes in striatal spiny neurons in R6/2 Huntington's disease transgenic mice. J. Neurophysiol. *86*, 2667-2677.

155. Koh,J.Y., Gwag,B.J., Lobner,D., and Choi,D.W. (1995). Potentiated necrosis of cultured cortical neurons by neurotrophins. Science *268*, 573-575.

156. Kopito,R.R. (2000). Aggresomes, inclusion bodies and protein aggregation. Trends Cell Biol. *10*, 524-530.

157. Kosinski,C.M., Cha,J.H., Young,A.B., Persichetti,F., MacDonald,M., Gusella,J.F., Penney,J.B., Jr., and Standaert,D.G. (1997). Huntingtin immunoreactivity in the rat neostriatum: differential accumulation in projection and interneurons. Exp. Neurol. *144*, 239-247.

158. Kremer,B. and . (2002). Clinical neurology of Huntington's Disease. In Huntington's Disease, G.P.Bates, P.S.Harper, and L.Jones, eds. Oxford university Press), pp. 28-61.

159. Kremer,H.P., Roos,R.A., Dingjan,G.M., Bots,G.T., Bruyn,G.W., and Hofman,M.A. (1991). The hypothalamic lateral tuberal nucleus and the characteristics of neuronal loss in Huntington's disease. Neurosci. Lett. *132*, 101-104.

160. Kuemmerle,S., Gutekunst,C.A., Klein,A.M., Li,X.J., Li,S.H., Beal,M.F., Hersch,S.M., and Ferrante,R.J. (1999). Huntington aggregates may not predict neuronal death in Huntington's disease. Ann. Neurol. *46*, 842-849.

161. Kuhn,A., Goldstein,D.R., Hodges,A., Strand,A.D., Sengstag,T., Kooperberg,C., Becanovic,K., Pouladi,M.A., Sathasivam,K., Cha,J.H., Hannan,A.J., Hayden,M.R., Leavitt,B.R., Dunnett,S.B., Ferrante,R.J., Albin,R., Shelbourne,P., Delorenzi,M., Augood,S.J., Faull,R.L., Olson,J.M., Bates,G.P., Jones,L., and Luthi-Carter,R. (2007). Mutant huntingtin's effects on striatal gene expression in mice recapitulate changes observed in human Huntington's disease brain and do not differ with mutant huntingtin length or wild-type huntingtin dosage. Hum. Mol. Genet. *16*, 1845-1861.

162. Landles,C., Sathasivam,K., Weiss,A., Woodman,B., Moffitt,H., Finkbeiner,S., Sun,B., Gafni,J., Ellerby,L.M., Trottier,Y., Richards,W.G., Osmand,A., Paganetti,P., and Bates,G.P. (2010). Proteolysis of mutant huntingtin produces an exon 1 fragment that accumulates as an aggregated protein in neuronal nuclei in Huntington disease. J. Biol. Chem. *285*, 8808-8823.

163. Lanska,D.J., Lanska,M.J., Lavine,L., and Schoenberg,B.S. (1988). Conditions associated with Huntington's disease at death. A case-control study. Arch. Neurol. *45*, 878-880.

164. Lawrence,A.D., Hodges,J.R., Rosser,A.E., Kershaw,A., ffrench-Constant,C., Rubinsztein,D.C., Robbins,T.W., and Sahakian,B.J. (1998). Evidence for specific cognitive deficits in preclinical Huntington's disease. Brain *121 (Pt 7)*, 1329-1341.

165. Lawrence,A.D., Sahakian,B.J., Hodges,J.R., Rosser,A.E., Lange,K.W., and Robbins,T.W. (1996). Executive and mnemonic functions in early Huntington's disease. Brain *119 (Pt 5)*, 1633-1645.

166. Lazic,S.E., Grote,H.E., Blakemore,C., Hannan,A.J., van Dellen,A., Phillips,W., and Barker,R.A. (2006). Neurogenesis in the R6/1 transgenic mouse model of Huntington's disease: effects of environmental enrichment. Eur. J. Neurosci. *23*, 1829-1838.

167. Legleiter,J., Lotz,G.P., Miller,J., Ko,J., Ng,C., Williams,G.L., Finkbeiner,S., Patterson,P.H., and Muchowski,P.J. (2009). Monoclonal antibodies recognize distinct conformational epitopes formed by polyglutamine in a mutant huntingtin fragment. J. Biol. Chem. *284*, 21647-21658.

168. Lemiere,J., Decruyenaere,M., Evers-Kiebooms,G., Vandenbussche,E., and Dom,R. (2004). Cognitive changes in patients with Huntington's disease (HD) and asymptomatic carriers of the HD mutation--a longitudinal follow-up study. J. Neurol. *251*, 935-942.

169. Levine,M.S., Klapstein,G.J., Koppel,A., Gruen,E., Cepeda,C., Vargas,M.E., Jokel,E.S., Carpenter,E.M., Zanjani,H., Hurst,R.S., Efstratiadis,A., Zeitlin,S., and Chesselet,M.F. (1999). Enhanced sensitivity to N-methyl-D-aspartate receptor activation in transgenic and knockin mouse models of Huntington's disease. J. Neurosci. Res. *58*, 515-532.

170. Li,H., Li,S.H., Cheng,A.L., Mangiarini,L., Bates,G.P., and Li,X.J. (1999). Ultrastructural localization and progressive formation of neuropil aggregates in Huntington's disease transgenic mice. Hum. Mol. Genet. *8*, 1227-1236.

171. Li,J.Y., Plomann,M., and Brundin,P. (2003). Huntington's disease: a synaptopathy? Trends Mol. Med. *9*, 414-420.

172. Li,S.H., Gutekunst,C.A., Hersch,S.M., and Li,X.J. (1998). Interaction of huntingtin-associated protein with dynactin P150Glued. J. Neurosci. *18*, 1261-1269.

173. Li,X.J., Li,S.H., Sharp,A.H., Nucifora,F.C., Jr., Schilling,G., Lanahan,A., Worley,P., Snyder,S.H., and Ross,C.A. (1995). A huntingtin-associated protein enriched in brain with implications for pathology. Nature *378*, 398-402.

174. Lin,C.H., Tallaksen-Greene,S., Chien,W.M., Cearley,J.A., Jackson,W.S., Crouse,A.B., Ren,S., Li,X.J., Albin,R.L., and Detloff,P.J. (2001). Neurological abnormalities in a knock-in mouse model of Huntington's disease. Hum. Mol. Genet. *10*, 137-144.

175. Lin,M.T. and Beal,M.F. (2006). Mitochondrial dysfunction and oxidative stress in neurodegenerative diseases. Nature *443*, 787-795.

176. Lione,L.A., Carter,R.J., Hunt,M.J., Bates,G.P., Morton,A.J., and Dunnett,S.B. (1999). Selective discrimination learning impairments in mice expressing the human Huntington's disease mutation. J. Neurosci. *19*, 10428-10437.

177. Lloret,A., Dragileva,E., Teed,A., Espinola,J., Fossale,E., Gillis,T., Lopez,E., Myers,R.H., MacDonald,M.E., and Wheeler,V.C. (2006). Genetic background modifies nuclear mutant huntingtin accumulation and HD CAG repeat instability in Huntington's disease knock-in mice. Hum. Mol. Genet. *15*, 2015-2024.

178. Lunkes,A. and Mandel,J.L. (1998). A cellular model that recapitulates major pathogenic steps of Huntington's disease. Hum. Mol. Genet. *7*, 1355-1361.

179. Maat-Schieman,M., Roos,R., Losekoot,M., Dorsman,J., Welling-Graafland,C., Hegeman-Kleinn,I., Broeyer,F., Breuning,M., and van Duinen,S. (2007). Neuronal intranuclear and neuropil inclusions for pathological assessment of Huntington's disease. Brain Pathol. *17*, 31-37.

180. Maat-Schieman,M.L., Dorsman,J.C., Smoor,M.A., Siesling,S., Van Duinen,S.G., Verschuuren,J.J., den Dunnen,J.T., van Ommen,G.J., and Roos,R.A. (1999). Distribution of inclusions in neuronal nuclei and dystrophic neurites in Huntington disease brain. J. Neuropathol. Exp. Neurol. *58*, 129-137.

181. Mangiarini,L., Sathasivam,K., Mahal,A., Mott,R., Seller,M., and Bates,G.P. (1997). Instability of highly expanded CAG repeats in mice transgenic for the Huntington's disease mutation. Nat. Genet. *15*, 197-200.

182. Mangiarini,L., Sathasivam,K., Seller,M., Cozens,B., Harper,A., Hetherington,C., Lawton,M., Trottier,Y., Lehrach,H., Davies,S.W., and Bates,G.P. (1996). Exon 1 of the HD gene with an expanded CAG repeat is sufficient to cause a progressive neurological phenotype in transgenic mice. Cell *87*, 493-506.

183. Markianos,M., Panas,M., Kalfakis,N., and Vassilopoulos,D. (2005). Plasma testosterone in male patients with Huntington's disease: relations to severity of illness and dementia. Ann. Neurol. *57*, 520-525.

184. Martin-Aparicio,E., Yamamoto,A., Hernandez,F., Hen,R., Avila,J., and Lucas,J.J. (2001). Proteasomal-dependent aggregate reversal and absence of cell death in a conditional mouse model of Huntington's disease. J. Neurosci. *21*, 8772-8781.

185. Martindale,D., Hackam,A., Wieczorek,A., Ellerby,L., Wellington,C., McCutcheon,K., Singaraja,R., Kazemi-Esfarjani,P., Devon,R., Kim,S.U., Bredesen,D.E., Tufaro,F., and Hayden,M.R. (1998). Length

of huntingtin and its polyglutamine tract influences localization and frequency of intracellular aggregates. Nat. Genet. *18*, 150-154.

186. Martinez-Vicente,M., Talloczy,Z., Wong,E., Tang,G., Koga,H., Kaushik,S., de Vries,R., Arias,E., Harris,S., Sulzer,D., and Cuervo,A.M. (2010). Cargo recognition failure is responsible for inefficient autophagy in Huntington's disease. Nat. Neurosci. *13*, 567-576.

187. Mason,S.T., Sanberg,P.R., and Fibiger,H.C. (1978). Kainic acid lesions of the striatum dissociate amphetamine and apomorphine stereotypy: similarities to Huntingdon's chorea. Science *201*, 352-355.

188. Mathai,A. and Smith,Y. (2011). The corticostriatal and corticosubthalamic pathways: two entries, one target. So what? Front Syst. Neurosci. *5*, 64.

189. Matsuyama,N., Hadano,S., Onoe,K., Osuga,H., Showguchi-Miyata,J., Gondo,Y., and Ikeda,J.E. (2000). Identification and characterization of the miniature pig Huntington's disease gene homolog: evidence for conservation and polymorphism in the CAG triplet repeat. Genomics *69*, 72-85.

190. McBride,J.L., Ramaswamy,S., Gasmi,M., Bartus,R.T., Herzog,C.D., Brandon,E.P., Zhou,L., Pitzer,M.R., Berry-Kravis,E.M., and Kordower,J.H. (2006). Viral delivery of glial cell line-derived neurotrophic factor improves behavior and protects striatal neurons in a mouse model of Huntington's disease. Proc. Natl. Acad. Sci. U. S. A *103*, 9345-9350.

191. Menalled,L.B., Sison,J.D., Dragatsis,I., Zeitlin,S., and Chesselet,M.F. (2003). Time course of early motor and neuropathological anomalies in a knock-in mouse model of Huntington's disease with 140 CAG repeats. J. Comp Neurol. *465*, 11-26.

192. Menalled,L.B., Sison,J.D., Wu,Y., Olivieri,M., Li,X.J., Li,H., Zeitlin,S., and Chesselet,M.F. (2002). Early motor dysfunction and striosomal distribution of huntingtin microaggregates in Huntington's disease knock-in mice. J. Neurosci. *22*, 8266-8276.

193. Metzler,M., Legendre-Guillemin,V., Gan,L., Chopra,V., Kwok,A., McPherson,P.S., and Hayden,M.R. (2001). HIP1 functions in clathrin-mediated endocytosis through binding to clathrin and adaptor protein 2. J. Biol. Chem. *276*, 39271-39276.

194. Milnerwood,A.J., Cummings,D.M., Dallerac,G.M., Brown,J.Y., Vatsavayai,S.C., Hirst,M.C., Rezaie,P., and Murphy,K.P. (2006). Early development of aberrant synaptic plasticity in a mouse model of Huntington's disease. Hum. Mol. Genet. *15*, 1690-1703.

195. Mink,J.W. (2003). The Basal Ganglia and involuntary movements: impaired inhibition of competing motor patterns. Arch. Neurol. *60*, 1365-1368.

196. Mitchell,I.J., Cooper,A.J., and Griffiths,M.R. (1999). The selective vulnerability of striatopallidal neurons. Prog. Neurobiol. *59*, 691-719.

197. Moffitt,H., McPhail,G.D., Woodman,B., Hobbs,C., and Bates,G.P. (2009). Formation of polyglutamine inclusions in a wide range of non-CNS tissues in the HdhQ150 knock-in mouse model of Huntington's disease. PLoS. One. *4*, e8025.

198. Montoya,A., Price,B.H., Menear,M., and Lepage,M. (2006). Brain imaging and cognitive dysfunctions in Huntington's disease. J. Psychiatry Neurosci. *31*, 21-29.

199. Morton,A.J., Glynn,D., Leavens,W., Zheng,Z., Faull,R.L., Skepper,J.N., and Wight,J.M. (2009). Paradoxical delay in the onset of disease caused by super-long CAG repeat expansions in R6/2 mice. Neurobiol. Dis. *33*, 331-341.

200. Morton,A.J., Lagan,M.A., Skepper,J.N., and Dunnett,S.B. (2000). Progressive formation of inclusions in the striatum and hippocampus of mice transgenic for the human Huntington's disease mutation. J. Neurocytol. *29*, 679-702.

201. Muchowski,P.J. (2002). Protein misfolding, amyloid formation, and neurodegeneration: a critical role for molecular chaperones? Neuron *35*, 9-12.

202. Murphy,K.P., Carter,R.J., Lione,L.A., Mangiarini,L., Mahal,A., Bates,G.P., Dunnett,S.B., and Morton,A.J. (2000). Abnormal synaptic plasticity and impaired spatial cognition in mice transgenic for exon 1 of the human Huntington's disease mutation. J. Neurosci. *20*, 5115-5123.

203. Myers,R.H., Vonsattel,J.P., Stevens,T.J., Cupples,L.A., Richardson,E.P., Martin,J.B., and Bird,E.D. (1988). Clinical and neuropathologic assessment of severity in Huntington's disease. Neurology *38*, 341-347.

204. Nasir,J., Floresco,S.B., O'Kusky,J.R., Diewert,V.M., Richman,J.M., Zeisler,J., Borowski,A., Marth,J.D., Phillips,A.G., and Hayden,M.R. (1995). Targeted disruption of the Huntington's disease gene results in embryonic lethality and behavioral and morphological changes in heterozygotes. Cell *81*, 811-823.

205. Nauta,H.J. (1979). A proposed conceptual reorganization of the basal ganglia and telencephalon. Neuroscience *4*, 1875-1881.

206. Naver,B., Stub,C., Moller,M., Fenger,K., Hansen,A.K., Hasholt,L., and Sorensen,S.A. (2003). Molecular and behavioral analysis of the R6/1

Huntington's disease transgenic mouse. Neuroscience *122*, 1049-1057.

207. Nithianantharajah,J., Barkus,C., Murphy,M., and Hannan,A.J. (2008). Gene-environment interactions modulating cognitive function and molecular correlates of synaptic plasticity in Huntington's disease transgenic mice. Neurobiol. Dis. *29*, 490-504.

208. O'Kusky,J.R., Nasir,J., Cicchetti,F., Parent,A., and Hayden,M.R. (1999). Neuronal degeneration in the basal ganglia and loss of pallido-subthalamic synapses in mice with targeted disruption of the Huntington's disease gene. Brain Res. *818*, 468-479.

209. Ordway,J.M. and Detloff,P.J. (1996). In vitro synthesis and cloning of long CAG repeats. Biotechniques *21*, 609-10, 612.

210. Orr,A.L., Li,S., Wang,C.E., Li,H., Wang,J., Rong,J., Xu,X., Mastroberardino,P.G., Greenamyre,J.T., and Li,X.J. (2008). N-terminal mutant huntingtin associates with mitochondria and impairs mitochondrial trafficking. J. Neurosci. *28*, 2783-2792.

211. Oyanagi,K., Takeda,S., Takahashi,H., Ohama,E., and Ikuta,F. (1989). A quantitative investigation of the substantia nigra in Huntington's disease. Ann. Neurol. *26*, 13-19.

212. Pandey,U.B., Nie,Z., Batlevi,Y., McCray,B.A., Ritson,G.P., Nedelsky,N.B., Schwartz,S.L., DiProspero,N.A., Knight,M.A., Schuldiner,O., Padmanabhan,R., Hild,M., Berry,D.L., Garza,D., Hubbert,C.C., Yao,T.P., Baehrecke,E.H., and Taylor,J.P. (2007). HDAC6 rescues neurodegeneration and provides an essential link between autophagy and the UPS. Nature *447*, 859-863.

213. Panov,A.V., Gutekunst,C.A., Leavitt,B.R., Hayden,M.R., Burke,J.R., Strittmatter,W.J., and Greenamyre,J.T. (2002). Early mitochondrial calcium defects in Huntington's disease are a direct effect of polyglutamines. Nat. Neurosci. *5*, 731-736.

214. Parent, A. Comparative Neurobiology of the Basal Ganglia. 1986. Wiley.
Ref Type: Generic

215. Parent,A. and Hazrati,L.N. (1995). Functional anatomy of the basal ganglia. I. The cortico-basal ganglia-thalamo-cortical loop. Brain Res. Brain Res. Rev. *20*, 91-127.

216. Paulsen,J.S., Langbehn,D.R., Stout,J.C., Aylward,E., Ross,C.A., Nance,M., Guttman,M., Johnson,S., MacDonald,M., Beglinger,L.J., Duff,K., Kayson,E., Biglan,K., Shoulson,I., Oakes,D., and Hayden,M. (2008). Detection of Huntington's disease decades before diagnosis: the Predict-HD study. J. Neurol. Neurosurg. Psychiatry *79*, 874-880.

217. Penney,J.B., Jr., Young,A.B., Shoulson,I., Starosta-Rubenstein,S., Snodgrass,S.R., Sanchez-Ramos,J., Ramos-Arroyo,M., Gomez,F., Penchaszadeh,G., Alvir,J., and . (1990). Huntington's disease in Venezuela: 7 years of follow-up on symptomatic and asymptomatic individuals. Mov Disord. *5*, 93-99.

218. Perutz,M.F., Johnson,T., Suzuki,M., and Finch,J.T. (1994). Glutamine repeats as polar zippers: their possible role in inherited neurodegenerative diseases. Proc. Natl. Acad. Sci. U. S. A *91*, 5355-5358.

219. Petersen,A., Mani,K., and Brundin,P. (1999). Recent advances on the pathogenesis of Huntington's disease. Experimental Neurology *157*, 1-18.

220. Pineda,J.R., Canals,J.M., Bosch,M., Adell,A., Mengod,G., Artigas,F., Ernfors,P., and Alberch,J. (2005). Brain-derived neurotrophic factor modulates dopaminergic deficits in a transgenic mouse model of Huntington's disease. J. Neurochem. *93*, 1057-1068.

221. Portera-Cailliau,C., Hedreen,J.C., Price,D.L., and Koliatsos,V.E. (1995). Evidence for apoptotic cell death in Huntington disease and excitotoxic animal models. J. Neurosci. *15*, 3775-3787.

222. Que,L., Jr., Holm,R.H., and Mortenson,L.E. (1975). Letter: Extrusion of Fe2S2 and Fe4S4 cores from the active sites of ferredoxin proteins. J. Am. Chem. Soc. *97*, 463-464.

223. Ransom,B., Behar,T., and Nedergaard,M. (2003). New roles for astrocytes (stars at last). Trends Neurosci. *26*, 520-522.

224. Ravikumar,B., Vacher,C., Berger,Z., Davies,J.E., Luo,S., Oroz,L.G., Scaravilli,F., Easton,D.F., Duden,R., O'Kane,C.J., and Rubinsztein,D.C. (2004). Inhibition of mTOR induces autophagy and reduces toxicity of polyglutamine expansions in fly and mouse models of Huntington disease. Nat. Genet. *36*, 585-595.

225. Reddy,P.H., Williams,M., Charles,V., Garrett,L., Pike-Buchanan,L., Whetsell,W.O., Jr., Miller,G., and Tagle,D.A. (1998). Behavioural abnormalities and selective neuronal loss in HD transgenic mice expressing mutated full-length HD cDNA. Nat. Genet. *20*, 198-202.

226. Reiner,A., Albin,R.L., Anderson,K.D., D'Amato,C.J., Penney,J.B., and Young,A.B. (1988). Differential loss of striatal projection neurons in Huntington disease. Proc. Natl. Acad. Sci. U. S. A *85*, 5733-5737.

227. Reiner,A., Del Mar,N., Deng,Y.P., Meade,C.A., Sun,Z., and Goldowitz,D. (2007). R6/2 neurons with intranuclear inclusions survive for prolonged periods in the brains of chimeric mice. J. Comp Neurol. *505*, 603-629.

228. Rigamonti,D., Bauer,J.H., De Fraja,C., Conti,L., Sipione,S., Sciorati,C., Clementi,E., Hackam,A., Hayden,M.R., Li,Y., Cooper,J.K., Ross,C.A., Govoni,S., Vincenz,C., and Cattaneo,E. (2000). Wild-type huntingtin protects from apoptosis upstream of caspase-3. J. Neurosci. *20*, 3705-3713.

229. Rigamonti,D., Sipione,S., Goffredo,D., Zuccato,C., Fossale,E., and Cattaneo,E. (2001). Huntingtin's neuroprotective activity occurs via inhibition of procaspase-9 processing. J. Biol. Chem. *276*, 14545-14548.

230. Robins Wahlin,T.B., Lundin,A., and Dear,K. (2007). Early cognitive deficits in Swedish gene carriers of Huntington's disease. Neuropsychology. *21*, 31-44.

231. Robitaille,Y., Lopes-Cendes,I., Becher,M., Rouleau,G., and Clark,A.W. (1997). The neuropathology of CAG repeat diseases: review and update of genetic and molecular features. Brain Pathol. *7*, 901-926.

232. Rodda,R.A. (1981). Cerebellar atrophy in Huntington's disease. J. Neurol. Sci. *50*, 147-157.

233. Roizin,L., Stellar S., and Liu J.C. (1979). Neuronal nuclear-cytoplasmic changes in Huntington's Chorea: Electron microscope investigations. In Advances in Neurology, Vol. 23, N.S.W.a.A.B.T.N Chase, ed. (New York: Raven Press), pp. 95-122.

234. Roizin,L., Stellar,S., Willson,N., Whittier,J., and Liu,J.C. (1974). Electron microscope and enzyme studies in cerebral biopsies of Huntington's chorea. Trans. Am. Neurol. Assoc. *99*, 240-243.

235. Roos,R.A. (2010). Huntington's disease: a clinical review. Orphanet. J. Rare. Dis. *5*, 40.

236. Roos,R.A. and Bots,G.T. (1983). Nuclear membrane indentations in Huntington's chorea. J. Neurol. Sci. *61*, 37-47.

237. Roos,R.A., Hermans,J., Vegter-van der Vlis,M., van Ommen,G.J., and Bruyn,G.W. (1993). Duration of illness in Huntington's disease is not related to age at onset. J. Neurol. Neurosurg. Psychiatry *56*, 98-100.

238. Roos,R.A., Pruyt,J.F., de Vries,J., and Bots,G.T. (1985). Neuronal distribution in the putamen in Huntington's disease. J. Neurol. Neurosurg. Psychiatry *48*, 422-425.

239. Rosas,H.D., Koroshetz,W.J., Chen,Y.I., Skeuse,C., Vangel,M., Cudkowicz,M.E., Caplan,K., Marek,K., Seidman,L.J., Makris,N., Jenkins,B.G., and Goldstein,J.M. (2003). Evidence for more widespread cerebral pathology in early HD: an MRI-based morphometric analysis. Neurology *60*, 1615-1620.

240. Rosas,H.D., Liu,A.K., Hersch,S., Glessner,M., Ferrante,R.J., Salat,D.H., van der,K.A., Jenkins,B.G., Dale,A.M., and Fischl,B. (2002). Regional and progressive thinning of the cortical ribbon in Huntington's disease. Neurology *58*, 695-701.

241. Rosas,H.D., Salat,D.H., Lee,S.Y., Zaleta,A.K., Pappu,V., Fischl,B., Greve,D., Hevelone,N., and Hersch,S.M. (2008). Cerebral cortex and the clinical expression of Huntington's disease: complexity and heterogeneity. Brain *131*, 1057-1068.

242. Ross,C.A. (1997). Intranuclear neuronal inclusions: a common pathogenic mechanism for glutamine-repeat neurodegenerative diseases? Neuron *19*, 1147-1150.

243. Ross,C.A., Becher,M.W., Colomer,V., Engelender,S., Wood,J.D., and Sharp,A.H. (1997). Huntington's disease and dentatorubral-pallidoluysian atrophy: proteins, pathogenesis and pathology. Brain Pathol. *7*, 1003-1016.

244. Rubinsztein,D.C. (2006). The roles of intracellular protein-degradation pathways in neurodegeneration. Nature *443*, 780-786.

245. Rubinsztein,D.C., Leggo,J., Coles,R., Almqvist,E., Biancalana,V., Cassiman,J.J., Chotai,K., Connarty,M., Crauford,D., Curtis,A., Curtis,D., Davidson,M.J., Differ,A.M., Dode,C., Dodge,A., Frontali,M., Ranen,N.G., Stine,O.C., Sherr,M., Abbott,M.H., Franz,M.L., Graham,C.A., Harper,P.S., Hedreen,J.C., Hayden,M.R., and . (1996). Phenotypic characterization of individuals with 30-40 CAG repeats in the Huntington disease (HD) gene reveals HD cases with 36 repeats and apparently normal elderly individuals with 36-39 repeats. Am. J. Hum. Genet. *59*, 16-22.

246. Rubinsztein,D.C., Wyttenbach,A., and Rankin,J. (1999). Intracellular inclusions, pathological markers in diseases caused by expanded polyglutamine tracts? J. Med. Genet. *36*, 265-270.

247. Ruocco,H.H., Lopes-Cendes,I., Li,L.M., Santos-Silva,M., and Cendes,F. (2006). Striatal and extrastriatal atrophy in Huntington's disease and its relationship with length of the CAG repeat. Braz. J. Med. Biol. Res. *39*, 1129-1136.

248. Sanchez,I., Mahlke,C., and Yuan,J. (2003). Pivotal role of oligomerization in expanded polyglutamine neurodegenerative disorders. Nature *421*, 373-379.

249. Sapp,E., Schwarz,C., Chase,K., Bhide,P.G., Young,A.B., Penney,J., Vonsattel,J.P., Aronin,N., and DiFiglia,M. (1997). Huntingtin localization in brains of normal and Huntington's disease patients. Ann. Neurol. *42*, 604-612.

250. Sathasivam,K., Lane,A., Legleiter,J., Warley,A., Woodman,B., Finkbeiner,S., Paganetti,P., Muchowski,P.J., Wilson,S., and Bates,G.P. (2010). Identical oligomeric and fibrillar structures captured from the brains of R6/2 and knock-in mouse models of Huntington's disease. Hum. Mol. Genet. *19*, 65-78.

251. Saudou,F., Finkbeiner,S., Devys,D., and Greenberg,M.E. (1998). Huntingtin acts in the nucleus to induce apoptosis but death does not correlate with the formation of intranuclear inclusions. Cell *95*, 55-66.

252. Saunders,H.M. and Bottomley,S.P. (2009). Multi-domain misfolding: understanding the aggregation pathway of polyglutamine proteins. Protein Eng Des Sel *22*, 447-451.

253. Schaffar,G., Breuer,P., Boteva,R., Behrends,C., Tzvetkov,N., Strippel,N., Sakahira,H., Siegers,K., Hayer-Hartl,M., and Hartl,F.U. (2004). Cellular toxicity of polyglutamine expansion proteins: mechanism of transcription factor deactivation. Mol. Cell *15*, 95-105.

254. Schiffer,N.W., Broadley,S.A., Hirschberger,T., Tavan,P., Kretzschmar,H.A., Giese,A., Haass,C., Hartl,F.U., and Schmid,B. (2007). Identification of anti-prion compounds as efficient inhibitors of polyglutamine protein aggregation in a zebrafish model. J. Biol. Chem. *282*, 9195-9203.

255. Schilling,G., Becher,M.W., Sharp,A.H., Jinnah,H.A., Duan,K., Kotzuk,J.A., Slunt,H.H., Ratovitski,T., Cooper,J.K., Jenkins,N.A., Copeland,N.G., Price,D.L., Ross,C.A., and Borchelt,D.R. (1999). Intranuclear inclusions and neuritic aggregates in transgenic mice expressing a mutant N-terminal fragment of huntingtin. Hum. Mol. Genet. *8*, 397-407.

256. Schwarcz,R., Whetsell,W.O., Jr., and Mangano,R.M. (1983). Quinolinic acid: an endogenous metabolite that produces axon-sparing lesions in rat brain. Science *219*, 316-318.

257. Seong,I.S., Ivanova,E., Lee,J.M., Choo,Y.S., Fossale,E., Anderson,M., Gusella,J.F., Laramie,J.M., Myers,R.H., Lesort,M., and MacDonald,M.E. (2005). HD CAG repeat implicates a dominant property of huntingtin in mitochondrial energy metabolism. Hum. Mol. Genet. *14*, 2871-2880.

258. Seredenina,T. and Luthi-Carter,R. (2011). What have we learned from gene expression profiles in Huntington's disease? Neurobiol. Dis.

259. Seto-Ohshima,A., Emson,P.C., Lawson,E., Mountjoy,C.Q., and Carrasco,L.H. (1988). Loss of matrix calcium-binding protein-containing neurons in Huntington's disease. Lancet *1*, 1252-1255.

260. Sharp,A.H., Loev,S.J., Schilling,G., Li,S.H., Li,X.J., Bao,J., Wagster,M.V., Kotzuk,J.A., Steiner,J.P., Lo,A., and . (1995).

Widespread expression of Huntington's disease gene (IT15) protein product. Neuron *14*, 1065-1074.

261. Shelbourne,P.F., Killeen,N., Hevner,R.F., Johnston,H.M., Tecott,L., Lewandoski,M., Ennis,M., Ramirez,L., Li,Z., Iannicola,C., Littman,D.R., and Myers,R.M. (1999). A Huntington's disease CAG expansion at the murine Hdh locus is unstable and associated with behavioural abnormalities in mice. Hum. Mol. Genet. *8*, 763-774.

262. Shin,J.Y., Fang,Z.H., Yu,Z.X., Wang,C.E., Li,S.H., and Li,X.J. (2005). Expression of mutant huntingtin in glial cells contributes to neuronal excitotoxicity. J. Cell Biol. *171*, 1001-1012.

263. Shirendeb,U., Reddy,A.P., Manczak,M., Calkins,M.J., Mao,P., Tagle,D.A., and Hemachandra,R.P. (2011). Abnormal mitochondrial dynamics, mitochondrial loss and mutant huntingtin oligomers in Huntington's disease: implications for selective neuronal damage. Hum. Mol. Genet. *20*, 1438-1455.

264. Simmons,D.A., Casale,M., Alcon,B., Pham,N., Narayan,N., and Lynch,G. (2007). Ferritin accumulation in dystrophic microglia is an early event in the development of Huntington's disease. Glia *55*, 1074-1084.

265. Simpson,J.M., Gil-Mohapel,J., Pouladi,M.A., Ghilan,M., Xie,Y., Hayden,M.R., and Christie,B.R. (2010). Altered adult hippocampal neurogenesis in the YAC128 transgenic mouse model of Huntington disease. Neurobiol. Dis.

266. Singaraja,R.R., Hadano,S., Metzler,M., Givan,S., Wellington,C.L., Warby,S., Yanai,A., Gutekunst,C.A., Leavitt,B.R., Yi,H., Fichter,K., Gan,L., McCutcheon,K., Chopra,V., Michel,J., Hersch,S.M., Ikeda,J.E., and Hayden,M.R. (2002). HIP14, a novel ankyrin domain-containing protein, links huntingtin to intracellular trafficking and endocytosis. Hum. Mol. Genet. *11*, 2815-2828.

267. Singhrao,S.K., Thomas,P., Wood,J.D., MacMillan,J.C., Neal,J.W., Harper,P.S., and Jones,A.L. (1998). Huntingtin protein colocalizes with lesions of neurodegenerative diseases: An investigation in Huntington's, Alzheimer's, and Pick's diseases. Exp. Neurol. *150*, 213-222.

268. Sisodia,S.S. (1998). Nuclear inclusions in glutamine repeat disorders: are they pernicious, coincidental, or beneficial? Cell *95*, 1-4.

269. Slow,E.J., Graham,R.K., and Hayden,M.R. (2006). To be or not to be toxic: aggregations in Huntington and Alzheimer disease. Trends Genet. *22*, 408-411.

270. Slow,E.J., Graham,R.K., Osmand,A.P., Devon,R.S., Lu,G., Deng,Y., Pearson,J., Vaid,K., Bissada,N., Wetzel,R., Leavitt,B.R., and

Hayden,M.R. (2005). Absence of behavioral abnormalities and neurodegeneration in vivo despite widespread neuronal huntingtin inclusions. Proc. Natl. Acad. Sci. U. S. A *102*, 11402-11407.

271. Slow,E.J., van Raamsdonk,J., Rogers,D., Coleman,S.H., Graham,R.K., Deng,Y., Oh,R., Bissada,N., Hossain,S.M., Yang,Y.Z., Li,X.J., Simpson,E.M., Gutekunst,C.A., Leavitt,B.R., and Hayden,M.R. (2003). Selective striatal neuronal loss in a YAC128 mouse model of Huntington disease. Hum. Mol. Genet. *12*, 1555-1567.

272. Smith,R., Chung,H., Rundquist,S., Maat-Schieman,M.L., Colgan,L., Englund,E., Liu,Y.J., Roos,R.A., Faull,R.L., Brundin,P., and Li,J.Y. (2006). Cholinergic neuronal defect without cell loss in Huntington's disease. Hum. Mol. Genet. *15*, 3119-3131.

273. Solomon,A.C., Stout,J.C., Johnson,S.A., Langbehn,D.R., Aylward,E.H., Brandt,J., Ross,C.A., Beglinger,L., Hayden,M.R., Kieburtz,K., Kayson,E., Julian-Baros,E., Duff,K., Guttman,M., Nance,M., Oakes,D., Shoulson,I., Penziner,E., and Paulsen,J.S. (2007). Verbal episodic memory declines prior to diagnosis in Huntington's disease. Neuropsychologia *45*, 1767-1776.

274. Sotrel,A., Paskevich,P.A., Kiely,D.K., Bird,E.D., Williams,R.S., and Myers,R.H. (1991). Morphometric analysis of the prefrontal cortex in Huntington's disease. Neurology *41*, 1117-1123.

275. Spargo,E., Everall,I.P., and Lantos,P.L. (1993). Neuronal loss in the hippocampus in Huntington's disease: a comparison with HIV infection. J. Neurol. Neurosurg. Psychiatry *56*, 487-491.

276. Speed,M.A., Wang,D.I., and King,J. (1996). Specific aggregation of partially folded polypeptide chains: the molecular basis of inclusion body composition. Nat. Biotechnol. *14*, 1283-1287.

277. Squitieri,F., Cannella,M., Sgarbi,G., Maglione,V., Falleni,A., Lenzi,P., Baracca,A., Cislaghi,G., Saft,C., Ragona,G., Russo,M.A., Thompson,L.M., Solaini,G., and Fornai,F. (2006). Severe ultrastructural mitochondrial changes in lymphoblasts homozygous for Huntington disease mutation. Mech. Ageing Dev. *127*, 217-220.

278. Squitieri,F., Falleni,A., Cannella,M., Orobello,S., Fulceri,F., Lenzi,P., and Fornai,F. (2009). Abnormal morphology of peripheral cell tissues from patients with Huntington disease. J. Neural Transm.

279. Squitieri,F., Gellera,C., Cannella,M., Mariotti,C., Cislaghi,G., Rubinsztein,D.C., Almqvist,E.W., Turner,D., Bachoud-Levi,A.C., Simpson,S.A., Delatycki,M., Maglione,V., Hayden,M.R., and Donato,S.D. (2003). Homozygosity for CAG mutation in Huntington disease is associated with a more severe clinical course. Brain *126*, 946-955.

280. Stack,E.C., Kubilus,J.K., Smith,K., Cormier,K., Del Signore,S.J., Guelin,E., Ryu,H., Hersch,S.M., and Ferrante,R.J. (2005). Chronology of behavioral symptoms and neuropathological sequela in R6/2 Huntington's disease transgenic mice. J. Comp Neurol. *490*, 354-370.

281. Steffan,J.S., Kazantsev,A., Spasic-Boskovic,O., Greenwald,M., Zhu,Y.Z., Gohler,H., Wanker,E.E., Bates,G.P., Housman,D.E., and Thompson,L.M. (2000). The Huntington's disease protein interacts with p53 and CREB-binding protein and represses transcription. Proc. Natl. Acad. Sci. U. S. A *97*, 6763-6768.

282. Strong,T.V., Tagle,D.A., Valdes,J.M., Elmer,L.W., Boehm,K., Swaroop,M., Kaatz,K.W., Collins,F.S., and Albin,R.L. (1993). Widespread expression of the human and rat Huntington's disease gene in brain and nonneural tissues. Nat. Genet. *5*, 259-265.

283. Tallaksen-Greene,S.J., Crouse,A.B., Hunter,J.M., Detloff,P.J., and Albin,R.L. (2005). Neuronal intranuclear inclusions and neuropil aggregates in HdhCAG(150) knockin mice. Neuroscience *131*, 843-852.

284. Telenius,H., Kremer,B., Goldberg,Y.P., Theilmann,J., Andrew,S.E., Zeisler,J., Adam,S., Greenberg,C., Ives,E.J., Clarke,L.A., and . (1994). Somatic and gonadal mosaicism of the Huntington disease gene CAG repeat in brain and sperm. Nat. Genet. *6*, 409-414.

285. Telenius,H., Kremer,H.P., Theilmann,J., Andrew,S.E., Almqvist,E., Anvret,M., Greenberg,C., Greenberg,J., Lucotte,G., Squitieri,F., and . (1993). Molecular analysis of juvenile Huntington disease: the major influence on (CAG)n repeat length is the sex of the affected parent. Hum. Mol. Genet. *2*, 1535-1540.

286. Tellez-Nagel,I., Johnson,A.B., and Terry,R.D. (1974). Studies on brain biopsies of patients with Huntington's chorea. J. Neuropathol. Exp. Neurol. *33*, 308-332.

287. Thu,D.C., Oorschot,D.E., Tippett,L.J., Nana,A.L., Hogg,V.M., Synek,B.J., Luthi-Carter,R., Waldvogel,H.J., and Faull,R.L. (2010). Cell loss in the motor and cingulate cortex correlates with symptomatology in Huntington's disease. Brain *133*, 1094-1110.

288. Timchenko,L.T. and Caskey,C.T. (1999). Triplet repeat disorders: discussion of molecular mechanisms. Cell Mol. Life Sci. *55*, 1432-1447.

289. Tippett,L.J., Waldvogel,H.J., Thomas,S.J., Hogg,V.M., Roon-Mom,W., Synek,B.J., Graybiel,A.M., and Faull,R.L. (2007). Striosomes and mood dysfunction in Huntington's disease. Brain *130*, 206-221.

290. Trottier,Y., Biancalana,V., and Mandel,J.L. (1994). Instability of CAG repeats in Huntington's disease: relation to parental transmission and age of onset. J. Med. Genet. *31*, 377-382.

291. Trueman,R.C., Brooks,S.P., Jones,L., and Dunnett,S.B. (2007). The operant serial implicit learning task reveals early onset motor learning deficits in the Hdh knock-in mouse model of Huntington's disease. Eur. J. Neurosci. *25*, 551-558.

292. Trueman,R.C., Brooks,S.P., Jones,L., and Dunnett,S.B. (2008). Time course of choice reaction time deficits in the Hdh(Q92) knock-in mouse model of Huntington's disease in the operant serial implicit learning task (SILT). Behav. Brain Res. *189*, 317-324.

293. Trueman,R.C., Brooks,S.P., Jones,L., and Dunnett,S.B. (2009). Rule learning, visuospatial function and motor performance in the Hdh(Q92) knock-in mouse model of Huntington's disease. Behav. Brain Res. *203*, 215-222.

294. Turmaine,M., Raza,A., Mahal,A., Mangiarini,L., Bates,G.P., and Davies,S.W. (2000). Nonapoptotic neurodegeneration in a transgenic mouse model of Huntington's disease. Proc. Natl. Acad. Sci. U. S. A *97*, 8093-8097.

295. Valjent,E., Bertran-Gonzalez,J., Herve,D., Fisone,G., and Girault,J.A. (2009). Looking BAC at striatal signaling: cell-specific analysis in new transgenic mice. Trends Neurosci. *32*, 538-547.

296. van Dellen,A., Cordery,P.M., Spires,T.L., Blakemore,C., and Hannan,A.J. (2008). Wheel running from a juvenile age delays onset of specific motor deficits but does not alter protein aggregate density in a mouse model of Huntington's disease. BMC. Neurosci. *9*, 34.

297. van Dellen,A., Grote,H.E., and Hannan,A.J. (2005). Gene-environment interactions, neuronal dysfunction and pathological plasticity in Huntington's disease. Clin. Exp. Pharmacol. Physiol *32*, 1007-1019.

298. van Dellen,A., Welch,J., Dixon,R.M., Cordery,P., York,D., Styles,P., Blakemore,C., and Hannan,A.J. (2000). N-Acetylaspartate and DARPP-32 levels decrease in the corpus striatum of Huntington's disease mice. Neuroreport *11*, 3751-3757.

299. van den Bogaard,S.J., Dumas,E.M., Acharya,T.P., Johnson,H., Langbehn,D.R., Scahill,R.I., Tabrizi,S.J., van Buchem,M.A., van der,G.J., and Roos,R.A. (2011). Early atrophy of pallidum and accumbens nucleus in Huntington's disease. J. Neurol. *258*, 412-420.

300. van der Burg,J.M., Winqvist,A., Aziz,N.A., Maat-Schieman,M.L., Roos,R.A., Bates,G.P., Brundin,P., Bjorkqvist,M., and Wierup,N. (2011). Gastrointestinal dysfunction contributes to weight loss in Huntington's disease mice. Neurobiol. Dis. *44*, 1-8.

301. van der,B.K. and Brundin,P. (2007). Reduced expression of PSA-NCAM in the hippocampus and piriform cortex of the R6/1 and R6/2 mouse models of Huntington's disease. Exp. Neurol. *204*, 473-478.

302. van Dijk,J.G., van der Velde,E.A., Roos,R.A., and Bruyn,G.W. (1986). Juvenile Huntington disease. Hum. Genet. *73*, 235-239.

303. van Oostrom,J.C., Maguire,R.P., Verschuuren-Bemelmans,C.C., Veenma-van der Duin,L., Pruim,J., Roos,R.A., and Leenders,K.L. (2005). Striatal dopamine D2 receptors, metabolism, and volume in preclinical Huntington disease. Neurology *65*, 941-943.

304. Van Raamsdonk,J.M., Murphy,Z., Slow,E.J., Leavitt,B.R., and Hayden,M.R. (2005a). Selective degeneration and nuclear localization of mutant huntingtin in the YAC128 mouse model of Huntington disease. Hum. Mol. Genet. *14*, 3823-3835.

305. Van Raamsdonk,J.M., Pearson,J., Murphy,Z., Hayden,M.R., and Leavitt,B.R. (2006). Wild-type huntingtin ameliorates striatal neuronal atrophy but does not prevent other abnormalities in the YAC128 mouse model of Huntington disease. BMC. Neurosci. *7*, 80.

306. Van Raamsdonk,J.M., Pearson,J., Slow,E.J., Hossain,S.M., Leavitt,B.R., and Hayden,M.R. (2005b). Cognitive dysfunction precedes neuropathology and motor abnormalities in the YAC128 mouse model of Huntington's disease. J. Neurosci. *25*, 4169-4180.

307. Velier,J., Kim,M., Schwarz,C., Kim,T.W., Sapp,E., Chase,K., Aronin,N., and DiFiglia,M. (1998). Wild-type and mutant huntingtins function in vesicle trafficking in the secretory and endocytic pathways. Exp. Neurol. *152*, 34-40.

308. Vidair,C.A., Huang,R.N., and Doxsey,S.J. (1996). Heat shock causes protein aggregation and reduced protein solubility at the centrosome and other cytoplasmic locations. Int. J. Hyperthermia *12*, 681-695.

309. Von Horsten,S., Schmitt,I., Nguyen,H.P., Holzmann,C., Schmidt,T., Walther,T., Bader,M., Pabst,R., Kobbe,P., Krotova,J., Stiller,D., Kask,A., Vaarmann,A., Rathke-Hartlieb,S., Schulz,J.B., Grasshoff,U., Bauer,I., Vieira-Saecker,A.M., Paul,M., Jones,L., Lindenberg,K.S., Landwehrmeyer,B., Bauer,A., Li,X.J., and Riess,O. (2003). Transgenic rat model of Huntington's disease. Hum. Mol. Genet. *12*, 617-624.

310. Vonsattel,J.P. (2008). Huntington disease models and human neuropathology: similarities and differences. Acta Neuropathol. *115*, 55-69.

311. Vonsattel,J.P. and DiFiglia,M. (1998). Huntington disease. J. Neuropathol. Exp. Neurol. *57*, 369-384.

312. Vonsattel,J.P., Myers,R.H., Stevens,T.J., Ferrante,R.J., Bird,E.D., and Richardson,E.P., Jr. (1985). Neuropathological classification of Huntington's disease. J. Neuropathol. Exp. Neurol. *44*, 559-577.

313. Waelter,S., Boeddrich,A., Lurz,R., Scherzinger,E., Lueder,G., Lehrach,H., and Wanker,E.E. (2001). Accumulation of mutant

huntingtin fragments in aggresome-like inclusion bodies as a result of insufficient protein degradation. Mol. Biol. Cell *12*, 1393-1407.

314. Wang,L.H. and Qin,Z.H. (2006). Animal models of Huntington's disease: implications in uncovering pathogenic mechanisms and developing therapies. Acta Pharmacol. Sin. *27*, 1287-1302.

315. Wanker,E.E., Rovira,C., Scherzinger,E., Hasenbank,R., Walter,S., Tait,D., Colicelli,J., and Lehrach,H. (1997). HIP-I: a huntingtin interacting protein isolated by the yeast two-hybrid system. Hum. Mol. Genet. *6*, 487-495.

316. Warrick,J.M., Paulson,H.L., Gray-Board, Bui,Q.T., Fischbeck,K.H., Pittman,R.N., and Bonini,N.M. (1998). Expanded polyglutamine protein forms nuclear inclusions and causes neural degeneration in Drosophila. Cell *93*, 939-949.

317. Weinstein,D.E., Shelanski,M.L., and Liem,R.K. (1991). Suppression by antisense mRNA demonstrates a requirement for the glial fibrillary acidic protein in the formation of stable astrocytic processes in response to neurons. J. Cell Biol. *112*, 1205-1213.

318. Weiss,A., Klein,C., Woodman,B., Sathasivam,K., Bibel,M., Regulier,E., Bates,G.P., and Paganetti,P. (2008). Sensitive biochemical aggregate detection reveals aggregation onset before symptom development in cellular and murine models of Huntington's disease. J. Neurochem. *104*, 846-858.

319. Wellington,C.L., Ellerby,L.M., Hackam,A.S., Margolis,R.L., Trifiro,M.A., Singaraja,R., McCutcheon,K., Salvesen,G.S., Propp,S.S., Bromm,M., Rowland,K.J., Zhang,T., Rasper,D., Roy,S., Thornberry,N., Pinsky,L., Kakizuka,A., Ross,C.A., Nicholson,D.W., Bredesen,D.E., and Hayden,M.R. (1998). Caspase cleavage of gene products associated with triplet expansion disorders generates truncated fragments containing the polyglutamine tract. J. Biol. Chem. *273*, 9158-9167.

320. Wexler,N.S., Lorimer,J., Porter,J., Gomez,F., Moskowitz,C., Shackell,E., Marder,K., Penchaszadeh,G., Roberts,S.A., Gayan,J., Brocklebank,D., Cherny,S.S., Cardon,L.R., Gray,J., Dlouhy,S.R., Wiktorski,S., Hodes,M.E., Conneally,P.M., Penney,J.B., Gusella,J., Cha,J.H., Irizarry,M., Rosas,D., Hersch,S., Hollingsworth,Z., MacDonald,M., Young,A.B., Andresen,J.M., Housman,D.E., De Young,M.M., Bonilla,E., Stillings,T., Negrette,A., Snodgrass,S.R., Martinez-Jaurrieta,M.D., Ramos-Arroyo,M.A., Bickham,J., Ramos,J.S., Marshall,F., Shoulson,I., Rey,G.J., Feigin,A., Arnheim,N., Acevedo-Cruz,A., Acosta,L., Alvir,J., Fischbeck,K., Thompson,L.M., Young,A., Dure,L., O'Brien,C.J., Paulsen,J., Brickman,A., Krch,D., Peery,S., Hogarth,P., Higgins,D.S., Jr., and Landwehrmeyer,B. (2004). Venezuelan kindreds reveal that genetic and environmental factors modulate Huntington's disease age of onset. Proc. Natl. Acad. Sci. U. S. A *101*, 3498-3503.

321. Wexler,N.S., Rose,E.A., and Housman,D.E. (1991). Molecular approaches to hereditary diseases of the nervous system: Huntington's disease as a paradigm. Annu. Rev. Neurosci. *14*, 503-529.

322. Wexler,N.S., Young,A.B., Tanzi,R.E., Travers,H., Starosta-Rubinstein,S., Penney,J.B., Snodgrass,S.R., Shoulson,I., Gomez,F., Ramos Arroyo,M.A., and . (1987). Homozygotes for Huntington's disease. Nature *326*, 194-197.

323. Wheeler,V.C., Auerbach,W., White,J.K., Srinidhi,J., Auerbach,A., Ryan,A., Duyao,M.P., Vrbanac,V., Weaver,M., Gusella,J.F., Joyner,A.L., and MacDonald,M.E. (1999). Length-dependent gametic CAG repeat instability in the Huntington's disease knock-in mouse. Hum. Mol. Genet. *8*, 115-122.

324. Wheeler,V.C., White,J.K., Gutekunst,C.A., Vrbanac,V., Weaver,M., Li,X.J., Li,S.H., Yi,H., Vonsattel,J.P., Gusella,J.F., Hersch,S., Auerbach,W., Joyner,A.L., and MacDonald,M.E. (2000). Long glutamine tracts cause nuclear localization of a novel form of huntingtin in medium spiny striatal neurons in HdhQ92 and HdhQ111 knock-in mice. Hum. Mol. Genet. *9*, 503-513.

325. White,F.J. and Wang,R.Y. (1986). Electrophysiological evidence for the existence of both D-1 and D-2 dopamine receptors in the rat nucleus accumbens. J. Neurosci. *6*, 274-280.

326. White,J.K., Auerbach,W., Duyao,M.P., Vonsattel,J.P., Gusella,J.F., Joyner,A.L., and MacDonald,M.E. (1997). Huntingtin is required for neurogenesis and is not impaired by the Huntington's disease CAG expansion. Nat. Genet. *17*, 404-410.

327. Wood,N.I., Pallier,P.N., Wanderer,J., and Morton,A.J. (2007). Systemic administration of Congo red does not improve motor or cognitive function in R6/2 mice. Neurobiol. Dis. *25*, 342-353.

328. Woodman,B., Butler,R., Landles,C., Lupton,M.K., Tse,J., Hockly,E., Moffitt,H., Sathasivam,K., and Bates,G.P. (2007). The Hdh(Q150/Q150) knock-in mouse model of HD and the R6/2 exon 1 model develop comparable and widespread molecular phenotypes. Brain Res. Bull. *72*, 83-97.

329. Yamamoto,A., Lucas,J.J., and Hen,R. (2000). Reversal of neuropathology and motor dysfunction in a conditional model of Huntington's disease. Cell *101*, 57-66.

330. Yang,S.H., Cheng,P.H., Banta,H., Piotrowska-Nitsche,K., Yang,J.J., Cheng,E.C., Snyder,B., Larkin,K., Liu,J., Orkin,J., Fang,Z.H., Smith,Y., Bachevalier,J., Zola,S.M., Li,S.H., Li,X.J., and Chan,A.W. (2008). Towards a transgenic model of Huntington's disease in a non-human primate. Nature *453*, 921-924.

331. Yang,W., Dunlap,J.R., Andrews,R.B., and Wetzel,R. (2002). Aggregated polyglutamine peptides delivered to nuclei are toxic to mammalian cells. Hum. Mol. Genet. *11*, 2905-2917.

332. Yohrling,G.J., Jiang,G.C., DeJohn,M.M., Miller,D.W., Young,A.B., Vrana,K.E., and Cha,J.H. (2003). Analysis of cellular, transgenic and human models of Huntington's disease reveals tyrosine hydroxylase alterations and substantia nigra neuropathology. Brain Res. Mol. Brain Res. *119*, 28-36.

333. Young,W.S., III, Bonner,T.I., and Brann,M.R. (1986). Mesencephalic dopamine neurons regulate the expression of neuropeptide mRNAs in the rat forebrain. Proc. Natl. Acad. Sci. U. S. A *83*, 9827-9831.

334. Yu,Z.X., Li,S.H., Evans,J., Pillarisetti,A., Li,H., and Li,X.J. (2003). Mutant huntingtin causes context-dependent neurodegeneration in mice with Huntington's disease. J. Neurosci. *23*, 2193-2202.

335. Zeitlin,S., Liu,J.P., Chapman,D.L., Papaioannou,V.E., and Efstratiadis,A. (1995). Increased apoptosis and early embryonic lethality in mice nullizygous for the Huntington's disease gene homologue. Nat. Genet. *11*, 155-163.

336. Zettlmeissl,G., Rudolph,R., and Jaenicke,R. (1979). Reconstitution of lactic dehydrogenase. Noncovalent aggregation vs. reactivation. 1. Physical properties and kinetics of aggregation. Biochemistry *18*, 5567-5571.

337. Zhang,Y., Leavitt,B.R., Van Raamsdonk,J.M., Dragatsis,I., Goldowitz,D., MacDonald,M.E., Hayden,M.R., and Friedlander,R.M. (2006). Huntingtin inhibits caspase-3 activation. EMBO J. *25*, 5896-5906.

338. Zuccato,C., Ciammola,A., Rigamonti,D., Leavitt,B.R., Goffredo,D., Conti,L., MacDonald,M.E., Friedlander,R.M., Silani,V., Hayden,M.R., Timmusk,T., Sipione,S., and Cattaneo,E. (2001). Loss of huntingtin-mediated BDNF gene transcription in Huntington's disease. Science *293*, 493-498.

339. Zuccato,C., Valenza,M., and Cattaneo,E. (2010). Molecular mechanisms and potential therapeutical targets in Huntington's disease. Physiol Rev. *90*, 905-981.